Functional Characterization of Outer Membrane Vesicles (OMVs) isolated from *Acinetobacter*baumannii DS002

Thesis submitted in partial fulfilment for the award of the degree

of

Doctor of Philosophy

By
Ganeshwari Dhurve
(15LAPH11)

Supervisor **Prof. S. Dayananda**



Department of Animal Biology
School of Life Sciences
University of Hyderabad-500046, India
June 2022



University of Hyderabad

(A central University established in 1974 by an act of Parliament) Hyderabad – 500046, INDIA

CERTIFICATE

This is to certify that the thesis entitled "Functional Characterization of Outer Membrane Vesicles (OMVs) isolated from Acinetobacter baumannii DS002" submitted by Ms. Ganeshwari Dhurve bearing registration number 15LAPH11 in partial fulfillment of the requirements for award of Doctor of Philosophy in the Department of Animal Biology, School of Life Sciences is a bonafide work carried out byher under my supervision and guidance. This thesis is free from plagiarism and has not been submitted previously in part or in full to this or any other University or Institution for award of any degree or diploma.

Publications:

1. Microbiology Spectrum, 2022 Apr 27;10(2) (PMID: 35266817)

Conference:

- 1. Poster presented at International conference organized by 'Association of Microbiologists of India (ASM-2019) at University of Hyderabad. 9th-12th December 2019.
- 2. Received Best Oral presentation award at "Proteomics in Agriculture and Healthcare" conference conducted during 13th-14th March 2021, University of Hyderabad.
- 3. Virtual presentation at "American Society of Microbiologist (ASM) 2022", 9th-13th June 2022, at Washington DC, USA.

Further, the student has passed the following courses towards the fulfillment of course work required for the award of Ph. D

Course Code	Name	Credits	Pass/Fail
AS 801	Seminar 1	1	Pass
AS 802	Research Ethics & Management	2	Pass
AS 803	Biostatistics	2	Pass
AS 804	Analytical Techniques	3	Pass
AS 805	Lab Work	4	Pass

Research Supervisor

Head of the Department

School of Life Sciences

Prof. S. DAYANANDA Dept. of Animal Biology. School of Life Sciences University of Hyderabad Hyderabad-500 046. T.S. अध्यक्ष / HEAD जंतु जैविकी विभाग Department of Animal Biology University of Hyderabad Hyderabad-500 046.



University of Hyderabad

(A central University established in 1974 by an act of Parliament) Hyderabad – 500046, INDIA

DECLARATION

This is to declare that the work embodied in this thesis entitled "Functional Characterization of Outer Membrane Vesicles (OMVs) isolated from Acinetobacter baumannii DS002" has been carried out by me under the supervision of Prof. S. Dayananda, Department of Animal Biology, School of Life Sciences. The work presented in this thesis is a bonafide research work and has not been submitted for any degree or diplomain any other University or Institute. A report on plagiarism statistics from the University Librarian is enclosed.

Date: 16-06-2022

Date: 16-06-2022 .

Ganeshwari Dhurve

15LAPH11

Prof. S. Dayananda

Supervisor

Prof. S. DAYANANDA Dept. of Animal Biology. School of Life Sciences University of Hyderabad Hyderabad-500 046. T.S.

<u>Acknowledgements</u>

First and foremost, I would like to express my deep and sincere gratitude to my supervisor, Prof: Dayananda Siddavattam for being an ideal teacher, mentor, and thesis supervisor, offering advice, immense support and encouragement: Prof: S: D: provided invaluable feedback in my research study, at times responding to emails late at night and early in the morning:

I thank my doctoral committee members $Dr \cdot K \cdot Gopinath$, especially for taking out time from his schedule and accompanying me during TEM imaging · Also, to $Prof \cdot M \cdot R \cdot Pongubala$ for his timely suggestions and critical assessment ·

I thank the current and former Deans, School of Life Sciences, Prof. S. Dayananda, Prof. K.V.A Ramaiah, and Prof. Reddanna for providing all the facilities in the school.

I thank Dr. Sreenivasulu Kurukuti, Head, Dept. of Animal Biology, and former Head's Prof. Anita Jagota and Prof. Jagan Pongubala for all the department facility.

This thesis would not have been possible without $Dr \cdot M \cdot V \cdot Jagannatham$, whose guidance in field of OMVs enabled me to develop an understanding and interest ·

I gratefully recognize the help of Prof. Kota Arun and his lab members for providing cell culture facility and their timely help during research work.

I thank the help and suggestions of all the faculty members in the School of Life Sciences, and for allowing me to use their laboratory facilities at different stages of my work.

I acknowledge the generous financial support from UGC (JRF and SRF), Biological E and Aurobindo pharma· I thank DBT, ICMR, UGC, UPE-II, UGC-SAP and DBT-CREBB for the infrastructural facility of the school·

My research work would have not been complete without the never-ending help and valuable suggestions by my seniors Dr. Sunil Parthasarathy, Dr. Ashok Madikonda, Dr. Ramurthy Gudla, Dr. Devyani, Dr. Hari and Dr. Aparna. I especially thank Dr. Emmanuel Paul for his valuable inputs in my research and thesis. I thank my current colleagues, Mr. Akbar, Dr. Sukhmeen and Ms. Sandhya. I must thank Dr. Harshita and Ms. Annapoorni for offering most friendly gesture and love in the lab. In addition, I would like to thank all project students Ms. Pooja, Mr. Kashif, Ms. Pardheepa, and Ms. Shailaja for filling my last days in lab with lots of fun and laughter.

Special thanks to all friends from school of Life Sciences for their support in my research and for the numerous fun filled discussions at the school canteen.

I thank non-teaching staff Mr. Krishna and Mr. Rajendra Prasad, Mr. Upendra, Mr. Praveen, Mr. Jagan, Mr. Srinu, Mr. Saleem and Mr. Sravan for their technical help.

I genuinely thank sports complex/ Badminton court facility at UOH for making past years much more enjoyable and keeping me sane throughout this journey.

I want to give my deepest appreciation to Ms· Amita, Dr· Nikhita, Mr· Deepak and Mr· Siddhartha for being wonderful friends and emotional support during this journey. Further, stay in Hyderabad was made fun and memorable by Ms· Pratibha, Dr· Ankita, Dr· Narender, and Ms· Rolly· They all have been family away from family and blessing in my life·

Lastly, my family deserves endless gratitude: My Father Mr· Bhagwan Singh Dhurve and my mother Mrs· Saroj Dhurve for teaching me good work etiquettes and values· Their belief in me has kept my spirits and motivation high during this process· I also thank my elder Brother Dr· Chandresh Dhurve and Sister Ms· Rameshwari Dhurve for always being there with family in needs so that I can focus in my research· I thank Yug (nephew) and Shri (niece) for being my stress buster·

Especially, I would like to thank and dedicate my thesis to my parents for all their hardships to bring me till this stage.

I thank God Almighty for filling my life with such wonderful people around and also for giving me the strength and patience needed to endure every difficulty encountered.



TABLE OF CONTENTS

CHAPTER 1: INTRODUCTION	1
1.1 Acinetobacter baumannii	2
1.2 Outer membrane vesicles (OMVs)	
1.2.1 Key discoveries	
1.2.2 Vesicle cargo composition	
1.2.3 Function of OMVs	6
1.3 Replication competent circular DNA	7
1.4 Hypothesis	3
1.5 Objectives of the present study	3
CHAPTER 2: GENERAL MATERIAL AND METHODS	4
2.1 Growth Media	7
2.1.1 Luria-Bertani (LB) medium	
2.1.2 Minimal Salts Medium	
2.2 Preparation of iron free media and solutions	
2.2.1 Preparation of high iron solution	
2.2.2 Preparation of low iron solution	
2.3 Preparation of iron free glassware	8
2.4 Antibiotic & Chemical stock solutions	8
2.4.1 Isopropyl β-D-1-thiogalactopyranoside (IPTG)	9
2.4.2 5-bromo-4-chloro-indolyl-β-D-galactopyranoside (X-Gal)	9
2.5 Solution and buffers for DNA manipulation and analysis:	
2.5.1 TAE (Tris-Acetate-EDTA) buffer	
2.5.2 6X Gel loading buffer	
2.5.3 Ethidium bromide	9
2.6 Agarose gel electrophoresis	10
2.7 Plasmid isolation by Alkaline Lysis method	
2.7.1 Solutions for plasmid isolation	
2.7.2 Procedure for Isolation of plasmid DNA	11
2.8 DNA Quantification	11
2.9 Polymerase Chain Reaction (PCR)	12
2.10 Colony PCR	12
2.11 Molecular Cloning	
2.11.1 Restriction Digestion of DNA	
2.11.2 Dephosphorylation of vector	
2.11.3 DNA Ligation	13
2.12 Gene transfer methods	
2.12.1 Preparation of Competent cells	
2.12.2 Bacterial transformation	14

2.12.4 Electroporation	14 14
2.13 Polyacrylamide gel electrophoresis	15
2.14 Protein Methods	16
2.14.1 Solutions for SDS-PAGE	
2.14.2 Solutions for Western Blotting	
2.14.3 Semi-Dry Western Blotting	
2.14.4 Protein precipitation by Methanol-Chloroform method	
CHAPTER 3: ISOLATION OF OMVS FROM ACINETOBACTER BAUMANNII DS	500220
3.1 Objective specific methodology	20
3.1.1 Isolation of outer membrane vesicle (OMVs)	
3.1.2 Cloning and Expression of ompA in pET28a vector	
3.1.3 Generation of polyclonal antibody against OmpA ^{N6XHis}	
3.1.4 Antibody purification	
3.1.5 Preparation of subcellular fractions	
3.1.6 Determination of OMV Purity and quantity	
3.1.7 Transmission Electron Microscopy (TEM)	
3.1.8 Nanoparticle tracking analysis (NTA)	
3.2 Results	25
3.2.1 Purification of OMVs	
3.2.2 Purity Assessment of OMVs	
3.2.3 Generation of anti-OmpA antibodies	
3.2.4 OMV isolated were pure	
3.2.5 Size distribution of OMVs	
3.3 Discussion	32
CHARTER A. PROTECNAE OF CNAVC	25
4.1 Objective specific methods	36
4.1 Objective specific methods	36
4.1 Objective specific methods	36 36
4.1 Objective specific methods	36 36 36
4.1 Objective specific methods	36 36 36 38
4.1 Objective specific methods	36 36 36 38
4.1 Objective specific methods	

5.1.5 Ligand blotting	78
5.1.6 AbDs1 and OMV interactions	
5.1.7 Generation of A. baumannii DS003	80
5.1.8 Role of OMVs in lateral mobility of DNA	81
5.1.9 Mobilization of Phage genome into eukaryotic cells	82
5.2 Results	83
5.2.1 Indigenous plasmids are associated with OMV	
5.2.2 Plasmids pTS486 and pTS9900 were found in the lumen of OMVs	85
5.2.3 Phage AbDs1 is associated with OMVs	
5.2.4 Microscopic observations	
5.2.5 AbDs1 anchors to OMVs by Interacting with OmpA	
5.2.6 Validation of OmpA and Orf96 interaction	
5.2.7 Genetic Evidence on phage AbDs1 with OMV interactions	
5.2.8 Isolation of OMVs from A. baumannii DS003	
5.2.9 OmpA is critical for AbDs1Association with OMVs	
5.2.10 Role of OMVs in lateral Mobility	
5.2.11 Tagging phage AbDs1 genome with GFP	104
5.3 Discussion	105
CONCLUSION	••••••
REFERENCES	
PUBLICATION	
ANTI-PLAGIARISM REPORT	•••••

LIST OF ABBREVIATIONS

Amp : Ampicilin

BBB : Blood-brain barrier

BMMF : Bovine meat and milk factors

BSA : Bovine serum albumin
CJD : Creutzfeldt-Jakob disease

Cm : Chloramphenicol CMI : Cow milk isolate

CNS : Central Nervous System

CP : Cytoplasmic

dNTPs : Deoxynucleoside triphosphate

Ent : Enterobactin

GFP : Green fluorescent proteinHAI : Hospital acquired infectionsHCBI : Healthy cattle blood isolateHGT : Horizontal Gene Transfer

ICU : Intensive Care Unit IM : Inner Membrane

IPTG : Isopropyl β -D-1-thiogalactopyranoside

Kan : Kanamycin Lpp : Lipoproteins

LPSs : Lipopolysaccharides
MDR : Multi Drug Resistant
MS : Multiple Sclerosis

MSBI : Multiple sclerosis brain isolate

OM : Outer Membrane

OMPs : Outer Membrane Proteins
OMVs : Outer Membrane Vesicles
PCR : Polymerase chain reaction
PPL : Priority Pathogen List

Sm : Streptomycin

SPHINX : Slow Progressive Hidden Infections of Variable (X) Latency

ssDNA : Single-stranded DNA

TEM : Transmission Electron Microscope

Tet : Tetracycline

TonB : TonB dependent transporter

TSE : Transmissible spongiform encephalopathies

WHO: World Health Organisation

X-gal : 5-bromo-4-chloro-indolyl-β-D-galactopyranoside

LIST OF TABLES

Table 2. 1 Antibiotics	4
Table 2. 2 Chemicals	4
Table 2. 3 Restriction enzymes and DNA modifying enzymes	6
Table 2. 4 Preparation of Antibiotics	9
Table 2. 5 PCR cycling conditions	
Table 2. 6 Composition of the resolving gel for SDS-PAGE	16
Table 2. 7 Composition of the stacking gel for SDS-PAGE	16
Table 4. 1 Gradient used for separating peptides	
Table 4. 2 Total list of OMV proteome identified using LC-ESI-MS/MS analysis	43
Table 4. 3 List of TonB dependent receptors proteins detected from OMVs of A. baumannii	63
Table 5. 1 Strains used in this study	73
Table 5. 2 Oligonucleotide primers used in this study	73
Table 5. 3 Plasmid Used in this study	75
Table 5. 4 Four circularized contigs obtained by assembly using SPAdes 3.15.3 assembler	83

LIST OF FIGURES

Figure 1. 1 OMVs contain diverse intracellular components, like proteins, lipids and genetic material	3
Figure 1. 2 The envelope of Gram-negative bacteria	3
Figure 1. 3 Biogenesis of outer-membrane vesicles (OMVs) is dependent on several factors	5
Figure 1. 4 Circular single-stranded DNA isolates from sources are grouped	
Figure 1. 5 Unrooted tree of BMMF isolates	
Figure 3. 1 Workflow followed during purification of OMVs from A. baumannii DS002	
Figure 3. 2 Isolation and purification of pure OMVs from A. baumannii DS002	
Figure 3. 3 Construction of pGD1.	
Figure 3. 4 Expression of OmpA ^{N6XHis}	
Figure 3. 5 Affinity purification of OmpA ^{N6XHis}	29
Figure 3. 6 Purification of anti-OmpA antibodies	29
Figure 3. 7 Checking purity of outer membrane vesicles (OMVs) from Acinetobacter baumannii DS002	30
Figure 3. 8 Size distribution of OMVs from A. baumannii DS002.	31
Figure 4. 1 Workflow followed during proteomic analysis of OMVs from A. baumannii DS002	27
Figure 4. 2 workflow for the preparation of ferric-Enterobactin	
Figure 4. 3 workflow for the labelling of OMVs with ferric-Enterobactin complex	
Figure 4. 4 Workflow representing, the iron uptake study by A. baumannii DS002	
Figure 4. 6 Origin of OMV proteome.	
Figure 4. 7 Cluster of orthologous group (COG) categorization of OMV proteins	
Figure 4. 8 Classification of OMV proteome of A. baumannii DS002	
Figure 4. 9 Representation of Proteins associated with OMV of A. baumannii DS002	
Figure 4. 11 TonB dependent transport system	
Figure 4. 12 Unrooted Phylogram constructed by including functionally characterized TonB dependent tr (TonRs) along with TonRs of OMVs of A. baumannii DS002	unsporter
Figure 4. 13 Molecular structure of siderophores.	
Figure 4. 14 Predicted transcription factor binding motifs overlapping TonR coding genes	
Figure 4. 15 The OMV assisted iron uptake in A. baumannii DS002	68
Table 5. 1 Strains used in this study	
Table 5. 2 Oligonucleotide primers used in this study	
Table 5. 3 Plasmid Used in this study	
Table 5. A Four circularized contine obtained by accomply using SPA dec 2.15.2 accompler	

Chapter 1: Introduction

Nosocomial infections are on the raise globally and is becoming serious threat to human health. On an average every year about 1.7 million patients suffer from hospital acquired infections (HAI), with 98,987 deaths (Klevens et al., 2007). In USA alone, 722,000 people suffered from HAI leading to 75,000 number of deaths (Magill et al., 2014). The leading cause of these infections are, growing number of antimicrobial resistant pathogens leading to emergence of multidrug resistant (MDR) strains. These bacterial infections are among the top three threats to global public health. In the year 2017, world health organization (WHO) has released the global priority pathogens list (PPL) by including 12 different drug resistant bacteria. Among them carbapenem resistant Acinetobacter baumannii was listed as the top critical pathogen needing development of new and effective antibiotic treatment (Shrivastava et al., 2018). The pathogens featured prominently in global PPL are Enterococcus faecium, Staphylococcus aureus, Acinetobacter baumannii, Klebsiella pneumoniae, Pseudomonas aeruginosa and Enterobacter sp. (Ramsamy et al., 2018). The Infectious Diseases Society of America termed them as 'ESCAPE' pathogens. The 'ESCAPE' pathogens not only cause huge percentage of nosocomial infections but have tendency to gain multiple resistance mechanisms to escape the biological activity of antibiotics.

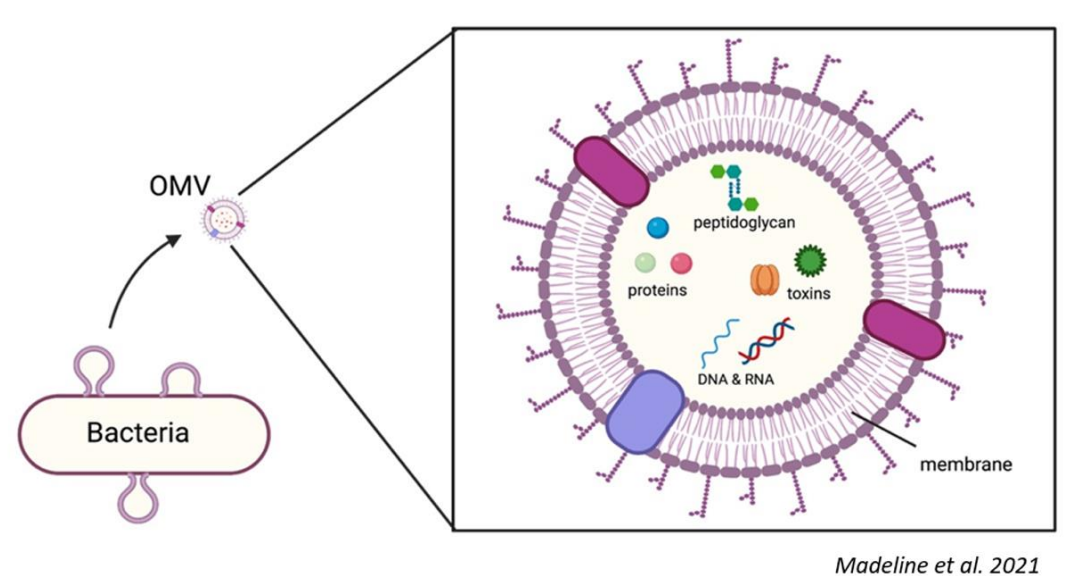
The genus *Acinetobacter* comprises Gram-negative, strictly aerobic, non-motile and non-fermenting bacteria which are ubiquitous in nature. In 1911, a Dutch microbiologist named Beijerinck isolated it from soil and named it Micrococcus calco-aceticus. Forty-three years later, the name *Acinetobacter* (coming from the Greek "akinetos" meaning non-motile) was introduced by Brisou and Prevot to differentiate it from rest of the motile organisms. Four decades later Brisou and Prevot proposed including it in the genus *Acromobacter*, due to their inability to move and lack of pigmentation. In the year 1968, Baumann et al. grouped all similar isolates into one genus named as *Acinetobacter*. Four years later, in 1971, the sub-committee on Taxonomy of Moraxella and Allied Bacteria, officially accepted Baumann's findings and given the official status to the genus *Acinetobacter*. The genus *Acinetobacter* now contains 65 validly published species (Nemec et al., 2021) and nearly half of them are either isolated from soil or water environments. The *A. calcoaceticus-baumannii* complex consists of *A. calcoaceticus*, *A. baumannii*, *A. pittii* and the fourth genospecies 13TU, *A. nosocomialis*. Among these genospecies *A. baumannii* has been identified as the most frequently isolated nosocomial pathogen and it is responsible for the highest mortality rate worldwide.

1.1 Acinetobacter baumannii

Acinetobacter baumannii has emerged as clinically significant pathogens. It acquired clinical significance due to the ability to quickly develops antibiotic resistance as well as survival capability on hospitals equipment and dry surfaces (Jawad et al., 1998). It is an opportunistic pathogen and can cause wide variety of infections, predominantly respiratory tract infections, bacteremia, urinary tract infections, skin and soft tissue infections, and intracranial infections. Nearly, 2–10% of all Gram-negative hospital infections are caused by A. baumannii (Joly-Guillou, 2005). The mortality associated with A. baumannii infections at intensive care unit (ICU) is observed around 40%. The number of multi-drug resistant (MDR) A. baumannii isolates have increased significantly due to incorrect and often excessive use of antibiotics. Apart from innate antibiotic resistance, A. baumannii has high genome plasticity. It is naturally competent to acquire exogenous DNA and quickly acquires genes from the environment that contribute to drug resistance. Natural competence to acquire antibiotic resistant genes, restricts effective therapeutic options to control A. baumannii which results in increased rate of mortality. Like other Gram-negative bacteria, A. baumannii also produces outer membrane vesicles (OMVs), which play important role in eliciting several physiological functions. However, studies establishing the relationship between multi-drug resistance and OMV assisted organismal fitness are scarce. There is virtually no information on virulence factors and DNA molecules associated with OMVs of A. baumannii.

1.2 Outer membrane vesicles (OMVs)

Outer membrane vesicles (OMVs) are spherical, non-replicating, nano sized particles ranging from 20-300 nm of size. These are composed of proteins, lipopolysaccharides (LPSs), phospholipids, DNA, RNA and lipids (Fig 1.1). Bacteria use OMVs as tools through which they interact with both biotic and abiotic factors. The secretion of membrane vesicles is a universal process. Organisms from all three domains of life, Eukarya, Archaea and Bacteria secrete membrane vesicles, called exosomes, agrosomes, microvesicles and outer membrane vesicles (OMVs). The vesicles produced by Gram-negative bacteria are called as outer membrane vesicle (OMVs) (Gill et al., 2019). Pathogenic and commensal, both Gram-negative bacteria secrete OMVs as a part of their natural growth.



Wadeline et al. 2021

Figure 1. 1 OMVs contain diverse intracellular components, like proteins, lipids and genetic material.

1.2.1 Key discoveries

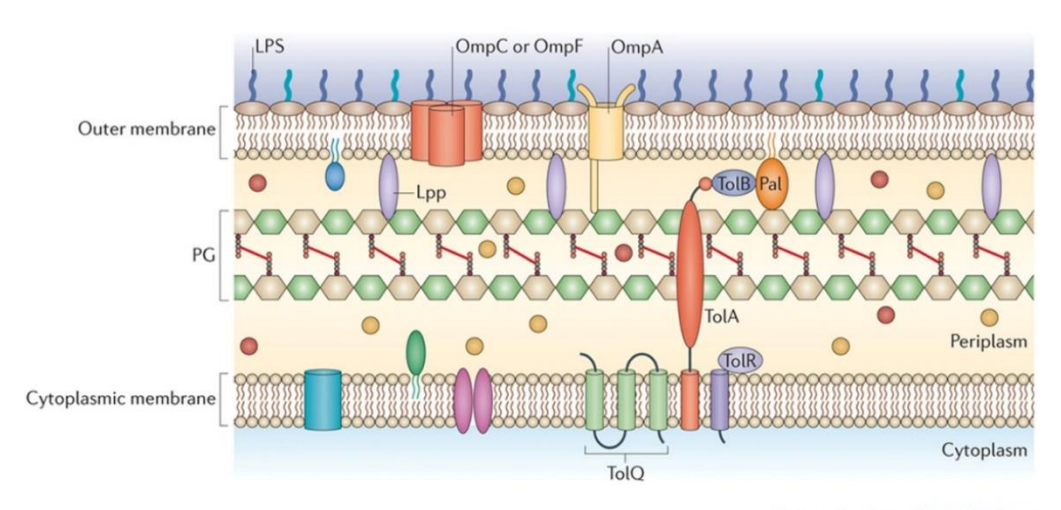
In 1965, the release of OMV was observed for the first time where the auxotrophic Escherichia coli strain released substantial amount of cell-free lipopolysaccharides (LPS) in a lysine-limiting growth conditions (Laboratories & Road, 1965). Later, in 1966 Knox and group observed it under electron microscopy, and found that these LPS elements were actually part of the membrane structure and proposed that these tiny structures called vesicles are derived from the outer membrane (OM) (Knox et al., 1966). Formation of these vesicles increased when cells are exposed to chloramphenicol and amino acid (Rothfield & Pearlman-Kothencz, 1969). Subsequently, many studies have observed and isolated OMVs from many gram-negative bacteria, such as Veillonella parvula (Mergenhagen et al., 1966), Vibrio cholerae (S. N. Chatterjee & Das, 1967), and Salmonella enterica ser. Typhimurium (Rothfield & Pearlman-Kothencz, 1969). OMVs are also detected in bacteria infecting animal tissue (DeVoe & Gilchrist, 1975). Despite of isolating OMVs from different sources, for a number of years, they were thought to be growth artifacts or products of cell lysis for a long time. Nevertheless, their physiological significance and their role in inter and intra-cellular communications, nutrient acquisition and lateral gene mobility is now established beyond reasonable doubt. Even the pathogenic bacteria, release OMVs. Over the years vesicle secretion by bacteria has regained interest due to finding of extensive biological roles, especially their role in microbial pathogenesis which has attracted the attention of scientists across the world (Jarzab et al., 2020; Rueter & Bielaszewska, 2020).

1.2.1.1 Envelope of gram-negative bacteria

In order to understand the mechanism behind OMV Biogenesis, discussing the membrane architecture of gram-negative bacteria is important. Gram-negative bacteria's envelope is made up of three major layers: an outer membrane (OM), a peptidoglycan cell wall, and an inner membrane (IM) (Fig 1.2). The 13 nm space between OM and IM is known as periplasmic space (Raetz & Dowhan, 1990). The membranes differ in lipid and protein composition. The OM is a lipid bilayer, the outer leaflet consists of glycolipids, principally lipopolysaccharide (LPS) and the inner leaflet of the bilayer is made up of phospholipids. Whereas both the leaflets of IM contain phospholipids. The viscous periplasmic space contains large number of proteins with non-reducing environment and has a rigid thin layer of peptidoglycan (PG) that is attached to IM and OM through lipoproteins (Braun's lipoprotein (Lpp) and OmpA. Proteins embedded in the OM are called as outer membrane proteins (OMPs) which are mostly folded in beta-barrel confirmation, whereas proteins present in IM are mostly alpha helical. Lipoproteins are the membrane anchored to a covalently anchored lipid moiety and are mostly destined to be on OM but sometimes also found in IM (Kleanthous & Armitage, 2015).

These envelopes are stabilized by crosslinking between them: the covalent crosslinking of Lpp in OM with PG sacculus. The non-covalent interaction between outer membrane protein A (OmpA) and peptidoglycan, and non-covalent interaction between the peptidoglycan and Tol-Pal (peptidoglycan-associated lipoprotein) complex, which spans the envelope from OM to the cytoplasmic (CP) membrane (Schwechheimer & Kuehn, 2015). Since, OMVs are known to be secreted by budding off the OM during growth, OMV biogenesis must be dependent on detachment of the OM from the underlying PG in areas lacking attachments which is followed by fission without causing any envelope instability. In principle, for an OMV to form, the outer membrane must be liberated from the underlying PG and bulge outwards until the budding vesicle membrane undergoes fission and detaches.

The envelope is the site for numerous essential functions like pathogenesis, adherence, nutrient acquisition, signalling, secretion and protection from the surrounding environment (Kulp & Kuehn, 2010b). Disruption of any layer of envelope is lethal to the bacterial cell. Release of OM and periplasm *via* OMVs is one of the evolved mechanisms to protect itself from environmental stress and for better survival.



Nature Reviews | Microbiology

Figure 1. 2 The envelope of Gram-negative bacteria. It consists of two membranes outer membrane and cytoplasmic membrane. In between the two membranes is the periplasmic space which consists of the peptidoglycan (PG) layer and periplasmic proteins. (LPS: Lipopolysaccharide, PG: Peptidoglycan, Lpp: lipoprotein).

1.2.1.2 Biogenesis of OMVs

Bacterial OMVs are extensively studied from past decades. However, there is no definitive mechanism to explain its biogenesis. Broadly, OMVs are originated by expanding and then budding off from the membrane (Anand & Chaudhuri, 2016). The release of OMVs is regulated and controlled at various physiological stages of bacterial cell growth, and there is no evidence so far, showing any Gram-negative bacteria not producing OMVs. Hence, the vesiculation process is most likely to be a conserved process (Kulp & Kuehn, 2010b). Evidences have shown that the release of OMV is completely independent process, it is a result of well-regulated mechanism, as shown by specific packaging of proteins and lipid contents or exclusion of contents from site of OMV release (Schertzer et al., 2012; Schwechheimer et al., 2013; Schwechheimer & Kuehn, 2015). This selectivity towards OMV content of proteins and lipids indicate that it is a systematic process, rather than random event. Furthermore, conditions like temperature, oxidation, nutrient availability, quorum sensing and antibiotics which target envelope can all influence the level of vesiculation. More importantly, careful analysis of bacterial mutants that contains modifications or deletions in genes coding for envelope components has shown that the process of vesiculation is not a consequence of bacterial lysis or disintegration of bacterial envelope, but would form vesicles with proteins and lipids components from all subcellular fractions of the bacteria (McBroom et al., 2006). OMVs may be an adaptive response for bacterial survival for removing undesirable components that are either soluble or insoluble. All these genetic and biochemical studies have led to several models for vesicle production. Although, many mechanisms have been put forth, there is a lack of sufficient evidence supporting these mechanisms. It is possible that there is a well-conserved mechanism for OMVs secretion. However, different types of OMVs are formed by different mechanisms. Different mechanisms proposed can be understood under three basic mechanisms explaining biogenesis of OMVs.

1.2.1.2.1 Loss of connection between the outer membrane and the peptidoglycan (PG) layer

One of the earliest mechanisms proposed for OMVs production is bulging of OM, in areas where proteins that attach the OM to peptidoglycan layer are not present (Fig 1.3 a). Such events are caused by membrane proteins like outer membrane protein A (OmpA) and outer membrane lipoprotein (Lpp). Previous studies have found that mutation or deletion LPP, Tol-Pal and OmpA results in hypervesiculation phenotypes along with cellular leakage as a consequence in membrane instability. However, because *lpp* has OM integrity defects, distinguishing OMV production from cell damage is difficult. This leads us to believe that naturally secreted OMVs are produced by more subtle process that depends on regulated disruption in the crosslinks.

1.2.1.2.2 Vesicle formation due to envelope stress

Often times OMVs are considered as an adaptive response for bacterial survival as they provide an effective mechanism for removal of undesirable soluble and insoluble components. OMV production relieves membrane stress by eliminating misfolded proteins, such as protease impairments, denaturants, or overexpressed toxic proteins, accumulated peptidoglycan fragments and lipopolysaccharides (LPS) from the periplasmic space (Haurat et al., 2011; McBroom & Kuehn, 2007; Schwechheimer et al., 2013). In areas containing accumulated envelope components or misfolded proteins, the crosslinks are either locally depleted or displaced, leading to bulging of the OM and hence increased OMV production (Fig 1.3 b).

1.2.1.2.3 Vesicle formation due to membrane curvature

In another model, alteration in lipid structure and topology due to the molecules that induce curvature, could lead to membrane bulging. For example, in *Pseudomonas* insertion of the quorum-sensing molecule, quinolone signal (PQS) into the outer leaflet of OM can also enhance curvature of the membrane and cause vesiculation, according to bilayer couple model (Mashburn & Whiteley, 2005b; Sciences et al., 2010). Accumulation of the PQS in outer leaflet of OM, promotes expansion of this leaflet compared to inner leaflet and creating tension between them. According to previous studies, this model is limited to gamma-proteobacteria, especially *Pseudomonas* and related species (Horspool & Schertzer, 2018). Notably, in bacteria which normally produce PQS, formation of vesicle can still occur in absence of the PQS producing genes (MacDonald & Kuehna, 2013; Sciences et al., 2010), revealing the redundancy of vesicle

biogenesis pathway in bacteria (Fig 1.3 c). It is expected that, the same bacteria can produce different OMV populations, with different compositions, depending on the pathway followed for OMV biogenesis. Future work is needed to get substantial insight into their different biogenesis mechanisms.

1.2.2 Vesicle cargo composition

Many biochemical analyses of the vesicle cargo have revealed selectivity during export, indicating the bona-fide secretary pathway of vesicle biogenesis. During biogenesis of OMVs different molecules can be incorporated: nucleic acids, proteins, lipids, and metabolites. Various quantitative proteomic and lipidomic studies have demonstrated that, the OMV composition does not mimic the envelope of the mother cell from which it is derived (Nagakubo et al., 2020; Orench-Rivera & Kuehn, 2021; Resch et al., 2016). Proteomic studies have revealed a large number of OM proteins (OMPs; OmpA, OmpF, and OmpC), periplasmic proteins and several virulence factors involved in the adhesion and invasion of the host cell (Jun et al., 2013). Selectivity of proteins in OMVs is greatly affected by protein cellular origin as studied in *H. pylori* and *Serratia marcescens* (McMahon et al., 2012; Olofsson et al., 2010).

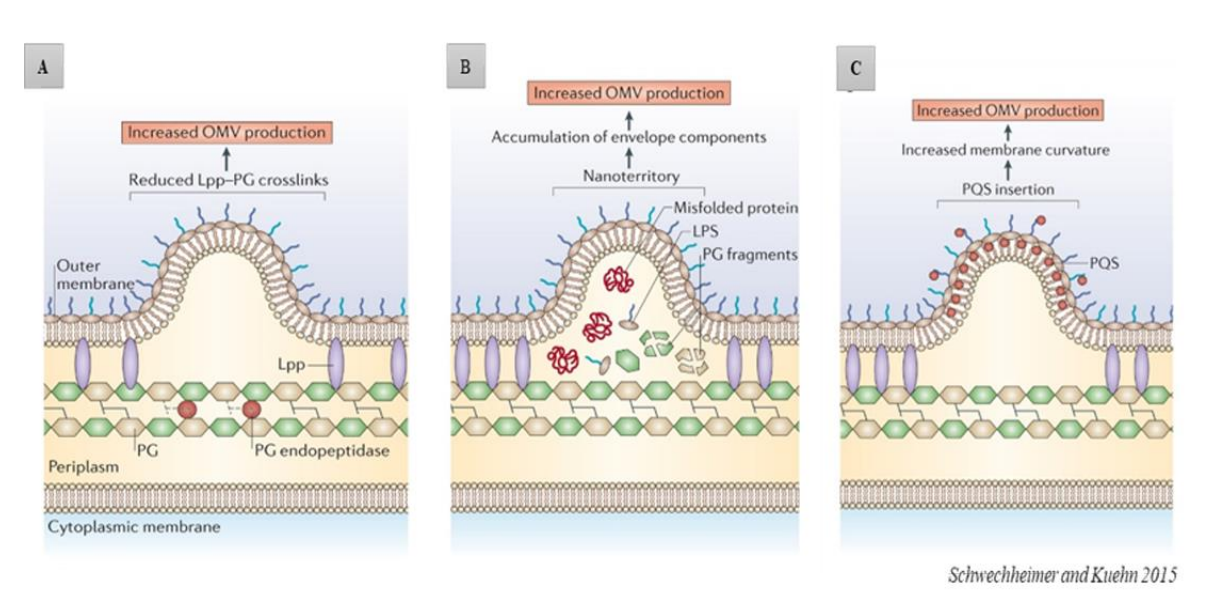


Figure 1. 3 Biogenesis of outer-membrane vesicles (OMVs) is dependent on several factors. (A) Peptidoglycan (PG) endopeptidases and other enzymes that are involved in regulating PG breakdown and synthesis govern the ability of the envelope to form crosslinks between Braun's lipoprotein (Lpp) and PG, hence increasing the OMV production in areas having reduced Lpp-PG crosslinks. (B) In areas where misfolded proteins or envelope components (LPS or PG fragments) accumulate, crosslinks get disturbed promoting bulging of membrane and increased OMV production. (C) Incorporation of Pseudomonas quinolone signal (PQS) into the outer membrane leaflet can lead to curvature formation hence increasing the OMV production.

Lipid is one of the essential structural biomolecules of gram negative OMVs. Though there is a similarity with OM lipid content (Chowdhury & Jagannadham, 2013; Kulkarni & Jagannadham, 2014), there are also reports showing presence of lipids exclusively in OMVs but not in OM (Kato et al., 2002). OMVs of enterotoxigenic *E. coli* contain glycerophospholipids, phosphatidylethanolamine, phosphatidylglycerol, and cardiolipin as major lipids that are associated with the curvature of OMVs during biogenesis (Horstman & Kuehn, 2000). Phosphatidylglycerol and phosphatidylethanolamine were found to be the important lipid components in the OMVs of *P. syringae* (Chowdhury & Jagannadham, 2013). Other studies have also demonstrated presence of phosphatidylglycerols as the major lipid content in OMVs (Tashiro et al., 2011). LPS is also a major component present in OMVs which facilitate adhesive functions during biofilm formation (Kulkarni et al., 2014).

OMVs are also known to carry both surface-associated as well as luminal nucleic acid. Presence of DNA, RNA, various plasmids and DNA of phage along with chromosomal DNA has been shown. Although how these molecules are selected is not known. The specific mechanism by which different types of cargo are selectively packaged in vesicles remain an area of active study. It is widely observed that the vesicles characterized to date likely consists of mixture of populations of vesicles with distinct composition.

1.2.3 Function of OMVs

As OMVs contain a variety of molecules, they play key role in biology of bacteria. Its secretion is one of the important mechanisms behind effects of many pathogenic, probiotic and symbiont bacteria. OMVs secretion aids bacteria in inter- and intraspecies communication, facilitating its interaction with host. Out of their diverse roles in pathological and physiological functions, OMVs are recognised for their function in antibiotic resistance, gene transfer, acquisition of nutrients, delivery of toxins, stress response, quorum sensing (Mashburn & Whiteley, 2005b), adhesion and delivery of virulence factor to evade host defence system.

1.2.3.1 Role of OMVs in lateral gene transfer

Horizontal gene transfer (HGT) is one of the major mechanism of gene transfer within the microorganisms (Bedhomme et al., 2019). HGT paves a way for bacterial evolution, facilitating bacterial adaptation, survival towards harshest environments (Bello-López et al., 2019; Davies, 1996; Emamalipour et al., 2020). There are three widely described mechanism of HGT for interchanging of genetic material between bacteria: transformation, conjugation and

transduction (Ely, 2020; Hall et al., 2020; Redondo-Salvo et al., 2020). In transformation, when bacterial cells are physiologically competent, they naturally uptake DNA from extracellular environment, and this process is facilitated by 20-50 proteins (Riva et al., 2020; Salvadori et al., 2019). Conjugation requires cell-to-cell contact for DNA transfer which occurs through the sexual pilus (Headd & Bradford, 2020). Transduction is a process of DNA transfer between bacteria through the bacteriophage infections, and it is host specific (Fillol-Salom et al., 2019). Recent findings have shown that OMVs facilitate horizontal gene transfer (Dell'annunziata et al., 2020; Domingues & Nielsen, 2017; Fulsundar et al., 2014; Tran & Boedicker, 2017).

Role of OMVs in HGT is established in *E. coli, Acinetobacter baumannii, Acinetobacter baylyi, , P. aeruginosa, Porphyromonas gingivalis and Thermus thermophilus* (Blesa & Berenguer, 2015; S. Chatterjee et al., 2017; Kolling et al., 1999). Vesicle release by *N. gonor-rhoeae* and *H. influenzae* can export DNA from mother bacterial strain to recipient cells. Studies have reported that vesicles released by *H. influenzae* and *N. gonorrhoeae* and can carry DNA from the producing strain and transfer it to recipient bacterial cells (David W Dorward et al., 1989; Kahn et al., 1983). Study on OMVs from *E. coli* shows presence of lumen associated virulent genes, and their transfer between bacteria of different species (Yaron et al., 2000). Rumbo and his associates have demonstrated that OMVs originated from *A. baumannii* act as vehicles for antibiotic resistance gene transfer. They showed presence of plasmid-borne *blaOXA*-24 gene in OMVs and they have bestowed carbapenems resistance to sensitive *Acinetobacter* strains (Rumbo et al., 2011). These evidences highlighted the role of OMVs in horizontal mobility and demonstrated the potential of OMVs in spreading antibiotic resistance and virulence.

1.3 Replication competent circular DNA

Over the last few years, several novel viral and phage genomes have been isolated from different mammalian tissues (Botsios & Manuelidis, 2016; Fernandez-Cassi et al., 2018; Whitley et al., 2014). These unusual discoveries have led to the proposition of new concept on pathogenesis of brain and other diseases like diabetes, atherosclerosis, colon, breast and prostate cancer (Bund et al., 2021; Manuelidis, 2011; zur Hausen et al., 2019). Brain diseases include all CNS disease such as Multiple Sclerosis (MS), amyotrophic lateral sclerosis, transmissible spongiform encephalopathies (TSE) / Prion - linked diseases, Alzheimer disease and Parkinson's (Oxley Jimmie, Smith James, Busby Taylor, 2022). According to this hypothesis, replication-competent circular DNA molecules and viruses are involved in generation of all these diseases. This concept is based on facts from several studies showing presence of replication-

competent circular DNA isolates, resembling to plasmid and phage genomes in various mammalian tissues and body fluids. In 2011, nuclease resistant, plasmid related sequences of circular DNA with the size 2.4 and 1.8 kb, were copurified along with other TSE infectious particles, from scrapie and CJD infected brain samples. SPHINX, an acronym for Slow Progressive Hidden INfections of Variable (X) Latency, was given to these infectious particles (Manuelidis, 2011).

Subsequently, in 2014, a study from Germany, reported SPHINX related circular DNAs molecules linked to Transmissible Spongiform Encephalopathy (TSE) particles isolated from Multiple sclerosis-affected human brain tissue, and Healthy Cattle Serum and Milk (Whitley et al., 2014). Eleven isolates shared nucleotide sequence similarity (ranging from 79% to 98%) with TSE isolates (Sphinx 1.76), among them two isolates were from cattle serum, HCBI6.159 (4 isolates from milk, CMI1.252 (CMI, cow milk isolate) and HCBI6.252 (HCBI, healthy cattle blood isolate) and CMI2.214, CMI3.168, and CMI4.158; and 2 isolates from brain tissue of human suffering from Multiple sclerosis, MSBI1.176 (MSBI, multiple sclerosis brain isolate) and MSBI2.176. In another report, same group has shown the presence of three replicationcompetent single-stranded DNA molecules sharing nucleotide similarity to sphinx 2.36 (Funk et al., 2014). HCBI1.225 and HCBI2.170 shares 81% and 75% nucleotide similarity to Sphinx 2.36. In same study, blood samples collected from healthy cattle and serum samples from patients with multiple sclerosis, they have shown the isolation of the genome sequences of three novel viruses which are related to Gemycircularvirus (Lamberto et al., 2014). One of the isolates MSSI1.162 from a multiple sclerosis patient serum sample had a nucleotide sequence that was distantly related to a *Psychrobacter* species plasmid. *Psychrobacter* is an opportunistic human pathogen (Gunst et al., 2014). This group has further expanded their study with more samples from cow milk and its product and have reported isolation of more 101 ssDNA isolates (97 as bovine meat and milk factors group 2 – BMMF2, and more 4 as BMMF1) (de Villiers et al., 2019). Very recently, such ssDNA is also found in milk of the domesticated Asian water buffalo, which belongs to the Bovinae subfamily (König et al., 2021).

With the discovery of various novel small circular single-stranded DNAs (probably of viral origin) from various bovine source samples, BMMF (bovine meat and milk factors) term was coined, and these were proposed to represent a particular class of infectious agents (zur Hausen et al., 2019). These circular single-stranded DNA molecules, ranging in size from 1084 and 2958 nucleotides were isolated, were isolated by performing in vitro replication strategies (Funk et al.,

2014; Gunst et al., 2014; Lamberto et al., 2014; Whitley et al., 2014). Based on their sequence homologies, the isolated BMMFs are divided into four groups BMMF1 through BMMF4 (Fig 1.4). BMMF1 and BMMF2 consists of isolates having similarities with the isolates of Sphinx 1.76 and Sphinx 2.36 respectively. BMMF3 group includes isolates which have been characterised as novel gemycircularviruses, belonging to the family Genomoviridae. Whereas the BMMF4 group contains single isolate resembling plasmid of *Psychrobacter* species. The terms CMI (cow milk isolate) and HCBI (healthy cattle blood isolate) are used to indicate their origin (zur Hausen et al., 2017). The common characteristic feature of all isolates is having of iteron-like tandem repeats and inverted repeats and presence of minimum one large open reading frame which codes for Rep protein. Few isolates also code for putative second ORF which is similar to a mobilization element (de Villiers et al., 2019).

In the context of diseases, these ssDNA sequences of BMMFs and sphinx have come into light due to their connection with breast cancer, colorectal cancer, and with neurodegenerative disorder Multiple Sclerosis (Zur Hausen, 2015). Compared to Asia, the detection of BMMF is known to be associated with higher incidence of breast and colorectal cancer in North America and Western Europe. BMMF ssDNA and Rep proteins have been reported in tissue of colon cancer patients and can result in chronic inflammation (Bund et al., 2021), and hence supporting the hypothesis of cancer induction to consuming meat and milk products from these animals. And these isolates are currently being taxonomically kept between bacterial plasmids and singlestranded DNA (ssDNA) viruses. This new class of microbial species, called as BMMFs isolates are consumed by human on regular day to day life, particularly from bovine milk, dairy products and serum, are presumably species - specific risk for cancer as well as multiple sclerosis (Zur Hausen, 2015; Zur Hausen & De Villiers, 2015). Up take of cow milk and other dairy products has also been linked to an increased risk of developing MS (Pantazou et al., 2015). These isolates of BMMFs and related MSBIs were further analysed for their ability to express and replicate in human cells (HEK293TT line). When the BMMFs designated as CMI3.168, CMI1.252, MSBI1.176 and MSBI2.176 were transfected into the cell lines (HEK293TT), all of them have transcribed and replicated in HEK293TT cells (Eilebrecht et al., 2018).

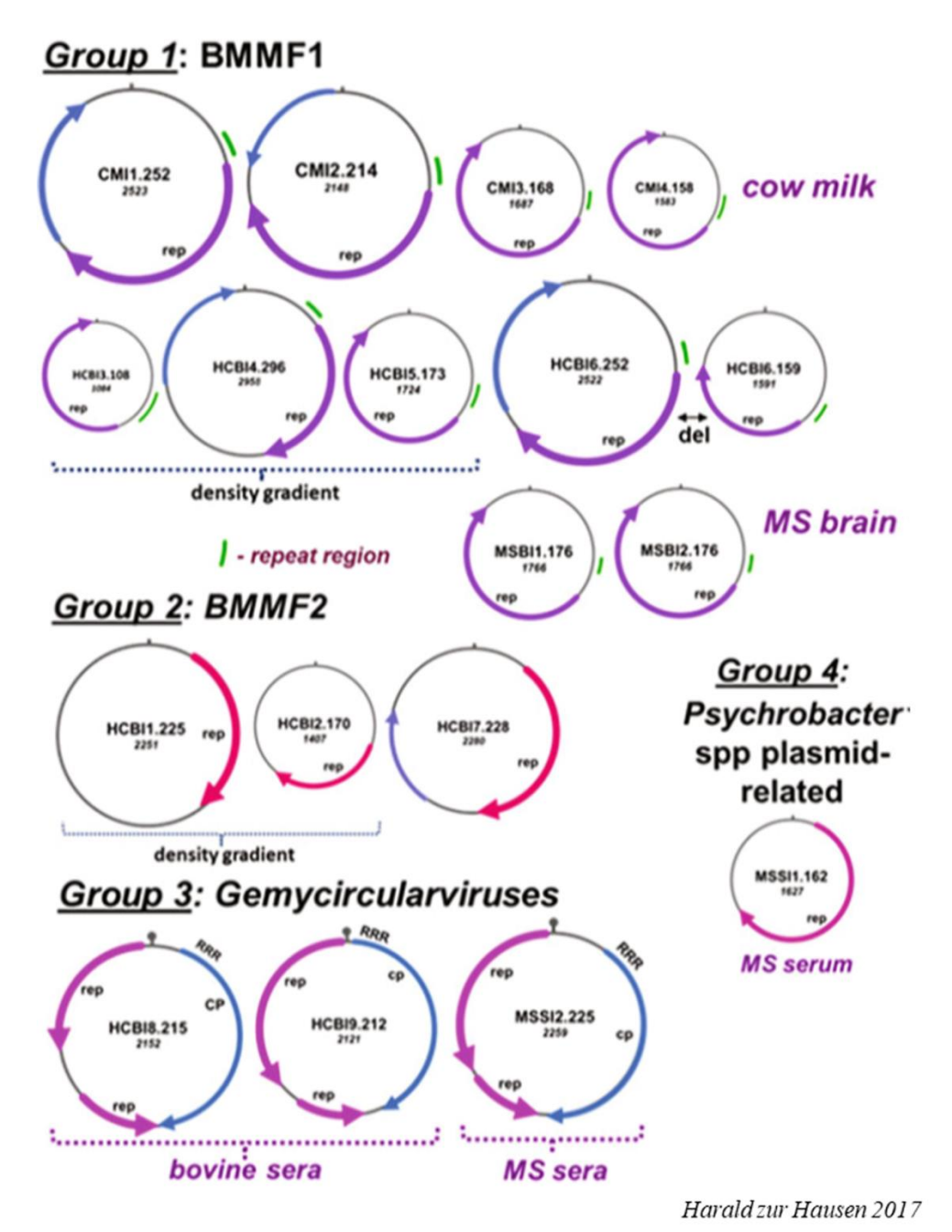


Figure 1. 4 Circular single-stranded DNA isolates from sources are grouped based on replication initiation proteins

In a study from our lab we have characterized bacteriophage AbDs1 of *Acinetobacter baumannii* DS002 (Longkumer et al., 2013). The genome of AbDs1 phage shows 67% sequence similarity to Sphinx 2.36 and 70 % to one of the group-2 BMMFs. Such high sequence similarity between phage AbDs1 genome and Sphinx and BMMF sequences points towards existence of a common origin. Further, the phylogenetic tree constructed by including all BMMF isolates and phage AbDs1 indicated formation of clades with AbDs1 and BMMFs (Fig 1.5).

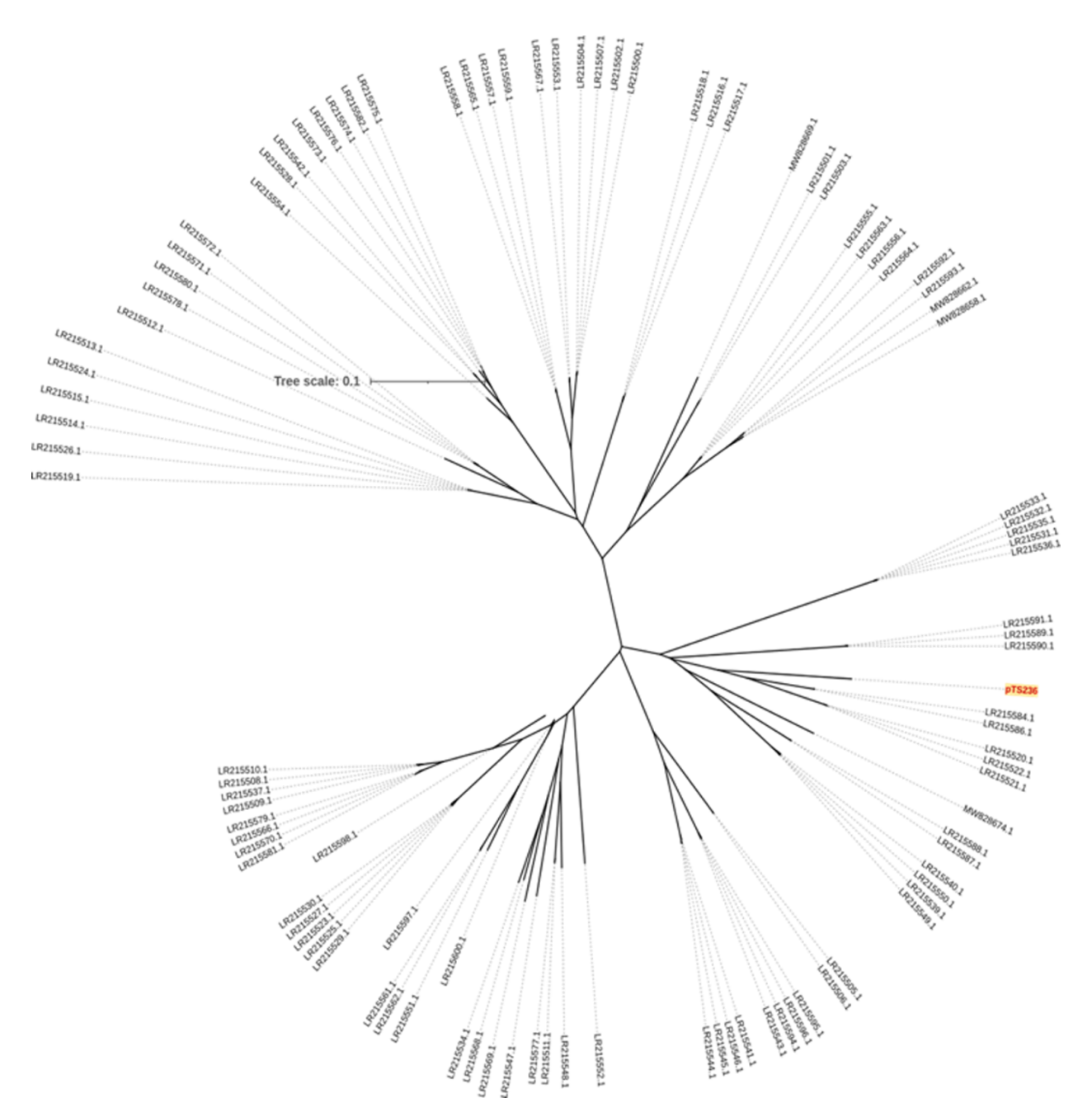


Figure 1. 5 Unrooted tree of BMMF isolates: The genome of AbDs1 phage isolated from *A. baumannii* DS002 is shown with red colour font.

Outer Membrane Vesicles (OMVs), as previously described, have a versatile role in the horizontal mobility of DNA. Their role in the interkingdom communications is also well established (Mashburn & Whiteley, 2005a). Additionally, OMVs have been also shown to reach bloodstream where they can reach various tissues and possibly including the brain (Stentz et al., 2018). The blood-brain barrier (BBB) regulates brain access *via* the bloodstream. The BBB is made up of brain microvascular endothelial cells that line brain capillaries in the brain and known regulate molecular and cellular trafficking between the neuronal tissue and bloodstream. The maintenance of this barrier is important for preventing potentially neurotoxic plasma

components, blood cells, and pathogens from entering the brain (Lippmann et al., 2014; Zhao et al., 2015). However, the OMVs cross BBB and deliver macromolecules like rRNA and rDNA (Emery et al., 2017; Zhan et al., 2016).

1.4 Hypothesis

The phage AbDs1 shows sequence similarity to Sphinx and BMMF sequences. Such extensive sequence similarities between these two circular DNA molecules indicate existence of common origin. Since OMVs have proven role in horizontal gene transfer and ability to cross blood brain barrier, the phage AbDs1 genome possibly reach mammalian tissue probably by associating with OMVs of *A. baumannii* DS002.

1.5 Objectives of the present study

The following objectives were framed based on the above hypothesis:

- Purification and characterization of Outer Membrane Vesicles (OMVs) from A. baumannii DS002.
- 2. Proteomics of OMVs and elucidation of functions of certain proteins enriched in OMVs.
- 3. Genomic of OMVs and establishing their role in inter- and intradomain horizontal gene transfer.

Chapter 2: General Material and Methods

Table 2. 1 Antibiotics

Name of the Antibiotic	Name of the supplier
Chloramphenicol	HIMEDIA
Streptomycin	HIMEDIA
Kanamycin Sulphate	HIMEDIA
Ampicillin sodium salt	HIMEDIA
Tetracycline hydrochloride	HIMEDIA

Table 2. 2 Chemicals

Name of the Chemical	Name of the Supplier
Absolute alcohol	SRL
Acetic Acid (Glacial)	SRL
Acetone	SRL
Acetonitrile	SRL
Acrylamide	Sigma-Aldrich
Agar	HIMEDIA
Agarose	SeaKem
Ammonium persulphate	GE Healthcare Lifesciences
Bovine serum albumin	HIMEDIA
β-Mercaptoethanol	Sigma-Aldrich
Bromophenol blue	SRL
Butanol	SRL
Calcium chloride	SRL
Calcium nitrate	SRL
Chloroform	SRL
Coomassie Brilliant Blue G-250	HIMEDIA
Coomassie Brilliant Blue R-250	HIMEDIA
Cobalt chloride	SRL
Dimethyl sulfoxide (DMSO)	Sigma-Aldrich
Ethylenediaminetetraacetic acid (EDTA)	SRL

Ethidium bromide	HIMEDIA
Ferrous sulphate	Sigma-Aldrich
Glucose	HIMEDIA
Glycerol	SRL
Glycine	SRL
Hydrochloric acid	SRL
L-Arginine	SRL
Iso-amyl alcohol	Fischer Scientific
Iso-propyl alcohol	Fischer Scientific
Isopropyl-ß-D-thiogalactopyranoside (IPTG)	G-biosciences
Lithium Chloride	SRL
Magnesium sulphate	SRL
Magnesium chloride	SRL
Manganese sulphate	SRL
Methanol	SRL
Nickle Chloride	SRL
N, N'-Methylene bis acrylamide	GE Healthcare Lifesciences
Potassium hydroxide	SRL
Potassium dihydrogen ortho phosphate	Merck
PMSF	GE Healthcare Life sciences
Protease inhibitor cocktail	Sigma-Aldrich
Skimmed milk powder	HIMEDIA
Sodium acetate	HIMEDIA
Sodium carbonate	HIMEDIA
Sodium citrate	SRL
Sodium chloride	SRL
Sodium dodecyl sulphate	SRL
Sodium hydrogen orthophosphate	SRL
Sodium hydroxide	SRL
Sucrose	SRL
RNase A	Thermo Fisher Scientific
Tetra ethyl methylene diamine (TEMED)	Sigma-Aldrich

Tris-base	SRL
Triton X-100	Sigma-Aldrich
Tryptone	HIMEDIA
Tween 20	AMRESCO
X-gal	SRL
Yeast extract	HIMEDIA

Table 2. 3 Restriction enzymes and DNA modifying enzymes

Name of the Enzyme	Name of the Supplier
BamHI	Thermo Fisher Scientific
BgIII	Thermo Fisher Scientific
EcoRI	Thermo Fisher Scientific
HindIII	Thermo Fisher Scientific
Ndel	Thermo Fisher Scientific
Notl	Thermo Fisher Scientific
Pstl	Thermo Fisher Scientific
Sall	Thermo Fisher Scientific
Smal	Thermo Fisher Scientific
Xhol	Thermo Fisher Scientific
Alkaline Phosphatase	Thermo Fisher Scientific
T4 DNA Ligase	Thermo Fisher Scientific
Pfu DNA polymerase	Thermo Fisher Scientific
Phusion® High-Fidelity DNA polymerase	New England Biolabs
Polynucleotide kinase	Thermo Fisher Scientific
T1 RNase	Thermo Fisher Scientific

Taq DNA polymerase	Thermo Fisher Scientific
T4 RNA polymerase	Thermo Fisher Scientific
Calf Intestinal Phosphatase	Thermo Fisher Scientific
Emerald Amp Max PCR master mix	Takara Bio
DNase-I	Thermo Fisher Scientific
RNase A	Thermo Fisher Scientific
1kb DNA Ladder	Thermo Fisher Scientific
20bp DNA ladder	Takara Bio
Unstained Protein Ladder, 10-200kDa	Thermo Fisher Scientific

2.1 Growth Media

E. coli and A. baumannii were cultured either on Luria-Bertani or on minimal medium. All prepared media were autoclaved at 15 psi for 20 min and trace element solutions by filtration through a sterile 0.2 μ filter membrane. While preparing solid media, 2 g of agar was added to 100 ml of broth and sterilized by autoclaving. Whenever required antibiotics Chloramphenicol (30 μ g/ml), Streptomycin (20 μ g/ml), ampicillin (100 μ g/ml), kanamycin (30 μ g/ml), and tetracycline (30 μ g/ml) were supplemented to the growth medium.

2.1.1 Luria-Bertani (LB) medium

LB media was prepared by dissolving peptone (10 g), yeast extract (5 g) and NaCl (10 g) in 800 ml of deionised H_2O , mixed thoroughly before adjusting the pH to 7.0 with 2 N NaOH. Later, water was added to the solution to prepare 1000 ml and sterilized as described above.

2.1.2 Minimal Salts Medium

Minimal salts medium was prepared by using the following composition which contained NH₄NO₃ (1 g), KH₂PO₄ (1.20 g), K₂HPO₄ (4.80 g) in 1000 ml of double distilled water (ddH₂O). The prepared solution was autoclaved and the complete minimal media was prepared by adding 2 ml of MgSO₄.7H₂O, 50 μ l of Fe2(SO4)3 and 100 μ l of CaNO₃.4H₂O from respective 1 M stock solutions. The prepared medium contains 0.4 mM of MgSO₄.7H₂O, 1.8 μ M of Fe₂(SO₄)₃ and 0.08 mM of CaNO₃.4H₂O. When required succinate, benzoate or lactate solution stocks were passed

through $0.2\mu m$ filter membrane and supplemented to the minimal salt's medium at a concentration of 5 mM.

2.2 Preparation of iron free media and solutions

Chelex 100 Chelating Resin (200–400 mesh, Bio-Rad) was used to make iron free minimal media and other solutions by following the manufacturers protocol. Briefly, to make 100 ml media iron free 5 g of resin was used. In order to make slurry, 5 g of resin was dissolved in 0.5 M sodium acetate buffer (pH 5.0). It was slowly poured into the column and once the resin bed is formed 4 bed volume of sodium acetate buffer was passed through it. Initially 5 to10 ml of milli-Q water was passed through resin and discarded into waste followed by passing 100 ml minimal media salt solution and collecting in iron free glassware. It was made sterile by autoclaving. Other trace elements were prepared in iron free milli-Q water prepared in similar manner followed by sterilization using syringe filter.

2.2.1 Preparation of high iron solution

Working concentration of 10 μ g Fe/ml was used for iron sufficient condition. To prepare the stock solution (10 mg/ml) of ferrous sulphate 0.1 g of FeSO₄.7H₂O was dissolved in 10 ml of iron free Milli-Q water. The stock solution was filter sterilised, and 10 μ l of it was mixed with 10 ml of culture medium to achieve 10 g Iron per ml.

2.2.2 Preparation of low iron solution

The iron limiting condition (0.02 μg Fe/ml) was prepared as follows. Stock solution of 2 ug/ml was prepared by adding 20 μl of 10 mg/ml primary stock solution to 20 ml of iron free Milli-Q H₂O. The secondary stock was filter sterilized and 100 μl of it was added to 10 ml of culture medium to give achieve 0.02 μg Iron per ml.

2.3 Preparation of iron free glassware

The glassware was soaked in 2% methanolic KOH for 24 h and rinsed thoroughly with H_2O and further soaked in 6N HCl for 24 h. Later, the glassware was thoroughly washed with deionised H_2O , left for drying till smell of HCl disappeared completely and autoclaved at 15 psi for 20 min.

2.4 Antibiotic & Chemical stock solutions

The stock solution for all the antibiotics were prepared in the respective solvent as mentioned in the following table. Stock solutions were made sterile by passing through 0.22 syringe filter, made into aliquots of 1 ml and stored at -20°C.

Table 2. 4 Preparation of Antibiotics

S. No.	Antibiotic	Solvent used to dissolve	Stock	Working
			concentration	conc.
1	chloramphenicol	70% ethanol	30 mg/ml	30 μg/μΙ
2	Streptomycin	Sterile milli-Q H2O	20 mg/ml	30 μg/μl
3	Ampicillin	Sterile milli-Q H2O	100 mg/ml	100 μg/ml
4	Kanamycin	Sterile milli-Q H2O	10 mg/ml	10 μg/μΙ
5	Tetracycline	70% ethanol	30 mg/ml	30 μg/μΙ

2.4.1 Isopropyl β-D-1-thiogalactopyranoside (IPTG)

One molar solution of IPTG (Isopropyl β -D-1-thiogalactopyranoside) (238 mg/ml of H2O) was made by mixing IPTG in 1ml of Milli-Q water and 100 μ l aliquots were made and stored at - 20°C.

2.4.2 5-bromo-4-chloro-indolyl-β-D-galactopyranoside (X-Gal)

X-gal stock solution (4% w/v) was made with 40 mg in 1ml of N, N'-di-methyl-formamide, stored at -20°C until use and was added to the medium to attain a working concentration of 0.004%.

2.5 Solution and buffers for DNA manipulation and analysis:

2.5.1 TAE (Tris-Acetate-EDTA) buffer

TAE buffer (50X) was prepared by adding 242 g of tris base, 100 ml of 0.5 M EDTA (pH 8.0) and 57.1 ml of glacial acetic acid. Finally, the volume was adjusted to 1000 ml with water. The working concentration of buffer (1X) was prepared by diluting the 50X TAE with water.

2.5.2 6X Gel loading buffer

DNA 6X loading dye was prepared by adding 12.5 mg of bromophenol blue, 12.5 mg of xylene cynol FF and 7.5 g of Ficoll (Type 400; Pharmacia) in 75 ml of ddH_2O and the volume was finally increased to 100 ml and kept at room temperature.

2.5.3 Ethidium bromide

The stock solution of ethidium bromide (1 mg/ml) was made by dissolving 10 mg of EtBr in 10 ml of ddH₂O, in an amber glass bottle and stored at room temperature. While preparing

agarose gel 5 μ l of the stock solution was added to 100 ml of gel solution to achieve a final concentration of 0.05 μ g/ml.

2.6 Agarose gel electrophoresis

Agarose gel electrophoresis was performed for resolving DNA fragments ranging in size from 50 bp to 25 kb. Gels of 0.8-2 % were prepared in 1X TAE buffer for resolution of DNA fragments. To prepare the gel appropriate amount of agarose was weighed and mixed to 100 ml of 1X TAE buffer, boiled until it was dissolved completely. Once this molten agarose was cooled to approximately 45°C, 0.5 µg/ml of EtBr was added to it and poured into the casting tray for it to solidify. Electrophoresis was performed after placing the gel in the tank with 1X tank-buffer keeping the wells towards the anode side. Samples were mixed with the required volume of 6X loading dye before being loaded into the wells alongside the DNA ladder in the adjacent well. Electrophoresis was performed by applying constant voltage (100 V) for 15 to 20 min. The migration of DNA was visualised under UVTech gel imaging system. The size of unknown DNA samples was determined by comparing its migration with DNA ladder loaded.

2.7 Plasmid isolation by Alkaline Lysis method

2.7.1 Solutions for plasmid isolation

2.7.1.1 Solution I (TEGL solution)

The solution I was prepared by mixing 10ml of glucose (250 mM), 6.25 ml of Tris (0.2 M pH 8.0),1ml of EDTA (0.5 M) was added to little amount of sterile ddH₂O and a solution of 50 ml volume was prepared with ddH₂O. The solution was autoclaved and stored at 4° C. When required stock solution of DNase free RNase A was mixed to it to achieve final concentration of 100 µg/ml.

2.7.1.2 Solution II

The solution II was prepared by mixing equal volumes of 0.4 N NaOH and 2% SDS solution.

2.7.1.3 Solution III (3M sodium acetate pH 4.8)

The solution III was made by adding 24.61 g of CH3COONa in 80 ml of sterile ddH2O followed by adjusting the pH 4.8. the volume was increased to 100 ml and stored at 4°C until further use.

2.7.1.4 Phenol chloroform solution (1:1)

Phenol chloroform was made by mixing equal volumes of water saturated phenol and chloroform. The required volume of above solution was always prepared freshly.

2.7.1.5 Chloroform Isoamyl alcohol solution (24:1)

About 96ml and 4ml of Chloroform and isoamyl alcohol were mixed and stored in amber coloured bottle.

2.7.1.6 TE buffer

About 100 ml of working solution of TE buffer was prepared by adding 5 ml of 0.2 M Tris-HCl, 0.2 ml of 0.5 M EDTA to 94.8 ml of deionised H_2O . The TE buffer was autoclaved to make it sterile.

2.7.2 Procedure for Isolation of plasmid DNA

Single colony of bacteria carrying desired plasmid was inoculated into 3 ml LB media containing appropriate antibiotic to maintain the plasmid, and was incubated for 12 h at 37°C under shaking. 1 ml of bacterial cells were taken and centrifuged at 13,000 rpm (1 min). The pellet was thoroughly resuspended in 100 μ l of TEGL solution by vertexing it vigorously. To this 200 μ l of freshly mixed lysis solution was added and incubated on ice for 4 to 5 min before adding 150 μ l of ice-cold solution-III (neutralizing solution). To complete the neutralisation process, the contents were thoroughly mixed by inverting the tubes end-to-end. The tubes were placed on ice for 3 to 5 min, centrifuged (13,000 rpm for 10 min) and the supernatant having the plasmid DNA was carefully collected into a new Eppendorf tube and is subjected to the following extractions: phenol - chloroform (1:1) and chloroform - iso-amyl alcohol (24:1) to remove proteins. The plasmid DNA was further precipitated by addition of 1/10th volume 3 M CH₃COONa (pH 3.8) and two volumes ice cold absolute alcohol by incubating the tubes at -20°C for 20 to 30 min. Centrifugation at 13000 rpm for 25 minutes at 4°C was used to collect the precipitated plasmid. The pellet obtained was washed with ice cold 70% ethanol, air dried and the obtained plasmid DNA was resuspended in 30 -50 μ l of TE buffer.

2.8 DNA Quantification

Nucleic acid concentration was determined spectrophotometrically by following the Beer-Lambert's law using Nano Drop ND-1000 system (Thermo Scientific). The absorbance was measured at 260 and 280nm by placing 1 μ l of DNA sample on the sample pedestal. The absorbance at 260 nm gives the DNA concentration while the ratio of 260/280 absorbance measurements indicate protein contamination. If the ratio is 1.8 the sample was considered pure and the DNA was used for further manipulation. Additionally, absorbance ratios at 260/230 with values between 1.8 to 2.2 indicate nucleic acid samples are without contamination.

2.9 Polymerase Chain Reaction (PCR)

PCR reactions of 50 μ l were carried out to amplify genes from genomic or plasmid DNA. The PCR reaction mixture contains 1X buffer, 2.5 mM MgCl₂, equimolar concentration of all dNTPs (0.2 mM dNTP: dATP, dCTP, dGTP and dTTP), primers (0.2 μ M), 1 unit of either Taq DNA polymerase or Phusion DNA polymerase, and 10-15 ng plasmid or genomic DNA as template. The PCR programme was tailored according to the amplicon size and annealing temperature of the primers. Amplicons were examined on an 0.8-1.0 percentage agarose gel.

2.10 Colony PCR

About 10 μ l PCR reactions were performed using EmeraldAmp® GT PCR Master Mix for identifying recombinant plasmids in colonies of bacteria. The colony of interest were independently dissolved in 20 μ l of sterile ddH₂O and boiled at 100°C for 5 min and 1 μ l of supernatant served as template for PCR. The PCR was performed on Bio-Rad thermal cycler with parameters set depending on the amplicon size and melting temperature (Tm) of the primers. The samples were examined on a 0.8 % agarose gel

Table 2. 5 PCR cycling conditions

Cycling Step	Temperature	Time	No. of cycles
Initial denaturation	94-98°C	3 min	1
Denaturation	94-98°C	15-30 seconds	
Annealing	55-65°C	30 seconds	3
Extension	94°C	30sec (1Kb per minute)	
Final extension	94°C	5-10 min	1

2.11 Molecular Cloning

2.11.1 Restriction Digestion of DNA

Standard restriction digestion was performed in 20-30 μ l of reaction mix consisting of digestion buffer, minimum 500 ng of vector or insert DNA to be digested and 1 unit of restriction enzyme per 1 μ g of DNA. Depending on the type of enzyme used, the reaction mixture was incubated at 37°C. The digestion reaction was stopped by thermal inactivation as per manufacturer's instructions.

2.11.2 Dephosphorylation of vector

Prior to ligation dephosphorylation of digested vector DNA was performed using alkaline phosphatase to remove the possibility of self-ligation. The reaction was carried out in a 20 μ l reaction mix having 1 μ g of vector and buffer (1X) supplied by the manufacturing company. To

above mixture 1 unit of alkaline phosphatase was added and was incubated at 37°C followed by heat inactivation according to manufacturer's instruction.

2.11.3 DNA Ligation

The vector already digested and insert DNA were ligated using T4 DNA ligase. The ligation reaction was carried out in 20 μ l reaction mix containing 1X ligase buffer, 100 ng of vector DNA, and insert DNA taken in a molar ratio of 1:3 and rest volume was made up using sterile MQ water. The reaction was incubated to 22°C (1 h) or at 4°C (12 h). The ligase enzyme was heat inactivated prior to transformation at 65°C for 20 min. The following equation was used to calculate vector insert ratio.

$$Plasmid\ (ng) \times \frac{Insert\#}{Plasmid\#} \times \frac{Insert\ length\ (bp)}{Plasmid\ size\ (bp)} = Insert\ needed(ng)$$

2.12 Gene transfer methods

2.12.1 Preparation of Competent cells

All the steps were performed inside laminar air flow, by maintaining proper sterile conditions. A single colony of *E. coli* DH5 α cell was taken from a freshly prepared LB plate and inoculated into a 10 ml LB media. The flask was incubated at 37°C with vigorous shaking at 180 rpm for 10 to16 h. This culture (1%) was added inoculum to grow cells in 250 ml of LB broth and incubated at 37°C with moderate agitation. The cells were grown till the OD of the reached to mid-log phase (0.4 to 0.5 OD₆₀₀). The cells were harvested by centrifuging the culture at 6000 rpm for 10 minutes at 4°C and the bacterial pellet obtained was suspended in 75 ml of pre-cooled solution of MgCl₂ (80 mM) and CaCl2 (20mM) by slowly swirling the tube on Ice. The above suspension was incubated on ice (30 min) and the cells were subsequently collected by centrifuging the culture at 6000 rpm for 10 minutes at 4°C. Finally, the pellet obtained was suspended in 10 ml of ice cold 100 mM CaCl₂ and 2ml of DMSO and incubated on ice (10 min). Immediately after incubation, these were distributed into sterile Eppendorf tubes in 100 μ l aliquots before snap frosting the cells by placing the tubes in liquid nitrogen. These cells were then stored at -80°C until further use (Sambrook & Russell David, 1989).

2.12.2 Bacterial transformation

All the steps were performed by maintaining sterile condition, whenever required laminar air flow was used. The frozen competent cells were taken out from -80°C storage, and directly placed over ice for thawing. Once thawed 10 to 20 μ l of ligation mixture or 30 to 50 ng of plasmid was mixed to competent cells and kept on ice for 30 minutes. Following incubation, cells were given heat shock at 42°C for 90 seconds and immediately kept back on ice for 2 min. To that, 1ml fresh LB broth was added and incubated at 37°C for 1 h under constant shaking. Cells were harvested at 6000 rpm for 5 min, were resuspended in 100 μ l of LB broth followed by plating them on to LB agar plates having appropriate antibiotics. The plates were kept at 37°C incubator, for 12 to 16 h to get the transformants.

2.12.3 Conjugation

Conjugation was performed using bi-parental method of conjugation (Figurski & Helinski, 1979). Before starting conjugation, the plasmid of interest was transformed to *E. coli* S17-1 and used as donor strain and the *Acinetobacter baumannii* DS002 served as recipient. Fresh overnight cultures of both donor and recipient strains were inoculated into 10 ml LB broth with suitable antibiotic and allowed to grow till mid-log phase (OD₆₀₀ 0.5) at 37°C and 30°C respectively. The cells were harvested at 6000 rpm at 4°C, and washed three times with 0.9% NaCl. The bacterial cell pellet was suspended in minimum volume of 0.9% NaCl such that the number of bacterial cells remain equal in both donor and recipient suspension vial. Mating mixture was prepared by mixing donor and recipient in 1:3 and 1:5 ratio and spotted on non-selective LB agar plates. The spots were allowed to air dry followed by incubation for 6 to 8 h at 30°C. The cell mass formed after incubation on plates were scraped and suspended in 1 ml of 0.9% NaCl. Serial dilution was made from above suspension and individually plated on LB agar plates having suitable antibiotic which only facilitate growth of exconjugants. The donor and recipient cells were treated in similar way and used as controls. The plates after spreading the cells were incubated at 30°C for 24 to 48 h to observe the growth of exconjugants.

2.12.4 Electroporation

Transformation of *A. baumannii* DS002 was achieved by electroporation. The competent cells were prepared by inoculating a single colony of *A. baumannii* DS002 was from solid LB agar

plate into 3 ml LB media, supplemented with 30 μ g/ μ l chloramphenicol and 20 μ g/ μ l streptomycin. The cells were grown overnight at 30°C and used it as inoculum (1%) to prepare 50 ml culture. The cells were grown till the OD (A₆₀₀₎ of the culture is reached to 0.8. The bacterial growth was interrupted by keeping the culture on ice (10 min) and the cells were collected by centrifuging it at 6000 rpm for 10 min at 4°C. Cells were twice washed with cold 10 % glycerol and resuspended in 500 μ l of 10% glycerol. Cell suspension (50 μ l) was taken in an Eppendorf tube and mixed with appropriate amount of DNA (2 to 5 μ g) before transferring the mixture to a 2 mm electroporation cuvette, followed by pulsing (voltage of 2.5 kV cm⁻¹, capacitance of 25 μ F, resistance of 200 Ω). Immediately 4 ml fresh LB was added to the cells and incubated at 30°C for minimum 2 h to facilitate recovery. The cells were spun down after incubation and the pellet obtained was suspended in 100 μ l of LB and spread with beads on to LB agar plate with suitable antibiotics and left at 30°C for 12 to 24h to facilitate the growth of transformants.

2.13 Polyacrylamide gel electrophoresis

Standard procedure for SDS-Polyacrylamide gel electrophoresis was used to separate the protein samples (Laemmli, 1970). MINI PROTEAN II Bio-Rad system was used to caste gels and to run SDS-PAGE. Clean spacer plate and thin plate were arranged into the casting stand. Initially, resolving gel of appropriate percentage was prepared and poured in space between both plates by leaving for stacking gel. Immediately, water saturated n-butanol was layered above the resolving gel solution to remove bubbles and left at room temperature for 15-20 min to polymerize. Water saturated butanol was removed after polymerisation by repeated washing, and any remaining traces of water were removed using filter paper. The prepared stacking gel was poured on top of resolving gel and appropriate size of comb was placed immediately to create wells in stacking gel, and was left to polymerize for 10 min. following polymerization the comb was slowly removed. The gel casted was placed into the electrophoresis tank with the electrode assembly and the 1X Tris-glycine buffer was filled up to the desired height. The protein samples ready to load were made by adding equal volumes of 2X SDS loading dye and kept for boiling in a hot water bath for 10 minutes. Sample were subjected to a short spin just before loading into wells along with protein ladder in one of the wells. The electrophoresis was performed at 100 volts until the tracking dye front entered anode end. The gel that was run was taken out from the plate with the help of wedge, and stained with Coomassie stain solution followed by distain or proceeded for transfer, if required.

Table 2. 6 Composition of the resolving gel for SDS-PAGE

Solution	12.5% for 5 ml	15% for 5 ml
H2O	1.7 ml	1.25 ml
Resolving Buffer (pH 8.8)	1.25 ml	1.25 ml
Acrylamide mix (30%)	2 ml	2.5 ml
APS (10%)	50 μΙ	50 μΙ
TEMED	5 μΙ	15 μΙ

Table 2. 7 Composition of the stacking gel for SDS-PAGE

Solutions	7.5% for 2.5 ml	
H2O	1.7 ml	
Stacking gel Buffer (pH 6.8)	0.625 ml	
Acrylamide mix (30%)	0.625 ml	
APS (10%)	25 μΙ	
TEMED	2.5 μΙ	

2.14 Protein Methods

2.14.1 Solutions for SDS-PAGE

2.14.1.1 Acrylamide mix Solution

A 30% stock solution of acrylamide was made by adding 30 g of acrylamide and 0.8 g of N, N'- methylene-bis-acrylamide in 70 ml of Milli-Q water. The mixture was gently stirred till the acrylamide is dissolved completely. Finally, the volume was increased to 100 ml by adding water and kept at 4°C until needed.

2.14.1.2 Resolving gel buffer

The resolving buffer (1.5 M Tris pH 8.8) was formulated by mixing 18.17 g of Tris base in 70 ml of Milli-Q water and the pH was adjusted to pH8.8 by adding required volume of concentrated HCl before adjusting the volume of the buffer to100ml by adding Milli-Q water. Above solution was autoclaved and 0.3% SDS was added to it before using. When required appropriate volume of resolving buffer was taken and mixed to the other gel components to get final working concentration of 390 mM Tris-HCl, pH 8.8. The solution was stored at room temperature.

2.14.1.3 Stacking gel buffer

The staking gel buffer (0.5 M, Tris pH 6.8) was made by adding 6.05 g of Tris base to 70 ml of Milli-Q water and the pH was adjusted to 6.8 by adding concentrated HCl of required volume. Finally, the solution volume was adjusted to 100 ml with Milli-Q water followed by autoclaving. The above stock solution of stacking buffer was mixed with appropriate amounts of SDS stock solution to adjust the concentration of SDS to a 0.3% and the buffer was kept at room temperature until needed. During SDS gel preparation appropriate volume of stock solution of staking buffer was mixed to other gel components to get working concentration of 130 mM Tris-HCL, pH 6.8.

2.14.1.4 Tris glycine electrophoresis buffer

A 30 g of Tris base, 140 g of Glycine, and 10 g of SDS were dissolved in 800 ml of ddH2O to make a 10X stock solution of tank buffer. The above mixture was kept for stirring till all the components were dissolved properly, and subsequently the volume was adjusted to 1L by adding ddH_2O . It was stored at room temperature and when required 1X (containing 25 mM tris base, 250 mM Glycine, and 0.1% SDS) solution was made by adding 900 ml ddH_2O to 100 ml of stock solution of Tris glycine SDS buffer.

2.14.1.5 2x SDS gel loading buffer

A stock solution of 2X SDS loading dye was formulated by mixing 5ml of 1M Tris-HCL pH 6.8 (100 mM), 2 g of SDS (4% SDS), 100 mg bromophenol blue (0.2% w/v) and 10 ml glycerol (20% v/v). The above solution was mixed with 0.699 ml of β -Mercaptoethanol (200 mM) before adjusting the volume to 50 ml by adding ddH₂O. The buffer was then distributed into 10 ml aliquots and stored at -20°C.

2.14.1.6 Staining solution

The solution was prepared in amber colour bottle by mixing 0.25 g of Coomassie brilliant blue R-250 in 50 ml of methanol. 10 ml of acetic acid was added to this solution before adjusting volume to 100 ml with ddH_2O . The contents were then filtered using Whatman's filter paper and stored at room temperature until further use.

2.14.1.7 Destaining solution

Detaining solution was made by adding methanol (30% v/v) and glacial acetic acid (10% v/v). For 100 ml destaining solution, 30 ml methanol and 10 ml acetic acid were added to 60 ml of ddH₂O.

2.14.2 Solutions for Western Blotting

2.14.2.1 Towbin buffer (protein transfer buffer)

Towbin buffer (Protein transfer buffer): Towbin buffer was prepared by dissolving 3 g of Tris base (25 mM), 14.4 g of glycine (192mM) in 500 ml of ddH₂O. Subsequently, 200 ml methanol (20% v/v) was added to above mixture and volume was adjusted to 1000 ml with ddH2O.

2.14.2.2 TBST Buffer

TBST buffer (20 ml) was prepared by taking 1M Tris-HCl (pH 7.6), 8 g NaCl and 1 ml tween-20 in a clean reagent bottle and dissolving the contents in minimal volume of ddH_2O . Once components were dissolved completely, the volume was adjusted to 1000 ml.

2.14.2.3 Blocking Reagent

Blocking solution was made freshly by mixing 1 g of skimmed milk powder in 10 ml of TBST and it was used to block PVDF membrane containing transferred proteins.

2.14.2.4 Ponceau S reagent

Ponceau S stain (0.1%) solution was made by dissolving 100 mg of ponceau in 100 ml of 5% acetic acid.

2.14.2.5 Membrane stripping solution

When required membrane stripping solution was prepared freshly. It was prepared by dissolving 1.5 g of glycine, 0.1 g of SDS and 1 ml tween 20 in 100 ml of ddH_2O . Later the pH was adjusted 2.2 with 6N HCl.

2.14.2.6 Primary antibody solution

The HRP conjugated anti-His antibody or anti-FLAG antibodies were diluted in a ratio of 1:10000 dilution by adding 1 μ l of antibody to 10 ml of 5% skimmed milk prepared in TBST. The antibody was stored at -20°C after usage and was used 2 to 3 times before discarding.

2.14.2.7 Secondary antibody solution

The HRP conjugated Goat anti-Mouse IgG/ Goat anti-Rabbit IgG secondary antibody was diluted in a ratio of 1:10000 dilution by adding 1 μ l of antibody to 10 ml of 5% skimmed milk prepared in TBST. The antibody was stored at -20°C after usage and was used 2 to 3 times before discarding.

2.14.3 Semi-Dry Western Blotting

Once protein samples were run on SDS-PAGE. Same gel was soaked in Towbin buffer for 5 minutes. Parallelly, PVDF membrane was cut into appropriate size and activated by soaking in methanol for 1 to 2 min, followed by in Towbin buffer for 5 minutes. All assembly process was performed using manufacturers instruction. Briefly, western pad pre-soaked in Towbin was placed on positive electrode of the transfer apparatus. The PVDF transfer membrane as placed carefully on the top of it. The SDS gel was taken out from Towbin and placed over PVDF membrane, subsequently another western pad was put in such a way that both gel and membrane get sandwiched between two western pads, where gel faced positive electrode and membrane faced negative electrode of the instrument. The transfer was carried out at 18V for 40 min in the transfer instrument.

Once transfer was completed, the membrane was taken out carefully with the help of forceps and placed in 10% blocking buffer at room temperature (1 h) or at 4°C (overnight), with constant shaking at 60 rpm. The blot was washed three times with TBST, 10 min each wash, followed by incubation with primary antibody for 1 h at room temperature or at 4°C overnight. The membrane was washed with TBST for 10 min and, if appropriate, incubated at RT with the secondary antibody for 1 h with mild shaking. Finally, the membrane was washed three to five times with TBST followed by developing it using ECL Western Blotting detection reagent according to manufacturer's instruction. The resulting chemiluminescence was captured by ChemiDocTM Touch imaging system (Bio-Rad).

2.14.4 Protein precipitation by Methanol-Chloroform method

Proteins were precipitated by adding two sample volumes of methanol and half of the sample volume of chloroform. The contents were vortexed and centrifuged at 13000 rpm (2 min) to separate the organic and aqueous phase. The aqueous phase found on the top was carefully discarded without disturbing the protein layer formed at the interface. Subsequently, the contents were mixed vigorously after adding two sample volumes of methanol. Centrifugation at 14000 rpm for 2 minutes at room temperature was used to collect the precipitated proteins from the organic layer. The supernatant was carefully removed and the protein precipitate was air dried before resuspending it in 2X SDS loading dye or any other buffer of choice.

Chapter 3: Isolation of OMVs from Acinetobacter baumannii DS002

As stated in the introduction, all gram-negative bacteria constitutively release OMVs in culture, in community and during host infection. The released OMVs perform a variety of functions that enables them to survive in harsh environmental conditions and to establish interand intracellular communications (Gao & van der Veen, 2020; Jan, 2017). Production of OMVs is affected by a variety of living conditions such as growth stage, nutritional status of growth medium, temperature and oxidative stress. Such an influence of abiotic factors on production of OMVs indicate their role in survival of bacteria under various stressful conditions. Intriguingly, the physicochemical properties significantly differ among OMVs isolated from different strains and species. The macromolecular cargo associated with OMVs determine their physiological role. *A. baumannii* strains gained notoriety due to their survival in harsh environmental conditions. They are tolerant to a variety of abiotic stresses and quickly adapt from a free-living state to a pathogenic life style. OMVs probably have a role behind such a robust life style of the opportunistic pathogen. However, studies linking OMVs in adaptive response of *A. baumannii* are scarce. In this chapter, the detailed procedures followed for isolation of these nanostructures is described and the results also include their purity and size distribution.

3.1 Objective specific methodology

3.1.1 Isolation of outer membrane vesicle (OMVs)

OMVs were isolated from *A. baumannii* DS002 culture supernatants following methods described elsewhere, with minor modifications (Fulsundar et al., 2015). Briefly, *A. baumannii* DS002 cultures (4 L) were grown at 30°C until the culture optical density at 600 nm reached 1.8, and cells were harvested by centrifuging the culture at $10,000 \times g$ for 30 min. The cell pellet was flash-frozen and stored at -80°C until it was used for preparing subcellular fractions following standard procedures (Kesty & Kuehn, 2004). The culture supernatant was taken into a sterile container and appropriate amounts of 500 mM EDTA (pH 8.0) stock was added until the EDTA concentration reached 1 mM. The supernatant was then passed through a $0.45\mu m$ vacuum filter (Millipore) to remove residual cells and cell debris. The cell-free culture supernatant was concentrated to 600 mL by passing it through a 100-kDa hollow fibre membrane (GE Healthcare).

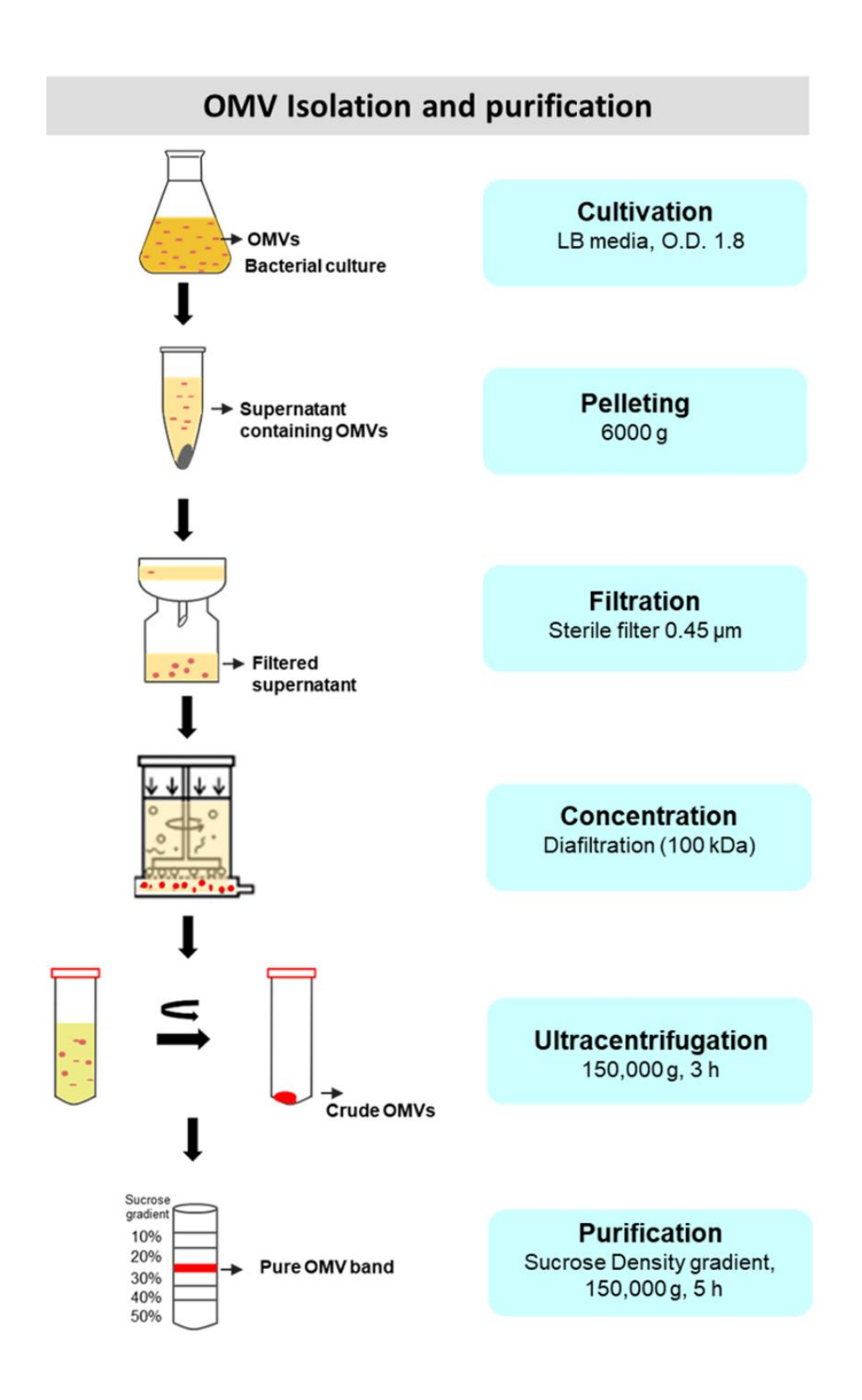


Figure 3. 1 Workflow followed during purification of OMVs from A. baumannii DS002.

The concentrated culture supernatant was again passed through a 0.45- μ m filter before centrifuging the contents using Ti70 rotor at 150,000 × g for 2 h to pellet the OMVs. The pellet containing OMVs were resuspended in 1 mL phosphate-buffered saline (PBS) buffer (pH 7.3), and carefully layered on a centrifuge tube containing a sucrose gradient ranging from 10% to 50%. The tube was then fitted to a swinging bucket rotor (SW32) and centrifuged for 5 h at 150,000 × g. The OMV band obtained between 20% and 30% sucrose was collected using a long syringe, and the collected OMVs were concentrated by centrifuging at 150,000 × g for 2 h. The pellet was resuspended in 500 μ l of PBS buffer and filtered through a 0.22- μ m syringe filter, and a portion of obtained vesicle suspension (10 μ g) was plated on an LB agar plate to check for bacterial contamination. Pure OMVs were then divided into small (50- μ l) aliquots and stored at -80°C until further use. The detailed procedures followed to isolated OMVs in their pure form is depicted in Fig 3.1.

3.1.2 Cloning and Expression of ompA in pET28a vector

Initially, *ompA* gene was amplified from genomic DNA of *A. baumannii* DS002, using primers GD1FP/GD1RP appended with *NdeI* and *XhoI* respectively (Table 5.2). The amplicon was checked on 0.8% agarose gel and purified before ligating it to pET28a digested with similar enzymes. After ligation, the DH5 α transformants obtained were selected on LB plates having with 50 µg/µl of kanamycin. The recombinant plasmid isolated from the transformed cells were screened for presence of insert by digesting it with *NdeI* and *XhoI* restriction enzymes and the recombinant plasmid was named pGD1.

3.1.2.1 Expression of OmpAN6XHis

Construct pGD1 coding OmpA N6XHis was transformed into E. coli. Nico strain and was grown in 10 mL LB media supplemented with 50 µg of kanamycin, to mid-logarithmic phase at 37oC and 1 mM IPTG was added. The culture was kept at 4oC for expression of OmpA N6XHis and 1 mL culture was collected at different time points 2h, 4h, 6h, 8h and 16h. The protein sample was analysed on 12% SDS-PAGE by staining with CBB stain. Western blot was also performed using anti-His antibody to further confirm the expression of OmpA N6XHis protein.

3.1.2.2 Purification of OmpA^{N6XHis} using affinity chromatography

E.~coli~Nico~ strain expressing OmpA^{N6XHis} was inoculated in LB containing 50 μg of kanamycin and grown overnight at 37°C. Inoculum equal to 1% was added to 1000 mL of LB and was grown till loge phase (OD₆₀₀ 0.5) followed by induction with 2 mM IPTG at 18°C for 12 h. The cells were collected at 6000 rpm for 10 min and the pellet was washed using PBS buffer

containing 10% glycerol. Cells were resuspended in lysis buffer (PBS+ 50 µg lysozyme+ 1mM PMSF+ protease arrest) and kept for end-to-end rotation at 4°C for 30 min. The cell suspension was then sonicated (20 sec on 40 sec off for 20 min) and the resulted cell lysate was centrifuged at 15,000 rpm for 20 min The clear supernatant was transferred to a sterile flask, and a stock solution of imidazole was added to bring the final concentration to 10 mM. The contents were then added to Ni-NTA column preequilibrated with equilibration buffer (PBS+ 10 mM imidazole + 5% glycerol). Flow through was collected and column was washed with 3 column volumes of wash buffer (PBS+ 50mM imidazole + 5% glycerol). Protein bound with the bead was eluted using PBS buffer having increased concentration (50 mM, 100 mM, 150 mM, 200 mM, 300 mM) of imidazole. These fractions were then separated on 12.5% SDS-PAGE to detect the presence of bound protein. These fractions collected were then pooled and dialyzed to remove imidazole. The Protein concentration was measured using Bradford method (Bio-Rad) and the pure OmpA^{NGXHis} was stored at -20°C until further use.

3.1.3 Generation of polyclonal antibody against OmpAN6XHis

Polyclonal antibodies against OmpAN6XHis protein were raised in rabbit by following standard protocol described elsewhere (cooper and Patterson, 2008). Briefly, prior to the immunization, rabbits were allowed to acclimatize in the animal house facility for a week. Before giving the first dose,10 ml of blood was taken and of serum was separated from it. Serum was collected by keeping the collected blood at room temperature for 1h followed by keeping it in refrigerator (4°C) for more than 12 h. The sample was centrifuged at 3000 rpm (5 min) at 4°C and the serum obtained was stored at -20°C until further use. The purified recombinant protein (250 μg) was diluted in 0.5 mL of PBS buffer and later mixed with 0.5 ml of complete Freund's adjuvant (Sigma). These contents were mixed thoroughly with the help of syringe to form a stable emulsion. The emulsion form was then injected subcutaneously near shoulder and intramuscularly into the large muscle of the rear legs. Four weeks after the first immunization, three immune booster doses were administrated each with an interval of two weeks. In each immune booster 125 µg of the antigen was taken in a final volume of 0.5 ml (addition of PBS to the antigen to 0.25 ml + 0.25 ml of incomplete Freund's adjuvant) and administrated intramuscularly as described earlier. One week after administration of each immune booster, blood samples were collected and the serum prepared from these samples were used to test generation of antibodies against OmpA protein. Finally, a 19-gauge needle was used to withdraw blood from the central ear artery, and the whole blood (15ml) was used to prepare serum, which was then followed by antibody purification.

3.1.4 Antibody purification

Affinity chromatography was carried out to purify IgG's from the serum collected from the immunized rabbit. The serum collected was diluted with equal volume of equilibration buffer (20 mM sodium phosphate buffer pH 7.0) and the diluted serum was applied to the protein A column, pre-equilibrated with the same buffer. Column was washed with 10 CV of equilibration buffer and IgG bound to the column was eluted using elution buffer (0.1 M glycine-HCL, pH 2.7) and stored in -20°C in 100 μ l aliquots until further use.

3.1.5 Preparation of subcellular fractions

An A. baumannii DS002 cell pellet obtained while preparing outer membrane vesicles (OMVs) was used for preparing subcellular fractions (Kesty & Kuehn, 2004). Briefly, the flashfrozen cell pellet was washed with phosphate-buffered saline (pH 7.3) before being resuspended (4 mL/g cells) in a 20% sucrose solution prepared using 20 mM Tris EDTA (100 mM) buffer (pH 8.0). The cell suspension was mixed with lysozyme (600 µg/g cells) and the contents were incubated on ice for 40 min. After lysozyme treatment, the appropriate amounts of MgCl₂ (0.16 mL/g cells) were added from a stock solution and the spheroplasts formed were separated by centrifuging the contents (95,000 × g) for 20 min. Supernatant was removed and the pellet containing spheroplasts were resuspended in ice-cold 10 mM Tris HCl (pH 8.0) and sonicated (10 sec on and 30 sec off) for 15 min. Unbroken cells were spun down by centrifugation at 8,000 × g for 20 min at 4°C, and the supernatant was centrifuged at 50,000 × g for 2 h to pellet the membrane from the cytoplasm. The supernatant contained the cytoplasmic fraction, and the pellet contained the crude membranes. The pellet was washed with 10 mM Tris-HCl (pH 8.0), then resuspended in 1 mL of sterile water. The dissolved membrane was then flash-frozen and thawed by placing it on an ice bucket. The membrane fraction was then adjusted to 0.5% (wt./vol) sarkosyl (sodium-N-lauryl sarcosine) and the contents were incubated at 25°C for 20 min with an end-to-end rotation. The contents were again centrifuged at 50,000 × g for 2 h at 4°C. The pellet containing outer membrane (OM) was dissolved in 10 mM Tris-HCl (pH 8.0) and stored at -80°C until further use. The supernatant containing inner membrane was collected into a separate sterile tube.

3.1.6 Determination of OMV Purity and quantity

The purity of OMVs was established by detecting marker proteins. The RepA was used as cytoplasmic protein marker, whereas the OmpA was used as OMV and outer membrane marker protein. The proteins of subcellular fractions prepared from *A. baumannii* DS002 were separated on 12% SDS-PAGE along with proteins of OMVs and independently probed with antibodies of either RepA or OmpA. If RepA specific signal was absent in OMV proteins then the OMV preparations were considered pure. Presence of OmpA exclusively in OMV and outer membrane fractions reconfirmed purity of OMVs. To quantify the amount of OMVs produced. Protein content of the OMV was measured using Bradford method of protein estimation

3.1.7 Transmission Electron Microscopy (TEM)

OMVs (0.5 μ g/ μ l protein concentration) dissolved in PBS were carefully placed on a copper grid (200 mesh) and the excess liquid was removed by gently touching the grid with filter paper. The copper grid was then left at a cool and dry place for 20 min to facilitate absorption of OMVs. The OMVs absorbed on copper grid were stained by floating the grid in 10 μ l of aqueous uranyl acetate (2%) for 60 seconds. The excess stain was removed by gently touching the grid with filter paper. The dried grid was then visualized under transmission electron microscope (JEM-1400 Electron microscope, JEOL) operating at 120 kV.

3.1.8 Nanoparticle tracking analysis (NTA)

Nanoparticle tracking analysis was done to measure the size distribution of OMVs prepared from *A. baumannii* DS002. The diluted pure OMVs (0.05 μ g/ml) were loaded onto the NTA chamber and the particle size was recorded for 60 seconds at the laser wavelength of 488 nm using particle matrix analyser (ZETAVIEW).

3.2 Results

3.2.1 Purification of OMVs

The procedure followed plays a crucial role in characterization of the OMVs. The primary goal and the topic of this present chapter is on isolation of pure OMVs from *A. baumannii* DS002. The method followed for isolation of OMVs from *A. baumannii* DS002 is described in methods section. In this method, isolation of OMVs was initiated from 4 L culture supernatant. The supernatant was passed through a membrane with molecular cut-off of 100 kDa column using diafiltration unit (BioRad) and this step has significantly reduced the volume (4 L to 400 ml) of culture medium. Further, the filtration step removed most of the extracellular proteins. The

ultracentrifugation of the filtered medium (Ti70 rotor, for 2 h, 150,000 x g) pelleted the most of the OMVs found in the filtered supernatant by removing the cell debris, protein and lipid aggregates and other non-OMV associated material. These crude OMVs were then dissolved in minimal volume of the buffer (PBS pH 7.3) and layered on the top of the sucrose solution layered between 10% to 50%. After ultracentrifugation, the OMVs appeared as a thick band between 20%-30% sucrose density (Fig 3.2 A). The protein content of the OMVs purified through gradient centrifugation was determined and the OMV content was measured as amount of protein per litre of the culture supernatant. The method followed in this study yielded 600 µg of protein per litre culture supernatant. The OMV proteins were then analysed on 12% SDS-PAGE (Fig 3.2 B) and the OMV protein profile was established by running them along with membrane proteins (Fig 3.2 B). The OMV protein profile matched with the profile of outer membrane indicating that the OMVs isolated following the method described in the methods section yielded pure OMVs. As seen in lane 4 of fig 3.2 B some unique protein bands were also seen in the lane loaded with OMV proteins. This clearly indicates that the OMV cargo contains proteins of inner membrane and cytoplasmic proteins along with outer membrane proteins. Before establishing the identity of OMV proteins further studies were conducted to establish the purity of isolated OMVs by detecting marker proteins.

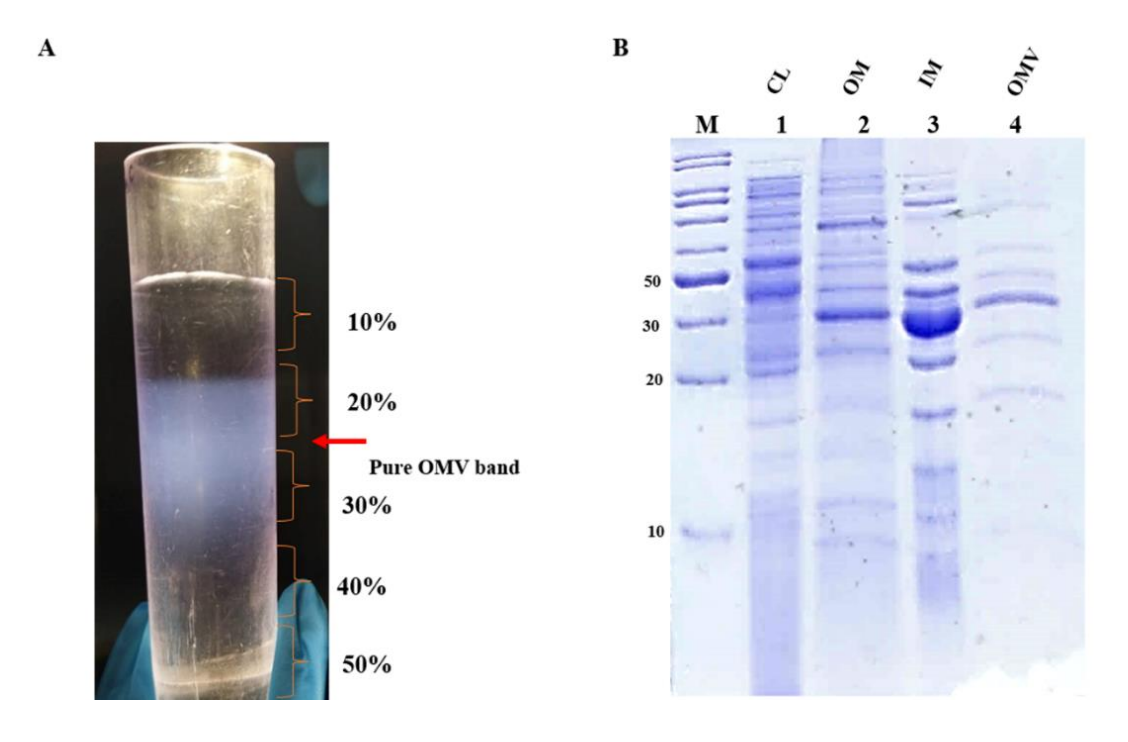


Figure 3. 2 Isolation and purification of pure OMVs from *A. baumannii* **DS002**. Panel A shows sucrose density gradient (10 to 50%) centrifugation. OMVs were banded out at a density of 20-30% sucrose. Panel B represents SDS-PAGE indicates protein profile of cytoplasmic fraction (lane 1), outer membrane proteins (lane 2) and inner membrane (lane 3). The total OMV protein profile is shown in lane 4.

3.2.2 Purity Assessment of OMVs

The purity of OMVs were established by detecting marker enzymes. Outer membrane porin, OmpA plays a critical role in the biogenesis and maintaining the integrity of OMVs (Moon et al., 2012). Since, it is exclusively present in the outer membrane, we have used it as an OMV-specific marker. The RepA protein involved in the rolling circle mode of DNA replication is used as a cytoplasmic protein marker (Longkumer et al., 2013). These two marker proteins were detected in OMV proteins by performing western blots. The anti-RepA antibodies available in our laboratory were used for the detection of RepA among OMV proteins. The anti-OmpA antibodies were generated for detecting OmpA among OMV proteins.

3.2.3 Generation of anti-OmpA antibodies

3.2.3.1 Cloning of ompA gene

Before proceeding to detect *ompA* the gene coding *ompA* was amplified using primer set GD1FP/GD1RP from the genomic DNA of *A. baumannii* DS002. The PCR reaction mix when analysed on 0.8% agarose gel showed presence of an amplicon of 1053 bp which corresponds to the size of *ompA* gene (Fig 3.3 A lane 2). As the primers were appended with *NdeI* and *XhoI* sites the amplicon was digested and ligated into similarly digested pET28a vector. The recombinant plasmid thus generated was digested and release of *ompA* from the vector was confirmed by analysing the digested plasmid on agarose gel (Fig 3.3 B lane 2). The expression plasmid was named pGD1 and codes for OmpA^{N6His} (Fig 3.3 C lane 3).

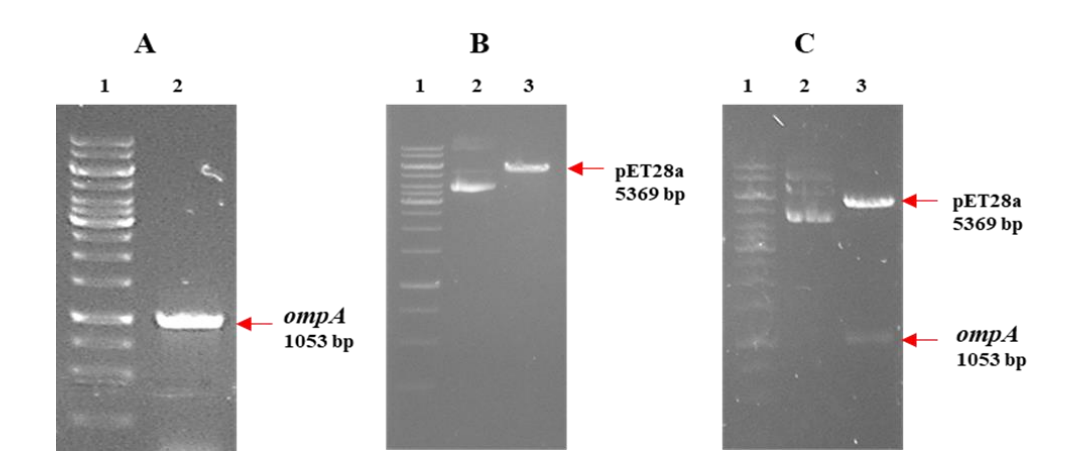


Figure 3. 3 Construction of pGD1. Panel A shows image of 0.8% agarose gel indicating molecular marker in lane 1, *ompA* amplicon in lane 2. Panel B shows image of 0.8% agarose gel with molecular marker (lane 1), undigested pET23b (lane 2) and pET23b digested with *Ndel/Xhol* (lane3). Panel C shows clone confirmation. Molecular weight marker (lane1), undigested pGD1 (lane2), pGD1 digested with *Ndel/Xhol*. The band corresponding to the vector and insert containing *ompA* gene are shown with arrows (lane 3).

3.2.3.2 Expression of OmpA

The pGD1 coding OmpA^{N6XHis} was transformed into *E. coli*. NiCo21 (DE3) strain and the expression of OmpA^{N6XHis} was induced as described in the methods section. Samples collected at different time points of induction were analysed on 12% SDS-PAGE. A thick band corresponding to the size of OmpA^{N6XHis} was observed in lanes loaded with proteins isolated from induced cultures. The western blot performed by using anti-His antibody further confirmed that the expressed protein at 37 kDa is OmpA^{N6XHis} (Fig 3.4 B lane 3 to 7).

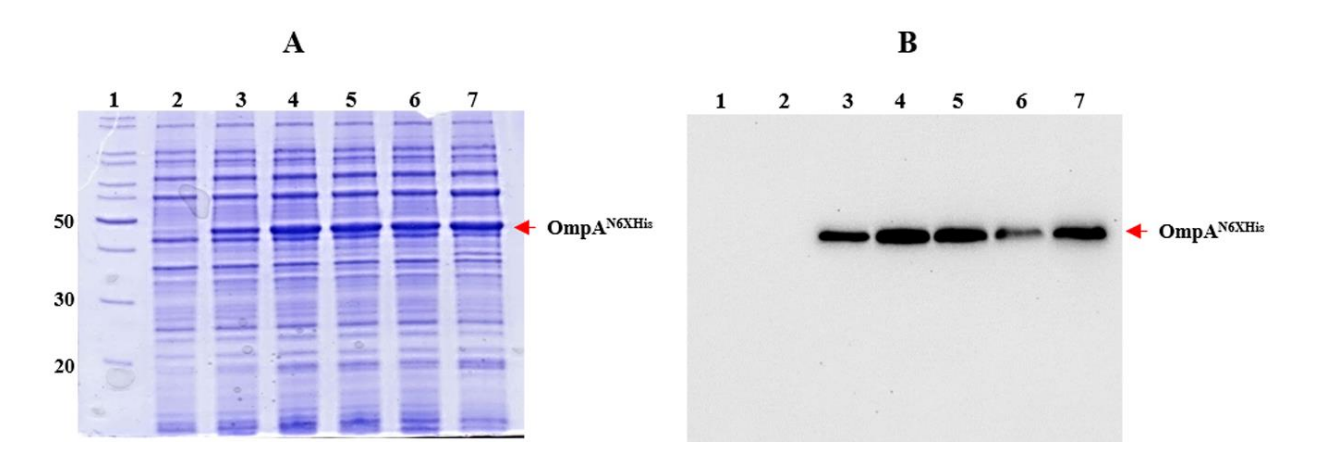


Figure 3. 4 Expression of OmpA^{N6XHis}. Panel A shows 12.5% SDS-PAGE showing the analysis of **OmpA**^{N6XHis} expression at different time points of induction. lane 1 shows the molecular weight marker, lane 2 is proteins from uninduced cultures. Lanes 3 to 7 are proteins from cultures induced for 2h, 4h, 6h, 8h and 16h respectively. Panel B shows corresponding western blot probed with anti-His antibody to confirm the expression of **OmpA**^{N6XHis}.

3.2.3.3 Purification of OmpA^{N6XHis}

After optimization of expression, the OmpA^{N6XHis} was purified using Ni-NTA matrix as described in method section. The cell lysate prepared from induced cultures was passed through Ni-NTA matrix and the beads were washed extensively to remove unbound proteins (Fig 3.5 A lane 5 and 6). The protein bound to Ni-NTA matrix was eluted by increasing the imidazole concentration from 100 to 300 mM (Fig 3.5 A lane 8 to 11). The eluted pure protein was dialysed and concentrated against PBS buffer (Fig 3.5 B lane 2).

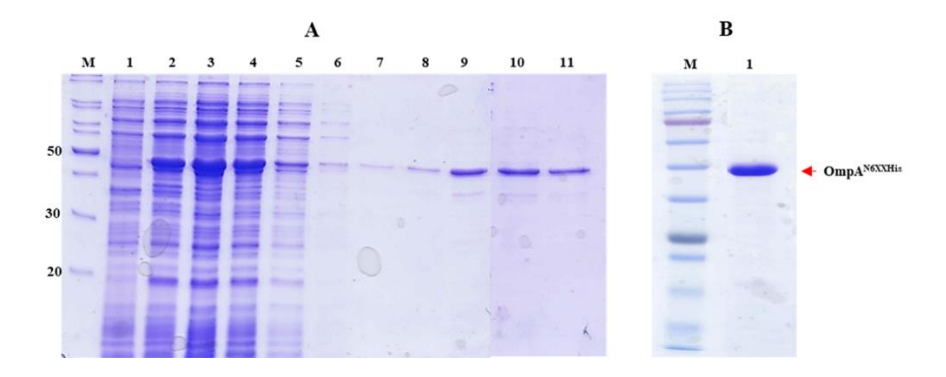


Figure 3. 5 Affinity purification of OmpA^{N6XHis}. The 12.5% SDS-PAGE showing different stages of **OmpA**^{N6XHis} purification. Lane M shows molecular size markers, lanes 1 and 2 show proteins found in lysates of uninduced and induced cultures. Lane 3 indicates soluble protein fraction containing **OmpA**^{N6XHis}, the proteins of flow through fraction are shown in lane 4. Lanes 5 and 6 represent proteins of wash fraction. Lanes 7 to 11 corresponds to fractions obtained while eluting the **OmpA**^{N6XHis} using 50 mM, 100 mM, 150 mM, 200 mM, 300 mM imidazole in wash buffer. Panel B indicates the dialysed and concentrated pure **OmpA**^{N6XHis}.

3.2.3.4 Immunization and preparation of anti-OmpA antibodies

The pure OmpA^{N6XHis} protein obtained was used to generate polyclonal antibodies against OmpA protein of *A. baumannii* DS002 in rabbit following procedures described in methods section. *A. baumannii* DS002 lysate gave no signal when probed with pre-immune serum suggesting that there were no anti-OmpA antibodies in the serum of the rabbit. However, when the *A. baumannii* DS002 lysate was probed using serum collected after three booster doses has shown good signal at the size of OmpA protein. Thus, blood serum collected from immunised rabbit was further purified using agarose-protein-A beads and purified antibodies were on 12% SDS-PAGE to confirm purity (Fig 3.6 lane 5 to 9).

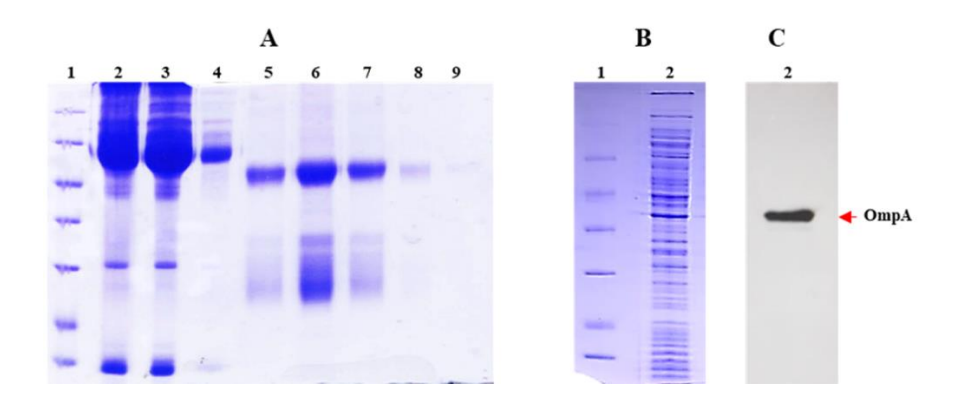


Figure 3. 6 Purification of anti-OmpA antibodies. Panel A shows SDS-PAGE showing different stages of anti-OmpA antibodies purification. Lanes 1 and 2 show molecular size marker and serum containing anti-OmpA antibodies. Proteins found in flowthrough and wash fraction are shown in lanes 3 and 4. Lanes 5 to 9. show eluted antibodies. Panel B shows 12.5% SDS-PAGE showing proteins of *A. baumannii* DS002 (lane 2) along with molecular marker (lane 1). The corresponding western blot developed using anti-OmpA antibodies is shown in panel C. The clear OmpA signal corresponding to the size of 37 kDa is shown with arrow.

The pure anti-OmpA antibodies were checked for their reactivity on OmpA protein by using it against *A. baumannii* DS002 lysate. The western blot results using OmpA antibody has shown a clear signal around 37 kDa (Fig 3.6 C), indicating successful generation anti-OmpA antibodies.

3.2.4 OMV isolated were pure

Due to the lack of well-established methodology for OMV isolation and purification, the purity of OMV is usually questioned. Therefore, in the present study we established the purity of OMVs before proceeding for their purification. At first, we analysed OMV, cytoplasmic, inner and outer membrane proteins on SDS-PAGE and later probed them with the antibodies of marker proteins to assess the purity of OMVs (Fig 3.7 B & D). The SDS-PAGE profile of OMV and outer membrane proteins shared significant similarities. Most of the protein bands seen in OMVs were also found in the outer membrane (Fig 3.7 A, lane 5 & 4). When these proteins were probed independently with antibodies raised against OmpA and RepA, the RepA specific signal was exclusively seen in the lane loaded with cytoplasmic proteins (Fig 3.7 C, lane 1). The RepA specific signals were not seen in lanes loaded with proteins extracted from OMVs and the outer membrane, suggesting that these fractions were not contaminated with cytoplasmic proteins (Fig 3.7 C, lane 2, 3 & 4).

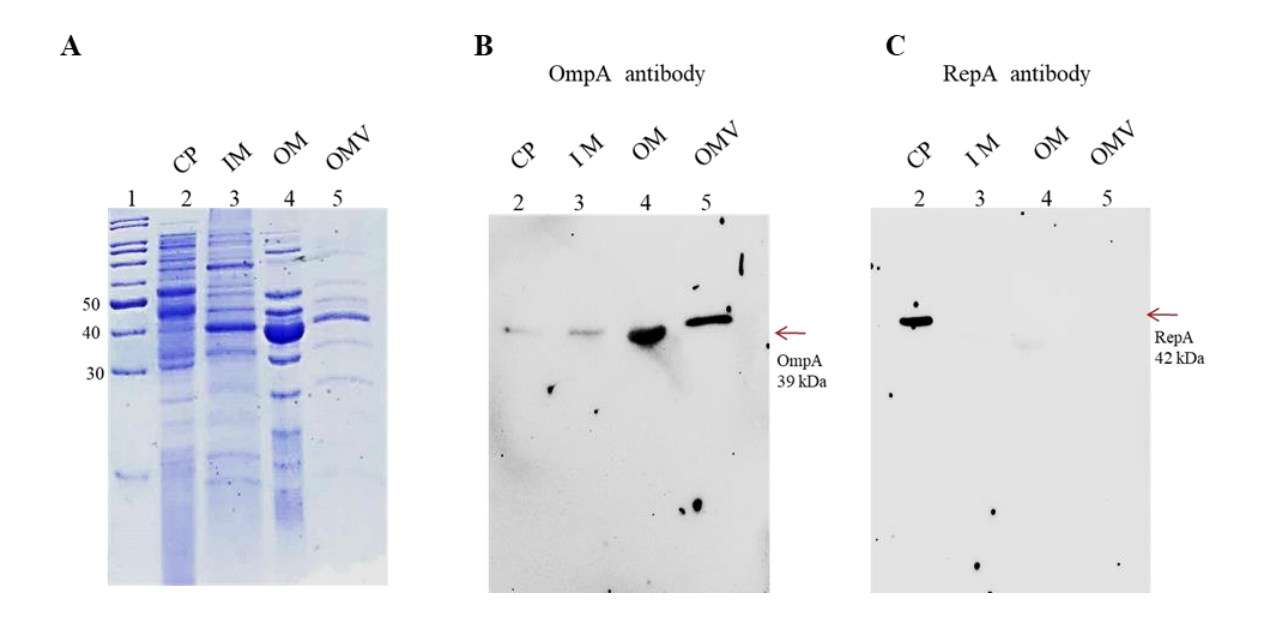


Figure 3. 7 Checking purity of outer membrane vesicles (OMVs) from *Acinetobacter baumannii* DS002. Panel A, SDS-PAGE (12%) showing the profiles of cytoplasmic (CP), inner membrane (IM), outer membrane (OM), and OMV proteins. Corresponding Western blots, developed by probing with either OmpA or RepA antibodies, are shown in panels C and D, respectively.

Inferring that the isolated OMVs are free from cytoplasmic fraction, the OmpA specific signals were only seen in lanes loaded with proteins of OM and OMVs but not in the lane loaded with proteins of cytoplasmic fraction (Fig 3.7 B, Lane 2, 3, 4 & 5).

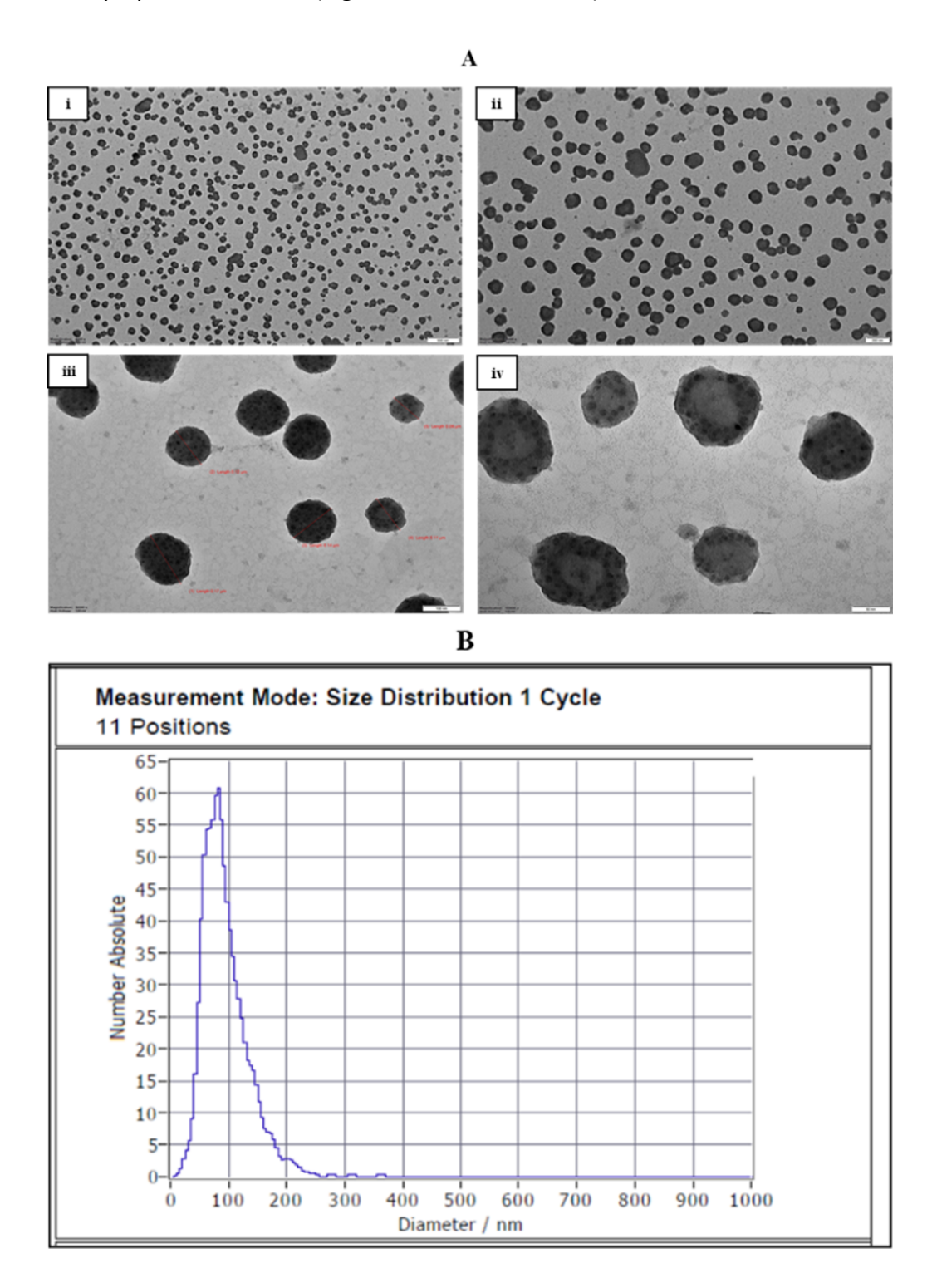


Figure 3. 8 Size distribution of OMVs from *A. baumannii* **DS002.** Panel A shows transmission electron microscopy (TEM) images of pure OMV sample. Images were taken at different resolution 500 nm (i), 200 nm (ii), 100 nm (iii) and 50 nm (iv). Size distribution of OMVs as measured by particle matrix analyser (ZetaView) is shown in panel B.

3.2.5 Size distribution of OMVs

After ascertaining purity of OMVs the size distribution and shape of OMVs were examined by taking the images of transmission electron microscopy (TEM) and nanoparticle tracking analysis. Initially, the TEM images of OMVs were captured at different resolution (Fig 3.8 A). *A. baumannii* DS002 OMVs were detected to have spherical shape which consists of a single lipid-bilayer with an electron dense surface layer. There were no cellular fragments in the purified OMV preparation (Fig 3.8 A). As described in the methods section, the size distribution profile of OMVs purified from three biological replicates was independently analysed. The size distribution of *A. baumannii* DS002 OMVs were 74 to 160 nm as determined by TEM and a fully hydrated size range of 20-300 nm as determined by nano track analysis (Fig 3.8 B), with a model vesicle mean diameter of 121 nm.

3.3 Discussion

A detailed investigations pertaining to the functional characterization of OMVs depend heavily on the methods followed in purification of OMVs. The main limitations in studying OMVs are the challenges associated with the isolation and purification methods that provide sufficient quantities of these small vesicular structures from culture supernatants. A number of methods have been developed for the isolation and enrichment of vesicles. In general, a typical OMV isolation procedure involves filtration of culture supernatant to remove bacteria and optionally pre-concentration followed by high-speed centrifugation (90 - 150,000 g) to pellet vesicles (Klimentová & Stulík, 2015). During cultivation, the medium composition, harvest time, and application of various stress conditions all influence the rate of vesiculation of OMV and its composition. Most of the bacteria were removed from the culture supernatants by following these two independent methods (E. Y. Lee et al., 2007). The culture filtrate is generally concentrated before ultracentrifugation which involves passing the culture filtrate through a membrane with a set molecular weight cut-off, typically 50–100 kDa, to remove the majority of proteins which are not associated with OMVs. Precipitation with ammonium sulfate is also followed in some studies to increase yield (Bauman & Kuehn, 2006). Subsequently, OMV is pelleted down using high speed ultracentrifugation, which gives crude OMVs containing non-OMV associated particles. Neither concentration nor ultracentrifugation completely separates OMV from other extracellular materials such as fimbria, flagella, any pili, and large protein aggregates (Kulp & Kuehn, 2010a). These components are primary impurities in OMVs and interfere with the subsequent studies aimed to functionally characterize OMVs. These impurities

were successfully removed by including one more step in OMV purification. The pelleted OMVs are subjected to gradient centrifugation or gel filtration. This additional purification step successfully removes non-OMV-associated materials. Because of their lipid content, OMVs have a lower density than soluble secreted proteins, pili and flagella. As a result, OMVs band out at a different density than proteins during density gradient centrifugation (Horstman & Kuehn, 2000). The most commonly used medium in density gradient method of purification of OMV is iodixanol (OptiPrepTM). Sucrose and dextran were also used to separate OMVs from contaminating proteins (Klimentová & Stulík, 2015). Quantifying OMV yield is a critical step in analyzing and comprehending the vesiculation process. The quantification is often done either by measuring protein or lipid concentration (Reimer et al., 2021). Proper analysis and quality check of Isolated OMV is important before their characterization. Various methods are used to evaluate OMV properties, of them only two main approaches are often followed in almost every study published. It includes techniques for visualizing and evaluating OMV content. Due to small size of OMVs its visualization by simple light microscopy is not possible. Therefore, OMVs are visualized under transmission electron microscopy (TEM) to show their presence, to describe their sizes, shape, overall appearance and to examine their purity depending on the presence of contaminating non-OMV materials such as large protein aggregates and flagella. TEM images of OMVs are typically taken after they have been negatively stained with uranyl acetate (Ojima et al., 2021).

The work described in the present chapter has focussed on two methods for isolating OMVs from *A. baumannii* DS002. The diafiltration followed by ultracentrifugation. Our results have shown a clear OMV band at lighter (20-30% sucrose) sucrose density (Fig 3.2 A). Similar results have been reported while isolating OMVs of *Escherichia coli* (Horstman & Kuehn, 2000), where OMV band is observed in lighter densities. Apparently, this is due to the lipid content of the OMVs and it has virtually eliminated secreted proteins, flagella, pili *etc.* from OMVs. *E. coli* OMV has reported to produce approximately, 2–3 mg of vesicles from 10 litres of ETEC 2 cell culture, which is approximately 300 µg/L. Results reported in this chapter are consistent with reported studies (Horstman & Kuehn, 2000). As revealed by protein estimation, the results from different batches of isolated OMVs on an average, 600 µg of OMVs per every litre of *A. baumannii* DS002 culture filtrate. This is indeed a 2-fold increase when compared to the yield obtained while isolating *E. coli* OMVs. As revealed by TEM images, the obtained OMVs are in the size range of 74 to 160 nm, which is within the range of OMVs isolated in other studies (Klimentová & Stulík, 2015). The nanoparticle tracking analysis has shown that the isolated OMVs were in the size

range of approximately 20 to 300 nm. This difference in size could be due to hydration of OMVs in liquid suspensions, or it may be due to the formation of aggregates in suspension.

The marker protein detection has shown that the isolated OMVs were free of other subcellular fractions. The OmpA protein was only detected in outer membrane and OMV fractions, whereas, detection of RepA protein, a cytoplasmic marker, was detected only in cytoplasmic fraction, but not in OMVs (Fig 3.7 B and C). The comparative, commissive stained SDS-PAGE of different subcellular fractions shows selective sorting of proteins from different location, in OMVs. Although a majority of proteins are from outer membrane, the banding pattern revealed presence of unique proteins in OMVs. This reveals selective incorporation of proteins in OMVs and suggests that they might be responsible for OMV mediated selective physiological roles. In subsequent chapters of the dissertation experiments performed to identify and characterize these unique OMV proteins are described.

Chapter 4: Proteome of OMVs

The cargo of macromolecules associated with the OMVs determine their role in contributing to the bacterial stress responses and adaptive potential. Therefore, several research have been carried to better understand the molecular composition of OMVs using several microorganisms as model systems. The molecular composition of OMVs is not universal, they differ from bacteria to bacteria and within same bacteria the composition of OMVs differ depending on the growth phase and nutritional status of growth medium. Essentially, OMVs contain lipopolysaccharide, proteins, lipids and DNA or RNA (E. Y. Lee et al., 2008). In some cases, active toxins and few virulence factors have been identified in OMVs produced by pathogenic bacteria (Horstman & Kuehn, 2000). OMV surface factors mediate vesicular component internalisation and adherence to host cells. In this regard, OMVs serve as a powerful vehicle for effector molecule transport into host cells. Pathogenic Gram-negative bacteria, including Escherichia coli (Hakami et al., 2017), Neisseria meningitidis (Pettit & Judd, 1992), Shigella (Kolling et al., 1999), Helicobacter pylori (Keenan et al., 2000), and Pseudomonas aeruginosa (Kadurugamuwa & Beveridge, 1995) secrete OMVs. Many virulence factors of pathogenic bacteria like cytolysin A and heat-labile toxin of *E. coli*, haemolytic phospholipase C, β-lactamase and alkaline phosphatase of P. aeruginosa, and VacA of H. pylori, enriched in OMVs, and their roles in bacterial pathogenesis are well understood.

As stated in introduction, *A. baumannii* DS002 is a soil isolate and survives in pesticide polluted agriculture soils by thriving on toxic phenolic wastes (Yakkala et al., 2019). Genome sequence information is available for strain DS002, and it contains a chromosome (3,430,799 bp) and six indigenous plasmids.

The genome of DS002 was recently compared to genome sequences of *A. baumannii* strains isolated from various habitats (Yakkala et al., 2019). Interestingly, the genome of DS002 revealed presence of several *tonB* paralogues coding TonB-dependent transporters (TonRs) involved in the transport of iron complexed with various siderophores. However, the genes encoding the corresponding siderophores are missing from the genome of *A. baumannii* DS002. Since, OMVs have a proven role in nutrient transport, detailed investigations were conducted to identify if TonRs were associated with OMVs. Experiments conducted in this study demonstrated selective enrichment of TonRs in OMVs of *A. baumannii* DS002 and proved their role in iron acquisition. In addition to TonB, various virulence-associated proteins and immune modulators

were associated with OMVs, indicating possible involvement of OMVs in transport of effector molecules into host cells.

4.1 Objective specific methods

4.1.1 Identification of OMV associated proteins

Two independent experiments were conducted while identifying the proteins associated with OMVs. The DS002 cultures were grown in LB medium till they reach identical OD and the culture supernatants were used to purify OMVs. The proteomic analysis was performed on these biological replicates and the proteins identified in both of them were taken as OMV associated proteins. Initially, the purified OMVs were resuspended in 2 X SDS-PAGE sample buffer and boiled for five min at 100°C. The OMVs corresponding to 30 μg (total protein concentration) of protein were taken and separated on 12% SDS-PAGE. The lane containing OMV proteins was divided into five zones and cut them into separate pieces and the proteins found in each gel piece were subjected to in-gel digestion with trypsin using standard protocols as described earlier (Kulkarni et al., 2014). Briefly, the gel pieces were washed with water and it was followed by a brief wash with 50 mM ammonium bicarbonate and acetonitrile (1:1). This step is continued till the stain was removed, and finally the gel pieces were treated with acetonitrile (ACN) before air drying the samples. The airdried samples were incubated with trypsin (10 ng/ml) at 37oC for 16-18 h. The in-gel digested peptides were extracted with 30% acetonitrile in water containing 0.1% TFA and concentrated with the help of speed vac concentrator. The peptides were desalted after dissolving them in 5% acetonitrile containing 0.1% TFA using Ziptips and analysed the sample on LC-MS/MS.

4.1.2 MALDI TOF/TOF:

The peptides generated from the in-gel digestion were used to spot on the MALDI target plate. Initially 2 μ l of the peptide sample was spotted and allowed it to dry before spotting 2 μ l of HCCA matrix. The MALDI plate was then inserted in to the MS instrument obtained from Bruker Daltonics, Bremen, Germany and the acquired MS and MS/MS spectra of different peptides. MS data was acquired from m/z 800-4000. Proteins were identified using MASCOT software.

4.1.3 Proteome analysis by LC-ESI-MS/MS

Peptides generated after trypsin digestion were subjected to LC-ESI-MS/MS using Q-Exactive mass spectrometer obtained from Thermo Fisher scientific. The peptides were separated on a PepMapTM RSLC, C18 nanocolumn with pore size 100 Å and particle size 3 µm

(Thermo fisher scientific) using a flow rate of 300 nl/min, on a 60 min gradient. Liquid Chromatography system was connected to ESI–MS/MS which recorded the collision induced dissociation (CID) MS of the peptides. The mass resolution of the precursor ion scans is 70,000. The mobile phases A and B were 0.1% formic acid in 5% ACN and 0.1% formic acid in 95% ACN respectively. The gradient used for separating peptides was shown in Table 4.1. The MS/MS spectrum of top 10 peptides with signal threshold of 500 counts was acquired with 30 sec activation time and a repeat duration of 30 sec. The MS/MS data was analysed using database of *Acinetobacter baumannii* DS002 from NCBI with accession number CP027704.1 using proteome discoverer 2.2.

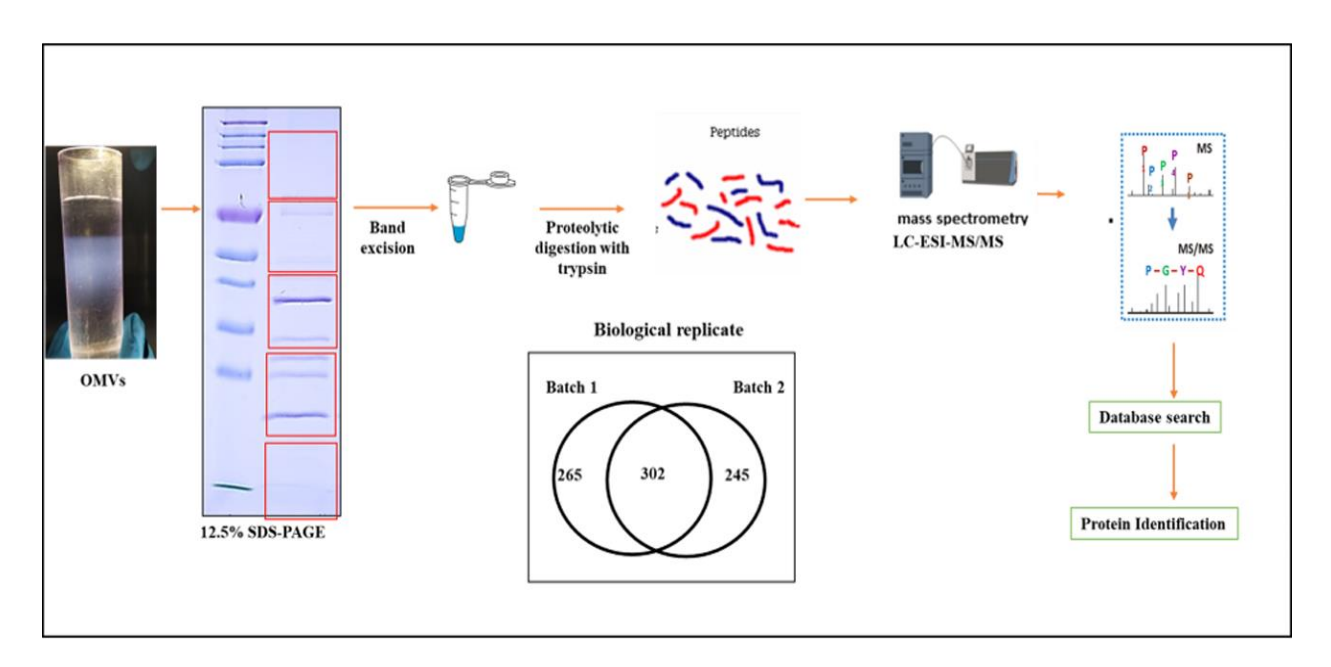


Figure 4. 1 Workflow followed during proteomic analysis of OMVs from A. baumannii DS002.

The precursor ion mass accuracy was set at 5 ppm and the fragment ion mass accuracy was set at 0.05 Da for the identification of proteins. Further, variable modification of oxidation of methionine and fixed modification carbamidomethyl were used for the identification of proteins. Two missed cleavages were allowed for trypsin and peptides with high confidence were selected. The proteomics data identified in this study was submitted to Proteome Exchange *via* PRIDE with identifier PXD026751.

Table 4. 1 Gradient used for separating peptides

Gradient: Solution A-5%ACN+.1%FA Solution B-95%ACN+0.1%FA

Time [mm:ss]	Duration [mm:ss]	Flow [nl/min]	Mixture [%B]
00:00	00:00	300	0
38:00	38:00	300	25
45:00	07:00	300	40
50:00	05:00	300	90
55:00	05:00	300	90
60:00	05:00	300	3

4.1.4 Bioinformatic analysis of the OMV proteins

4.1.4.1 Subcellular localization of identified proteins

The *A. baumannii* DS002 genome coded proteins were downloaded in a FASTA format from NCBI database (Accession No.: CP027704.1). The protein subcellular localization was predicted using Psortb V3.0 (https://www.psoort.org/psortb/). The score 7 out of 10 was used to predict the localization of protein with a reasonable confidence. If this tool failed to predict the localization, such proteins were further analysed using the program CELLO2GO (http://cello.life.nctu.edu.tw/cello2go/).

4.1.4.2 Functional annotation of identified proteins

Function of the identified proteins from the OMVs were predicted using EggNOG-mapper tool version 5.0 (http://eggnog-mapper.embl.de/). FASTA sequence file was uploaded, search filter was used as default and taxonomic scope was selected as gamma-proteobacteria. Result was obtained in excel format. Where COG category was mentioned for the successfully annotated proteins.

4.1.4.3 Prediction of OMV-host protein interaction network

In order to detect the interaction of pathogenic proteins from OMVs with human cellular proteins. Proteome of *Homo sapiens* (human) (Proteome id: UP000005640; 71, 599) from UniProt was used. The Host-Pathogen Interaction Database (HPIDB) was used to predict protein-protein interactions (PPI) between the MV proteome and the host proteome (Ammari et al., 2016). The protein data from OMVs was submitted in FASTA format, and homology-based search

results with virulence properties were obtained in the tabular form. The pathogenic protein having 98% query coverage were chosen and the interaction was studied with Human proteins.

4.1.5 OMVs in iron uptake

4.1.5.1 Preparation of radiolabeled ferric-enterobactin

Radiolabeled iron enterobactin complexes were prepared and purified using the following procedure, optimized by our laboratory (Parapatla et al., 2020). Initially, a stock solution of desferri-enterobactin (Sigma-Aldrich, USA) was prepared by dissolving 1 mg of desferri-enterobactin in 100 mL of dimethyl sulfoxide. About 3 mL of enterobactin stock solution was taken in a sterile Eppendorf tube, and 5 mL of ⁵⁵Fe was added from 0.2 mmol of ⁵⁵Fe stock (Specific activity, 44.6 mCi/mg, American Radiolabeled Chemicals, MO, USA) and incubated at room temperature for 5 min. The contents were made up to 50 mL with PBS buffer (pH 7.3) and unbound ⁵⁵Fe was removed by passing the reaction mix through a Sephadex G-25 column. The radiolabeled ferric-enterobactin eluted in the flowthrough was collected, and radioactivity was determined by taking 2 mL of ⁵⁵Fe-Ent into 5 mL of scintillation fluid [2,5-diphenyloxazole and 1, 4-bis (5 phenyl-2-oxazolyl) benzene]. The amount of radioactivity found in purified ⁵⁵Fe-Ent was measured using a Perkin Elmer Tri-Carb 2910TR scintillation counter. The work flow of this procedure is indicated in fig 4.2.



Figure 4. 2 Workflow for the preparation of ferric-Enterobactin.

4.1.5.2 Labeling of OMVs with ⁵⁵Fe-Ent

The ⁵⁵Fe-Ent (25 mL/166 pmol) was incubated with 200 mL of OMV (400mg protein) and the mixture was then incubated at 4°C for 2 h with end-to-end rotation, as shown in fig 4.3. After incubation, the OMVs were repurified by centrifuging the contents at 150,000 g for 2 h at 4°C. The supernatant was carefully removed, and the pelleted OMVs were redissolved and repurified by repeating the process until negligible counts were seen in the supernatant. The labelled OMVs were then resuspended in 50mL PBS (pH 7.3) and the amount of ⁵⁵Fe-Ent bound to OMVs was

determined by measuring the radioactivity. The labelled OMVs were then stored at -80°C until further use.

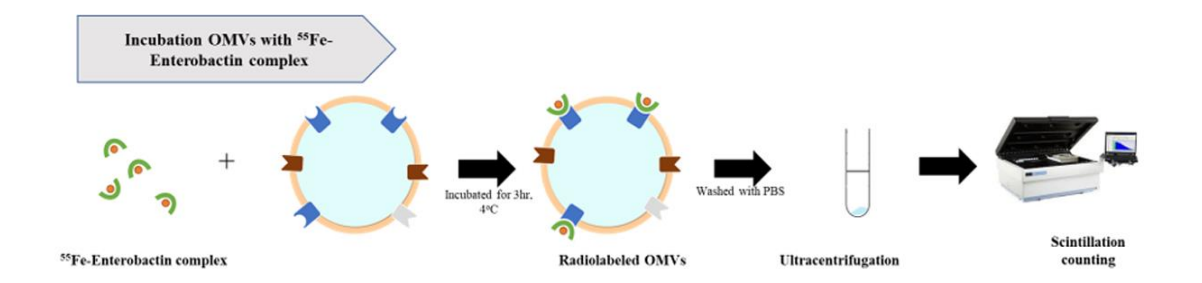


Figure 4. 3 Workflow for labelling of OMVs with ferric-Enterobactin complex.

4.1.5.3 Iron uptake studies

Initially, the *A. baumannii* DS002 cells were acclimatized to grow in minimal medium by growing them in iron sufficient (0.2 mg/mL) minimal medium. Once the culture OD₆₀₀ reached 0.7, the cells were harvested and reinoculated (OD₆₀₀ 0.05) in iron-limiting (0.002 mg/mL) minimal medium and allowed to grow at 30°C until the OD₆₀₀ reached 0.5. The cells were then harvested and washed twice with iron-free minimal salt medium. The cell pellet was then resuspended in iron-limiting medium to obtain a cell suspension of 1.0 OD₆₀₀. The cell suspension (100 mL) was incubated with ⁵⁵Fe-Ent labelled OMV (equivalent to 12 pmol of ⁵⁵Fe). Cells incubated with unlabelled OMVs served as a negative control. These cell suspensions were incubated overnight at 30°C to facilitate iron uptake. Cells were harvested from both the control and experimental samples and extensively washed (twice with 0.1 M LiCl2, then once with cold iron-free minimal medium) to remove surface-bound ⁵⁵Fe-Ent from the cells. The washed cell pellets were resuspended in 100 mL minimal media and the associated radioactivity was determined by pipetting 2 mL of the cells into 5 mL scintillation fluid (Fig 4.4).

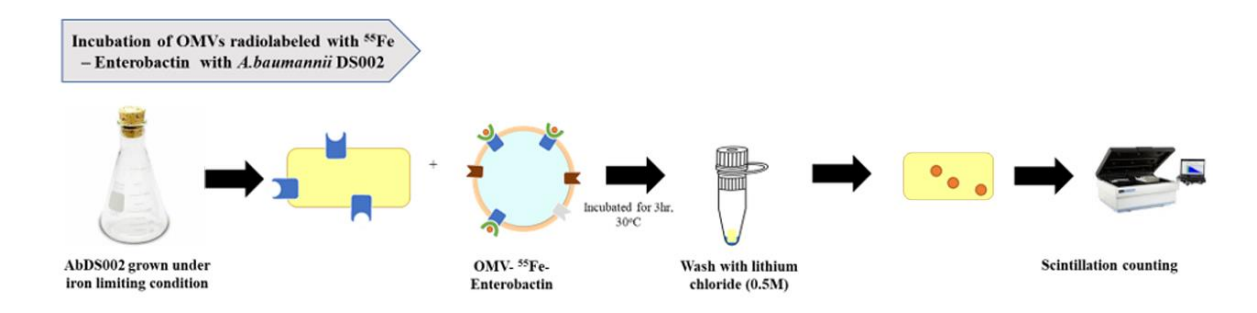


Figure 4. 4 Workflow representing the iron uptake study by *A. baumannii* DS002 grown under iron limiting conditions.

4.2 Results

The functional diversity of OMVs can be better assed and analysed by accurately identifying their protein composition. Therefore, the work described in the present chapter is entirely devoted to identify the proteins associated with OMVs of *A. baumannii* DS002. The functions of identified proteins were either predicted by using bioinformatic tools or validated by conducting experiments.

4.2.1 Identification of OMV proteome of A. baumannii DS002:

For gaining more insights into the identity of proteins associated with OMVs, we initially performed matrix-assisted laser desorption ionization-tandem time of flight (MALDI-TOF/TOF) analysis. The lane containing OMV proteins was divided into five zones, and the proteins present in each zone were identified by determining the peptide mass fingerprint and tandem mass spectrometry (MS-MS) analysis, as detailed in the Methods section (Fig 4.5 A, B & C). The prominent protein band in the lane was identified as OmpA by excising it from the gel and performing both MALDI and ESI-MS/MS studies (Fig 4.5 D, E & F).

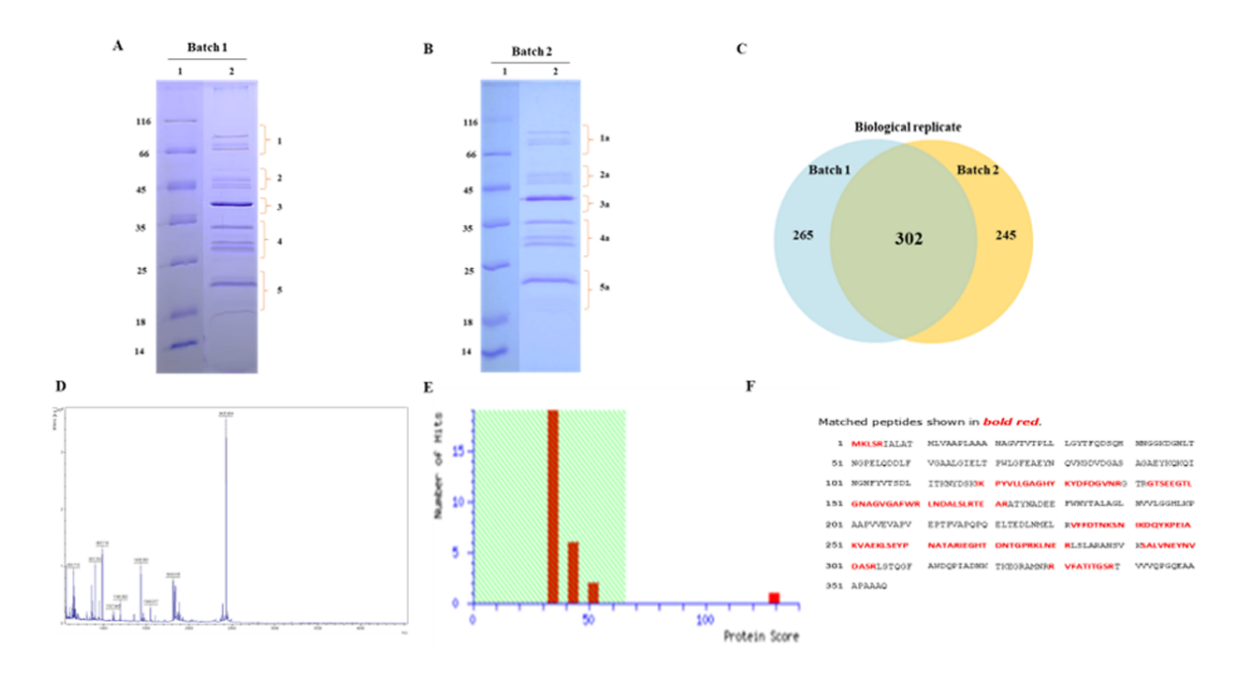


Figure 4. 5 Analysis of OMV proteins. Panels A and B show SDS-PAGE (12.5%) profile of total proteome extracted from OMVs isolated from culture supernatant collected from two independent *A. baumannii* DS002 cultures. Lanes 1 and 2 represent molecular size markers and OMV proteins respectively. Panel C is a Venn diagram showing the total 302 OMV proteins commonly identified from two biological replicates. The mass profile of tryptic digested peptide fragments and corresponding Mascot ID generated for prominent protein band is shown in panels D and E. Panel F shows the sequence of OmpA. The sequence highlighted in red colour indicate identity between the generated peptide sequences through MS/MS and OmpA.

The rest of the proteome of the OMVs was identified using LC-ESI-MS/MS analysis. OMVs isolated from two independent culture batches were used to minimize detection errors and to improve the identity of the number of proteins in OMVs. In total, 302 proteins were detected in OMVs isolated from *A. baumannii* DS002. Of these 302 proteins, the identities of 265 and 245 proteins were established from OMVs isolated from the first and second batches, respectively (Fig 4.5 C).

4.2.2 Subcellular origin of OMV proteome

Before analysing the functions of OMV proteins they were segregated into different groups based on their subcellular localization. Proteins use signature sequences, known as signal peptides to reach subcellular destinations. Once reached, the signal peptide is cleaved from precursor proteins. A number of online tools are available to predict presence of signal peptides from the precursor proteins and to suggest their subcellular localization. Online tool PSORTb version 3. was used to predict the subcellular origin of OMV proteins. The subcellular localization of the 302 proteins were predicted using PSORTb version 3. The online tools revealed segregated all 302 OMV proteins into various subcellular groups. As shown in fig 4.6 about 32% of the OMV proteins belong to outer membrane, 22% are periplasmic proteins, 27% are of cytoplasmic origin, 11% of inner membrane origin and 8% belong to extracellular proteins. Almost 54% of proteins are of OM and periplasmic origin suggesting that the OMVs prepared were pure (Fig 4.6)

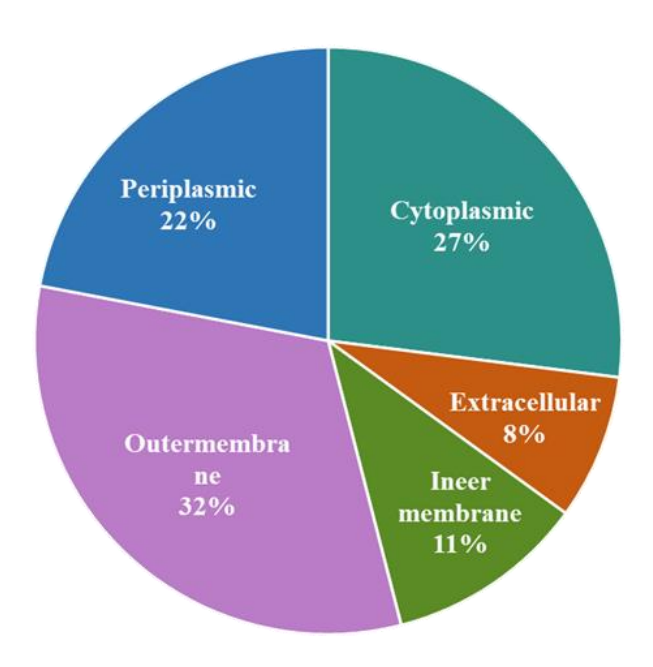


Figure 4. 6 Origin of OMV proteome. Pie chart indicating subcellular origin of OMV proteins as predicted by PSORTb version 3 and CELLO2GO.

Acc. No.	Protein Name	Description by EggNOG Mapper	COG category	FUNCTION CLASS	FUNCTION
AVP32905.1	Outer-membrane lipoprotein carrier protein	Participates in the translocation of lipoproteins from the inner membrane to the outer membrane. Only forms a complex with a lipoprotein if the residue after the N-terminal Cys is not an aspartate (The Asp acts as a targeting signal to indicate that the lipoprotein should stay in the inner membrane)	М	CELLULAR PROCESSES AND SIGNALING	Cell wall / membrane / envelope biogenesis (M)
AVP32912.1	Multidrug efflux pump subunit AcrA	Belongs to the membrane fusion protein (MFP) (TC 8.A.1) family	М	CELLULAR PROCESSES AND SIGNALING	Cell wall / membrane / envelope biogenesis (M)
AVP32993.1	Outer membrane protein Omp38	Belongs to the ompA family	М	CELLULAR PROCESSES AND SIGNALING	Cell wall / membrane / envelope biogenesis (M)
AVP33066.1	Photosystem I P700 chlorophyll a apoprotein A2	Belongs to the ompA family	М	CELLULAR PROCESSES AND SIGNALING	Cell wall / membrane / envelope biogenesis (M)
AVP33362.1	hypothetical protein C6W84_03545	Nucleoside-specific channel-forming protein, Tsx	М	CELLULAR PROCESSES AND SIGNALING	Cell wall / membrane / envelope biogenesis (M)
AVP33433.1	L-AlaD-Glu endopeptidase	Peptidase family M23	М	CELLULAR PROCESSES AND SIGNALING	Cell wall / membrane / envelope biogenesis (M)
AVP33493.1	Membrane-bound lytic murein transglycosylase B	Lytic murein transglycosylase	М	CELLULAR PROCESSES AND SIGNALING	Cell wall / membrane / envelope biogenesis (M)
AVP33501.1	Peptidyl-prolyl cis-trans isomerase A	PPlases accelerate the folding of proteins. It catalyzes the cis-trans isomerization of proline imidic peptide bonds in oligopeptides	М	CELLULAR PROCESSES AND SIGNALING	Cell wall / membrane / envelope biogenesis (M)
AVP33616.1	Vitamin B12 transporter BtuB	TonB dependent receptor	М	CELLULAR PROCESSES AND SIGNALING	Cell wall / membrane / envelope biogenesis (M)
AVP33651.1	D-alanyl-D-alanine endopeptidase	Belongs to the peptidase S11 family	М	CELLULAR PROCESSES AND SIGNALING	Cell wall / membrane / envelope biogenesis (M)
AVP33863.1	Tail-specific protease	Belongs to the peptidase S41A family	М	CELLULAR PROCESSES AND SIGNALING	Cell wall / membrane / envelope biogenesis (M)
AVP33874.1	Outer membrane protein assembly factor BamB	Part of the outer membrane protein assembly complex, which is involved in assembly and insertion of beta-barrel proteins into the outer membrane	М	CELLULAR PROCESSES AND SIGNALING	Cell wall / membrane / envelope biogenesis (M)
AVP33882.1	Toxin and drug export protein A	Outer membrane efflux protein	М	CELLULAR PROCESSES AND SIGNALING	Cell wall / membrane / envelope biogenesis (M)
AVP33884.1	LPS-assembly lipoprotein LptE	Together with LptD, is involved in the assembly of lipopolysaccharide (LPS) at the surface of the outer membrane. Required for the proper assembly of LptD. Binds LPS and may serve as the LPS recognition site at the outer membrane	М	CELLULAR PROCESSES AND SIGNALING	Cell wall / membrane / envelope biogenesis (M)
AVP34056.1	Outer-membrane lipoprotein LolB	Plays a critical role in the incorporation of lipoproteins in the outer membrane after they are released by the LoIA protein	М	CELLULAR PROCESSES AND SIGNALING	Cell wall / membrane / envelope biogenesis (M)
AVP34059.1	Outer membrane protein assembly factor BamD	Part of the outer membrane protein assembly complex, which is involved in assembly and insertion of beta-barrel proteins into the outer membrane	М	CELLULAR PROCESSES AND SIGNALING	Cell wall / membrane / envelope biogenesis (M)
AVP34094.1	putative lipoprotein YiaD	Belongs to the ompA family	М	CELLULAR PROCESSES AND SIGNALING	Cell wall / membrane / envelope biogenesis (M)
AVP34115.1	Gamma- glutamyltranspeptidase	Gamma-glutamyltranspeptidase	М	CELLULAR PROCESSES AND SIGNALING	Cell wall / membrane / envelope biogenesis (M)

AVP34209.1	Membrane-bound lytic murein	COG0741 Soluble lytic murein transglycosylase and related	М	CELLULAR PROCESSES	Cell wall / membrane / envelope
	transglycosylase D	regulatory proteins (some contain LysM invasin domains)		AND SIGNALING	biogenesis (M)
AVP34252.1	Putative lipoprotein	Curli production assembly/transport component CsgG	M	CELLULAR PROCESSES	Cell wall / membrane / envelope
				AND SIGNALING	biogenesis (M)
AVP34296.1	Metalloprotease LoiP	Peptidase family M48	M	CELLULAR PROCESSES	Cell wall / membrane / envelope
				AND SIGNALING	biogenesis (M)
AVP34558.1	hypothetical protein	Outer membrane protein (OmpH-like)	М	CELLULAR PROCESSES	Cell wall / membrane / envelope
	C6W84 11740			AND SIGNALING	biogenesis (M)
AVP34598.1	Putative phospholipase A1	Phospholipase	М	CELLULAR PROCESSES	Cell wall / membrane / envelope
7.1.0.000.1	T dtdt/f priosprionpase/ii	· mosphonpase		AND SIGNALING	biogenesis (M)
AVP34773.1	Major outer membrane	Gram-negative porin	М	CELLULAR PROCESSES	Cell wall / membrane / envelope
AVI 54775.1	protein P.IB	Grain negative porm	141	AND SIGNALING	biogenesis (M)
AVP34862.1	Chaperone SurA	Chaperone involved in the correct folding and assembly of outer	М	CELLULAR PROCESSES	Cell wall / membrane / envelope
AVP34002.1	Chaperone SurA	membrane proteins. Recognizes specific patterns of aromatic	IVI	AND SIGNALING	biogenesis (M)
		residues and the orientation of their side chains, which are found		AND SIGNALING	biogenesis (IVI)
		•			
		more frequently in integral outer membrane proteins. May act in			
		both early periplasmic and late outer membrane-associated steps			
		of protein maturation			
AVP34890.1	Beta-lactamase OXA-133	Penicillin binding protein transpeptidase domain	М	CELLULAR PROCESSES	Cell wall / membrane / envelope
				AND SIGNALING	biogenesis (M)
AVP35121.1	Membrane-bound lytic murein	Transglycosylase SLT domain	M	CELLULAR PROCESSES	Cell wall / membrane / envelope
	transglycosylase B			AND SIGNALING	biogenesis (M)
AVP35122.1	Endolytic peptidoglycan	Lytic transglycosylase with a strong preference for naked glycan	M	CELLULAR PROCESSES	Cell wall / membrane / envelope
	transglycosylase RlpA	strands that lack stem peptides		AND SIGNALING	biogenesis (M)
AVP35163.1	Putative L,D-transpeptidase	ErfK YbiS YcfS YnhG family protein	M	CELLULAR PROCESSES	Cell wall / membrane / envelope
	YkuD			AND SIGNALING	biogenesis (M)
AVP35285.1	Peptidoglycan-associated	Belongs to the ompA family	M	CELLULAR PROCESSES	Cell wall / membrane / envelope
	lipoprotein			AND SIGNALING	biogenesis (M)
AXU43350.1	Antibiotic efflux pump outer	Outer membrane efflux protein	М	CELLULAR PROCESSES	Cell wall / membrane / envelope
	membrane protein ArpC	, , , , , , , , , , , , , , , , , , ,		AND SIGNALING	biogenesis (M)
AXU43351.1	Solvent efflux pump outer	Outer membrane efflux protein	М	CELLULAR PROCESSES	Cell wall / membrane / envelope
7000 13331.1	membrane protein SrpC	outer memorane emax protein	***	AND SIGNALING	biogenesis (M)
AXU43387.1	Porin B	Carbohydrate-selective porin, OprB family	М	CELLULAR PROCESSES	Cell wall / membrane / envelope
AAO43367.1	TOTAL	Carbonydrate-selective porm, Opro family	IVI	AND SIGNALING	biogenesis (M)
AVII/12/127 1	AXU43427.1	COG0741 Soluble lytic murein transglycosylase and related	M	CELLULAR PROCESSES	Cell wall / membrane / envelope
AXU43427.1	AXU43427.1		IVI		T
AVIII 42 C22 4	harathatian and the	regulatory proteins (some contain LysM invasin domains)		AND SIGNALING	biogenesis (M)
AXU43632.1	hypothetical protein	Has lipid A 3-O-deacylase activity. Hydrolyzes the ester bond at the	М	CELLULAR PROCESSES	Cell wall / membrane / envelope
	C6W84_1565	3 position of lipid A, a bioactive component of lipopolysaccharide		AND SIGNALING	biogenesis (M)
		(LPS), thereby releasing the primary fatty acyl moiety			
AXU43670.1	putative FKBP-type peptidyl-	peptidyl-prolyl cis-trans isomerase	М	CELLULAR PROCESSES	Cell wall / membrane / envelope
	prolyl cis-trans isomerase FkpA			AND SIGNALING	biogenesis (M)
AXU43672.1	Polysialic acid transport	Polysaccharide biosynthesis/export protein	M	CELLULAR PROCESSES	Cell wall / membrane / envelope
	protein KpsD			AND SIGNALING	biogenesis (M)
43/11/42742	Soluble lytic murein	Transglycosylase SLT domain	М	CELLULAR PROCESSES	Cell wall / membrane / envelope
AXU43713.1	Soluble lytic murein	Transgrycosylase ser domain			
AXU43/13.1	transglycosylase	Transgrycosyluse SET domain		AND SIGNALING	biogenesis (M)
AXU43713.1 AXU43751.1	- T	OmpW family	M		

AXU43838.1	hypothetical protein C6W84 2595	OmpA family	М	CELLULAR PROCESSES AND SIGNALING	Cell wall / membrane / envelope biogenesis (M)
AXU43869.1	putative phospholipid-binding lipoprotein MlaA	MlaA lipoprotein	М	CELLULAR PROCESSES AND SIGNALING	Cell wall / membrane / envelope biogenesis (M)
AXU44210.1	Outer membrane protein assembly factor BamA	Part of the outer membrane protein assembly complex, which is involved in assembly and insertion of beta-barrel proteins into the outer membrane	М	CELLULAR PROCESSES AND SIGNALING	Cell wall / membrane / envelope biogenesis (M)
AXU44211.1	Outer membrane protein assembly factor BamA	Part of the outer membrane protein assembly complex, which is involved in assembly and insertion of beta-barrel proteins into the outer membrane	M	CELLULAR PROCESSES AND SIGNALING	Cell wall / membrane / envelope biogenesis (M)
AXU44499.1	hypothetical protein C6W84_5900	OmpW family	М	CELLULAR PROCESSES AND SIGNALING	Cell wall / membrane / envelope biogenesis (M)
AXU44500.1	hypothetical protein C6W84_5905	OmpW family	М	CELLULAR PROCESSES AND SIGNALING	Cell wall / membrane / envelope biogenesis (M)
AXU43614.1	hypothetical protein C6W84_1475	Gram-negative-bacterium-type cell outer membrane assembly	М	CELLULAR PROCESSES AND SIGNALING	Cell wall / membrane / envelope biogenesis (M)
AXU44343.1	LPS-assembly protein LptD	lipopolysaccharide transport	М	CELLULAR PROCESSES AND SIGNALING	Cell wall / membrane / envelope biogenesis (M)
AXU43372.1	putative NTE family protein	Esterase of the alpha-beta hydrolase superfamily	М	CELLULAR PROCESSES AND SIGNALING	Cell wall / membrane / envelope biogenesis (M)
AVP35179.1	D-alanyl-D-alanine carboxypeptidase DacA	Belongs to the peptidase S11 family	М	CELLULAR PROCESSES AND SIGNALING	Cell wall / membrane / envelope biogenesis (M)
AVP34631.1	Porin B	wide pore channel activity	М	CELLULAR PROCESSES AND SIGNALING	Cell wall / membrane / envelope biogenesis (M)
AVP35300.1	hypothetical protein C6W84 16625	Outer membrane efflux protein	М	CELLULAR PROCESSES AND SIGNALING	Cell wall / membrane / envelope biogenesis (M)
AVP34177.1	Lipoprotein NIpE	regulation of cell-substrate adhesion	М	CELLULAR PROCESSES AND SIGNALING	Cell wall / membrane / envelope biogenesis (M)
AVP32981.1	putative thiol:disulfide interchange protein DsbC	Required for disulfide bond formation in some periplasmic proteins. Acts by transferring its disulfide bond to other proteins and is reduced in the process	0	CELLULAR PROCESSES AND SIGNALING	Post-translational modification, protein turnover, and chaperones (O)
AVP33025.1	hypothetical protein C6W84_01290	META domain	0	CELLULAR PROCESSES AND SIGNALING	Post-translational modification, protein turnover, and chaperones (O)
AVP33520.1	Thiol:disulfide interchange protein DsbA	Thiol disulfide interchange protein	0	CELLULAR PROCESSES AND SIGNALING	Post-translational modification, protein turnover, and chaperones (O)
AXU44584.1	Periplasmic pH-dependent serine endoprotease DegQ	Belongs to the peptidase S1C family	0	CELLULAR PROCESSES AND SIGNALING	Post-translational modification, protein turnover, and chaperones (O)
AVP35272.1	hypothetical protein C6W84_16425	protein with SCP PR1 domains	0	CELLULAR PROCESSES AND SIGNALING	Post-translational modification, protein turnover, and chaperones (O)
AVP34606.1	ATP-dependent Clp protease ATP-binding subunit ClpA	Belongs to the ClpA ClpB family	0	CELLULAR PROCESSES AND SIGNALING	Post-translational modification, protein turnover, and chaperones (O)

			1	1	
AVP34461.1	Peptidyl-prolyl cis-trans isomerase cyp18	PPlases accelerate the folding of proteins. It catalyzes the cis-trans isomerization of proline imidic peptide bonds in oligopeptides	0	CELLULAR PROCESSES AND SIGNALING	Post-translational modification, protein turnover, and chaperones (O)
AVP34317.1	Alkyl hydroperoxide reductase subunit C	alkyl hydroperoxide reductase	0	CELLULAR PROCESSES AND SIGNALING	Post-translational modification, protein turnover, and chaperones (O)
AVP33947.1	Thioredoxin C-2	Belongs to the thioredoxin family	0	CELLULAR PROCESSES AND SIGNALING	Post-translational modification, protein turnover, and chaperones (O)
AVP33530.1	putative FKBP-type peptidyl- prolyl cis-trans isomerase FkpA	Peptidyl-prolyl cis-trans isomerase	0	CELLULAR PROCESSES AND SIGNALING	Post-translational modification, protein turnover, and chaperones (O)
AVP32929.1	Modulator of FtsH protease HflK	stress-induced mitochondrial fusion	0	CELLULAR PROCESSES AND SIGNALING	Post-translational modification, protein turnover, and chaperones (O)
AVP34707.1	Biopolymer transport protein ExbD	Biopolymer transport protein ExbD/ToIR	U	CELLULAR PROCESSES AND SIGNALING	Intracellular trafficking, secretion, and vesicular transport (U)
AVP34963.1	hypothetical protein C6W84_14240	hemolysin activation secretion protein	U	CELLULAR PROCESSES AND SIGNALING	Intracellular trafficking, secretion, and vesicular transport (U)
AVP35284.1	Protein TolB	Involved in the TonB-independent uptake of proteins	U	CELLULAR PROCESSES AND SIGNALING	Intracellular trafficking, secretion, and vesicular transport (U)
AXU43834.1	hypothetical protein C6W84_2575	TIGRFAM conserved repeat domain	U	CELLULAR PROCESSES AND SIGNALING	Intracellular trafficking, secretion, and vesicular transport (U)
AVP35252.1	Signal peptidase I	signal peptide processing	U	CELLULAR PROCESSES AND SIGNALING	Intracellular trafficking, secretion, and vesicular transport (U)
AVP33228.1	Type IV pilus biogenesis and competence protein PilQ	Type ii and iii secretion system protein	U	CELLULAR PROCESSES AND SIGNALING	Intracellular trafficking, secretion, and vesicular transport (U)
AXU44519.1	Beta-lactamase	Beta-lactamase	V	CELLULAR PROCESSES AND SIGNALING	Defense mechanisms (V)
AXU44520.1	Beta-lactamase	Beta-lactamase	V	CELLULAR PROCESSES AND SIGNALING	Defense mechanisms (V)
AVP34562.1	Cell division coordinator CpoB	TolA binding protein trimerisation	D	CELLULAR PROCESSES AND SIGNALING	Cell cycle control, cell division, chromosome partitioning (D)
AXU43953.1	Septum site-determining protein MinD	cell division	D	CELLULAR PROCESSES AND SIGNALING	Cell cycle control, cell division, chromosome partitioning (D)
AVP33531.1	Tyrosine-protein kinase ptk	protein tyrosine kinase activity	D	CELLULAR PROCESSES AND SIGNALING	Cell cycle control, cell division, chromosome partitioning (D)
AVP34373.1	hypothetical protein C6W84_10445	Universal stress protein	Т	CELLULAR PROCESSES AND SIGNALING	Signal transduction mechanisms (T)
AVP33997.1	Transcriptional regulatory protein RstA	Transcriptional regulatory protein, C terminal	Т	CELLULAR PROCESSES AND SIGNALING	Signal transduction mechanisms (T)

AVP33077.1	50S ribosomal protein L13	This protein is one of the early assembly proteins of the 50S ribosomal subunit, although it is not seen to bind rRNA by itself. It	J	INFORMATION STORAGE AND PROCESSING	Translation, ribosomal structure and biogenesis (J)
AVP33078.1	30S ribosomal protein S9	is important during the early stages of 50S assembly Belongs to the universal ribosomal protein uS9 family	J	INFORMATION STORAGE AND PROCESSING	Translation, ribosomal structure and biogenesis (J)
AVP33090.1	hypothetical protein C6W84_01765	Belongs to the RNase T2 family	J	INFORMATION STORAGE AND PROCESSING	Translation, ribosomal structure and biogenesis (J)
AVP33112.1	50S ribosomal protein L17	Ribosomal protein L17	J	INFORMATION STORAGE AND PROCESSING	Translation, ribosomal structure and biogenesis (J)
AVP33114.1	30S ribosomal protein S4	One of the primary rRNA binding proteins, it binds directly to 16S rRNA where it nucleates assembly of the body of the 30S subunit	J	INFORMATION STORAGE AND PROCESSING	Translation, ribosomal structure and biogenesis (J)
AVP33115.1	30S ribosomal protein S11	Located on the platform of the 30S subunit, it bridges several disparate RNA helices of the 16S rRNA. Forms part of the Shine-Dalgarno cleft in the 70S ribosome	J	INFORMATION STORAGE AND PROCESSING	Translation, ribosomal structure and biogenesis (J)
AVP33119.1	50S ribosomal protein L15	binds to the 23S rRNA	1	INFORMATION STORAGE AND PROCESSING	Translation, ribosomal structure and biogenesis (J)
AVP33122.1	50S ribosomal protein L18	This is one of the proteins that binds and probably mediates the attachment of the 5S RNA into the large ribosomal subunit, where it forms part of the central protuberance	J	INFORMATION STORAGE AND PROCESSING	Translation, ribosomal structure and biogenesis (J)
AVP33123.1	50S ribosomal protein L6	This protein binds to the 23S rRNA, and is important in its secondary structure. It is located near the subunit interface in the base of the L7 L12 stalk, and near the tRNA binding site of the peptidyltransferase center	J	INFORMATION STORAGE AND PROCESSING	Translation, ribosomal structure and biogenesis (J)
AVP33124.1	30S ribosomal protein S8	One of the primary rRNA binding proteins, it binds directly to 16S rRNA central domain where it helps coordinate assembly of the platform of the 30S subunit	J	INFORMATION STORAGE AND PROCESSING	Translation, ribosomal structure and biogenesis (J)
AVP33126.1	50S ribosomal protein L5	This is 1 of the proteins that binds and probably mediates the attachment of the 5S RNA into the large ribosomal subunit, where it forms part of the central protuberance. In the 70S ribosome it contacts protein S13 of the 30S subunit (bridge B1b), connecting the 2 subunits	J	INFORMATION STORAGE AND PROCESSING	Translation, ribosomal structure and biogenesis (J)
AVP33128.1	50S ribosomal protein L14	Binds to 23S rRNA. Forms part of two intersubunit bridges in the 70S ribosome	J	INFORMATION STORAGE AND PROCESSING	Translation, ribosomal structure and biogenesis (J)
AVP33131.1	50S ribosomal protein L16	Binds 23S rRNA and is also seen to make contacts with the A and possibly P site tRNAs	J	INFORMATION STORAGE AND PROCESSING	Translation, ribosomal structure and biogenesis (J)
AVP33132.1	30S ribosomal protein S3	Binds the lower part of the 30S subunit head. Binds mRNA in the 70S ribosome, positioning it for translation	J	INFORMATION STORAGE AND PROCESSING	Translation, ribosomal structure and biogenesis (J)
AVP33135.1	50S ribosomal protein L2	One of the primary rRNA binding proteins. Required for association of the 30S and 50S subunits to form the 70S ribosome, for tRNA binding and peptide bond formation. It has been suggested to have peptidyltransferase activity	J	INFORMATION STORAGE AND PROCESSING	Translation, ribosomal structure and biogenesis (J)
AVP33136.1	50S ribosomal protein L23	One of the early assembly proteins it binds 23S rRNA. One of the proteins that surrounds the polypeptide exit tunnel on the outside of the ribosome. Forms the main docking site for trigger factor binding to the ribosome	J	INFORMATION STORAGE AND PROCESSING	Translation, ribosomal structure and biogenesis (J)
AVP33138.1	50S ribosomal protein L3	One of the primary rRNA binding proteins, it binds directly near the 3'-end of the 23S rRNA, where it nucleates assembly of the 50S subunit	J	INFORMATION STORAGE AND PROCESSING	Translation, ribosomal structure and biogenesis (J)

AVP33206.1	50S ribosomal protein L19	This protein is located at the 30S-50S ribosomal subunit interface	1	INFORMATION STORAGE	Translation, ribosomal structure
AVI 33200.1	303 Hb030Hai protein E13	and may play a role in the structure and function of the aminoacyl-	,	AND PROCESSING	and biogenesis (J)
		tRNA binding site		7.110 1 110 02331110	and biogenesis (s)
AVP33686.1	50S ribosomal protein L11	Forms part of the ribosomal stalk which helps the ribosome	J	INFORMATION STORAGE	Translation, ribosomal structure
AVI 33000.1	303 fib030fffat protein E11	interact with GTP-bound translation factors	,	AND PROCESSING	and biogenesis (J)
AVP33687.1	50S ribosomal protein L1	Binds directly to 23S rRNA. The L1 stalk is quite mobile in the	J	INFORMATION STORAGE	Translation, ribosomal structure
AVP33087.1	505 fibosoffiai protein L1		J		
11/2010701	200 11 1 1 1 27	ribosome, and is involved in E site tRNA release		AND PROCESSING	and biogenesis (J)
AVP34079.1	30S ribosomal protein S7	One of the primary rRNA binding proteins, it binds directly to 16S	J	INFORMATION STORAGE	Translation, ribosomal structure
		rRNA where it nucleates assembly of the head domain of the 30S		AND PROCESSING	and biogenesis (J)
		subunit. Is located at the subunit interface close to the decoding			
		center, probably blocks exit of the E-site tRNA			
AVP34081.1	Elongation factor Tu	This protein promotes the GTP-dependent binding of aminoacyl-	J	INFORMATION STORAGE	Translation, ribosomal structure
		tRNA to the A-site of ribosomes during protein biosynthesis		AND PROCESSING	and biogenesis (J)
AVP34447.1	hypothetical protein	Part of the outer membrane protein assembly complex, which is	J	INFORMATION STORAGE	Translation, ribosomal structure
	C6W84_10985	involved in assembly and insertion of beta-barrel proteins into the		AND PROCESSING	and biogenesis (J)
		outer membrane			
AVP35129.1	30S ribosomal protein S2	Belongs to the universal ribosomal protein uS2 family	J	INFORMATION STORAGE	Translation, ribosomal structure
				AND PROCESSING	and biogenesis (J)
AXU43962.1	Outer membrane protein	Part of the outer membrane protein assembly complex, which is	J	INFORMATION STORAGE	Translation, ribosomal structure
	assembly factor BamE	involved in assembly and insertion of beta-barrel proteins into the		AND PROCESSING	and biogenesis (J)
		outer membrane			
AXU43769.1	30S ribosome-binding factor	rRNA processing	J	INFORMATION STORAGE	Translation, ribosomal structure
	_			AND PROCESSING	and biogenesis (J)
AXU43566.1	hypothetical protein	regulation of translation	J	INFORMATION STORAGE	Translation, ribosomal structure
	C6W84_1235			AND PROCESSING	and biogenesis (J)
AVP35171.1	50S ribosomal protein L31	rRNA binding	J	INFORMATION STORAGE	Translation, ribosomal structure
	·	-		AND PROCESSING	and biogenesis (J)
AVP35168.1	Elongation factor P	translation elongation factor activity	J	INFORMATION STORAGE	Translation, ribosomal structure
				AND PROCESSING	and biogenesis (J)
AVP35128.1	Elongation factor Ts	Associates with the EF-Tu.GDP complex and induces the exchange	J	INFORMATION STORAGE	Translation, ribosomal structure
		of GDP to GTP. It remains bound to the aminoacyl-tRNA.EF- Tu.GTP		AND PROCESSING	and biogenesis (J)
		complex up to the GTP hydrolysis stage on the ribosome			S ,
AVP35062.1	30S ribosomal protein S21	Belongs to the bacterial ribosomal protein bS21 family	J	INFORMATION STORAGE	Translation, ribosomal structure
	·	,		AND PROCESSING	and biogenesis (J)
AVP34819.1	30S ribosomal protein S20	rRNA binding	J	INFORMATION STORAGE	Translation, ribosomal structure
	, , , , , , , , , , , , , , , , , , ,			AND PROCESSING	and biogenesis (J)
AVP34553.1	Ribosome-recycling factor	cytoplasmic translational termination	J	INFORMATION STORAGE	Translation, ribosomal structure
		7,15,151		AND PROCESSING	and biogenesis (J)
AVP34407.1	30S ribosomal protein S6	Binds together with S18 to 16S ribosomal RNA	1	INFORMATION STORAGE	Translation, ribosomal structure
. () 1 107.1	CCC TIDOSOMAI PROCEIT SO	Sinds to potitor with 510 to 100 hb030illul lift.		AND PROCESSING	and biogenesis (J)
AVP34405.1	50S ribosomal protein L9	rRNA binding	1	INFORMATION STORAGE	Translation, ribosomal structure
AVI 34403.1	303 HD030Hai protein E3	THUS SHIGHING		AND PROCESSING	and biogenesis (J)
AVP34406.1	30S ribosomal protein S18	rRNA binding	1	INFORMATION STORAGE	Translation, ribosomal structure
AVF 34400.1	303 Hb030Hai protein 318	THINA MINNING	,	AND PROCESSING	and biogenesis (J)
AVP34078.1	30S ribosomal protein S12	rRNA binding	1	INFORMATION STORAGE	Translation, ribosomal structure
AVP34U/8.1	303 HDOSOIHai protein 312	Triva biliding	,		
				AND PROCESSING	and biogenesis (J)

AVP33936.1	50S ribosomal protein L20	Binds directly to 23S ribosomal RNA and is necessary for the in vitro	J	INFORMATION STORAGE	Translation, ribosomal structure
		assembly process of the 50S ribosomal subunit. It is not involved in the protein synthesizing functions of that subunit		AND PROCESSING	and biogenesis (J)
AVP33755.1	Polyribonucleotide	polyribonucleotide nucleotidyltransferase activity	J	INFORMATION STORAGE	Translation, ribosomal structure
	nucleotidyltransferase	, , , , , , , , , , , , , , , , , , , ,		AND PROCESSING	and biogenesis (J)
AVP33689.1	50S ribosomal protein L7/L12	mitochondrial gene expression	J	INFORMATION STORAGE	Translation, ribosomal structure
				AND PROCESSING	and biogenesis (J)
AVP33688.1	50S ribosomal protein L10	Forms part of the ribosomal stalk, playing a central role in the	J	INFORMATION STORAGE	Translation, ribosomal structure
		interaction of the ribosome with GTP-bound translation factors		AND PROCESSING	and biogenesis (J)
AVP33209.1	30S ribosomal protein S16	mitochondrial translation	J	INFORMATION STORAGE	Translation, ribosomal structure
AVP33139.1	30S ribosomal protein S10	o tanlarmia translation	1	AND PROCESSING INFORMATION STORAGE	and biogenesis (J) Translation, ribosomal structure
AVP33139.1	303 ribosomai protein 310	cytoplasmic translation	J	AND PROCESSING	and biogenesis (J)
AVP33137.1	50S ribosomal protein L4	Forms part of the polypeptide exit tunnel	1	INFORMATION STORAGE	Translation, ribosomal structure
	Joseph Margaretta	The state of the polypoptide data talline.		AND PROCESSING	and biogenesis (J)
AVP33134.1	30S ribosomal protein S19	Protein S19 forms a complex with S13 that binds strongly to the 16S	J	INFORMATION STORAGE	Translation, ribosomal structure
		ribosomal RNA		AND PROCESSING	and biogenesis (J)
AVP33133.1	50S ribosomal protein L22	The globular domain of the protein is located near the polypeptide	J	INFORMATION STORAGE	Translation, ribosomal structure
		exit tunnel on the outside of the subunit, while an extended beta-		AND PROCESSING	and biogenesis (J)
		hairpin is found that lines the wall of the exit tunnel in the center			
AVP33127.1	50S ribosomal protein L24	of the 70S ribosome One of the proteins that surrounds the polypeptide exit tunnel on	J	INFORMATION STORAGE	Translation, ribosomal structure
AVI 33127.1	303 Hb030Hai protein L24	the outside of the subunit	,	AND PROCESSING	and biogenesis (J)
AVP33125.1	30S ribosomal protein S14	Binds 16S rRNA, required for the assembly of 30S particles and may	J	INFORMATION STORAGE	Translation, ribosomal structure
		also be responsible for determining the conformation of the 16S		AND PROCESSING	and biogenesis (J)
		rRNA at the A site			
AVP33121.1	30S ribosomal protein S5	rRNA binding	J	INFORMATION STORAGE	Translation, ribosomal structure
A) (D22447.4	500 (1)	Polonosta tha hasta dal d'accomplanta a ha 20 fe cell	1	AND PROCESSING	and biogenesis (J)
AVP33117.1	50S ribosomal protein L36	Belongs to the bacterial ribosomal protein bL36 family	J	INFORMATION STORAGE AND PROCESSING	Translation, ribosomal structure and biogenesis (J)
AVP33116.1	30S ribosomal protein S13	Located at the top of the head of the 30S subunit, it contacts	1	INFORMATION STORAGE	Translation, ribosomal structure
7.01 55110.1	303 Haddelliai protein 313	several helices of the 16S rRNA. In the 70S ribosome it contacts the		AND PROCESSING	and biogenesis (J)
		23S rRNA (bridge B1a) and protein L5 of the 50S subunit (bridge			
		B1b), connecting the 2 subunits			
AVP32907.1	50S ribosomal protein L21	This protein binds to 23S rRNA in the presence of protein L20	J	INFORMATION STORAGE	Translation, ribosomal structure
				AND PROCESSING	and biogenesis (J)
AVP32940.1	hypothetical protein C6W84 00745	long-chain fatty acid transport protein	1	INFORMATION STORAGE AND PROCESSING	Lipid transport and metabolism (I)
AVP34156.1	Lipase 1	Alpha beta hydrolase	1	INFORMATION STORAGE	Lipid transport and metabolism
AVI 54150.1	Lipuse 1	Alpha beta flyarolase		AND PROCESSING	(I)
AVP33525.1	Non-hemolytic phospholipase	nuclear-transcribed mRNA catabolic process, deadenylation-	К	INFORMATION STORAGE	Transcription (K)
	C	dependent decay		AND PROCESSING	
AVP33113.1	DNA-directed RNA	RNA polymerase activity	К	INFORMATION STORAGE	Transcription (K)
	polymerase subunit alpha			AND PROCESSING	
AVP32848.1	Glycerophosphodiester	Glycerophosphoryl diester phosphodiesterase family	С	METABOLISM	Energy production and
	phosphodiesterase,				conversion (C)
	periplasmic				

AVP32886.1	Succinate dehydrogenase iron- sulfur subunit	succinate dehydrogenase	С	METABOLISM	Energy production and conversion (C)
AVP32887.1	Succinate dehydrogenase flavoprotein subunit	Belongs to the FAD-dependent oxidoreductase 2 family. FRD SDH subfamily	С	METABOLISM	Energy production and conversion (C)
AVP33604.1	ATP synthase subunit beta 1	Produces ATP from ADP in the presence of a proton gradient across the membrane. The catalytic sites are hosted primarily by the beta subunits	С	METABOLISM	Energy production and conversion (C)
AVP35306.1	Electron transfer flavoprotein subunit alpha	Electron transfer flavoprotein	С	METABOLISM	Energy production and conversion (C)
AVP35307.1	Electron transfer flavoprotein subunit beta	electron transfer activity	С	METABOLISM	Energy production and conversion (C)
AVP35144.1	Superoxide dismutase	Destroys radicals which are normally produced within the cells and which are toxic to biological systems	С	METABOLISM	Energy production and conversion (C)
AVP34412.1	Cytochrome bo(3) ubiquinol oxidase subunit 2	oxidoreductase activity, acting on a heme group of donors, oxygen as acceptor	С	METABOLISM	Energy production and conversion (C)
AVP34003.1	NADH-quinone oxidoreductase subunit I	NDH-1 shuttles electrons from NADH, via FMN and iron-sulfur (Fe-S) centers, to quinones in the respiratory chain. The immediate electron acceptor for the enzyme in this species is believed to be ubiquinone. Couples the redox reaction to proton translocation (for every two electrons transferred, four hydrogen ions are translocated across the cytoplasmic membrane), and thus conserves the redox energy in a proton gradient	С	METABOLISM	Energy production and conversion (C)
AVP34001.1	NADH-quinone oxidoreductase subunit G	ATP synthesis coupled electron transport	С	METABOLISM	Energy production and conversion (C)
AVP34000.1	NADH-quinone oxidoreductase subunit F	NDH-1 shuttles electrons from NADH, via FMN and iron- sulfur (Fe-S) centers, to quinones in the respiratory chain	С	METABOLISM	Energy production and conversion (C)
AVP33998.1	NADH-quinone oxidoreductase subunit B	NDH-1 shuttles electrons from NADH, via FMN and iron-sulfur (Fe-S) centers, to quinones in the respiratory chain. The immediate electron acceptor for the enzyme in this species is believed to be ubiquinone. Couples the redox reaction to proton translocation (for every two electrons transferred, four hydrogen ions are translocated across the cytoplasmic membrane), and thus conserves the redox energy in a proton gradien	С	METABOLISM	Energy production and conversion (C)
AVP32883.1	Dihydrolipoyllysine-residue succinyltransferase component of 2-oxoglutarate dehydrogenase complex	S-acyltransferase activity	С	METABOLISM	Energy production and conversion (C)
AVP32882.1	Dihydrolipoyl dehydrogenase	cell redox homeostasis	С	METABOLISM	Energy production and conversion (C)
AVP32881.1	SuccinateCoA ligase [ADP- forming] subunit beta	Succinyl-CoA synthetase functions in the citric acid cycle (TCA), coupling the hydrolysis of succinyl-CoA to the synthesis of either ATP or GTP and thus represents the only step of substrate-level phosphorylation in the TCA. The alpha subunit of the enzyme binds the substrates coenzyme A and phosphate, while succinate binding and nucleotide specificity is provided by the beta subunit	С	METABOLISM	Energy production and conversion (C)

AVP32880.1	SuccinateCoA ligase [ADP-	Succinyl-CoA synthetase functions in the citric acid cycle (TCA),	С	METABOLISM	Energy production and
	forming] subunit alpha	coupling the hydrolysis of succinyl-CoA to the synthesis of either			conversion (C)
		ATP or GTP and thus represents the only step of substrate-level phosphorylation in the TCA. The alpha subunit of the enzyme binds			
		the substrates coenzyme A and phosphate, while succinate binding			
ODV16400.1	Law (Na Mal hinding anatain	and nucleotide specificity is provided by the beta subunit		NATTA DOLICA A	Austra asid transport and
QDX16480.1	Leu/Ile/Val-binding protein (plasmid)	Receptor family ligand binding region	E	METABOLISM	Amino acid transport and metabolism (E)
QDX16481.1	hypothetical protein C6W84_16901 (plasmid)	Receptor family ligand binding region	E	METABOLISM	Amino acid transport and metabolism (E)
AXU44003.1	Esterase TesA	Lysophospholipase L1 and related esterases	E	METABOLISM	Amino acid transport and metabolism (E)
AVP34673.1	Endonuclease YhcR	5'-nucleotidase, C-terminal domain	F	METABOLISM	Nucleotide transport and metabolism (F)
AXU43517.1	Nuclease	DNA RNA non-specific endonuclease	F	METABOLISM	Nucleotide transport and metabolism (F)
AVP33460.1	hypothetical protein	TRAP-type C4-dicarboxylate transport system periplasmic	G	METABOLISM	Carbohydrate transport and
	C6W84_04265	component	_		metabolism (G)
AVP34135.1	Poly-beta-1,6-N-acetyl-D- glucosamine N-deacetylase	Hypothetical glycosyl hydrolase family 13	G	METABOLISM	Carbohydrate transport and metabolism (G)
AXU44186.1	6-phosphogluconolactonase	Lactonase, 7-bladed beta-propeller	G	METABOLISM	Carbohydrate transport and metabolism (G)
AXU43991.1	Aldose 1-epimerase	converts alpha-aldose to the beta-anomer	G	METABOLISM	Carbohydrate transport and metabolism (G)
AXU43615.1	Aldose sugar dehydrogenase	pyrroloquinoline quinone binding	G	METABOLISM	Carbohydrate transport and
	Ylil				metabolism (G)
AVP34386.1	Aldose sugar dehydrogenase YliI	pyrroloquinoline quinone binding	G	METABOLISM	Carbohydrate transport and metabolism (G)
AVP33022.1	Vitamin B12 transporter BtuB	TonB dependent receptor	Р	METABOLISM	Inorganic ion transport and metabolism (P)
AVP33193.1	Superoxide dismutase [Cu-Zn]	Destroys radicals which are normally produced within the cells and	Р	METABOLISM	Inorganic ion transport and
		which are toxic to biological systems			metabolism (P)
AVP33218.1	Bacterioferritin	Iron-storage protein, whose ferroxidase center binds Fe(2) ions, oxidizes them by dioxygen to Fe(3), and participates in the subsequent Fe(3) oxide mineral core formation within the central cavity of the protein complex	Р	METABOLISM	Inorganic ion transport and metabolism (P)
AVP33597.1	High-affinity zinc uptake system protein ZnuA	Zinc-uptake complex component A periplasmic	Р	METABOLISM	Inorganic ion transport and metabolism (P)
AVP33656.1	Fe(2+) transporter FeoB	Ferrous iron transport protein B	Р	METABOLISM	Inorganic ion transport and metabolism (P)
AVP34155.1	Ferric enterobactin receptor	TonB dependent receptor	Р	METABOLISM	Inorganic ion transport and metabolism (P)
AVP34214.1	Ferrichrome-iron receptor	TonB dependent receptor	Р	METABOLISM	Inorganic ion transport and metabolism (P)
AVP34241.1	Copper resistance protein B	Copper resistance protein B precursor (CopB)	Р	METABOLISM	Inorganic ion transport and metabolism (P)
AVP34247.1	Membrane lipoprotein TpN32	NLPA lipoprotein	Р	METABOLISM	Inorganic ion transport and metabolism (P)

AVP34394.1	Membrane lipoprotein TpN32	NLPA lipoprotein	Р	METABOLISM	Inorganic ion transport and metabolism (P)
AVP34448.1	hypothetical protein C6W84_10985	Domain of unknown function (DUF4198)	Р	METABOLISM	Inorganic ion transport and metabolism (P)
AVP34597.1	putative TonB-dependent receptor BfrD	TonB dependent receptor	Р	METABOLISM	Inorganic ion transport and metabolism (P)
AVP34668.1	Molybdate-binding periplasmic protein	Bacterial extracellular solute-binding protein	Р	METABOLISM	Inorganic ion transport and metabolism (P)
AVP35155.1	Colicin I receptor	TonB dependent receptor	Р	METABOLISM	Inorganic ion transport and metabolism (P)
AVP35190.1	Phosphate-binding protein PstS	PBP superfamily domain	Р	METABOLISM	Inorganic ion transport and metabolism (P)
AVP35260.1	Sulfate-binding protein	sulfate ABC transporter	Р	METABOLISM	Inorganic ion transport and metabolism (P)
AVP35425.1	Ferric aerobactin receptor	TonB dependent receptor	Р	METABOLISM	Inorganic ion transport and metabolism (P)
AXU43383.1	hypothetical protein C6W84_0320	TonB dependent receptor	Р	METABOLISM	Inorganic ion transport and metabolism (P)
AXU43384.1	Ferric aerobactin receptor	TonB dependent receptor	Р	METABOLISM	Inorganic ion transport and metabolism (P)
AXU43402.1	putative TonB-dependent receptor	TonB-dependent receptor	Р	METABOLISM	Inorganic ion transport and metabolism (P)
AXU43592.1	Ferrichrome receptor FcuA	TonB-dependent Receptor Plug Domain	Р	METABOLISM	Inorganic ion transport and metabolism (P)
AXU43593.1	Ferrichrome receptor FcuA	TonB-dependent Receptor Plug Domain	Р	METABOLISM	Inorganic ion transport and metabolism (P)
AXU43696.1	Ferrichrome-iron receptor	TonB dependent receptor	Р	METABOLISM	Inorganic ion transport and metabolism (P)
AXU43811.1	putative TonB-dependent receptor BfrD	TonB dependent receptor	Р	METABOLISM	Inorganic ion transport and metabolism (P)
AXU43812.1	putative TonB-dependent receptor BfrD	TonB dependent receptor	Р	METABOLISM	Inorganic ion transport and metabolism (P)
AXU44011.1	hypothetical protein C6W84_3460	Capsule assembly protein Wzi	Р	METABOLISM	Inorganic ion transport and metabolism (P)
AXU44161.1	FhuE receptor	TonB dependent receptor	Р	METABOLISM	Inorganic ion transport and metabolism (P)
AXU44162.1	Ferripyoverdine receptor	Receptor	Р	METABOLISM	Inorganic ion transport and metabolism (P)
AXU44299.1	FhuE receptor	TonB dependent receptor	Р	METABOLISM	Inorganic ion transport and metabolism (P)
AXU44326.1	Vitamin B12 transporter BtuB	TonB dependent receptor	Р	METABOLISM	Inorganic ion transport and metabolism (P)
QDX16513.1	Fe(3+) dicitrate transport protein FecA (plasmid)	TonB dependent receptor	Р	METABOLISM	Inorganic ion transport and metabolism (P)
QDX16557.1	Ferrichrome-iron receptor (plasmid)	TonB dependent receptor	Р	METABOLISM	Inorganic ion transport and metabolism (P)

AVP34153.1	Arylsulfatase	Arylsulfatase A and related enzymes	Р	METABOLISM	Inorganic ion transport and metabolism (P)
AXU43452.1	putative phospholipid-binding protein MIaC	MlaC protein	Q	METABOLISM	Secondary metabolites biosynthesis, transport, and catabolism (Q)
AXU44046.1	Copper resistance protein A	Multicopper oxidase	Q	METABOLISM	Secondary metabolites biosynthesis, transport, and catabolism (Q)
AVP35097.1	hypothetical protein C6W84_15235	COG0457 FOG TPR repeat	Н	METABOLISM	Coenzyme transport and metabolism (H)
AVP32927.1	putative NTE family protein	Patatin-like phospholipase	S	POORLY CHARACTERIZED	Function unknown (S)
AVP32953.1	hypothetical protein C6W84 00820	Protein of unknown function (DUF1176)	S	POORLY CHARACTERIZED	Function unknown (S)
AVP32954.1	hypothetical protein C6W84 00825	Domain of unknown function (DUF4850)	S	POORLY CHARACTERIZED	Function unknown (S)
AVP32982.1	Secretory immunoglobulin A- binding protein EsiB	Sel1-like repeats.	S	POORLY CHARACTERIZED	Function unknown (S)
AVP33073.1	hypothetical protein C6W84_01640	Uncharacterized protein conserved in bacteria (DUF2147)	S	POORLY CHARACTERIZED	Function unknown (S)
AVP33095.1	hypothetical protein C6W84_01800	Protein of unknown function (DUF3108)	S	POORLY CHARACTERIZED	Function unknown (S)
AVP33169.1	hypothetical protein C6W84_02255	Lysozyme inhibitor Lprl	S	POORLY CHARACTERIZED	Function unknown (S)
AVP33311.1	hypothetical protein C6W84_03245	Putative general bacterial porin	S	POORLY CHARACTERIZED	Function unknown (S)
AVP33352.1	hypothetical protein C6W84_03490	Uncharacterized protein conserved in bacteria (DUF2147)	S	POORLY CHARACTERIZED	Function unknown (S)
AVP33356.1	hypothetical protein C6W84_03510	Putative MetA-pathway of phenol degradation	S	POORLY CHARACTERIZED	Function unknown (S)
AVP33613.1	hypothetical protein C6W84_05275	LysM domain	S	POORLY CHARACTERIZED	Function unknown (S)
AVP33624.1	hypothetical protein C6W84_05365	Esterase-like activity of phytase	S	POORLY CHARACTERIZED	Function unknown (S)
AVP33637.1	Porin D	outer membrane porin, OprD family	S	POORLY CHARACTERIZED	Function unknown (S)
AVP33638.1	hypothetical protein C6W84_05455	Bacterial protein of unknown function (Gcw_chp)	S	POORLY CHARACTERIZED	Function unknown (S)
AVP33837.1	hypothetical protein C6W84_06755	Bacterial protein of unknown function (DUF839)	S	POORLY CHARACTERIZED	Function unknown (S)
AVP33838.1	hypothetical protein C6W84_06760	Bacterial protein of unknown function (DUF839)	S	POORLY CHARACTERIZED	Function unknown (S)
AVP33844.1	Secretory immunoglobulin A- binding protein EsiB	Sel1-like repeats.	S	POORLY CHARACTERIZED	Function unknown (S)
AVP33891.1	hypothetical protein C6W84_07095	TIGRFAM conserved repeat domain	S	POORLY CHARACTERIZED	Function unknown (S)
AVP34205.1	hypothetical protein C6W84_09380	BON domain	S	POORLY CHARACTERIZED	Function unknown (S)

AVP34250.1	Putative lipoprotein	Putative bacterial lipoprotein (DUF799)	S	POORLY CHARACTERIZED	Function unknown (S)
AVP34251.1	hypothetical protein C6W84_09710	Domain of unknown function (DUF4810)	S	POORLY CHARACTERIZED	Function unknown (S)
AVP34383.1	hypothetical protein C6W84_10550	ABC-type transport auxiliary lipoprotein component	S	POORLY CHARACTERIZED	Function unknown (S)
AVP34662.1	hypothetical protein C6W84_12355	Bacterial protein of unknown function (Gcw_chp)	S	POORLY CHARACTERIZED	Function unknown (S)
AVP34766.1	hypothetical protein C6W84_13005	TonB C terminal	S	POORLY CHARACTERIZED	Function unknown (S)
AVP34785.1	hypothetical protein C6W84 13125	Histidine phosphatase superfamily (branch 2)	S	POORLY CHARACTERIZED	Function unknown (S)
AVP34883.1	Protein Ycel	Ycel-like domain	S	POORLY CHARACTERIZED	Function unknown (S)
AVP34945.1	hypothetical protein C6W84_14120	Tetratricopeptide repeat	S	POORLY CHARACTERIZED	Function unknown (S)
AVP35115.1	hypothetical protein C6W84_15360	Secretory lipase	S	POORLY CHARACTERIZED	Function unknown (S)
AVP35195.1	hypothetical protein C6W84_15930	Protein of unknown function (DUF541)	S	POORLY CHARACTERIZED	Function unknown (S)
AVP35212.1	putative zinc protease	Belongs to the peptidase M16 family	S	POORLY CHARACTERIZED	Function unknown (S)
AVP35370.1	hypothetical protein C6W84_07080	Domain of unknown function DUF11	S	POORLY CHARACTERIZED	Function unknown (S)
AVP35404.1	hypothetical protein C6W84_10920	Protein of unknown function (DUF2799)	S	POORLY CHARACTERIZED	Function unknown (S)
AXU43373.1	hypothetical protein C6W84_0270	Entericidin EcnA/B family	S	POORLY CHARACTERIZED	Function unknown (S)
AXU43553.1	hypothetical protein C6W84_1170	Putative general bacterial porin	S	POORLY CHARACTERIZED	Function unknown (S)
AXU43836.1	hypothetical protein C6W84_2585	cell adhesion involved in biofilm formation	S	POORLY CHARACTERIZED	Function unknown (S)
AXU44089.1	hypothetical protein C6W84_3850	Peptidase M15	S	POORLY CHARACTERIZED	Function unknown (S)
AXU44481.1	Ferri-bacillibactin esterase BesA	Putative esterase	S	POORLY CHARACTERIZED	Function unknown (S)
QDX16474.1	Porin-like protein NicP (plasmid)	outer membrane porin, OprD family	S	POORLY CHARACTERIZED	Function unknown (S)
QDX16497.1	hypothetical protein C6W84_16917 (plasmid)	Spore Coat Protein U domain	S	POORLY CHARACTERIZED	Function unknown (S)
QDX16498.1	hypothetical protein C6W84_16918 (plasmid)	Spore Coat Protein U domain	S	POORLY CHARACTERIZED	Function unknown (S)
QDX16499.1	hypothetical protein C6W84_16919 (plasmid)	Spore Coat Protein U domain	S	POORLY CHARACTERIZED	Function unknown (S)
QDX16502.1	F1 capsule-anchoring protein (plasmid)	Outer membrane usher protein	S	POORLY CHARACTERIZED	Function unknown (S)
AXU43623.1	hypothetical protein C6W84_1520	START domain	S	POORLY CHARACTERIZED	Function unknown (S)

Proteome of OMVs

AVP34588.1	hypothetical protein C6W84_11915	Uncharacterized protein conserved in bacteria (DUF2057)	S	POORLY CHARACTERIZED	Function unknown (S)
AVP34366.1	Lipopolysaccharide export system protein LptA	lipopolysaccharide binding	S	POORLY CHARACTERIZED	Function unknown (S)
AVP33805.1	hypothetical protein C6W84_06540	Lysozyme inhibitor Lprl	S	POORLY CHARACTERIZED	Function unknown (S)
AVP35175.1	Murein hydrolase activator NIpD	Peptidase family M23	DM		
AVP34941.1	Glutaminase-asparaginase	Asparaginase	EJ		
AVP34920.1	Glutamate/aspartate import solute-binding protein	Bacterial periplasmic substrate-binding proteins	ET		
AVP35112.1	Lysine/arginine/ornithine- binding periplasmic protein	Bacterial periplasmic substrate-binding proteins	ET		
AXU43664.1	putative oxidoreductase YciK	KR domain	IQ		
AVP32926.1	hypothetical protein C6W84_00650	Forms passive diffusion pores that allow small molecular weight hydrophilic materials across the outer membrane	MU		
AXU43745.1	Outer membrane protein TolC	Outer membrane efflux protein	MU		
AVP33220.1	Fimbrial protein	Belongs to the N-Me-Phe pilin family	NU		
AVP35185.1	hypothetical protein C6W84_15855	Domain of unknown function	NU		
AXU43819.1	Lipopolysaccharide assembly protein B	Tetratricopeptide repeat	NU		
QDX16500.1	putative fimbrial chaperone YadV (plasmid)	Pili and flagellar-assembly chaperone, PapD N-terminal domain	NU		
AVP34824.1	Oligopeptide transport system permease protein OppC	ABC-type dipeptide oligopeptide nickel transport systems permease components	EP		
AVP33889.1	Ketol-acid reductoisomerase (NADP(+)	ketol-acid reductoisomerase activity	EH		
AVP32856.1	hypothetical protein C6W84_00190	Not Detected			
AVP33009.1	hypothetical protein C6W84_01200	Not Detected			
AVP33028.1	hypothetical protein C6W84_01320	Not Detected			
AVP33176.1	hypothetical protein C6W84_02305	Not Detected			
AVP33177.1	hypothetical protein C6W84_02310	Not Detected			
AVP33248.1	hypothetical protein C6W84_02790	Not Detected			
AVP33279.1	hypothetical protein C6W84_03020	Not Detected			
AVP33373.1	hypothetical protein C6W84_03620	Not Detected			
AVP33580.1	hypothetical protein C6W84_05085	Not Detected			

AVP33692.1	hypothetical prote C6W84_05820	in Not Detected		
AVP33693.1	hypothetical prote C6W84_05825	in Not Detected		
AVP33699.1	hypothetical prote C6W84_05865	in Not Detected		
AVP33802.1	hypothetical prote C6W84_06525	in Not Detected		
AVP33804.1	hypothetical prote C6W84_06535	in Not Detected		
AVP34186.1	hypothetical prote C6W84_09235	in Not Detected		
AVP34268.1	hypothetical prote C6W84_09800	in Not Detected		
AVP34313.1	hypothetical prote C6W84_10080	in Not Detected		
AVP34423.1	hypothetical prote C6W84_10805	in Not Detected		
AVP34425.1	hypothetical prote C6W84_10815	in Not Detected		
AVP34632.1	hypothetical prote C6W84_12180	in Not Detected		
AVP34767.1	hypothetical prote C6W84_13010	in Not Detected		
AVP35073.1	hypothetical prote C6W84_15080	in Not Detected		
AVP35178.1	hypothetical prote C6W84_15815	in Not Detected		
AVP35249.1	hypothetical prote C6W84_16295	in Not Detected		
AVP35266.1	hypothetical prote C6W84_16390	in Not Detected		
AVP35269.1	hypothetical prote C6W84_16410	in Not Detected		
AVP35311.1	hypothetical prote C6W84_16710	in Not Detected		
AVP35340.1	hypothetical prote C6W84_03585	in Not Detected		
AXU44227.1	hypothetical prote C6W84_4540	in Not Detected		
AXU44229.1	hypothetical prote C6W84_4550	in Not Detected		
QDX16346.1	hypothetical prote C6W84_16836 (plasmid)	in Not Detected		
QDX16454.1	hypothetical prote C6W84_16874 (plasmid)	in Not Detected		

AXU43671.1	hypothetical protein	Not Detected	I	
	C6W84_1760			
AXU43832.1	hypothetical protein	Not Detected		
	C6W84_2565			
AXU44012.1	hypothetical protein	Not Detected		
	C6W84_3465			
QDX16345.1	hypothetical protein	Not Detected		
	C6W84_16835 (plasmid)			
QDX16527.1	hypothetical protein	Not Detected		
	C6W84_16947 (plasmid)			
QDX16528.1	hypothetical protein	Not Detected		
	C6W84_16948 (plasmid)			
AXU43800.1	hypothetical protein	Not Detected		
	C6W84_2405			
AVP35177.1	hypothetical protein	Not Detected		
A) (D2 4772 4	C6W84_15810	N. D. L. L.		
AVP34770.1	hypothetical protein	Not Detected		
AV/D246464	C6W84_13030	Not Potential		
AVP34616.1	hypothetical protein	Not Detected		
AVP34515.1	C6W84_12080	Not Detected		
AVP34515.1	hypothetical protein C6W84 11490	Not Detected		
AVP33197.1	hypothetical protein	Not Detected		
AVP33197.1	C6W84 02440	Not Detected		
AVP33179.1	hypothetical protein	Not Detected		
AVI 33173.1	C6W84 02335	Not betetted		
AVP33107.1	hypothetical protein	Not Detected		
AVI 55107.1	C6W84 01910	Not beteeted		
AVP32961.1	hypothetical protein	Not Detected		
	C6W84 00880	1		
AVP32904.1	hypothetical protein	Not Detected		
	C6W84 00515			

After establishing the identity and subcellular localization of the OMV proteins, these proteins were further clustered them into orthologous groups (COG) using EggNOG mapper tool. The names of these 302 proteins given as input to the EggNOG mapper tool is shown in Table 4.2. The online EggNOG mapper could only assign functions to 254 proteins out of 302 OMV proteins. The COG clustering included 76 OMV proteins with cellular process and signalling, 63 with metabolism, and 56 with information storage and processing. Surprisingly, 46 proteins were identified within the group of poorly characterized proteins (Fig 4.7). The COG categorization showed that the majority of OMV proteins are related to inorganic ion transport and storage, cell wall/membrane biogenesis, and pathogenesis (Fig 4.07).

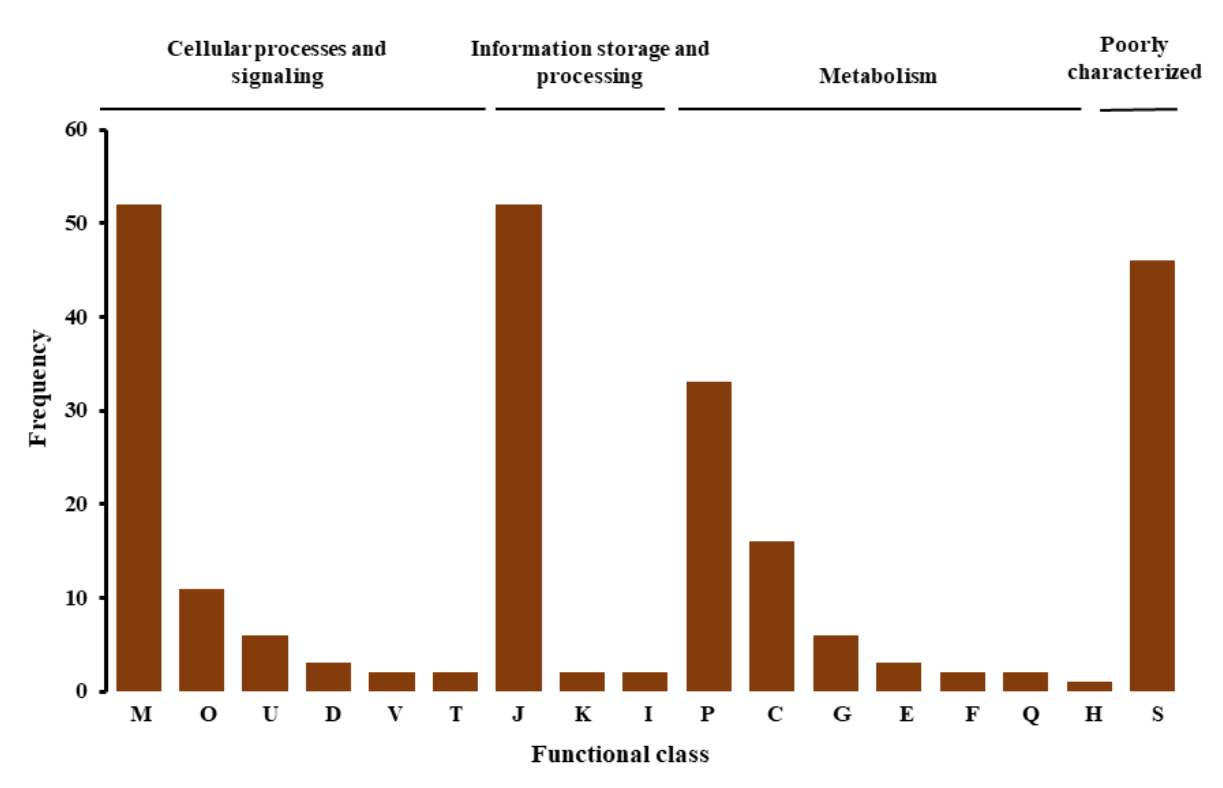


Figure 4. 7 Cluster of orthologous group (COG) categorization of OMV proteins: The letters in X-axis indicate proteins performing various functions: M, cell wall/membrane/envelope biogenesis; O, posttranslational modification, protein turnover, and chaperones; U, intracellular trafficking, secretion, and vesicular transport; D, cell cycle control, cell division, and chromosome partitioning; V, defence mechanisms; T, signal transduction mechanisms; J, translation, ribosomal structure and biogenesis; K, transcription; I, lipid transport and metabolism; P, inorganic ion transport and metabolism; C, energy production and conversion; G, carbohydrate transport and metabolism; E, amino acid transport and metabolism; F, nucleotide transport and metabolism; Q, secondary metabolites biosynthesis, transport, and catabolism; H, coenzyme transport and metabolism; and S, function unknown.

The biological functions of the OMV proteins were also assessed by performing gene ontology studies. According to the gene ontology, the majority of OMV proteins are involved in biological processes such as transport, translation, and pathogenesis (Fig 4.8 A). Ion binding,

transmembrane transport, and RNA binding appear to be the other main molecular functions of OMV proteins (Fig 4.8 B).

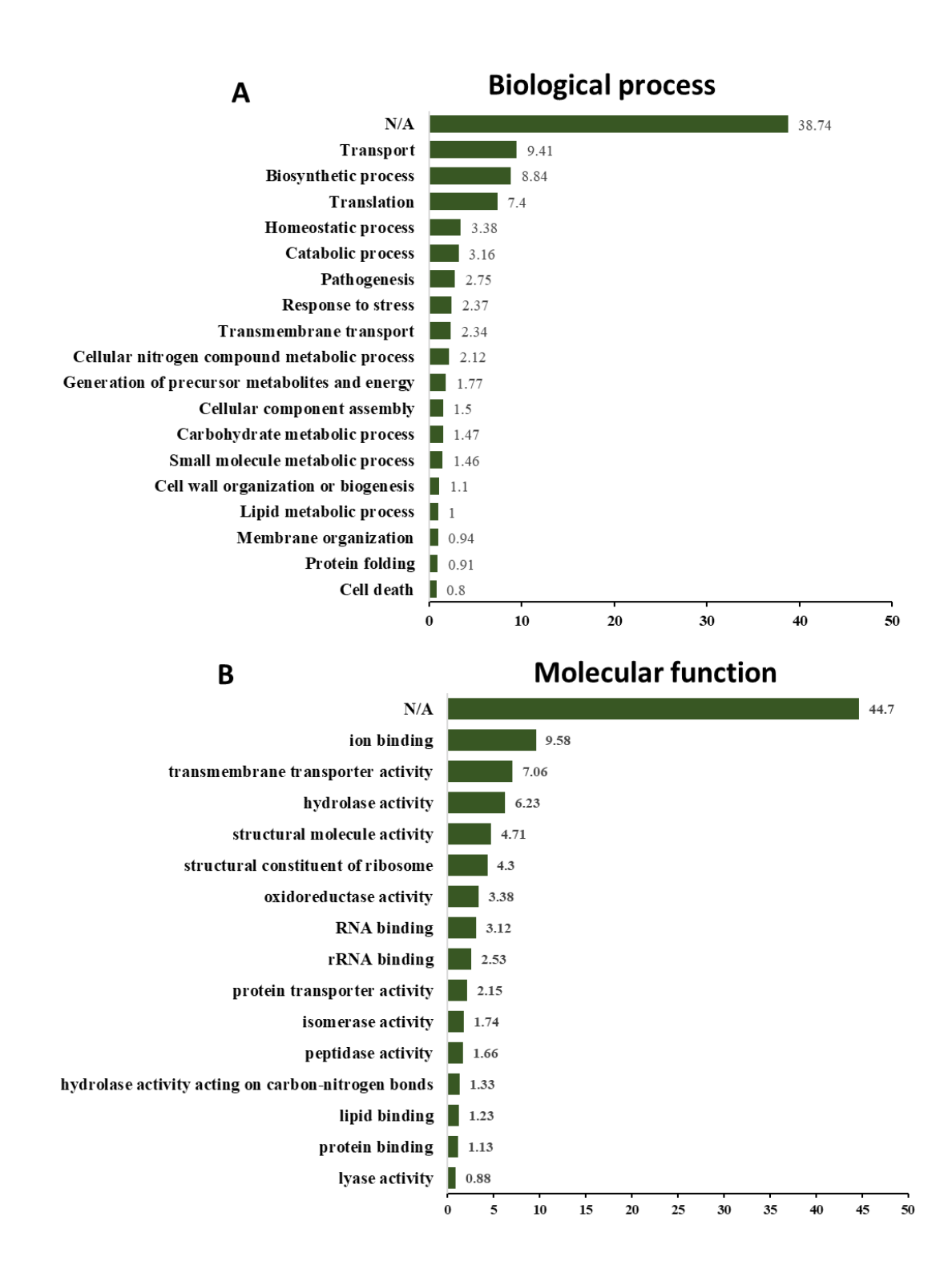


Figure 4. 8 Classification of OMV proteome of *A. baumannii* **DS002.** MV associated proteins were grouped based on their GO (A) Biological processes (BP). (B) Molecular functions (MF).

4.2.3 Significant Proteins of OMVs:

The OMVs contain Beta lactamases, multidrug efflux proteins like AroC, SrpC, TolC and other proteins playing an important role in drug resistance and increasing the survival of the bacteria. They are also a set of proteins modulating the host immune response like Porins, lipoproteins, YiaD, TpN32, peptidoglycan associated lipoprotein and serine endo protease DegQ, superoxidase dismutase and bacterioferritin (Fig 4.9).

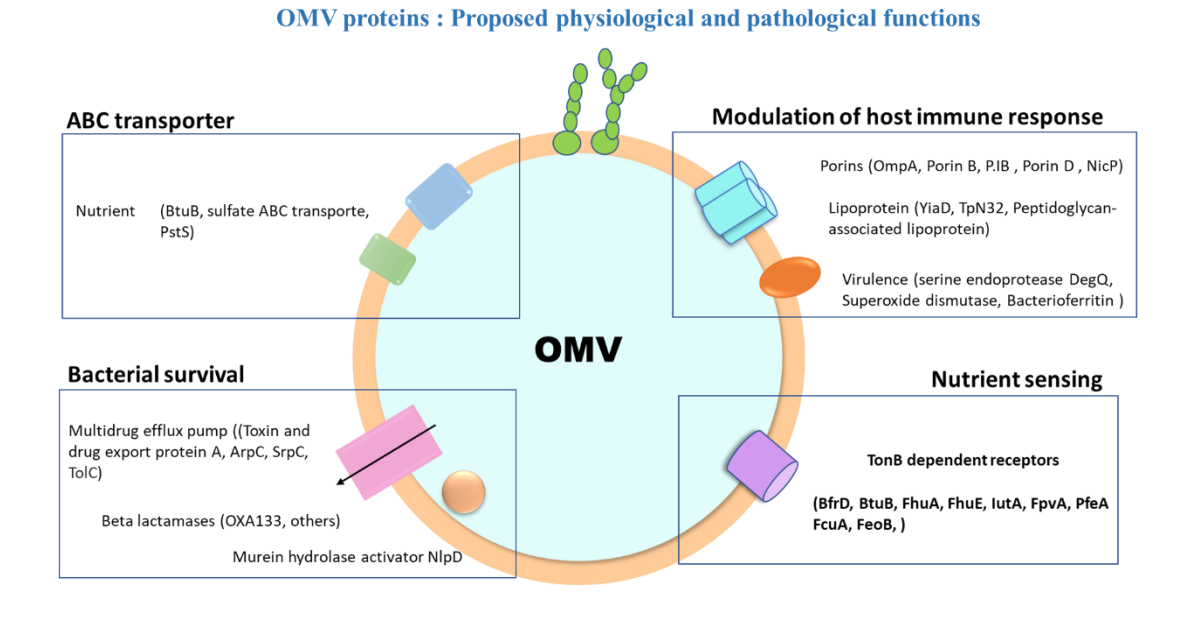


Figure 4. 9 Representation of Proteins associated with OMV of *A. baumannii* DS002 with important functions.

4.2.4 EF-TU is among the OMV-associated proteins

Proteins such as elongation factor Tu (EF-Tu), curli protein transporter, CsgG, SdhA, SdhB and peptidyl prolyl cis-trans isomerase are also detected in the OMV proteome. As virulence factors were seen among OMV proteins and interaction network map was generated by including the OMV proteins with human proteome (Fig 4.10). The Host-Pathogen Interaction Database (HPIDB) predicted interactions of OMV proteins with key human proteins that influence immune response, transcription factors and proteins that mediate inflammation etc. The detailed interaction map is shown in fig 4.10. As shown in the predicted interaction map, elongation factor, EF-Tu is part of OMV proteome that interacts with several crucial human proteins. Identification of EF-Tu with outer membrane and OMVs is not uncommon. A number of studies have highlighted its existence in OMVs and its moonlighting activities (Bai et al., 2014; Dineshkumar et al., 2020). EF-Tu is known to interact with immune system regulators such as

Factor H, substance P, and plasminogen, and thus increases virulence by helping immune system evasion (N'Diaye et al., 2019). Recent studies have also demonstrated a decreased bacterial load in subjects with antibodies against EF-Tu (Harvey et al., 2019). EF-Tu has also been shown to interact with fibronectins and glycosaminoglycans to facilitate adhesion of bacteria to human cells (Henderson et al., 2011). Peptidyl-prolyl isomerases (PPIs) play a key role in protein folding by catalysing the cis-trans isomerisation of peptide bonds N-terminal to proline residues. The isomerization process contributes to the mechanical properties of materials required to generate various extracellular matrices (Kumawat et al., 2020). Extracellular matrices are also generated during biofilm formation. Therefore, the association of EF-Tu and PPI with OMVs, which have a proven role in biofilm formation, is not surprising.

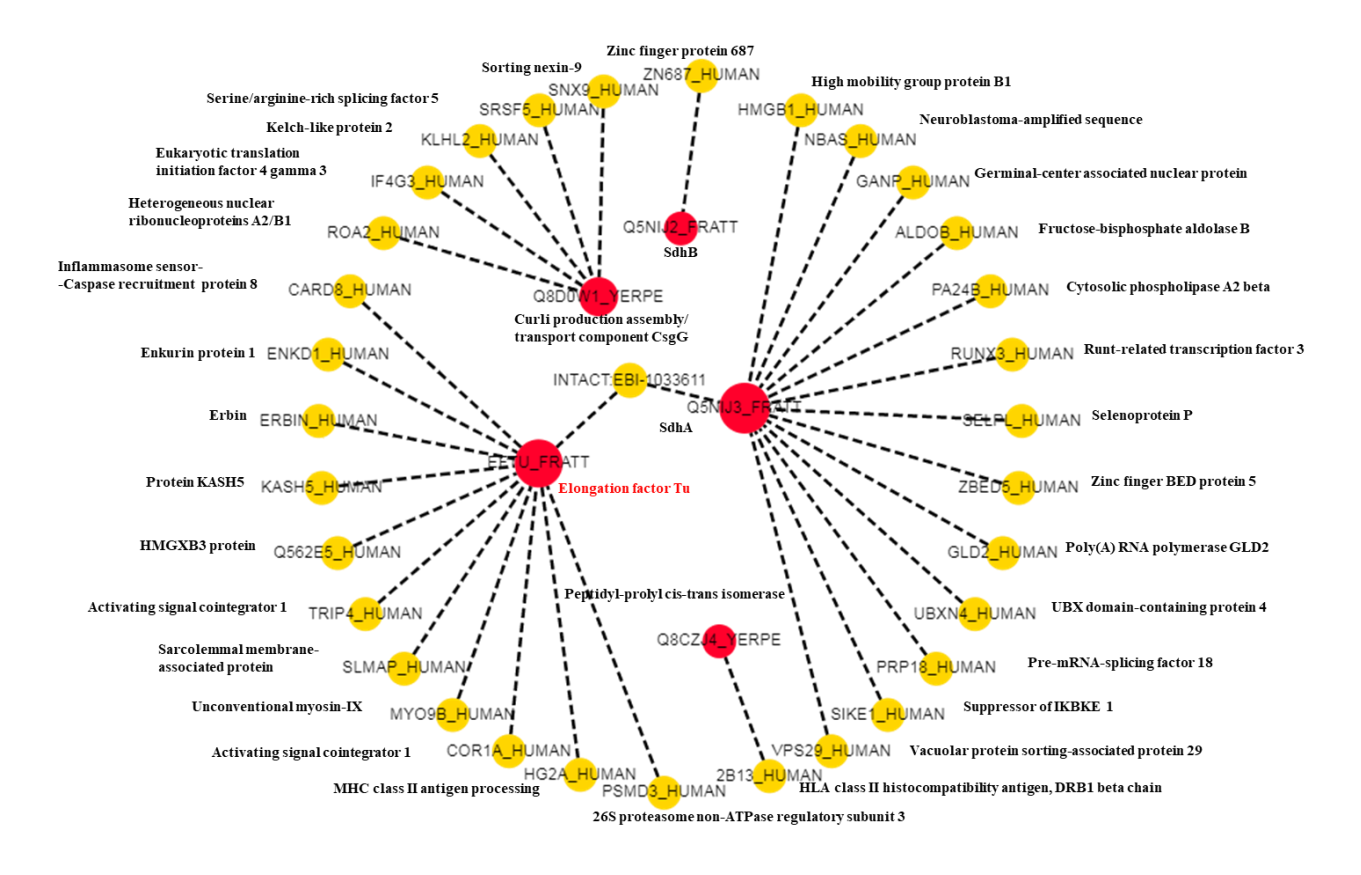


Figure 4. 10 Virulence proteins in OMVs of A. baumannii DS002.

4.2.5 TonB-dependent transporters are enriched in OMVs

The TonB-dependent transporters (TonRs) actively transport several nutrients, including iron, across the energy-deprived outer membrane of Gram-negative bacteria (Ferguson & Deisenhofer, 2002). They use energy generated by the inner membrane-associated Ton-complex while transporting siderophores complexed to iron across the outer membrane. The genome of *A. baumannii* DS002 codes for several TonRs, which transport all three major types of

Proteome of OMVs

siderophores. Intriguingly, the genetic repertoire required for the synthesis of corresponding siderophores are absent in the genome of DS002 (Yakkala et al., 2019). In the absence of siderophores, DS002 cells must acquire iron using siderophores synthesized and secreted by cohabiting bacteria. Outer membrane vesicles (OMVs) play a critical role in meeting the nutritional requirements of the host. They carry various nutrients, including iron, due to the presence of membrane transporters and iron-binding proteins.

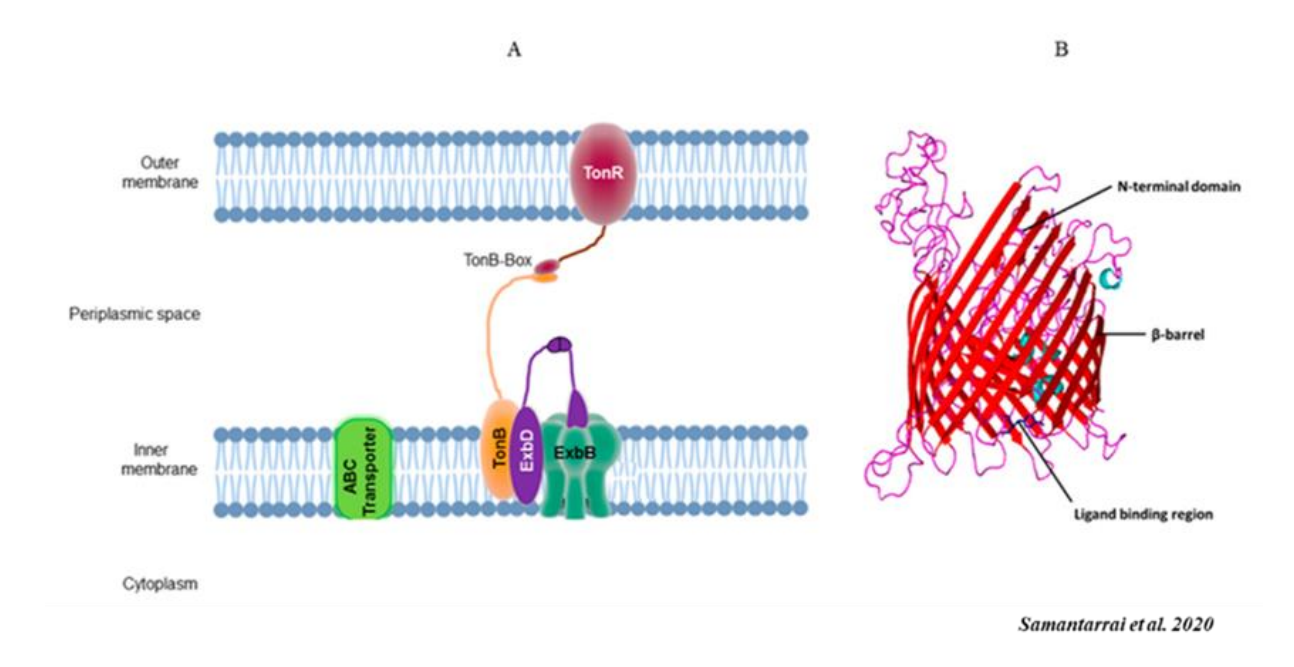


Figure 4. 11 TonB dependent transport system: (A) Schematic representation of TonB-dependent transport system. (B) Typical structure of an outer membrane transporter (TBDT), representing 22 β -barrel structure with N-terminal plug domain, and substrate binding motif.

A majority of OMV proteins performing transport functions are TonB-dependent transporters (TonRs). TonRs play a key role in the active transport of nutrients across energy-deprived outer membranes. TonRs are different from outer membrane porins. Substrates pass through porins by diffusion, whereas in TonRs, nutrients exceeding 600 Da in size cross the outer membrane by utilizing the energy generated by the inner membrane-localized Ton-complex (Wiener, 2005). The Ton-complex contains ExbB/ExbD and TonB, where the proton motive force (PMF) components, ExbB/ExbD, generate energy and TonB harvests energy and transduces it to outer membrane-localized TonRs (Ahmer et al., 1995; Larsen et al., 1996) (Fig 4.11). TonRs have unique structural features that are very distinct from porins. The C-terminal region of TonR contains 22 antiparallel β -strands which form a membrane-spanning barrel domain, and it is significantly bigger than the barrel domain of porins (Ferguson & Deisenhofer, 2002). In addition, the TonRs contain an N-terminal plug domain which obstructs the passage of solutes. Substrates to be transported are specifically recognized by the plug domain or by the external loops of the

barrel, independent of the involvement of the energy transducer TonB (Usher et al., 2001). However, the translocation of substrate into periplasmic space requires a functional Toncomplex. The five-amino acids-long TonB box motif (ETVIV) found at the plug domain interacts with the C-terminal domain of the energy transducer TonB to obtain the energy required for transporting a substrate bound to plug domain (Noinaj et al., 2010; Tuckman & Osburne, 1992).

The EggNOG mapper identified 24 OMV proteins as TonRs (Table 2.3). These TonR sequences were then re-examined to verify whether the OMV-associated TonRs had sequence motifs typically seen in well-characterized TonRs. Out of 24 TonR sequences, only 19 were full-length TonRs, and the rest of the 5 had either C-terminal or N-terminal truncations. Only 19 full-length TonRs of OMV proteome was taken for further analysis (Table 4.3).

Table 4. 3 List of TonB dependent receptors proteins detected from OMVs of A. baumannii

Accession no. (gi no)	Protein name	Gene name	Mol. weight (kDa)	PI	sequence coverage (%)	#peptides
1472139223	putative TonB-dependent receptor BfrD	bfrD_1	67.1	6.96	58	36
1472139224	putative TonB-dependent receptor BfrD	bfrD_2	19.7	8.94	52	11
1367986576	putative TonB-dependent receptor BfrD	bfrD_3	77.9	6.15	48	36
1367985001	Vitamin B12 transporter BtuB	btuB_1	67.9	5.27	68	43
1367985595	Vitamin B12 transporter BtuB	btuB_2	77.4	6.19	37	25
1472139738	Vitamin B12 transporter BtuB	btuB_3	45	5.2	9	3
1472138795	hypothetical protein C6W84_0320	C6W84_0320	16.7	5.07	9	1
1472138814	putative TonB-dependent receptor	C6W84_0415	16.7	5.07	8	3
1367986745	hypothetical protein C6W84_13005	C6W84_13005	14.2	5.24	67.5	6
1367987134	Colicin I receptor	cirA_2	100.8	7.66	5	3
1472139004	Ferrichrome receptor FcuA	fcuA_1	26	6.55	15	4
1472139005	Ferrichrome receptor FcuA	fcuA_2	41.4	6.8	28	7
1714623787	Fe(3+) dicitrate transport protein FecA (plasmid)	fecA	77.2	5.47	57	29
1367985635	Fe(2+) transporter FeoB	feoB	67.5	7.05	2	1
1472139108	Ferrichrome-iron receptor	fhuA_3	80.1	6.02	11	6
1367986193	Ferrichrome-iron receptor	fhuA_4	78.2	5.81	37	21
1714623831	Ferrichrome-iron receptor (plasmid)	fhuA_5	76.6	5.47	43	32
1472139573	FhuE receptor	fhuE_1	52.3	4.91	4	1
1472139711	FhuE receptor	fhuE_2	79.2	5.06	25	14
1472139574	Ferripyoverdine receptor	fpvA	11.7	8.88	10	1
1472138796	Ferric aerobactin receptor	iutA_1	63.3	5.82	14	8
1367987404	Ferric aerobactin receptor	iutA_3	80.7	5.35	53	37
1367986134	Ferric enterobactin receptor	pfeA	82.8	5.78	15	11
1472139893	Ferri-bacillibactin esterase BesA	besA	35.6	8.9	5	1

4.2.6 Functional classification of OMV TonRs:

Since, TonRs are known to transport many nutrients in addition to iron, two independent approaches were followed to ascertain the putative functions of OMV-associated TonRs. In the first approach, a phylogenetic tree for OMV-associated TonRs was constructed by including

functionally characterized TonR sequences (Letunic & Bork, 2007). Based on the cladding pattern, putative functions were assigned to the TonRs of OMVs (Fig 4.12). The generated phylogram contained eight clades, numbered from C-I to C-VIII (Fig 4.12). Interestingly, clades C-I and C-II represent TonRs of pathogenic bacteria, transporting ferritin, heme, and carbohydrates such as maltodextrin and sucrose. Interestingly, none of the OMV TonRs of DS002 are found in these two clades. Most of the TonRs of OMVs of DS002 are identified in clades C-VI, C-VII, and C-VIII. The clade C-VI contains six OMV TonRs, and they have clustered with TonRs transporting both catecholate (Fiu) and phenolate (FyuA) type siderophores. Incidentally, all OMV TonRs of DS002 have branched out to form a separate sub-clade, suggesting that they are unique from TonRs transporting phenolate and catecholate type siderophores (Noinaj et al., 2010). Clades V-II and V-III represent six TonRs of DS002, two of which formed clade C-VII by clustering with TonRs transporting pyochelin (FptA), alcaligin (FauA), and pyoverdine (FpvA), and the remaining four DS002 TonRs formed clade C-VIII by aligning well with FoxA and FhuA, which transport iron complexed with ferrioxamine (FoxA) and ferrichrome (FhuA). The cladding pattern suggests that the six TonRs present in these two clades might also transport iron complexed with five deferent types of siderophores. In addition to iron transporters, clade C-III, with its two sub-clades, contained both copper- and zinc-transporting TonRs. There are two DS002 TonRs in these two sub-clades: BtuB2, aligned with copper transporters NosA and OprC (H. S. Lee et al., 1991; Yoneyama & Nakae, 1996); and TonR1, with zinc transporter ZnuD (Mobarak Qamsari et al., 2020). Likewise, clade C-IV also contains two sub-clades, and in one of them, two DS002 TonRs, BtuB1 and CirA, have clustered with cobalamin-transporting BtuB (Shultis et al., 2006). Sub-clade 2 of clade C-IV contains one DS002 TonR, which seems to align well with the ferric enterobactin (Fe-Ent) transporter, FepA. Clade C-V, with five TonRs is divided into two sub-clades. In sub-clade S1, plasmid-encoded TonR (AbFecA*) is clustered with FecA of E. coli. Similarly, in sub-clade S2, OMV TonR, annotated as AblutA3, is clustered with BfnH of A. baumannii ATCC 19606. BfnH transports iron bound to acinetobactin (Aghajani et al., 2019; Eijkelkamp et al., 2011). AblutA3 seems to have a role in the transport of acinetobactin complexed with iron.

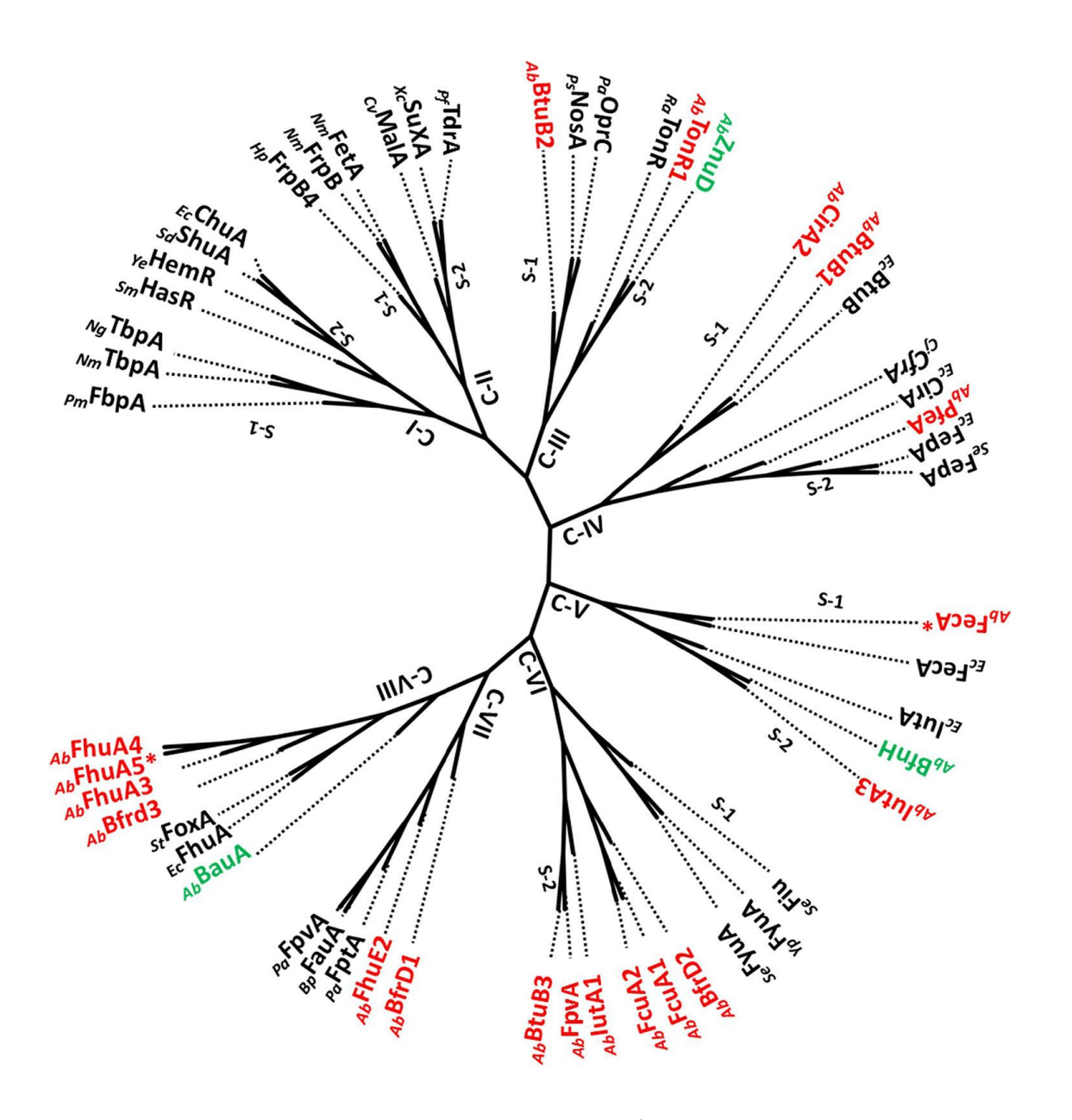


Figure 4. 12 Unrooted Phylogram constructed by including functionally characterized TonB dependent transporters (TonRs) along with TonRs of OMVs of A. baumannii DS002. TonRs shown in black colour font are functionally characterized. The TonRs shown in green colour font are functionally characterized TonRs from A. baumannii strains. The OMV associated TonRs are shown with red colour font. The plasmid coded TonRs are indicated with '*' symbol. The TonRs of Pasteurella multocida (PmFbpA), Neisseria meningitidis (NmTbpA, NmFrpB, NmFetA), Neisseria gonorrhoeae (NgTbpA), Serratia marcescens (SmHasR), Yersinia enterocolitica (YeHemR), Shigella dysenteriae (SdShuA), Escherichia coli (EcChuA, EcBtuB, EcCirA, EcFepA, EcFecA, EclutA, EcFhuA), Helicobacter pylori (HpFrpB4), Caulobacter vibrioides, (CvMalA), Xanthomonas campestris (XcSuxA), Pseudomonas fluorescens (PfTdrA), Pseudomonas stutzeri (PsNosA), Pseudomonas aeruginosa (PaOprC, PaFptA, PaFpvA), Riemerella anatipestifer (RaTonR), Campylobacter jejuni (CjCfrA), Salmonella_enterica (SeFiu, SeFyuA), Yersinia pestis (YpFyuA), Bordetella pertussis (BpFauA), Salmonella typhimurium (StFoxA) were included while constructing phylogram.

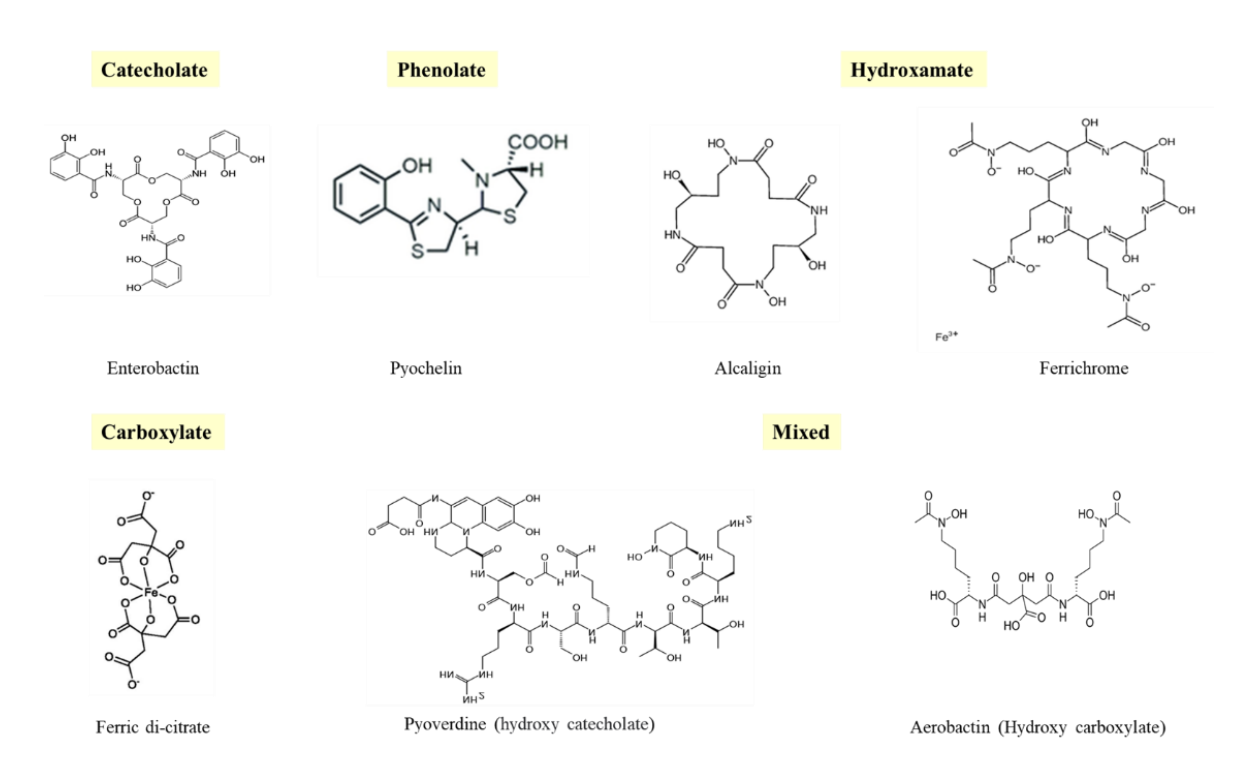


Figure 4. 13 Molecular structure of siderophores. Represents different class of siderophores based on functional groups attached to along with the examples from each group.

4.2.7 Transcription factor Fur regulates expression of TonRs:

In the cladogram described in fig 4.12, some of the TonRs of OMVs have clustered with functionally characterized TonB-dependent transporters. These TonRs transport iron complexed with many different types of siderophores. Such alignment of OMV proteins with functionally characterized TonRs suggests their involvement in iron transport through sideraphores. Proteins involved in iron acquisition are coded by genes regulated by ferric uptake regulatory protein (Fur). Fur is a dual-transcription regulator and regulates genes in response to the intracellular iron concentration (Escolar et al., 1999). Since, Fur binds to the conserved fur-box motif, the upstream region of tonR coding gene were examined to identify fur-box motif (Bailey et al., 2015). The analysis revealed the presence of a well-conserved fur-box overlapping the promoters of seven TonR-coding genes (Fig 4.14). In addition to the fur-box motif, certain tonR genes contained conserved sequence motifs overlapping their promoter regions. These sequence motifs serve as targets for the transcription factors LexA and OmpR. These two transcription factors respond to oxidative stress and osmolarity, respectively (Chakraborty & Kenney, 2018; Leaden et al., 2018). Iron deficiency is known to induce oxidative stress, and LexA and OmpR counter this stress by modulating the expression of several genes (Leaden et al., 2018). However,

the existence of TonRs under the control of LexA and OmpR is rather unusual and warrants further studies to explain the relationship between TonR expression and extracellular osmolarity.

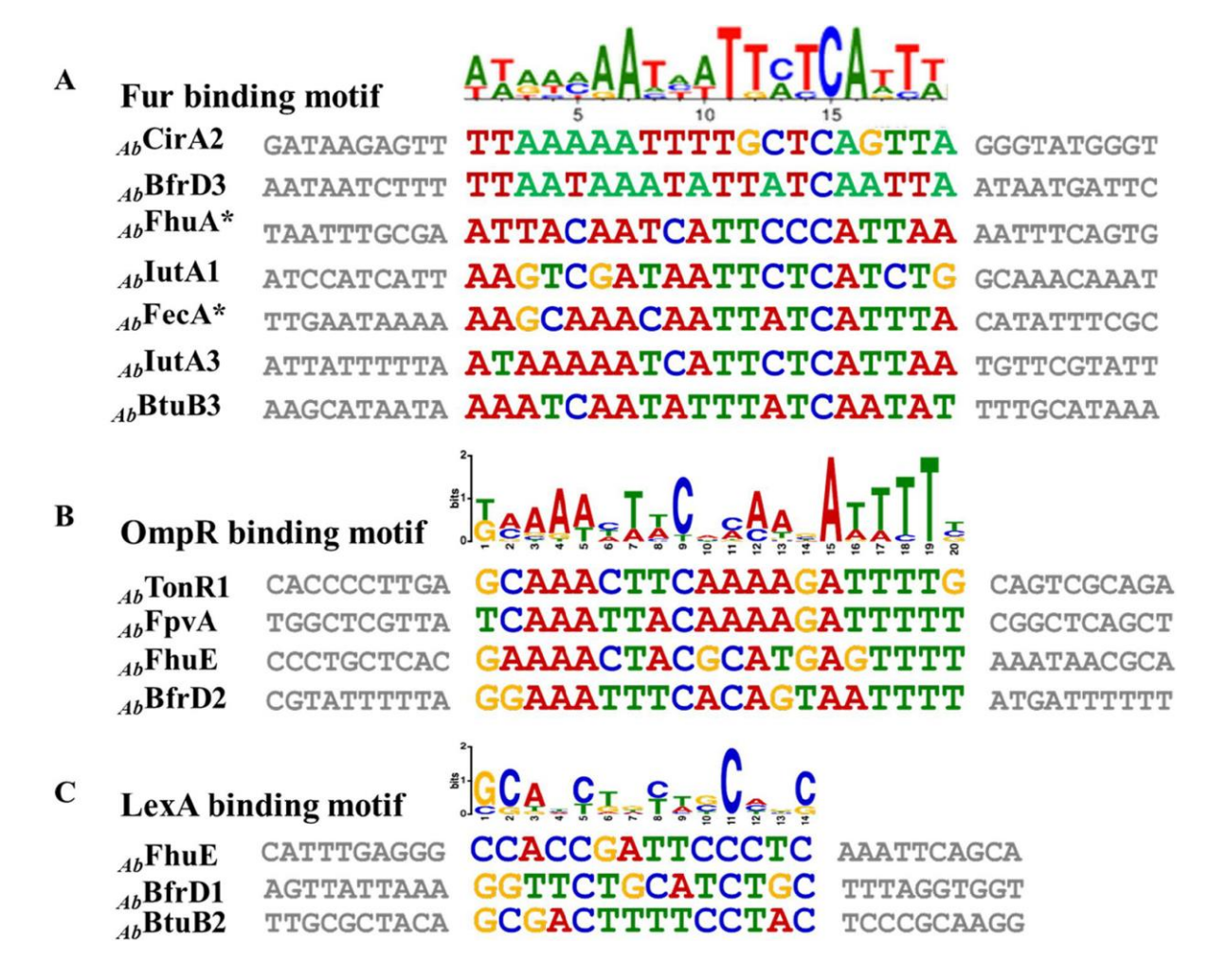


Figure 4. 14 Predicted transcription factor binding motifs overlapping TonR coding genes. Panel A shows fur-box motif predicted overlapping the promoters of genes coding AbCirA2, AbBfrD3, AbFhuA*, AbIutA1, AbFecA*, AbIutA3, AbBtuB3. The OmpR binding sites identified overlapping the AbFpvA, AbFhuE and AbBfrD2 and LexA binding sites found at the promoters of AbFhuE, AbBfrD1 and AbBtuB2 coding genes are shown in panels B and C respectively.

4.2.8 OMVs capture iron complexed with enterobactin.

The presence of large number of iron-transporting TonRs in nanostructures like OMVs is expected to increase surface area, enabling them to efficiently capture siderophores. This hypothesis was tested by using radiolabeled ferric iron (55Fe) complexed with enterobactin (Ent). Initially, the pure ferric-enterobactin (Fe-Ent) was prepared by incubating commercially procured enterobactin with 55Fe (American Radiolabeled Chemicals, ARX-0109) (Fig 4.15 A). The 55Fe-Ent was then purified and incubated with OMVs, as described in the methods section. The OMVs complexed with 55Fe -Ent were then repurified following density gradient centrifugation. Since the binding of 55Fe-Ent requires no energy, Fe-Ent bound strongly with the OMVs. The bound 555Fe-Ent did not dissociate from OMVs, even after the OMVs were repurified through density

gradient centrifugation. About 72 pmol of 55 Fe was bound to 200 µg of OMVs (Fig 4.15 B). The OMVs complexed with 55 Fe-Ent were then used to test whether they can transport iron into DS002 cells. The cells (8 × 108 cells) grown under iron-limiting conditions were then incubated with 34 µg of OMVs (12 pmol of 55 Fe) for 12 h.

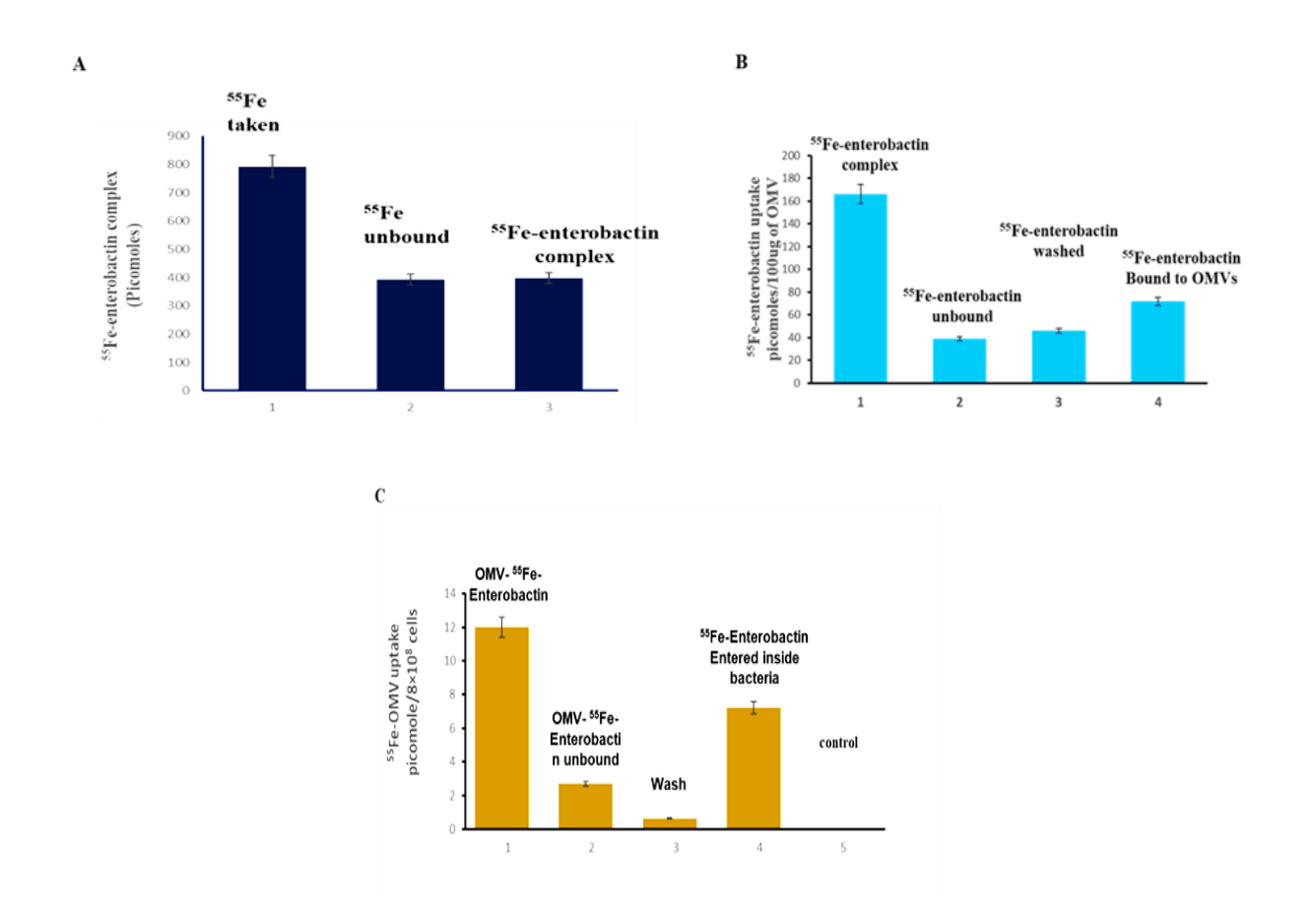


Figure 4. 15 The OMV assisted iron uptake by *A. baumannii* DS002. Panel A indicates binding of radiolabelled iron to enterobactin. Panel B shows the labelling of OMVs with ferric enterobactin-complex. Uptake of radiolabelled iron via OMV is shown in panel C. Lane 1 indicates amount of ⁵⁵Fe-Ent bound to OMVs. The cells after incubating with OMVs associated with ⁵⁵Fe-Ent were collected and washed with lithium chloride to remove surface associated 55Fe-Ent. The unbound or cell surface associated 55Fe-Ent is shown in lanes 2 and 3 respectively. Lane 4 shows ⁵⁵Fe present inside the cells after washing with lithium chloride. The control unlabelled OMVs incubated with cells shown in lane 5.

These cells were then used to examine whether radiolabeled iron was found inside the cells. The surface-accumulated iron was removed by washing the cells with lithium chloride, and the actual amount of 55 Fe translocated into the cytoplasm was measured as described in the Methods section. About 7.2 pmol iron was transported into DS002 cells when incubated with 34 µg of OMVs (Fig 4.15 C). These results clearly demonstrate the ability of OMVs to transport iron into DS002 cells by utilizing Fe-Ent. TonRs of OMVs have aligned with TonRs transporting iron bound to all three major classes of siderophores (Fig 4.12). OMVs also have TonRs that

aligned well with zinc (AbTonR1) and copper (AbButB2) transporters (Fig 4.12). If these are available in the vicinity, the OMVs might also capture and transport them into *A. baumannii* DS002 cells along with iron and other nutrients.

4.3 DISCUSSION

In Gram-negative bacteria, the outer membrane hinders the uptake of nutrients which exceed the pore size of outer membrane porins (U. Choi & Lee, 2019). Such nutrients, and nutrients which are scarcely available in the environment, require active transport. Active transport across energy deprived outer membrane is dependent on the inner membraneassociated Ton-complex comprised of the proton motive force components ExbB/ExbD and TonB (Ahmer et al., 1995). The TonB harvests energy from PMF components and transduces it to the outer membrane-located TonR. This TonR uses that energy to translocate bound substrates across the outer membrane (Ahmer et al., 1995). The outer membrane active transport system, otherwise known as the TonB-dependent-transport (TBDT) system, was discovered in E coli while deciphering the mode of phage T1 infection (Killmann et al., 1995). Subsequent studies have shown its role in the transport of vitamin B12 and iron complexed with siderophores (Schauer et al., 2008). Several studies have linked the TBDT system with iron acquisition and shown that the expression of TonR-coding gene are under the transcriptional control of ferric iron uptake regulator (Fur) protein (Escolar et al., 1999). Therefore, the TBDT system became synonymous with iron acquisition. However, recent studies have demolished this myth and shown that TonBenergized transport is also required for the transport of nickel, copper, zinc, and carbohydrates such as maltodextrins and sucrose (Schauer et al., 2008). In fact, the expression of a nickelspecific TonR, FrpB4, of the human pathogen Helicobacter pylori, is strongly regulated by nickel ions (Davis et al., 2006; Ernst et al., 2006). Likewise, the expression of MalA is upregulated only when maltodextrins were used as sole source of carbon (K. H. Choi et al., 2013). Genomes of Gram-negative bacteria contain several TonR-coding sequences, and their number increases with the complexity of their habitat (Schauer et al., 2008). TonRs are proposed to have roles in the transport of complex nutrients and to facilitate organismal survival in complex environments.

Gram-negative bacteria, without exception, produce OMVs. The cargo carried by OMVs contains proteins and secondary metabolites that perform various cellular activities (Schwechheimer & Kuehn, 2015). OMV-associated proteins influence pathogenesis, immune response, signalling activities, and transport functions (Kulp & Kuehn, 2010a). Interestingly, the OMVs isolated from *A. baumannii* DS002 contain 19 different TonRs. Of these, FecA and FhuA5 are encoded by the large indigenous plasmid pTS134338. The genomic island involved in iron

acquisition contains two TonRs, FcuA1 and FcuA2, and the rest of the TonR-coding sequences have been identified on the chromosome. Among these TonRs, only seven are under the transcriptional control of Fur protein. These Fur-regulated TonRs showed structural similarities to the TonRs involved in the transport of iron complexed with siderophores such as enterobactin, aerobactin, alcaligin, and hydroxy carboxylates (Fig 4.13). Due to the presence of these TonRs, the OMVs are expected to capture different types of siderophores synthesized and secreted by cohabiting bacteria. These OMVs when bound to these siderophores would probably facilitate ferric iron transport into *A. baumannii* DS002. Thus, the OMV-mediated transport mechanism is expected to contribute to the survival of *A. baumannii* DS002, especially in a nutrient-limiting polymicrobial environment.

The true physiological significance of the TonB-dependent transport (TBDT) system is slowly unfolding (Noinaj et al., 2010). Besides iron, the TBDT system facilitates the transport of several nutrients and carbon sources (Samantarrai, Sagar, et al., 2020). The presence of multiple TonRs in nano-structures, such as OMVs, serve to capture nutrients and carbon resources which are scarcely available in the environment. Since, ligand binding to the plug domain of the receptor is energy independent, the TonRs load nutrients/carbon sources onto OMVs (De Biase et al., 2021; Kulp & Kuehn, 2010a; Prados-Rosales et al., 2014). These nutrient-loaded OMVs, when fused to the outer membrane of *A. baumannii*, gain access to the inner membrane-located Toncomplex to gain the energy required to translocate the nutrients into the periplasmic space.

Several studies have highlighted the role of OMVs in intra- and interspecies delivery (Jones et al., 2020; Kulkarni et al., 2015; MacDonald & Kuehn, 2012). Once released from their mother cells, OMVs travel to distant places and deliver associated macromolecules to species that share no obvious taxonomic relationship (Berleman & Auer, 2013). If these findings are viewed together with the structural diversity of OMV-associated TonRs, the role of OMVs in meeting the nutrient requirements of the microbial community is evident. These nanostructures, with increased surface area and TonR diversity, promote the survival of the microbial community by capturing and delivering scarcely available nutrients, including iron. The COG categorization included nearly 50% of the OMV-associated proteins as proteins of unknown functions. Unless their functions are known, it is hard to realize the complete role of OMVs in the physiology and adaptive potential of *A. baumannii* DS002.

Chapter 5: Genomics of OMVs of Acinetobacter baumannii DS002

Work described in current chapter deals with identification and characterisation of the DNA associated with OMVs. As stated in the introduction, OMVs have diverse functions, these capabilities are the result of vesicles being versatile secretion mechanism that allows cells to transport both hydrophilic and hydrophobic molecules through the extracellular milieu (Biller et al., 2017). Vesicles can be specifically enriched or depleted in individual components rather than simply mimicking cellular contents (Bonnington & Kuehn, 2014). Perhaps One of the most notable characteristics of OMVs is the ability to contain nucleic acids (Biller et al., 2014; David W Dorward et al., 1989; Rumbo et al., 2011). Plasmid DNA, viral DNA as well as genomic DNA fragments ranging in size from hundreds of base pairs to 420 kb have been identified in vesicles of Gram-negative bacteria, gram positive bacteria, archaea and eukaryotes (D. W. Dorward & Garon, 1990; Gaudin et al., 2014; Grande et al., 2015; Jiang et al., 2014; Klieve et al., 2005a; Soler et al., 2008; Yáñez-Mó et al., 2015). First it was reported in 1989, since then, a growing number of studies have described the presence of plasmid and/or chromosomal DNA in MVs (Biller et al., 2014; Renelli et al., 2004; Turnbull et al., 2016). Vesicles are reported to function as vehicles of horizontal gene transfer (Klieve et al., 2005b; Renelli et al., 2004; Yaron et al., 2000). Lateral mobility of DNA plays a critical role during acquisition and spread of drug resistance genes. In general, indigenous plasmids carrying drug resistance genes disseminate resistance through conjugation (von Wintersdorff et al., 2016). However, A. baumannii strains show competence to undergo natural transformation by acquiring DNA from environment (Domingues et al., 2019; Hu et al., 2022). Such natural competence facilitates A. baumannii to acquire antimicrobial resistance from taxonomically unrelated bacterial species (Fournier et al., 2006). In fact, the drug resistant genes identified in the genomic island of multidrug resistant A. baumannii AYE strain are laterally acquired from *Pseudomonas aeruginosa* (Fournier et al., 2006).

Acinetobacter baumannii DS002 was isolated from the soil polluted with insecticides and other agrochemicals (Longkumer et al., 2013). It survives even using phenolic compounds as sole source of carbon. The genome of DS002 contains seven replicons. One of them with a size of 3430798 bp is designated as chromosome and the rest of the replicons are plasmids of various sizes (Yakkala et al., 2019). We have recently compared these plasmid genome sequences with A. baumannii plasmid database and generated plasmid network. The network indicated presence of extensive similarities among A. baumannii plasmids indicating lateral mobility and recombination among A baumannii plasmids (Samantarrai, Yakkala, et al., 2020). Only one

plasmid pTS37365 was not found as part of the plasmid network (Fig 5.1). These plasmid sequences were further examined to identify genetic modules that contribute for their lateral mobility. Interestingly, most of them contained origin of transfer (oriT) but none of them have shown presence of *tra* genes that encode for the type 4 secretary system (T4SS), a critical component required to facilitate lateral mobility. The *tra* sequences were also not found in the chromosomal DNA of DS002 strain. Since, lateral mobility and extensive recombination among plasmids is evident among *A. baumannii* plasmids, we have investigated, if alternate mechanisms exist in lateral mobility of plasmid sequences among *A. baumannii* strains. In this study, we demonstrated association of four out of five plasmids with outer membrane vesicles (OMVs) and show role of OMVs in lateral mobility of the episomal DNA.

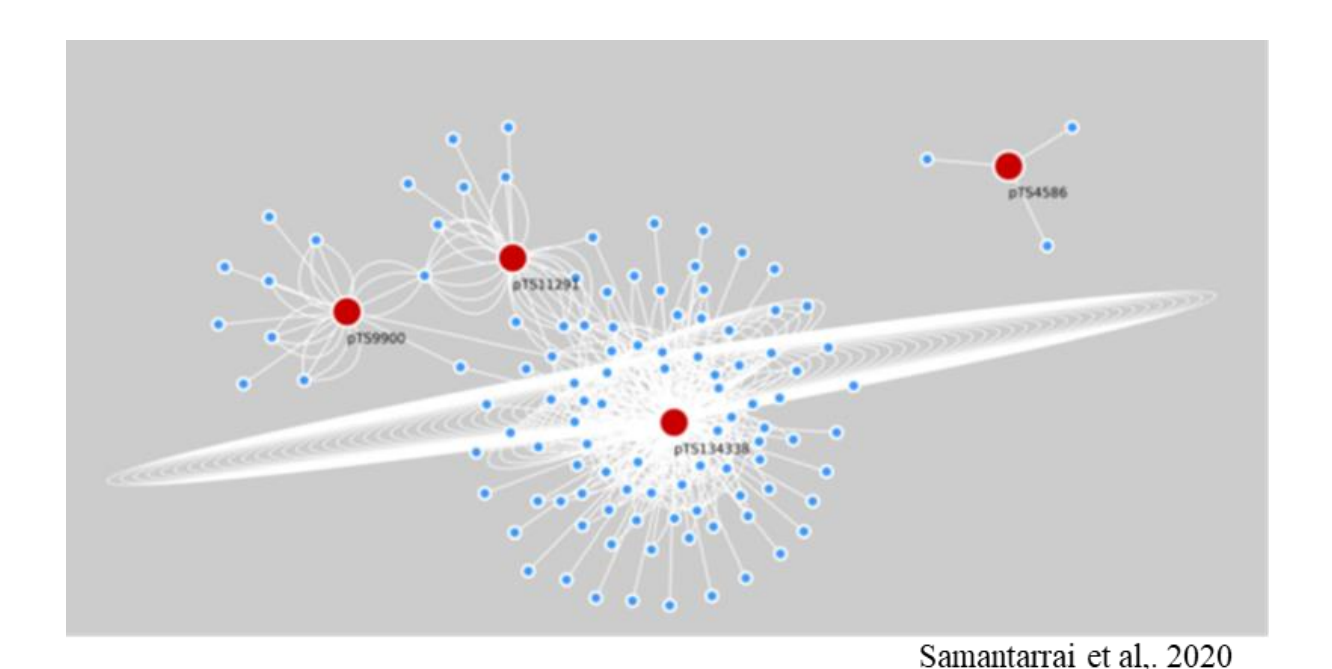


Figure 5. 1 Gene-sharing network. The red dots represent indigenous plasmids of *A. baumannii* DS002 and each blue dots represent 493 plasmids of *Acinetobacter* species included in the gene-sharing network. The number of white edges (connections) between the blue and red dots indicate the number of proteins with 100% identity.

5.1 Objective specific Methodology

Table 5. 1 Strains used in this study

Strains	Genotype	Reference
E. coli DH5α	λsupE44, ΔlacU169 (Δ80	(Hanahan, 1983)
	lacZΔM15) hsdR17 recA1	
	endA1 gyrA96 thi1 relA1	
Acinetobacter baumannii DS002	Cm ^r , Sm ^r	Harshita et al., 2019
Acinetobacter baumannii DS003	Cm ^r , Sm ^r , Tet ^r , <i>ompA</i> KO,	This work
	ompA gene replaced with	
	tetracycline	
E. coli BL21	hsdS gal (λclts857 ind1 sam7	Studier and Moffat, 1986
	nin5lac uv5 T7 gene 1)	
E. coli pir 116	F-mcrA Δ(mrr-hsdRMS-	Epicentre
	mcrBC) φ80dlacZΔM15	Biotechnologies, USA
	ΔlacX74 recA1 endA1	
	araD139 Δ (ara, leu)7697	
	galU galK λ- rpsL nupG	
	pir+(DHRF)	

Table 5. 2 Oligonucleotide primers used in this study.

Primer Name	Sequence	Purpose
GD1FP	GCCTCACATATGAAATTGAGTCGTATTGCACTTG	Primers used to amplify
GD1RP	TTGACTCTCGAGTTGAGCTTGTTGACCAGGTT	ompA gene as Ndel and Xhol fragment
GD2 FP	GCATTGATGGCAGTTGCAGAAC	Primers used to amplify
GD2 RP	GGGTCTATGACACAAAAATCGCC	plasmid pTS4586 specific sequence.
GD3 FP	CTAATTCACGCTTTCCGCCAAAAACC	Primers used to amplify
GD3 RP	CAGAGATAAATACAGCTTTAGTGTGTTCTG	plasmid pTS11291 specific sequence.
GD4 FP	CGATTTCTACCAGCTGGTATTGC	Primers used to amplify
GD4 RP	GATAATTAGTGCTATCCACTTTAACCC	plasmid pTS9900 specific sequence.
GD5 FP	GTCATGCCACAAGCTCAAGCAGG	Primers used to amplify
GD5 RP	GTCTGCATTGATGGACCTACG	plasmid pTS37365 specific sequence.
GD5 FP A	CCCTGTAGAAGATCGTGATCCTGC	Primers used to amplify
GD5 RP A	GCTAACAAATGGTTGAAGCTCAACAAACC	plasmid pTS37365 specific sequence.
GD6 RP	CGTCTGCCTGAATTTGATGAATGGCTAG	Primers used to amplify
GD6 RP	CTCGTCCAATACCTGCTTCTTTCGC	plasmid pTS134338 specific sequence.
GD6 RP A	GGCTGGAAATGCATATGCTGAC	

GD6 RP A	GGTGAGCTGACGAGAATCATC	Primers used to amplify
		plasmid pTS134338 specific sequence.
GD6 RP B	CGACATAATGGAGTAGTCAGCACTAG	Primers used to amplify
GD6 RP B	CATCTTCCCAACGGAGTTCACG	plasmid pTS134338 specific sequence.
GD7 FP	TACTCG <u>CATATG</u> AAATTGAGTCGTATTGCACTTG CTACTA	Forward primer used to amplify <i>ompA</i> gene of <i>A. baumannii</i> DS002. The <i>Ndel</i> site appended to facilitate cloning in pET23b is underlined.
GD7 RP	TATCA <u>AAGCTT</u> TTACTTGTCGTCATCGTCTTTGTA GTCTTGAGCTGCTGCAGGAGCTG	Reverse primer used to amplify <i>ompA</i> gene of <i>A. baumannii</i> DS002.The sequence specifying FLAG tag downstream of stop codon is shown with bold case. The <i>Hind</i> III site appended to facilitate cloning in pET23b is underlined.
T7 FP	CCTT <u>AGATCT</u> TAATACGACTCACTATAGG	Forward and reverse
T7 RP	CCTT <u>AGATCT</u> CTAGTTATTGCTCAGCGGTGGC	primers specific to pET23b vector, used to amplify variant of <i>ompA</i> from pGD2. The <i>Bgl</i> II site appended to facilitate cloning into pRGOOD is underlined.
GD8 FP	TAGAAT <u>GTCGAC</u> GGTAATCACTTTATAGAG	Forward and reverse primer
GD8 RP	TGGCA <u>CTCGAG</u> TTTGAGTTCTTGAACAAAAAG C	to amplify 1kb upstream region of <i>ompA</i> gene. The <i>Sal</i> I and <i>XhoI</i> sites appended to facilitate cloning in pBSKS cloning vector are underlined.
GD9 FP	TATCA <u>CTCGAG</u> GGATATCCTCCAGAGATAACAAT TG	Forward and reverse primer to amplify 1kb upstream
GD9 RP	CAGTA <u>GAATTC</u> TAATCTCCGATTGTTCTTAA	region of <i>ompA</i> gene. The <i>Xho</i> I and <i>EcoR</i> I sites appended to facilitate cloning in pBSKS cloning vector are underlined.
GD10 RP	CGA <u>GGATCC</u> CGTTACATAACTTACGGTAAATG	Forward and reverse
GD10 RP	GGCAT <u>GTCGAC</u> TTATAAGATACATTGATGAGTTT GGAC	primers to amplify eukaryotic GFP from pEGFP-C1 vector. restriction site BamHI and SalI restriction site appended to facilitate

	cloning	in	pTS236-K1
	plasmid a	re und	erlined.

Table 5. 3 Plasmid Used in this study

Plasmid name	Description	Source
pET23b	Amp ^r , expression vector, codes proteins of cloned	
	genes with C-terminal His-tag.	
pT96W	Amp ^r , Generated by ligating orf96 of pTS236 as EcoRI	(Toshisangba et al.,
	and <i>XhoI</i> fragment to pET23b. Codes for Orf96 ^{C6His}	2013)
pT113W	Amp ^r , Generated by ligating orf113 of pTS236 as EcoRI	(Toshisangba et al.,
	and <i>XhoI</i> fragment to pET23b. Codes for Orf113 ^{C6His.}	2013)
pTS236-K1	S236-K1 Kan ^r , Variant of phage genome, pTS236. Generated by	
	inserting kanamycin region with R6Ky origin of	2013)
	replication and MCS site at unique Mlul site of	
	pTS236.	
pTS4586	Kan ^r , A. baumannii DS002 plasmid rescue cloned by	(Toshisangba et al.,
	tagging mini-transposon <ez-tn5 <r6kγori="" kan-2=""> to</ez-tn5>	2013)
	indigenous plasmid, pTS5486 of A. baumannii DS002.	
	Replication in <i>E. coli</i> pir116.	
pGD1	Km ^r , Expression plasmid, Codes for OmpA ^{N6xHis}	This study This study
pGD 2	Amp ^r , Expression plasmid. Generated by ligating	
	ompA in pET23b as Ndel and HindIII. Codes for	
	OmpA ^{CFLAG} .	
pGD 3	Cm ^r , Expression plasmid. Generated by ligating <i>ompA</i>	This study
	in pRGOOD vector as <i>Bgl</i> II fragment. Codes OmpA ^{CFLAG}	
	from an arabinose inducible PBAD promoter.	
pGD 6	Am ^r , generated by ligating <i>ompA</i> flanking sequences	This study
	as Sall and EcoRI fragment. Contains unique Xhol site	
	in place of <i>ompA</i> gene.	
pGD 4	Amp ^r , Tet ^r , Generated by ligating tetracycline	This study
	resistance gene at unique restriction site of pGD6.	
	Contains tet ^r gene in place of <i>ompA</i> gene.	This study
pGD 5		
	gene in pTS236-K1 as <i>BamH</i> I and <i>Sal</i> I fragment. Codes	
	GFP from CMV promoter.	
pAT02	Amp ^r , Codes for RecET recombinase system from <i>A</i> .	Tucker, et al 2019
	baumannii strain IS-123.	

5.1.1 OMV genomics

5.1.1.1 Isolation of total DNA from OMVs

Purified OMVs 20 μ l (50 μ g protein concentration) were used for DNA isolation. Initially, Triton X-100 was added to the OMVs to attain a final concentration of 2% of by adding appropriate amounts of stock solution. The contents were then mixed and incubated for 10 min at 55°C. Triton X-100 treated OMVs were then used to isolate DNA by using Genomic DNA isolation kit (DNeasy, QIAGEN) by following the manufacturer's protocol. Briefly, Triton X-100 treated OMVs (50 μ g protein) were mixed with equal volume of binding buffer and loaded onto genomic DNA extraction column. The column was washed twice with wash buffer and finally eluted in 20 μ l of sterile MQ water.

5.1.1.2 Isolation of DNA from the lumen of OMVs

Similar procedures were followed while isolating total DNA from the lumen of OMVs, except that the OMVs were treated with DNase prior to Triton X-100 treatment. The OMVs were incubated with 2 Units of DNase for 30 minutes at 37°C to eliminate surface associated DNA. After treatment with DNase, the OMVs were left at 80°C for 10 min to inactivate DNase. The DNase free OMVs were then subjected to Triton X-100 treatment to dissolve membranes of OMVs. The lumen content released after Triton X-100 treatment was used to isolate DNA by following the procedure described above.

5.1.1.3 Sequencing of OMV associated DNA

The total DNA isolated from OMVs were sequenced and assembled and the contigs exceeding the size of 4.00 kb were aligned with the genomic sequence of *A. baumannii* DS002 (accession number: CP027704.1) following established procedures. Briefly, sequencing of OMV isolated DNA was carried out using paired end illumina sequencing platform and the raw reads obtained were subjected for adapter finding using BBMerge tool (Bushnell B. et al). Further, adapter was trimmed using Trimmomatic tool (Bolger et al. 2014) and the SPAdes 3.15.3 assembler was used to assemble reads from genome (Bankevich A. et al 2012). The contigs were then mapped against a reference genome of *Acinetobacter* using CONTIGuator web server (http://combo.dbe.unifi.it/contiguator). Genome annotation was performed using RAST Server (Aziz et al 2008) and the annotated genome sequence was visualised using Gview Server (https://server.gview.ca/).

5.1.2 Detection of plasmids and Phage AbDs1 in OMVs

Polymerase chain reaction (PCR) was performed to detect OMV associated episomal DNA. The DNase treated and untreated OMVs were taken as templates and oligos specific to indigenous plasmids and phage AbDs1 were used as primers (Table 5.2). If plasmid/phage specific amplicons were obtained both in DNase treated and untreated OMVs they were considered as present in the lumen. If the amplicons were seen only in DNase untreated OMVs then it was concluded as present on the surface of the OMVs.

5.1.3 Detection of AbDs1 protein in OMVs

5.1.3.1 Western blots with Orf96 antibody

To determine the presence of phage proteins in OMVs, western blot was performed. OMV proteins equivalent to 30 μ g was separated on 12 % SDS gel followed by electro-transfer to PVDF membrane using semidry method of transfer. The blots were blocked with 10% non-fat skim milk before being incubated with Orf96 antibody produced in our lab (Longkumer et al., 2013). Followed by primary incubation, secondary antibody conjugated to horseradish peroxidase was added and incubated. The membrane was developed using an enhanced chemiluminescence system after being washed properly with TBST.

5.1.3.2 Immunogold labelling

OMVs were visualized under Transmission Electron Microscopy following protocols standardized in our laboratory (Dhurve et al., 2022). While detecting both OmpA and phage, AbDs1 coded protein Orf96 in OMVs, immuno-gold labelling studies were conducted. After purification of OMVs, different concentrations of OMVs were carefully spotted on the copper grids and were rinsed by floating it on a droplet of distilled water. The grids were then incubated with blocking buffer (0.3% BSA in PBS buffer) for 15 to 30 min. After incubation, the grids were carefully picked, excess liquid was removed, and incubated independently with both primary antibodies raised against OmpA and Orf96 (Diluted in blocking buffer) for 2 h. Each grid was washed 5 times independently with wash buffer (0.03% BSA in PBS buffer). After the last wash, grids were transferred over the droplet of Gold conjugated secondary antibody (diluted in blocking buffer) for 1 h, followed by washing 5 times with wash buffer, and three times with water. Excess liquid was removed with the help of filter paper and the grids were stained with 2 percent uranyl acetate for 1 min before being visualized under TEM.

5.1.4 Purification of Orf96^{C6His} and Orf113^{C6His}

In a previous study from our laboratory, orf96 and orf113 were cloned into expression vector pET23b and recombinant plasmids were named as pT96W and pT113W which encode for Orf96^{C6His} and Orf113^{C6His} respectively. In order to purify Orf96^{C6His} and Orf113^{C6His} proteins, both constructs were transformed into E. coli BL21 independently and purification experiments were performed by affinity chromatography using Ni-NTA column. E. coli BL21 (pT96W) bacteria were grown in 250 mL of LB broth till the culture reached to mid log phase (OD₆₀₀, 0.5). IPTG (0.5 mM) was used to induce Orf96 expression. After that, the induced cultures were incubated at 18°C for 16 h. After overnight induction cells were harvested and cells were washed twice in binding buffer (20 mM Tris-HCL having pH 8.0, 50 mM NaCl) followed by resuspension (10 ml/1 g) in lysis buffer (5 mM imidazole and 10 % glycerol in binding buffer). The suspension was sonication for 10 min (pulse on 30 sec/pulse off 30 sec) at 4°C. The sonicated sample was centrifuged at 15,000 rpm for 30 minutes and the supernatant obtained was slowly passed through column having Ni-NTA Sepharose beads, pre-equilibrated with the binding buffer. After protein binding, it was washed with wash buffer (50 mM imidazole in binding buffer) to remove loosely bound proteins, and the proteins strongly bound to the beads were eluted using a gradient of elution buffer (0-500 mM imidazole in binding buffer). Purification of Orf113^{C6His} protein obtained was performed in similar manner. Or f 96^{C6His} and Orf 113^{C6His} proteins obtained from two independent purification process were analyzed on SDS-PAGE and pure protein was dialyzed and concentrated using 3 kDa cutoff centricon tubes

5.1.5 Ligand blotting

OMV proteins isolated from *A. baumannii* DS002 strain were separated on 12% SDS-PAGE and electro-transferred onto a PVDF membrane. After blocking the membrane with 3% BSA in TBST, it was incubated at room temperature for one hour separately with 1 μ g/ml of purified 96^{C6His} and 113^{C6His} protein diluted in TBST containing 0.2% BSA. The unbound proteins were removed by three washes with TBST. The membrane was then incubated with anti-His-HRP conjugated antibody at room temperature for 1h. After three washes with TBST, the blots were developed and analysed.

5.1.6 AbDs1 and OMV interactions

5.1.6.1.1 Expression of OmpA with C-terminal FLAG-tag

The gene *ompA* was amplified from genomic DNA with primer set GD7FP and GD7RP having FLAG sequence overhang as *NdeI* and *HindIII* fragment. The PCR amplicon was then

digested and cloned into pET23b vector digested with same enzymes. The construct was named as pGD2. The *ompA* coding OmpA^{CFLAG} was amplified from pGD2 using primers T7 FP *BgI*II and T7 RP *BgI*II and cloned into a broad host range mobilizable expression plasmid pRGOOD digested with *BamH*I. The resulting recombinant plasmid pGD3 is then transformed into *E. coli* BL21 (DE3) and expression of OmpA^{CFLAG} checked by carrying out western blots with anti-FLAG antibodies.

5.1.6.2 Pulldown Strategy

5.1.6.2.1 Two plasmid Assays

The expression plasmids pGD3 and pT96W/pT113W coding OmpACFLAG and Orf96^{C6His}/Orf113^{C6His} are derivatives of plasmids pRGOOD and pET23b. Therefore, they are compatible plasmids and replicate in the same host. The E. coli BL21 DE3 (pGD3) cells expressing OmpA^{CFLAG} was independently transformed with the expression plasmid coding either Orf96^{C6His} (pT96W) or Orf113^{C6His} (pT113W). The BL21 (pGD3 + pT96W) cultures was grow to mid log phase in 10 ml LB media and the expression of OmpA^{CFLAG} and Orf96^{C6His} were induced with 1 mM IPTG and allowed to grow overnight at 30°C. The bacterial cells were collected at 6000 rpm (10 min) and were washed two times with wash buffer (PBS pH 7.4, 150 mM NaCl and 5% glycerol). The cell pellet obtained after washing was resuspended in 2 ml of lysis buffer (PBS pH 7.4, 150 mM NaCl, 5% glycerol, 50 μg lysozyme and 1 mM PMSF) and protease inhibitor cocktail (10 μl) was added before lysing the cell by sonication for 10 min (10 sec ON and 40 sec OFF for 5 min). The cell lysate was then subjected to centrifugation for 20 min at 13,000 rpm and the clear lysate (1 ml) was mixed with Ni-NTA magnetic beads (30 µl slurry). The contents were kept at 4°C for overnight on head-to-head rotation and the magnetic beads were collected to the bottom of the tube with the help of magnet. The clear supernatant was taken into clean eppendorf tube. The collected beads were washed 3 to 4 times with PBS pH 7.4 (150mM NaCl, 5% glycerol) and each wash fraction was collected into separate sterile eppendorf tube. The washed beads were dissolved in 50 μ l of 2x SDS-PAGE sample buffer and stored at -20°C until further use. Appropriate amounts of supernatant, wash fractions were taken into separate tubes and mixed with 2X SDS-PAGE sample buffer and boiled along with washed beads stored at -20°C for 5 min before analyzing all of them on 12.5% SDS-PAGE. The separated proteins were detected by performing western blots with either anti-His antibody (to detect Orf96^{C6His} or Orf113^{C6His}) or anti-flag antibodies. Cell lysate made from E. coli cells expressing OmpACFLAG and Orf96C6His were independently treated in a similar manner and used as controls. Similarly, pull down assays were performed using ANTI-FLAG® M2 Magnetic Beads to check the interactions between OmpACFLAG and Orf113^{C6His} independently.

5.1.7 Generation of *A. baumannii* DS003

The knockout of *ompA* was generated following homologous recombination method described by Tucker et al. (Tucker et al., 2014). Plasmid pTA02 codes for IPTG inducible recombinase used to generate *ompA* knock out of *A. baumannii* DS002. Plasmid pTA02 was a gift from Dr. Bryan Davies, Department of Molecular Biosciences, University of Texas, USA. Initially pAT02 was electroporated into *A. baumannii* DS002 and the cells expressing recombinase were made competent and used to generate knockout. Since, a recombineering PCR product with tetracycline cassette with flanking regions of *ompA* gene was required. Therefore, pGD4 was constructed which had tetracycline cassette flanked by the upstream and downstream of the *ompA* gene.

5.1.7.1 Construction of pGD4

A tetracycline resistance marker (TetR) was released as Xhol fragment from pTZ-TetR plasmid to create recombineering PCR product. Size corresponding to 1kb, was amplified as Sall and XhoI using primer set GD8FP/GD8RP from upstream region of ompA gene and designated as fragment A. Similarly, 1kb region downstream of ompA gene was also amplified as XhoI and EcoRI fragment, using primer set GD9FP/GD9RP and designated as B fragment. Above PCR products were then digested with XhoI and ligated to join fragment A and fragment B. These ligated A B fragment was amplified using forward primer GD8FP specific to fragment A and reverse primer GD9RP specific to fragment B. The A-B fragment thus generated contains a unique restriction site XhoI in place of ompA. Fragment AB was digested with SalI and EcoRI and ligated to cloning vector pBSKS digested with similar enzymes and the resulting plasmid is named as pGD6. Above construct, pGD6 was then digested with XhoI enzyme and ligated to the tetracycline resistance cassette, transformed into E. coli DH5α and selected on tetracycline plates. Colonies obtained were grown in LB media containing tetracycline and plasmid was digestion with Sall and EcoRI to release 3.1 kb release of A-tetR-B fragment. The construct was designated as pGD4. When necessary, the A-tetR-B fragment was amplified using GD5FP and GD6RP and electroporated into A. baumannii DS002 (pTA02) cells.

5.1.7.2 Electroporation of A-TetR-B fragment in A. baumannii DS002 (pTA02)

The *A. baumannii* DS002 (pAT02) were grown at 30°C in LB medium in presence of ampicillin to maintain the plasmid. Expression of recombinase was induced by adding 2 mM IPTG. After 3 washes with 10% ice-cold glycerol the pellet obtained was dissolved in 500 µl of 10%

glycerol. Electrocompetent cells (100 μ l) were taken in a 2 mm electroporation cuvette and mixed with 5 μ g of recombineering product (A-TetR-B) and pulsed at 2.5 kV in a GenePulser Xcell (Bio-RAD). The electroporated cells were grown for overnight in 4 ml rich medium containing 2 mM IPTG and the bacteria were centrifuged and the pellet was plated on LB agar plates containing 5 μ g/ml tetracycline. The plates were incubated at 37°C till colonies appeared. *A. baumannii* DS002 (pTA02) electroporated without the addition of recombineering product served as control.

5.1.7.3 PCR verification of ompA mutant of A. baumannii DS002

The colonies obtained on tetracycline plates were patched on tetracycline plate and tested for deletion of *ompA* gene by performing colony PCR using the primer set (GD8FP/GD9RP) specific to the upstream and downstream regions of *ompA* gene. Colonies which gave shift in amplicon size due to insertion of tetracycline were further screened with *ompA* specific primers to check the absence of *ompA*. The Positive colonies were subsequently pathed for three to four generations on LB plates supplemented only with tetracycline and Chloramphenicol, no ampicillin was supplemented to facilitate the removal of pAT02 plasmid. The resulting *ompA* deletion mutant strain was named *A. baumannii* DS003.

5.1.8 Role of OMVs in lateral mobility of DNA

5.1.8.1 Generation of AbDs1 derivatives

In a previous study from our laboratory pT236-K1 was constructed by tagging it with kanamycin resistance cassette at unique restriction site *Mlu*I between *repA* and *orf113*. Briefly, a primer pair (DS00119/DS00120) having *Mlu*I site was used to amplify the region (2kb) of minitransposon (EZ-Tn5™<R6Kγori/ KAN-2>) containing MCS, R6Kγori and Kanamycin cassette. The PCR amplicon was digested with *Mlu*I and then ligated to *Mlu*I digested pTS4 plasmid and the construct is named pTS236-K1. This R6Kγ origin containing plasmid can only replicate in *E. coli pir*116 (Longkumer et al., 2013).

5.1.8.2 Horizontal mobility in bacteria

The construct pTS236-K1 was transformed into *A. baumannii* DS002. OMVs were isolated from *A. baumannii* DS002 (pTS236-K1) by using procedures as explained before. Gene transfer experiments were based on previous studies (Yaron et al., 2000). The recipient strain used include gram negative *E. coli Pir*116, *Pseudomonas stutzeri*, *A. baumannii* DS002 as well as gram positive *Bacillus subtilis*. All recipient cells were grown in LB medium at 30°C except *E. coli* which

was grown at 37°C with shaking (180 rpm) for 3 to 4 h to an optical density of 0.6. (OD $_{600}$). Cells were harvested, washed and resuspended in cold SOC medium (2% tryptone, 0.5% yeast extract, 10 mM NaCl, 2.5 mM KCl, 10mMMgCl $_2$, 10m M MgSO $_4$, and 20mM glucose) to produce a bacterial suspension of 2×10 4 CFUml $^{-1}$. The cell suspension of 100 μ l was added to 800 μ l of SOC medium and 100 μ l of OMV suspension with increasing concentration (20 μ g, 40 μ g, 60 μ g and 100 μ g protein concentration). The suspension was kept statically at 30°C for 1 h followed by additional 2 h with shaking at 180 rpm. Further, 10 ml of LB medium was mixed to each culture and incubated for an additional 21 h. bacterial cells were pelleted, resuspended in 1 ml of SOC medium and plated on LB plates supplemented with kanamycin followed by incubation at 37°C for *E. coli* or at 30°C for other recipient bacteria. Colonies obtained were screened by performing PCR with kanamycin specific primers.

5.1.9 Mobilization of Phage genome into eukaryotic cells

5.1.9.1 Tagging GFP coding sequence to AbDs1 genome

To monitor mobilization of page genome into eukaryotic cells, phage genome derivative pTS236-K1 was tagged with GFP having eukaryotic promoter and terminator. As explained previously, pTS236-K1 has MCS which was explored for tagging it with kanamycin resistance cassette. The sequence coding GFP was amplified along with CMV promoter and SV40_PA_terminator from pEGFP-C1 plasmid using primer set pGD7FP and pGD7RP appended with *Bam*HI and *Sal*I restriction site. The amplicon was digested with *Bam*HI and *Sal*I enzyme and ligated to similarly digested plasmid pTS236-K1. The ligation mix was used to transform *E. coli Pir*116 cells and the transformants were selected on Kanamycin plates. Colonies obtained were sub-cultured and used to isolate phage genome tagged with GFP coding sequence. Presence of sequence coding GFP was determined by digesting the genome with *Bam*HI and *Sal*I enzyme. The resulting phage genome derivative was designated as pGD6.

5.1.9.2 Phage genome mobility in neuronal cell lines

Plasmid pGD6 was electroporated into *A. baumannii DS002* strain and OMVs were isolated as described before. To test the phage genome mobilization neuronal cell line Neu2A was used and experimental procedure followed were based on previously published report with slight modification (Kwon et al., 2009). Neuronal cell line Neu2A were grown in Dulbecco's Modified Eagle's Medium (DMEM) having 10% fetal bovine serum (FBS) and incubated at 37°C in 5% CO₂. Cells were taken and seeded on the glass coverslip at a density of 5×10⁴ a day before the

assay. On the subsequent day, cells were checked for 70 to 80% confluency and media was replaced with fresh DMEM media. Pure and sterile 20 µg of OMVs from *A. baumannii* (pGD6) were added to cells and incubated further for 6h, 12h and 24h time points. After the incubation period, the cells were washed with PBS, fixed with 4% paraformaldehyde, mounted over a microscopic slide and visualized under fluorescence microscopy.

5.2 Results

This study was designed to understand the lateral mobility of plasmids in the absence of genetic machinery coding for Type 4 Secretary System (T4SS). In a number of studies, OMVs have been shown to be vehicles for lateral mobility of DNA (Pérez-Cruz et al., 2015). The OMVs isolated from drug resistant clinical isolates of *A. baumannii* have successfully transformed drug sensitive strains into drug resistant strains (Park et al., 2021). In the light of these observations, we have investigated for the ability of OMVs, isolated from *A. baumannii* DS002, in lateral mobility of plasmids or plasmid encoded genes.

5.2.1 Indigenous plasmids are associated with OMV

Pure OMVs equal to 50 μg of protein concentration were used to Isolate DNA associated with OMVs. The procedure described in material and methods yielded about 0.2 μg of DNA for every 50 μg of OMVs. The pure OMV associated DNA was successfully sequenced using illumine sequencing platform. The assembled sequence was then aligned with the genome sequence of strain DS002. Interestingly, the contigs obtained showed sequence similarity to four indigenous plasmids of *A. baumannii* DS002, namely pTS4586, pTS9900, pTS11291 and ptTS134338, but none of the contigs matched to the 37 kb plasmid pTS37365 (Table 5.4). Further, the contigs obtained were mapped against a reference genome of *Acinetobacter* using CONTIGuator web server. Genome annotation was performed using RAST Server. Annotated files were visualised using Gview Server (Fig 5.2).

Table 5. 4 Four circularized contigs obtained by assembly using SPAdes 3.15.3 assembler

S.No.	Reference replicon	Reference length (bp)	Mapped contig (bp)
1	CP042210.1	134338	109538
2	CP042208.1	11291	12162
3	CP042207.1	9900	10035
4	CP042206.1	4586	4708

•

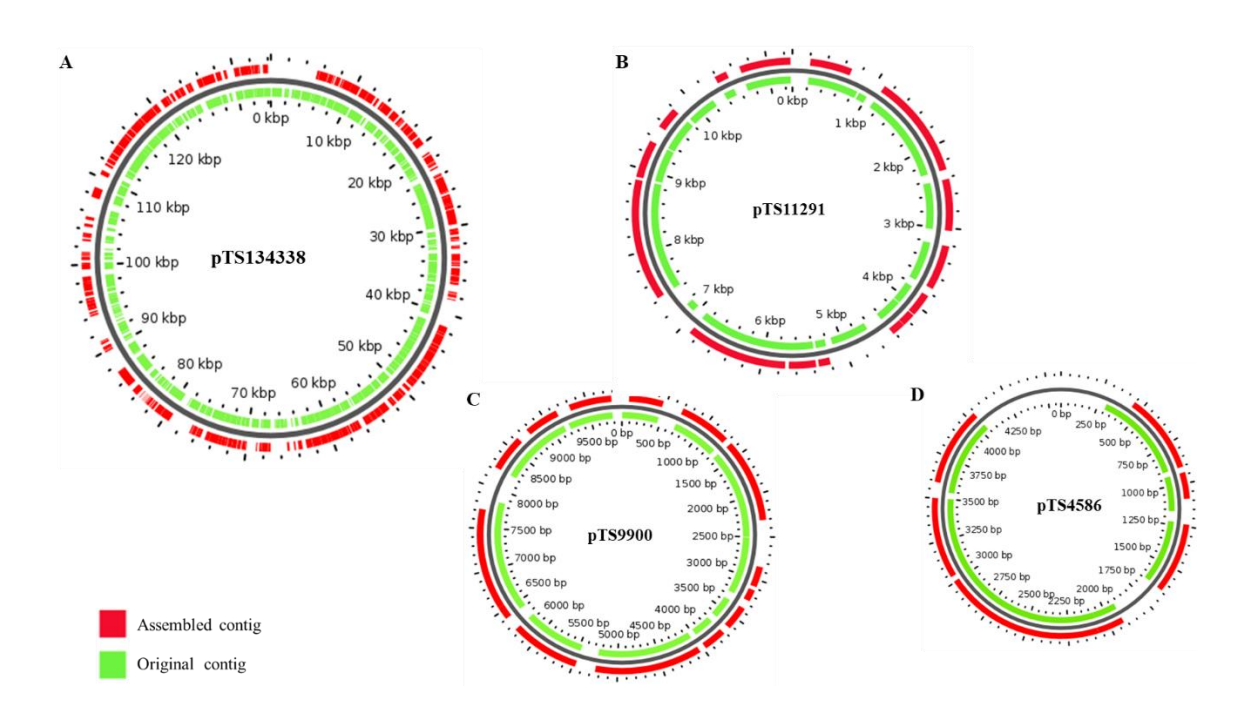


Figure 5. 2 Blast atlas original vs assembled sequence generated using GView server. Panel A show the comparative map of pTS134338 where original sequence is highlighted in red colour and assembled sequence highlighted in green colour. Panels B, C and D are comparative maps generated for pTS11291, pTS9900 and pTS4586 respectively.

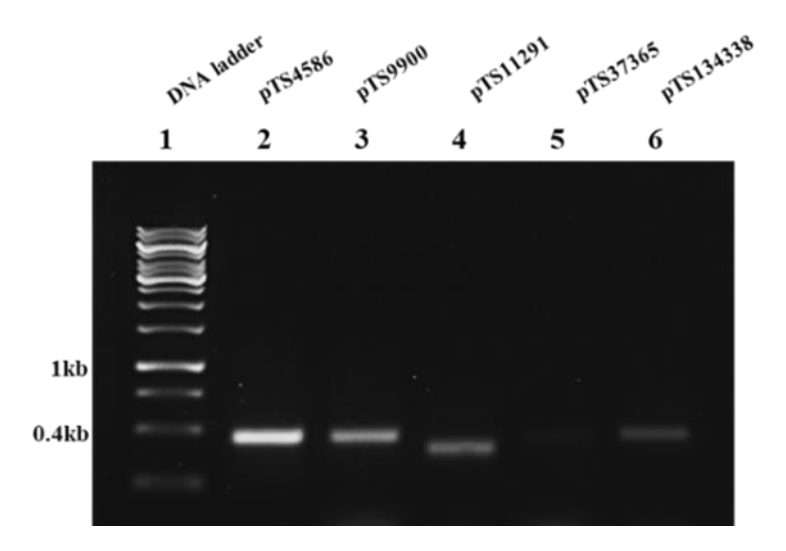


Figure 5. 3 PCR amplification of plasmids associated with vesicular DNA of *A. baumannii* **DS002.** The image represents agarose gel showing amplification of a regions specific to four plasmids, *viz.* pTS4586 (lane 2), pTS9900 (lane 3), pTS11291(lane 4), and pTS13433 (lane 6). Lane 5 represents reaction mix having primers to plasmid pTS37365. No amplification is observed indicating absence of plasmid pTS37365 in OMVs.

The sequence data was further validated by randomly amplifying the plasmid specific sequences using vesicular DNA as template. Strengthening the sequencing results, which indicated selective absence of pTS37365 in OMVs, no pTS37365 specific sequences were amplified in PCR reactions

(Fig 5.3 D lane 5). Similar experiments were performed to reconfirm the presence of other four indigenous plasmids in OMVs. Three primer pairs were designed to amplify three different regions of these plasmids (Table 5.2). In all of them amplicons of expected size were generated, suggesting that plasmids pTS4586, pTS9900, pTS11291 and pTS134338 are associating with OMVs isolated from *A. baumannii* DS002. (Fig 5.3 lane 2, 3, 4 & 6).

5.2.2 Plasmids pTS486 and pTS9900 were found in the lumen of OMVs

After ascertaining the association of four indigenous plasmids of *A. baumannii* DS002 with OMVs, further experiments were conducted to establish their localization in OMVs. Initially, the OMVs were treated with DNase to remove DNA associated on the surface of the OMVs and then the DNase treated OMVs were used to isolate DNA. This DNase treated vesicular DNA was then used as a template in the PCR reactions to amplify all four OMV associated plasmids. Interestingly, only plasmid pTS4586 and pTS9900 specific regions were amplified when DNase treated OMVs were used as template (Fig 5.4, panel B & C lane 3). Such amplification was not seen in the reaction mixes prepared using pTS11291 and pTS134338 specific primers (Fig 5.4, panel D & E lane 3).

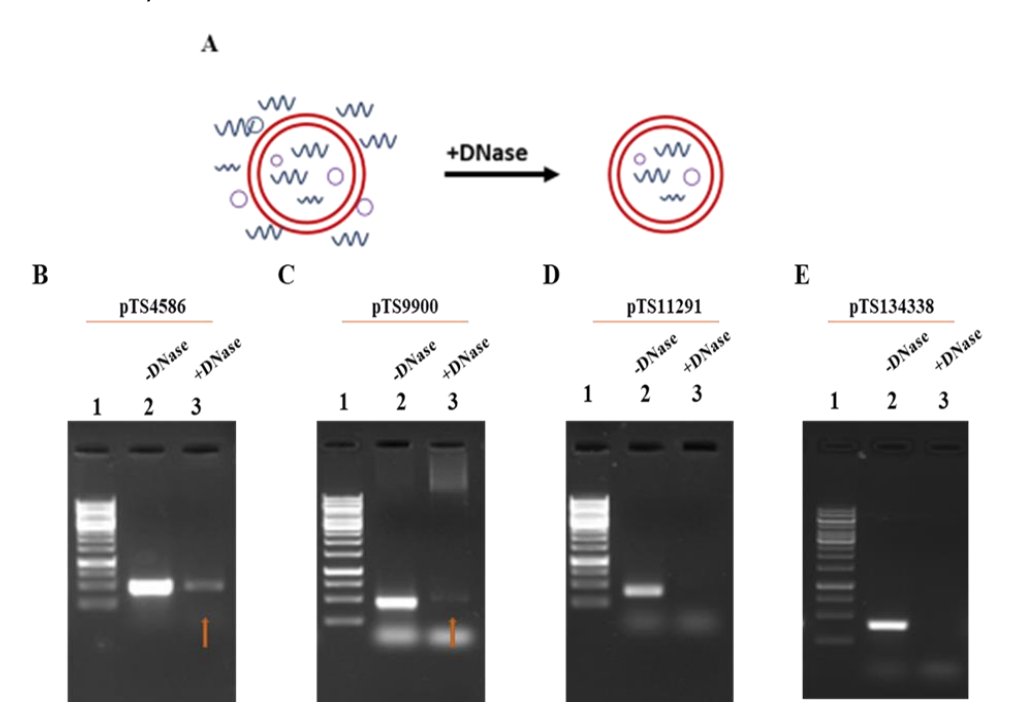


Figure 5. 4 Plasmids present inside the lumen of OMVs. Panel A represents procedures followed to treat OMVs with DNase: DNA associated with the OMV is both outside and inside (lumen) of OMV. After DNase treatment DNA inside the lumen of OMVs is protected from DNase degradation. Panels B, C, D and E show PCR amplification of pTS4586, pTS9900, pTS11291 and pTS134338 respectively. In all panel Lane 1 is DNA molecular weight marker, lane 2 represents PCR amplification using DNase untreated OMVs as a template. Lane 3 represents PCR amplification obtained using DNase treated OMVs. The amplicons obtained in DNase treated OMVs are shown with red arrow.

The plasmids pTS4586 and pTS9900 were alone available for PCR amplification as they were rescued from DNase digestion as membrane of OMV prevented from gaining access to these plasmids. These two independent studies have given clear indication about the presence of plasmids pTS4586 and pTS9900 in the lumen and pTS11291 and pTS134338 on the surface of OMVs. Experiments such as sequencing and PCR studies were performed as two biological replicates and, in both cases, we have obtained identical results.

5.2.3 Phage AbDs1 is associated with OMVs

The OMV DNA sequence didn't reveal presence of phage AbDs1 DNA, probably due to usage of more than 4 kb length contigs while aligning with genome sequence of *A. baumannii* DS002. However, one of the proteins (Orf96) coded by phage AbDs1 were found in the total proteome identified using mass spectrometry data presented in chapter-II. This preliminary lead was then verified by detecting phage coded protein, Orf96 in OMVs by performing western blots. The OMV proteins were initially probed using antibodies raised against phage AbDs1 coded protein, Orf96. As shown in corresponding western blot in Fig 5.5 B lane 2 containing OMV protein, a clear Orf96 specific signal appeared in the form of a ladder. Such signals were also found in the lanes loaded with affinity purified Orf96^{C6His} (lane 3) and *A. baumannii* DS002 cell lysate (lane 4). Multimerization SDS resistant protein is quite common, especially in virus coded proteins (Yang et al., 2001). Since similar trend is seen with respect Orf96 it is assumed that Orf96 is the coat protein of AbDs1. Appearance of signal in OMV associated proteins clearly suggests association of phage AbDs1 with OMVs (Fig 5.5).

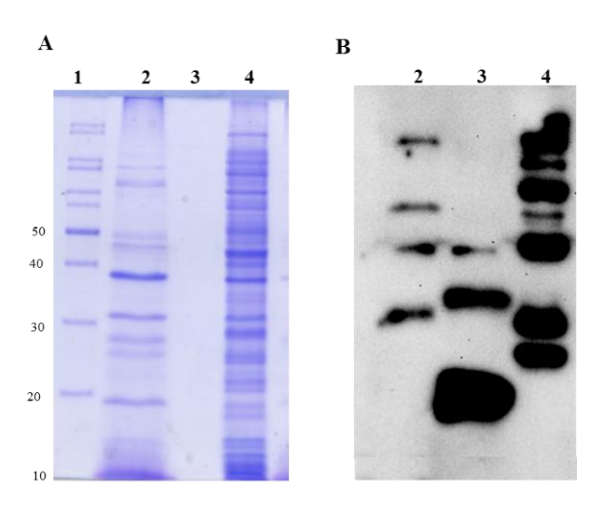


Figure 5. 5 Detection of phage AbDs1 proteins into OMVs. Panel A shows 12% SDS-PAGE. Lane 1 represents protein ladder, lane 2 is OMV proteome, lane 3 contains pure Orf96C6XHis protein and 4 shows total lysate of *A. baumannii* DS002. Panel B is the corresponding western blot probed with antibody specific to Orf96.

These results were further confirmed by performing PCR using primers that amplify all ORFs and also entire AbDs1 genome pTS236 by using vesicular DNA as template. Amplicon corresponding to the size of all the three ORFs, orf 96, orf113, repA and also complete genome of AbDs1 was seen in PCR reaction performed (Fig 5.6). After ascertaining AbDs1 existence in OMVs further experiments were conducted to identify its localization. PCR was performed using AbDs1 genome specific primers and DNase treated and untreated OMVs as template. Interestingly, no amplicon was detected in reaction mix used DNase treated Vesicular DNA as a template, indicating that AbDs1 presence on the surface of OMVs.

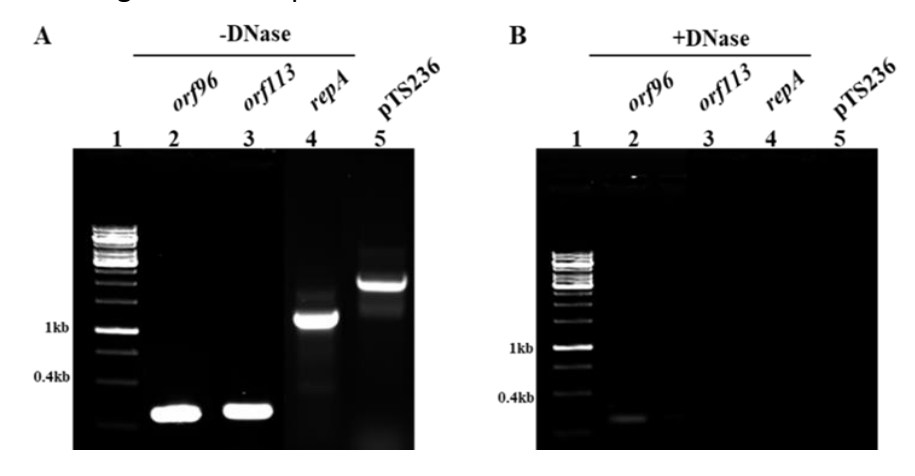


Figure 5. 6 Association of phage AbDs1 with OMVs. Panels A and B show agarose gel image indicating amplification of phage genome using primers specific to different ORFs of phage AbDs1 genome (pTS236). The panels A and B represent amplicons obtained by using DNase treated (Panel A) and untreated (Panel B) OMVs as templates. Lanes 2, 3 and 4 are amplicons specific to orf96 (291 bp), orf113 (342 bp) and repA (1137 bp). Lane 4 shows amplification of complete pTS236 sequence using repA specific FP and orf113 specific RP. In OMVs treated with DNase gave no amplification of phage genome (pTS236) specific fragments suggesting that the phage AbDs1 is associated with OMVs by establishing surface interactions.

5.2.4 Microscopic observations

Final studies were conducted to establish phage AbDs1 association with OMVs by obtaining TEM images of OMVs after treating them with Orf96 specific primary antibodies and gold-labelled secondary antibody. As described in methods sections when TEM images were obtained after incubating the grids containing OMVs with Orf96 antibodies and gold-labelled secondary antibodies. The TEM images showed presence of OMVs in the size range of 30 to 90 nm on copper grid. However, the association of gold -labelled secondary antibodies on the surface of OMVs clearly indicated existence of phage AbDs1 on the surface of OMVs (Fig 5.6 Panel A). Similar studies done by treating with OmpA specific antibodies.

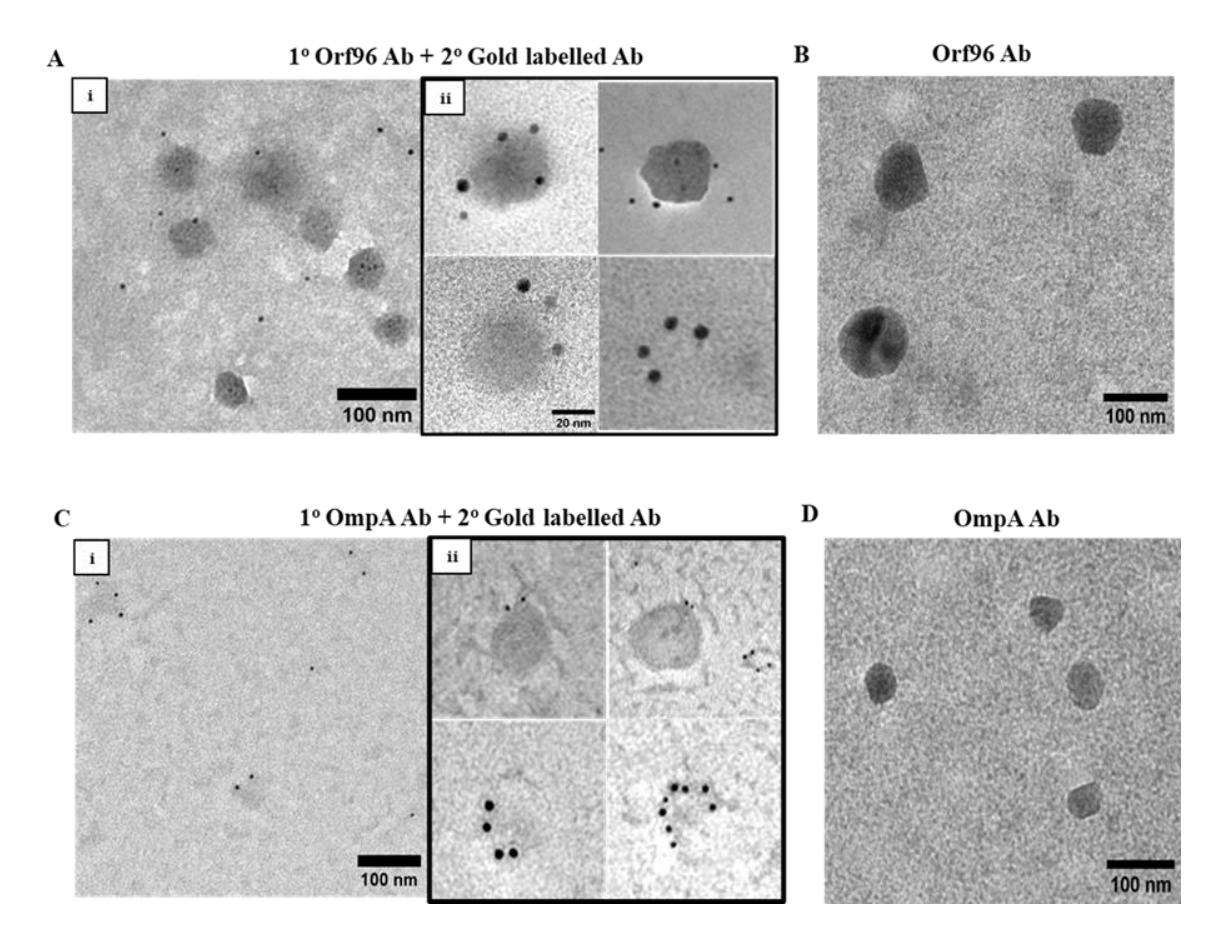


Figure 5. 7 Transmission Electron microscopy (TEM) images of OMVs. Panel A shows TEM image of OMVs after performing immunogold labelling using orf96 antibody. A (i) indicates a broad field used to take image showing presence of gold particles around OMVs. A (ii) represents single OMV molecules showing presence of gold particles around it. Similarly, panel C represents TEM images of OMVs after performing immunogold labelling using anti-OmpA antibody as primary and gold labelled secondary antibody. Where C (i) is broad field used to take image and C (ii) represent a picture of single OMV surrounded with gold particles. Panel B and D are control TEM images of OMVs after treating with either only anti-Orf96/anti-OmpA antibody.

5.2.5 AbDs1 anchors to OMVs by Interacting with OmpA

The above-described experiments gave very clear clues on presence of AbDS1 on the surface of OMVs. However, the mechanistic details facilitating interactions between these two macromolecules (OMVs and AbDs1) are not clear. Both genetic and biochemical studies were performed to understand the mechanism underlying their association. Initially ligand blot assays were conducted to identify *A. baumannii* proteins interacting with phage AbDs1. As stated in the earlier section's phage AbDs1 genome encode for three proteins; RepA, Orf96 and Orf113. RepA has and established function in the replication (Longkumer et al., 2013). The other two are proteins of unknown function and probably playing a role in establishing effective contact with *A. baumannii* DS002 proteins. Initially, these two proteins were expressed in *E. coli* with C-terminal His-tag and affinity purified following standard protocol.

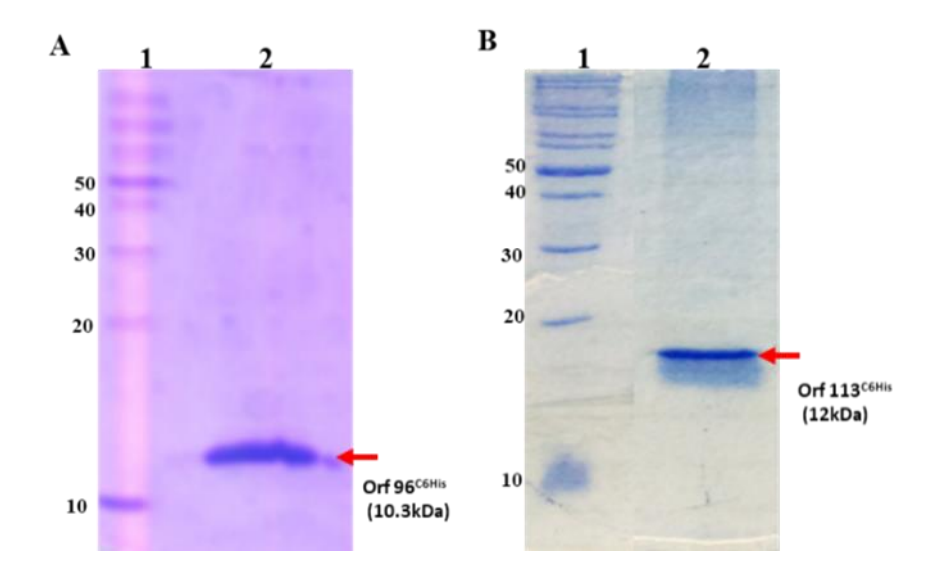


Figure 5. 8 Purification of Orf96^{C6XHis} **and Orf113**^{C6XHis}. Panel A shows 15% SDS-PAGE. Lane 1 is molecular weight marker and lane 2 represents affinity purified Orf96^{C6XHis} shown with red arrow mark. Panel B indicate purification of Orf113^{C6XHis} where lane 1 represents molecular weight marker and lane 2 affinity purified of Orf113^{C6XHis} shown with a red colour arrow.

After obtaining pure Orf96^{C6XHis} and Orf113^{C6XHis} (Fig 5.8 A & B) they were used to perform ligand blot assays. The proteins of *A. baumannii* OMV were separated on 12.5% SDS-PAGE and immobilized on PVDF membrane and incubated independently with affinity purified Orf96^{C6His} and Orf113^{C6XHis}. After incubation the membrane was extensively washed and western blots were carried out using anti-His antibodies. A protein with below 40 kDa size gave signal (Fig 5.9 A & B) in membranes incubated with only Orf96^{C6XHis} and such signal was not seen when membrane was incubated with Orf113^{C6XHis} (Fig 5.9 C). Pure Orf96^{C6His} and Orf113^{C6XHis} were used as positive control for western blot (Fig 5.9 B & C, lane 3).

The OMV protein interacting with Orf96^{C6His} was identified by performing mass spectrophotometry. The band interacting with Orf96 was excised from the SDS-PAGE and its identity was established by performing MALDI-ToF/ToF following procedures described in methods section (chapter 2 method section) The protein that interacted with Orf96^{C6His} gave a mass profile that resembles with OmpA protein of *A. baumannii* DS002. Further the sequence of peptides determined by performing MS/MS matched with OmpA sequence. The sequence of four fragments matched exactly with the sequence of OmpA at various positions suggesting that the Orf96 interacting partner is OmpA (Fig 5.10 A, B, C & D).

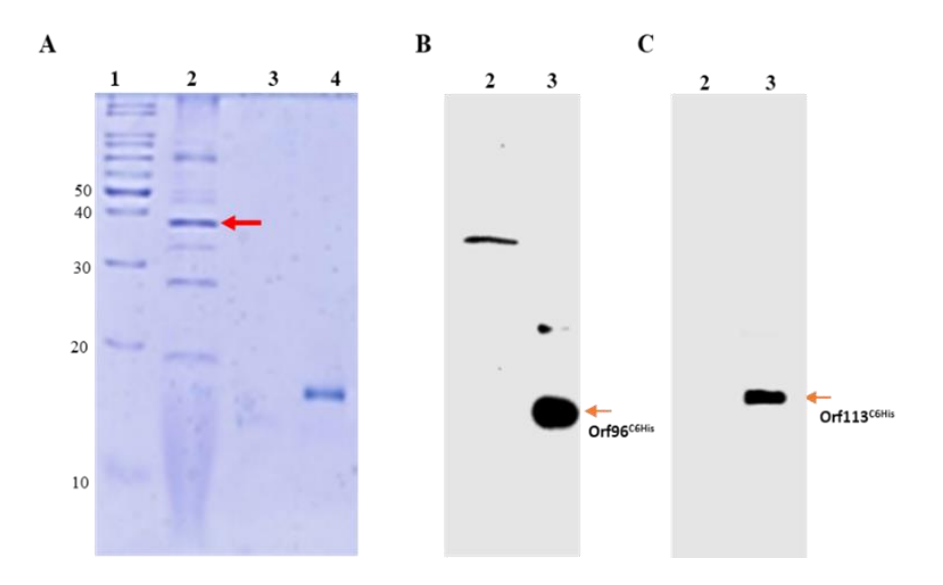


Figure 5. 9 Ligand blot assay for detection of proteins interacting with phage structural proteins. Panel A shows 12.5% SDS-PAGE stained with Coomassie blue. Lane 1 represents protein ladder, lane 2 shows OMV protein, lane 3 and 4 are pure Orf96^{C6Xhis} and pure Orf113^{C6XHis} respectively used as positive controls. The proteins resolved on SDS-PAGE were then transferred on to a PVDF membrane and incubated with either Orf96^{C6XHis} and Orf113^{C6XHis}. After incubation the membrane was probed with anti-His antibodies. Panel B represents the ligand blotting results performed by incubating membrane with pure Orf96^{C6Xhis} protein and developed using anti-His antibody. Lane 2 A clear signal was detected below the size of 40 kDa (lane 2) and lane 3 shows signal obtained for pure Orf96^{C6Xhis} (11 kDa). Similar blot generated by incubating with pure Orf113^{C6XHis} protein is shown in panel C. There was no signal in lane loaded with OMVs (lane 2) whereas clear signal was seen at the size of Orf113^{C6XHis} protein in lane 3.

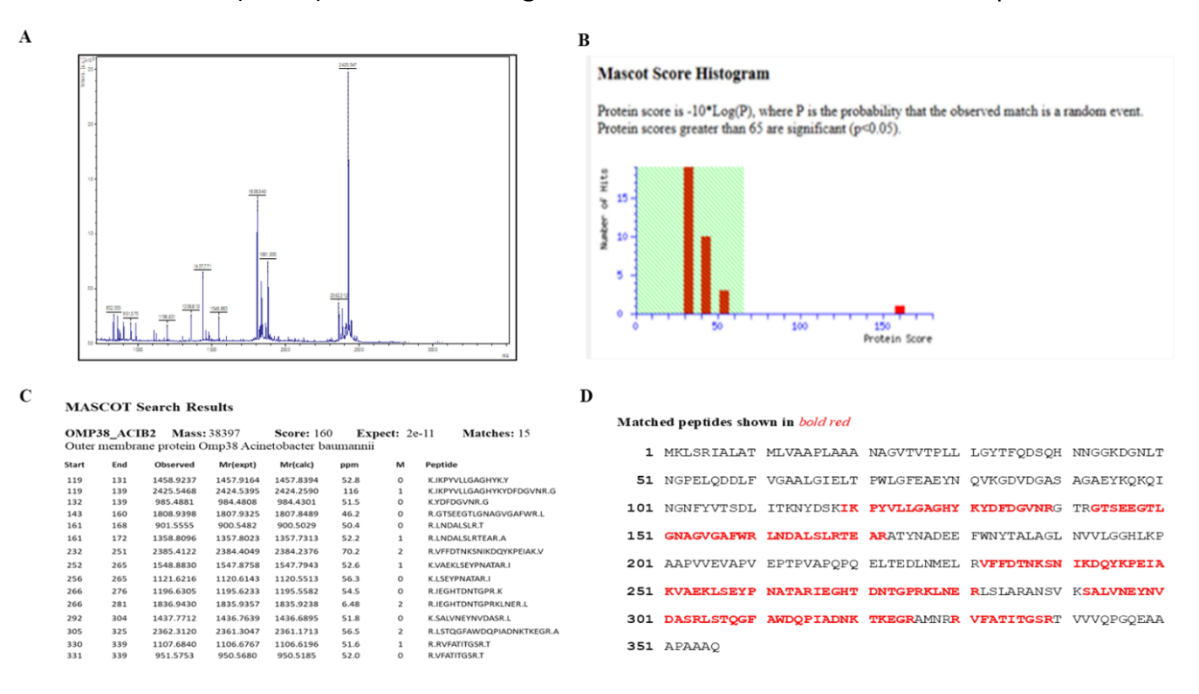


Figure 5. 10 Mascot score of Orf96 interacting protein. The mass profile of tryptic digested peptide fragments and corresponding Mascot ID generated for 14kDa protein band is shown in panels A and B. The sequence of selected peptide generated through MS/MS analysis shown in panel C. The sequence of OmpA highlighted in red colour indicate identity between the generated peptide sequences through MS/MS and the sequence of OmpA predicted from the genome sequence of *A. baumannii* ATCC 19606 (panel D).

5.2.6 Validation of OmpA and Orf96 interaction

The results obtained from ligand blot assay were confirmed by performing both biochemical and genetic studies. Reciprocal pulldowns were performed by co-expressing both OmpA^{CFLAG} and Orf96^{C6XHis} or Orf113^{C6XHis}.

5.2.6.1 Expression and Purification of OmpACFLAG

The schematic representation of strategy used for construction of pGD2 is shown in Fig 5.8 A. Initially, *ompA* gene was amplified using primer set GD7FP/GD7RP. The forward primer GD7FP is designed taking the initiation codon of *ompA* sequence and introduced *NdeI* site overlapping initiation codon, ATG (Fig 5.11 B). The reverse primer designed taking the 3' region of *ompA* gene replacing stop codon of the *ompA* gene and by adding additional codons specifying FLAG epitope. After FLAG epitope specific sequence, a stop codon followed by *HindIII* site was introduced in the reverse primer. The amplicon of 1102 bp was digested with *NdeI* and *HindIII* and were ligated in to pET23b digested with *NdeI* and *HindIII* (Fig 5.11 C).

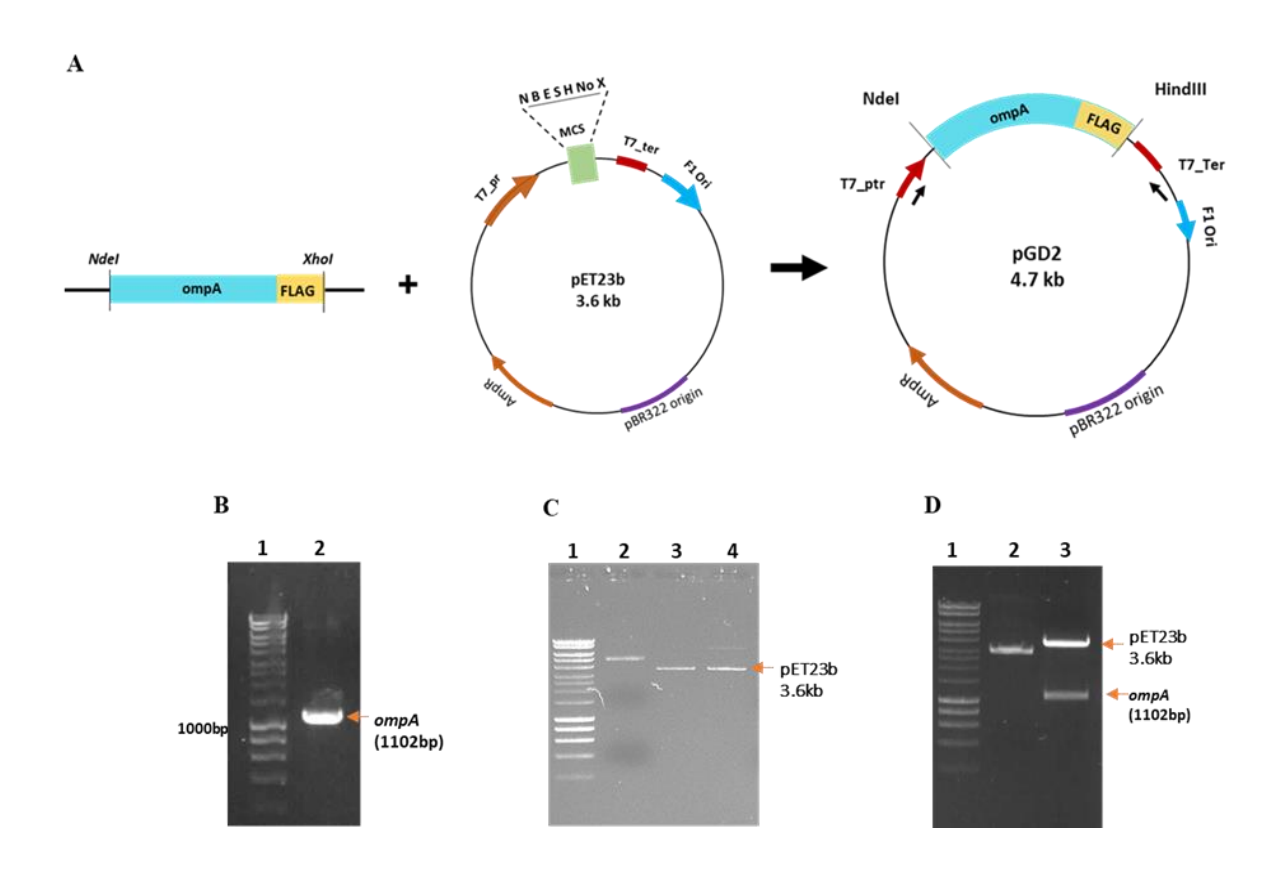


Figure 5. 11 Construction of expression plasmid coding OmpA^{CFLAG}. Panel A shows strategy followed for the construction of pGD2. Panel B shows PCR amplification of *ompA*. Lanes 1 & 2 show 1 Kb DNA ladder and PCR amplicon of *ompA* (1.1 Kb). Digestion of pET23b is shown in panel C. Lane 1 is 1 Kb DNA ladder, lane 2 shows uncut pET23b. lane 3 and 4 indicate pET23b digested with Ndel and HindIII respectively. Ligation of *ompA* in pET23b is shown in panel D. Lanes 1 show 1 Kb DNA ladder. Lane 2 & 3 are uncut pGD2 and release of insert *ompA* from pGD2 upon digestion with *Ndel* and *HindIII* enzymes.

The resulting recombinant plasmid was named as pGD2 and codes for OmpA^{CFLAG} (Fig 5.11 D). The expression of OmpA^{CFLAG} was then confirmed by inducing its expression in BL21 (pGD2) and detecting OmpA^{CFLAG} by performing western blots using anti-FLAG antibodies (Fig 5.12).

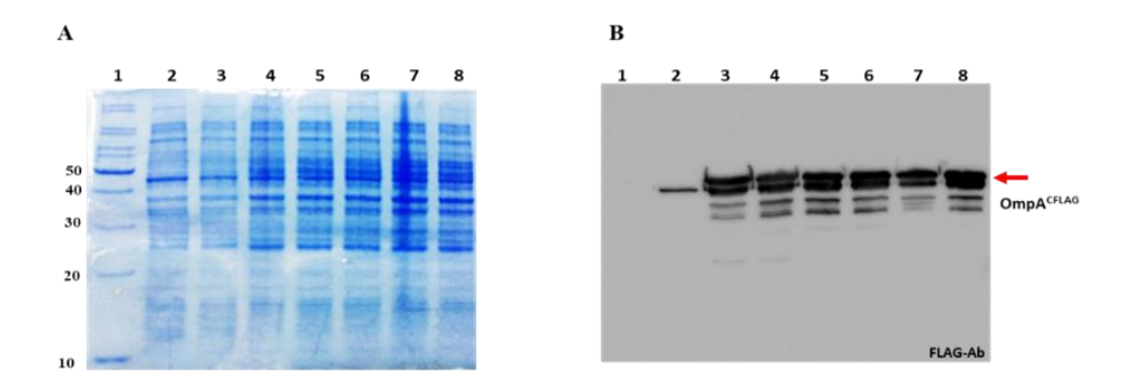


Figure 5. 12 Expression of OmpA^{CFLAG} in *E. coli* **BI21 DE3 cells.** Panel A shows 12.5% SDS-PAGE indicating expression of OmpA^{CFLAG} induced with 1mM IPTG. Cells were collected at various time points after induction and the OmpA^{CFLAG} expression levels were detected by performing western blot with anti-FLAG antibody. Lane 1 shows protein ladder, lane 2 is uninduced sample and lanes 3 to 8 were loaded with proteins extracted from *E. coli* BL21 (pGD2) cells collected at different time points after induction. Panel B shows corresponding western blot developed using anti-FLAG antibody. Degradation of OmpA protein can be seen in all the lanes (B, lane 3 to lane 8).

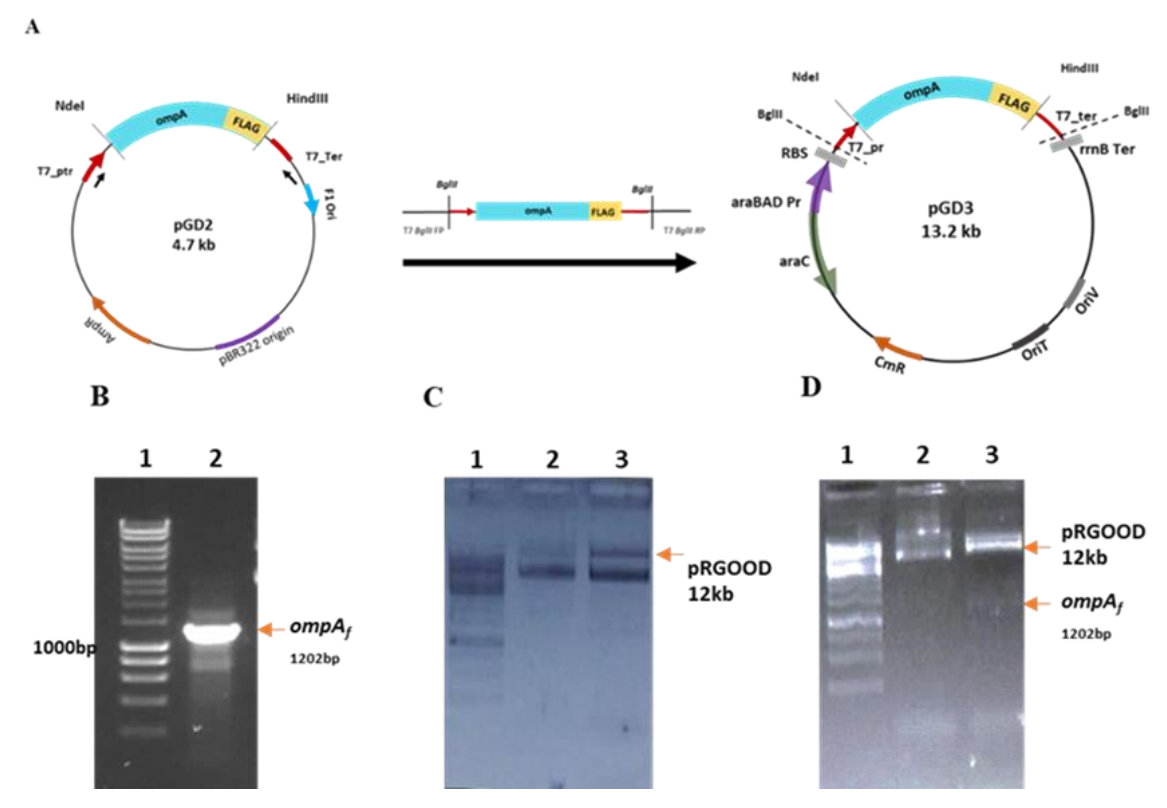


Figure 5. 13 Generation of pGD3 expressing OmpA^{CFLAG}. Panel A shows strategy followed for the construction of pGD3. Panel B shows PCR amplification of *ompA* using T7FP/T7RP appended with *Bg/*II. Lanes 1 & 2 show 1 Kb DNA ladder and PCR amplicon of *ompA* (1.2 Kb). Digestion of pRGOOD is shown in panel C. Lane 1 is 1 Kb DNA ladder, lane 2 & 3 indicate undigested & digested pRGOOD with *Bg/*II respectively. Ligation of *ompA* in pRGOOD is shown in panel D. Lanes 1 show 1 Kb DNA ladder. Lane 2 & 3 are uncut pGD3 and release of insert *ompA* from pGD3 upon digestion with *Bg/*II enzymes.

After ascertaining OmpA expression in BL21 the *ompA* gene coding OmpA^{CFLAG} was amplified using primer set (T7FP/T7RP) as Bg/II fragment and cloned into pRGOOD digested with similar enzyme. The recombinant plasmid was designated as pGD3 codes for OmpA^{CFLAG} under the control of an arabinose inducible P_{Bad} promoter (Fig 5.13). The expression of OmpA^{CFLAG} was further confirmed by inducing the $E.\ coli\ BL21\ (pGD3)$ cells with 1% arabinose. Expression of OmpA^{CFLAG} protein in $E.\ coli\ BL21\ (pGD3)$ cells were detected by performing western blots using anti-FLAG antibodies. Specific signal without any degradation corresponding to the size of OmpA at 40 kDa was seen in arabinose induced cultures (Fig 5.14).

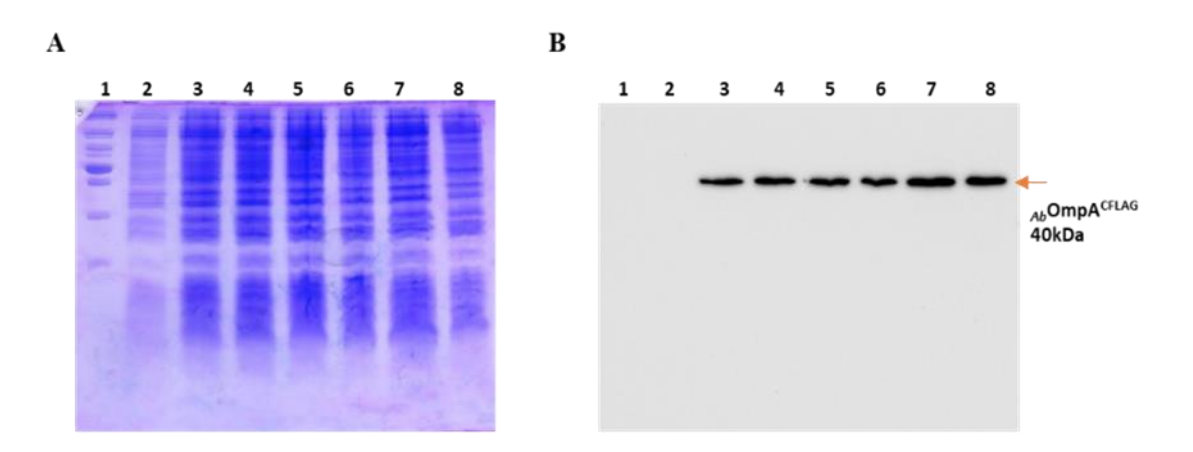


Figure 5. 14 Expression of OmpA^{CFLAG} in *E. coli* **BL21 DE3 cells.** Panel A shows SDS-PAGE (12.5%) indicating expression of OmpA^{CFLAG} induced with 1% arabinose. Cells were withdrawn at various time points after induction and the levels of OmpA^{C6His} expression was determined by performing western blots using anti-FLAG antibodies. Lane 1 shows protein ladder, lane 2 is uninduced sample and lanes 3 to 8 were loaded with proteins extracted from *E. coli* BL21 (pGD3) cells collected after various time points of induction. Panel B shows corresponding western blot developed using anti-FLAG antibody. There was no signal in lanes-2 loaded with proteins collected from uninduced cells. A clear band at 40 kDa was seen in lanes loaded with proteins collected from induced cells (lane 3 to lane 8).

5.2.6.2 Co-expression of OmpA^{CFLAG} and Orf96^{C6XHis}

E. coli BL21(pGD3 + pT96W) cells expressing OmpA^{CFLAG} and Orf96^{C6XHis} were induced by adding 1% arabinose and 1mM IPTG to the cultures grown to mid log phase. After induction the cells were lysed and the clear lysate obtained after centrifuging the lysate at 13,000 rpm was taken to perform SDS-PAGE and western blots with anti-His and anti-FLAG antibodies respectively. Both OmpA^{CFLAG} and Orf96^{C6His} specific signals were detected in western blots (Fig 5.15). A 40 kDa signal equal to the size of OmpA was seen in blot probed with anti-FLAG antibody and a 12 kDa signal corresponding to the size of Orf96^{C6XHis} was seen in blot probed with anti-His antibody (Fig 5.15 B & C).

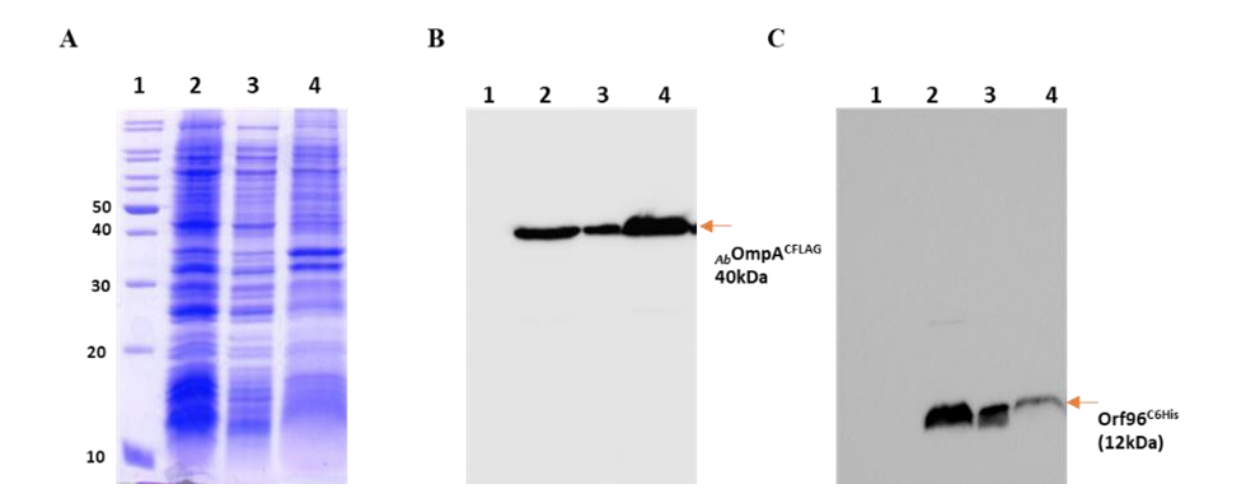


Figure 5. 15 Co-expression of Orf96^{C6XHis} **and OmpA**^{CFLAG}. Panel A shows SDS-PAGE image of cell lysate obtained from *E. coli* BL21 (pGD3 + pT96W) cells. Lane 1 is protein molecular weight marker, lane 2 shows lysate from *E. coli* expressing Orf96^{C6XHis} and OmpA^{CFLAG}. Lanes 3 and 4 indicate supernatant and inclusion body fractions respectively. Panel B and C are corresponding western blot probed using either anti-FLAG (panel B) and anti-His (Panel C) antibodies respectively. The OmpA^{CFLAG} and Orf96^{C6XHis} specific signals were observed in all the lanes. The lysate fraction containing both OmpA^{CFLAG} and Orf96^{C6XHis} was used to perform pulldown assays.

5.2.6.3 Pull down Assays

The cell lysate of *E. coli* BL21 (pGD3 + pT96W) containing both the soluble proteins OmpA^{CFLAG} and Orf96^{C6XHis} was used to perform pull-downs by using either nickel magnetic beads or with anti-FLAG antibody magnetic beads. The proteins purified using magnetic beads were then analyzed on SDS-PAGE and western blots were performed by using either anti-FLAG or anti-His antibodies. When nickel-magnetic beads were used to pulldown His-tagged Orf96 along with it we have always seen co-elution of OmpA^{CFLAG} (Fig 5.16 A). In similar pull-down experiments performed using magnetic-anti-FLAG tag antibodies along with OmpA^{CFLAG} we have seen co-elution of Orf96^{C6His} (Fig 5.16 B). These reciprocal pulldown assays clearly indicate interactions of AbDs1phage coded protein, Orf96 with OmpA. We have also performed similar experiments by co-expressing Orf113^{C6XHis} and OmpA^{CFLAG} but could not observe any interactions of Orf113 with OmpA (Fig 5.17 A).

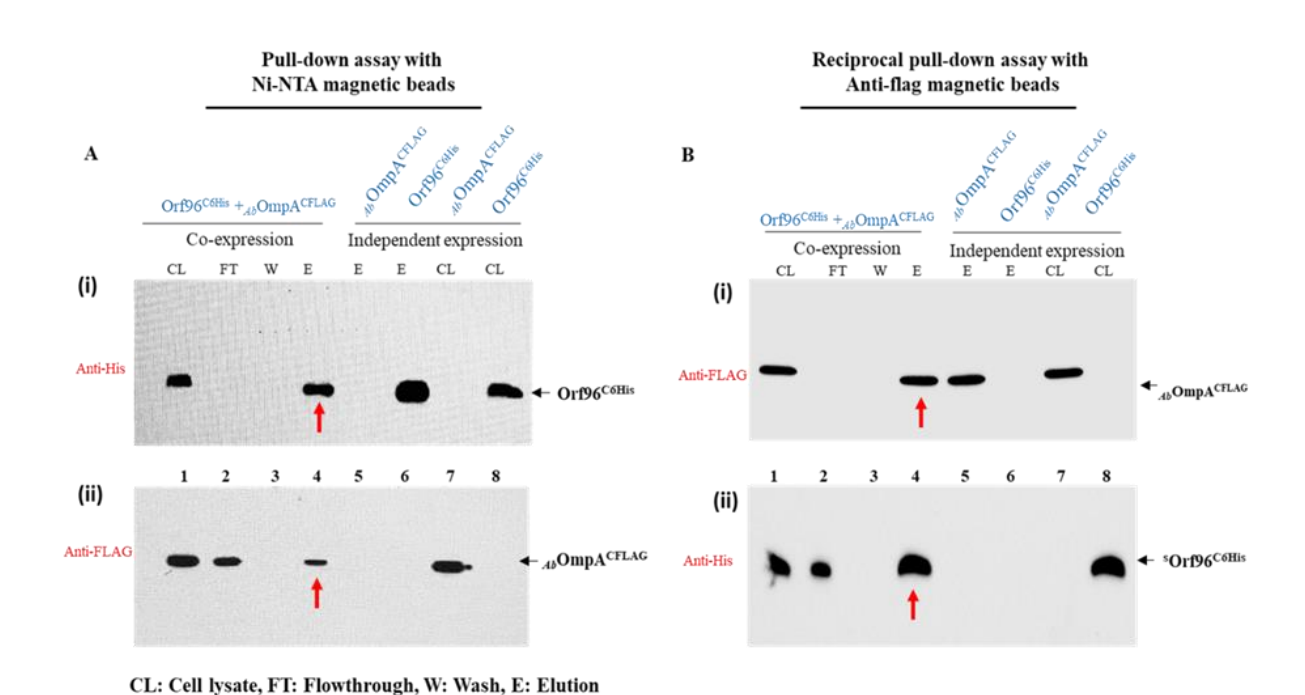
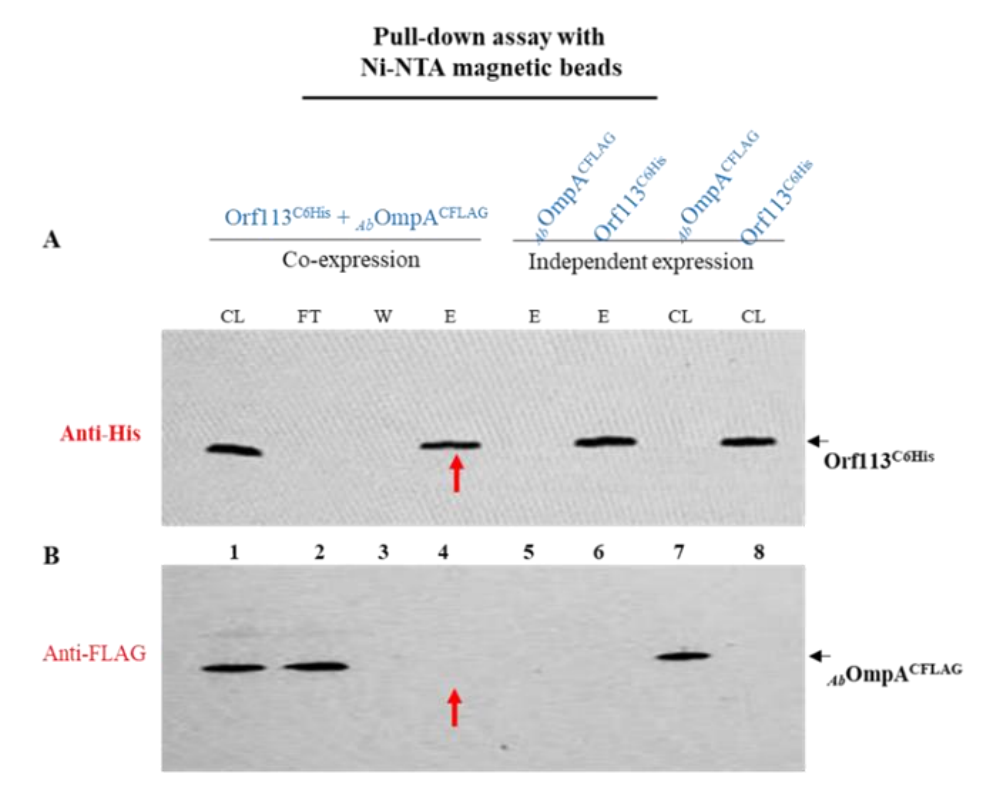


Figure 5. 16 Pulldown assays: Pulldown assays were performed to demonstrate interactions between Orf96 and OmpA. Pulldown assays performed using Ni-NTA and FLAG magnetic beads are shown in panels A and B respectively. The cell lysates prepared from cells (pGD3+pT96W) co-expressing OmpA^{CFLAG} and Orf96^{C6His} and separately (Independent expression) were used to perform pulldown assays. CL represents cell lysate used as input. The FT, W and E indicate flowthrough, wash and elution fractions respectively. Panel A-I indicates western blots performed using anti-his antibodies. Similar experiments done using anti-FLAG antibodies are shown in panel A-II. Lane CL contains both OmpA^{CFLAG} and Orf96^{C6His} specific signal. Significant amount of OmpA^{CFLAG} is seen in lane FT. No signals were seen in lane W loaded with wash due to dilution of wash fraction. The OmpA^{CFLAG} co-eluted along with Orf96^{C6His} is shown with red arrow. Reciprocal pulldown shown in panel B indicate similar loading and blotting pattern. The Orf96^{C6His} co-eluted with OmpA^{CFLAG} is shown with red arrow (Panel B-II).



CL: Cell lysate, FT: Flowthrough, W: Wash, E: Elution

Figure 5. 17 Pulldown assays performed to detect Orf113 and OmpA^{CFLAG} **interactions**: Pulldowns performed using Ni-NTA magnetic beads incubated with cell lysate obtained from *E. coli* BL21 cells (pGD3+pT113W) is shown in panels A and B. The cell lysates prepared from cells (pGD3+pT113W) expressing both OmpA^{CFLAG} and Orf113^{CGXHis} (co-expression) and separately (Independent expression) were used to perform pulldown assays. CL represents cell lysate used as input. The FT, W and E indicate flowthrough, wash and elution fractions respectively. Cell lysate contains both Orf113^{CGXHis} and OmpA^{CFLAG} specific signals, whereas elution fraction showed only Orf113^{CGXHis} specific signal but not signal specific to OmpA^{CFLAG} (shown with red arrow).

5.2.7 Genetic Evidence on phage AbDs1 with OMV interactions

Biochemical assays performed in the form of reciprocal pulldown assays have clearly indicated that the phage AbDs1 interaction with OMVs is through establishing physical interactions between OMV borne OmpA and phage genome coded Orf96. If these are the only interactions that facilitate phage AbDs1 and OMV interactions, the OMVs isolated from the *ompA* negative strains should not contain phage AbDs1. While testing this hypothesis *ompA* negative strain of *A. baumannii* DS002 was generated. The OMVs isolated from the *ompA* negative strain of *A. baumannii* DS002 was screened for the presence of AbDs1.

5.2.7.1 Generation of *ompA* mutant

The *ompA* knockout strain was generated by replacing the *ompA* gene with tetracycline cassette by following the procedures described in methods section. Pictorial representation of the complete strategy is shown in Fig 5.15 A. Initially, the regions of DNA flanking to *ompA* gene were amplified as A and B fragments and these two fragments were then ligated by using a

unique *Xho*I site (Fig 5.18). The unique *Xho*I site was then used to ligate tetracycline cassette amplified as *Xho*I fragment. The linier DNA fragment contains tetracycline resistant gene in place of *ompA* (Fig 5.18 E).

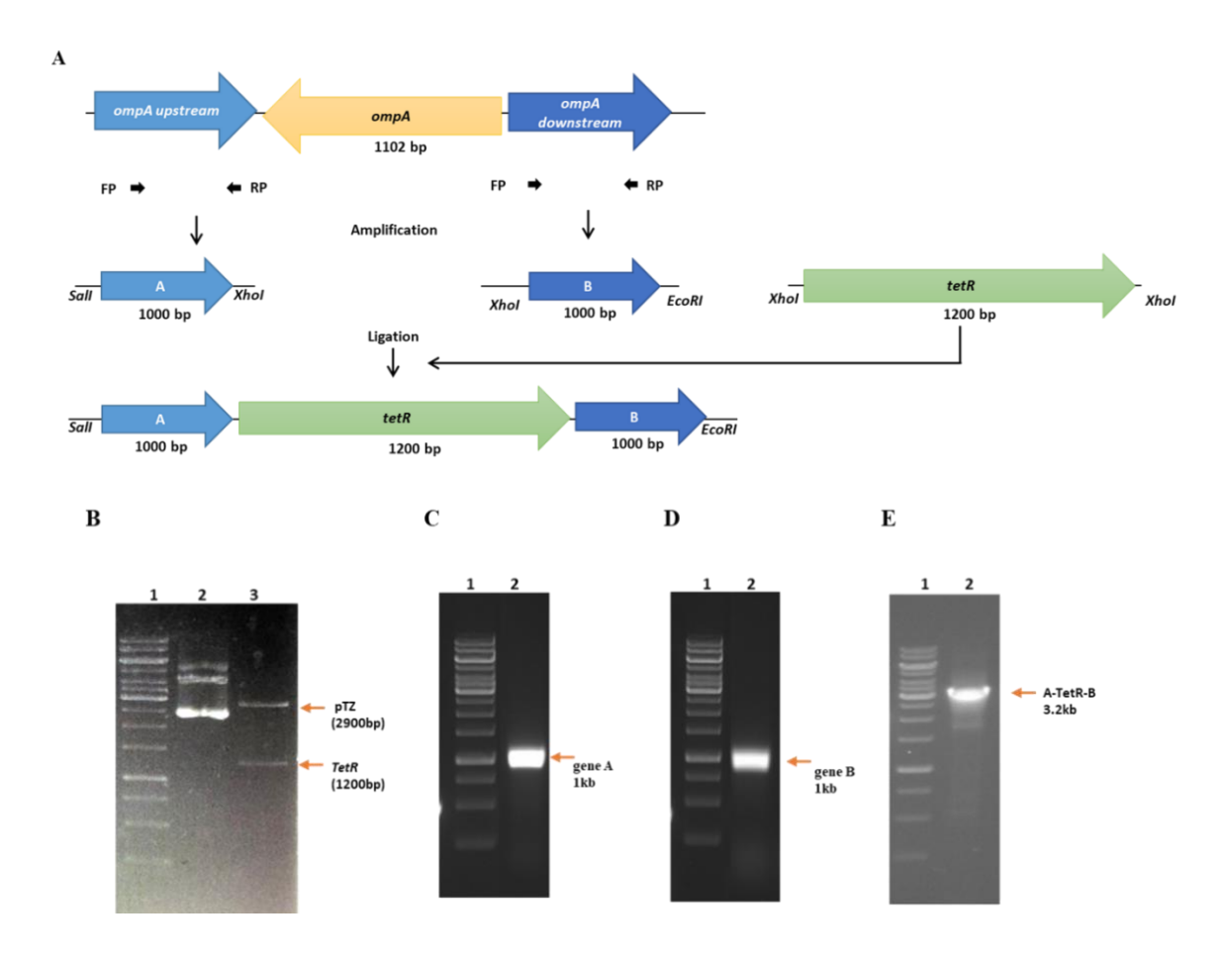


Figure 5. 18 Strategy for generation of *A. baumannii* **DS003.** Panel A shows the schematic representation of *ompA* knockout in *A. baumannii* DS002 strain. Panel C shows release of tetracycline resistance gene from pTZ-TetR vector using *Xho*I enzyme (lane 3), undigested vector is shown in lane 2. Panel C and D indicate amplification of fragment A and B respectively. Panel E shows PCR product after amplification at 3.2 kb for A-TetR-B fragment. Lane 1 in all the panels represents 1 kb DNA ladder.

The linear amplicon A-TetR-B was electroporated in *A. baumannii* (pATO2) having ectopically expressed recombinase coded by a plasmid pATO2 (Tucker et al., 2014). The transformants were selected on a tetracycline plate and about 20 to 30 colonies were screened by performing colony PCR to detect presence of *tet* gene in the genome. The *ompA* locus was amplified by using the primers (GD8 FP and GD9 RP) designed taking flanking sequence of *ompA*. In the wildtype strain, an amplicon with a size of 3.1 kb corresponding to the region congaing fragment A, *ompA* gene, and fragment B were amplified (Fig 5.19 A lane 2). However, in knockout strains a shift in amplicon size from 3.1 to 3.2 kb was observed due to incorporation of tetracycline resistant gene in place of *ompA* (Fig 5.19 A lane 3) indicating absence of *ompA* gene. The *ompA* specific signal

was absent in knockout strains (Fig 5.19 B 2) when PCR was performed using *ompA* internal primers. A 1.1 Kb *ompA* specific amplicon was seen only in wild type strains of *A. baumannii* DS002 (Fig 5.19 B lane 3). The strain having deletion in *ompA* gene is designated as *A. baumannii* DS003.

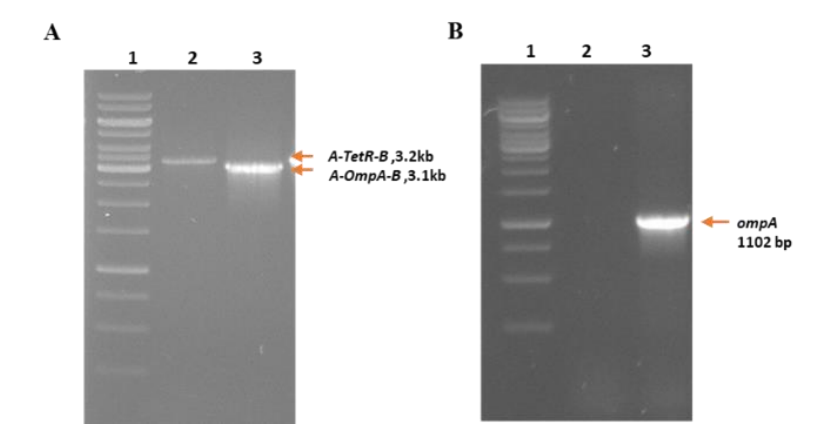


Figure 5. 19 Deletion of *ompA* **from** *A. baumannii* **DS002**: Panel A shows the incorporation of tetracycline cassette at the *ompA* gene locus. Lane 1 represents 1 Kb molecular weight marker. Lane 2 & 3 represents the amplification of *ompA* locus with fragment A forward (GD8 FP) fragment B reverse (GD9 RP) primers using colonies appeared on tetracycline plate and a colony of DS002 strain respectively. Panel B Lane 2 shows lack of amplification of *ompA* in tetracycline resistant colony when gene specific internal primers GD7 FP/RP were used in PCR reaction mix. The *ompA* deletion mutant was the designated as *A. baumannii* DS003

5.2.8 Isolation of OMVs from A. baumannii DS003

The OMVs were prepared from the *A. baumannii* DS003 strain using similar procedures that were followed for isolating OMVs from wild type strain. Upon sucrose density gradient a single band of OMVs were observed between 20% and 30 % sucrose (Fig 5.20 A). The SDS-PAGE profile of OMV proteins isolated from DS002 (WT) and DS003 (*ompA* mutant) strain revealed interesting facts. The protein profile of OMVs isolated from DS003 strain showed presence of a greater number of proteins, especially at high molecular weight range (Fig 5.20 B, lane 3). The corresponding western blots developed using OmpA antibody gave no OmpA specific signal indicating the absence of OmpA in OMVs of DS003 strain (Fig 5.20 C). TEM images were also obtained for OMVs isolated from DS003. As seen in Fig 5.18 D i & iii the OMVs of DS003 have lost the proper shape of OMVs (Fig 5.20 D i & iii) due to loss of membrane integrity. However, the OMVs isolated from DS002 strains retained shape and membrane integrity (Fig 5.20 D ii & iv). The size distribution analysis performed using particle track analysis for OMVs isolated from strain DS003 showed OMVs with greater diameter (Fig 5.20 E).

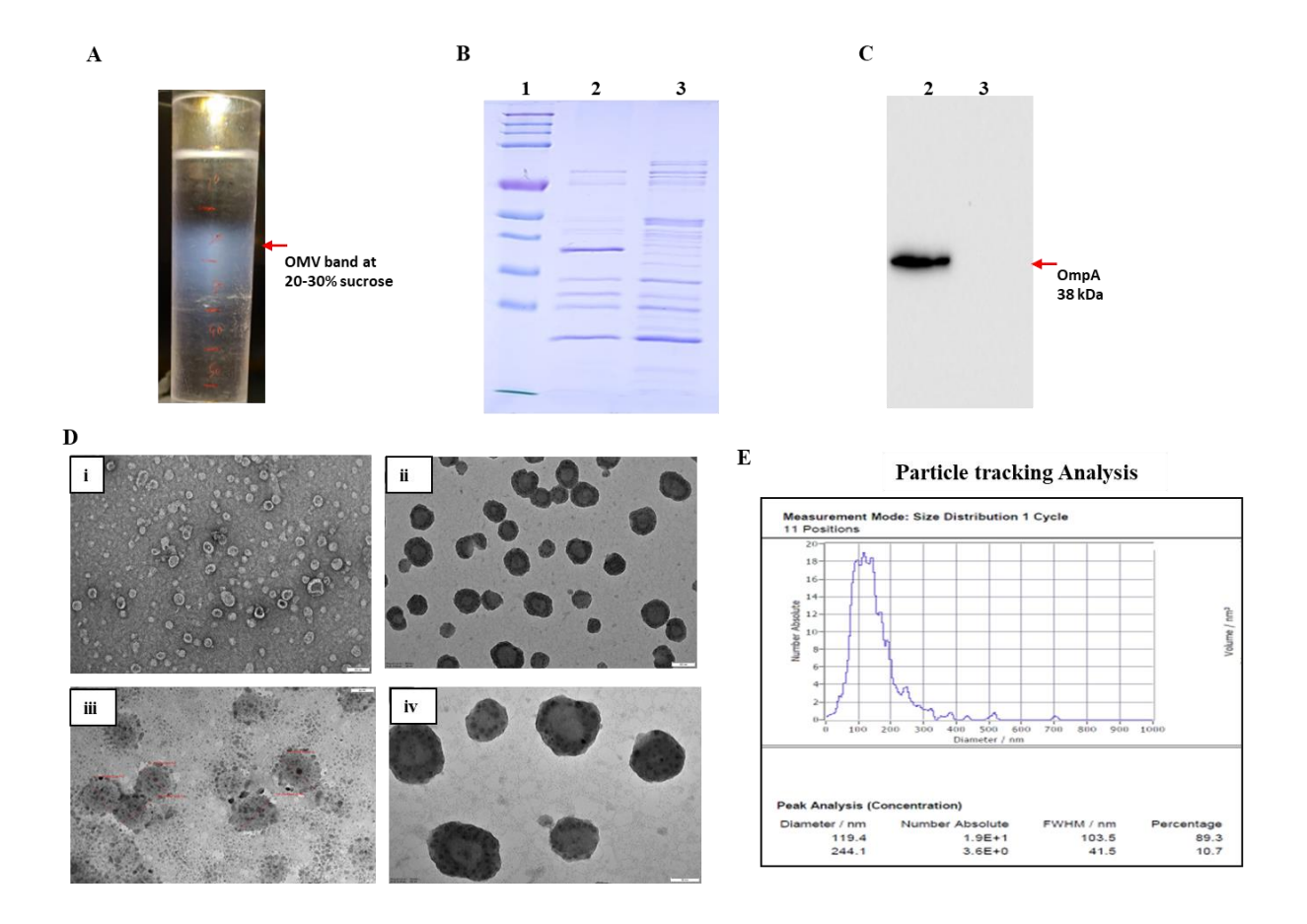


Figure 5. 20 Isolation of OMVs from *A. baumannii* **DS003 strain.** Panel A shows OMV band formed in sucrose density gradient at the range of 20% and 30%. Panel B shows SDS-PAGE profile of proteins isolated from WT (DS002) and *ompA* KO (DS003) in lane 2 and 3 respectively. The corresponding western blot probed using anti-OmpA antibody, indicates absence of OmpA specific signal in the lane loaded with OMV proteins isolated from DS003 (Panel C, Lane 3). However, a clear signal corresponding to the size of OmpA is seen in lane 2 loaded with WT OMV. Panel D is comparison of TEM images of OMVs isolated from WT and *ompA* KO strains. D (i) and (ii) represent TEM images of *ompA* KO strain. D (iii) and D (iv) show TEM images of WT OMV. Panel E is particle tracking analysis of OMVs isolated from *ompA* KO strain DS003.

5.2.9 OmpA is critical for AbDs1 Association with OMVs

After physical characterization of OMVs isolated from strain DS003 they were then used to detect phage AbDs1. Initially, these OMVs were used as templates in a PCR reaction performed using primers specific for the genome of phage AbDs1. Surprisingly, no amplification was observed correspondent to any of the ORFs specific to AbDs1 genome (Fig 5.21). This observation has provided very conclusive evidence on association of AbDs1 to OMVs by establishing physical interactions between OmpA of OMVs and Orf96 of phage AbDs1.

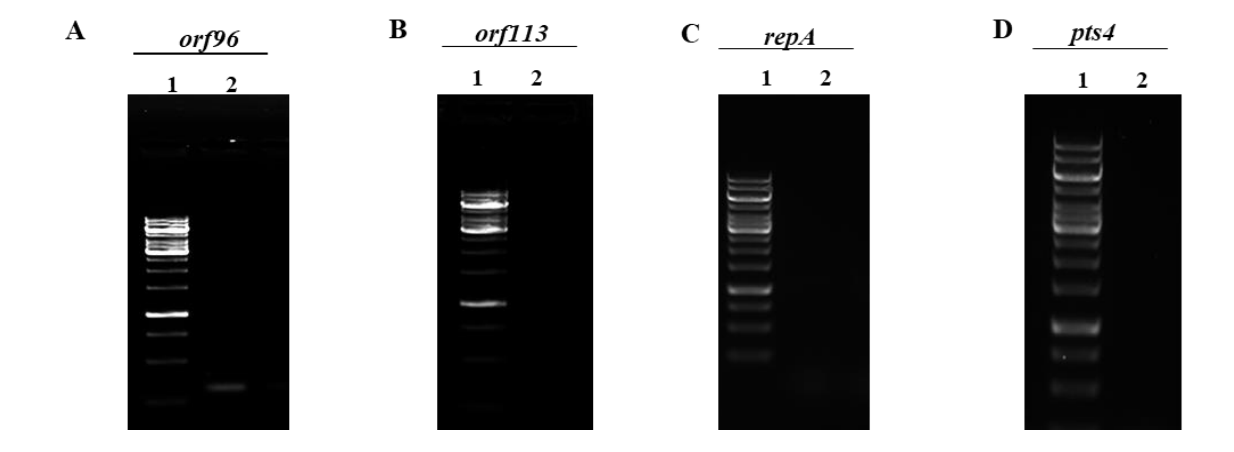


Figure 5. 21 PCR amplification of phage genome pTS236 from OMVs isolated from strain DS003. Panel A, B, C and D indicate amplification of *orf96, orf113, repA* and pTS4 complete genome. In all the panels Lane 1 shows 1kb DNA ladder and lane 2 is loaded with PCR reaction mix used to amplify ORFs of phage AbDs1 genome. No pTS236 specific amplification was observed when OMVs of DS003 were used as template.

5.2.10 Role of OMVs in lateral Mobility

After ascertaining presence of plasmid and phage, further experiments were conducted to demonstrate the role of OMV in lateral mobility of phage and plasmid DNA. Before proceeding to conduct experiments to demonstrate the role of OMVs in lateral mobility of plasmid and phage, the phage and plasmid pTS5486 derivatives were generated. The pTS4586 is 4.5 kb plasmid identified in A. baumannii DS002 and its presence is also established in the lumen of OMVs. In order to monitor the lateral mobility of plasmid, the plasmid pTS4586 was tagged with drug resistance gene. Further, the stability of the laterally transferred plasmid in the recipient strain depends on its replication machinery of the host. Since, plasmid pTS4586 having narrow host replicative origin, its replication in other gram-negative bacteria is uncertain. Therefore, the kanamycin resistance cassette with R6KY replicative origin is inserted in plasmid pTS5486 by performing in vitro transposition and rescue cloned into E coli pir116 cells (Longkumer et al., 2013). This mini transposon tagged pTS4586-K (pTS4586-K) was electroporated into A. baumannii DS002 strain and the transformants were propagated in LB medium containing kanamycin to facilitate retaining of pTS4586-K derivate containing kanamycin resistance cassette. The OMVs isolated from this culture were screened using kanamycin specific primers to ascertain incorporation of pTS4586-K into the OMVs. As expected, the OMVs isolated from A. baumannii DS002 (pTS4586-K) gave amplicon showing the presence of pTS4586-K in OMVs (Fig 5.22). These OMVs were used to demonstrate the lateral mobility of pTS4586-K. Since, kanamycin cassette contains R6Ky replication origin the E. coli pir116 cells were used as recipient while demonstrating OMV mediated lateral mobility of pTS4586-K plasmid. Mid log phase grown pir116 cells were harvested and the cell pellet was resuspended in cold SOC medium. Pure OMV (20 µg) was added and incubated for outgrowth as detailed in method section. After incubation for 12 h, cells were plated on kanamycin containing LB plates. No kanamycin resistant colonies were observed even after incubating cells with OMVs for 12 h, indicating that no lateral mobility of plasmid pTS4586-K was possible under the experimental condition followed in the study.

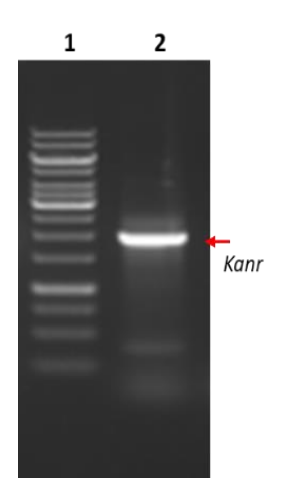


Figure 5. 22 Existence of plasmid pTS4586-K in OMVs isolated from *A. baumannii* (pTS4586-K). lane 1 shows 1 kb DNA ladder. Lane 2 indicates amplification of kanamycin cassette at 2kb.

5.2.10.1 Lateral mobility of phage AbDs1 genome

Several experiments were performed to show the OMVs mediated lateral mobility of phage AbDs1 into bacterial as well as mammalian cells. The experiments to demonstrate lateral mobility of phage genome into mammalian cell lines were performed due to the existence of reports showing high sequence similarity between phage genome and close covalent circular DNA identified in brain tissue of mammals suffering from transmissible spongiform encephalopathies (TSEs), such as Creutzfeldt–Jakob Disease (CJD), Kuru in humans, Scrapie in sheep, and BSE in cows (Manuelidis, 2011). These are claimed to be a group of related, but not well characterized infectious agents. Further, recent studies done at German Cancer Research Institute, Heidelberg, Germany had demonstrated the presence of circular replication competent DNA molecules in Brain, meat and milk samples of cattle which are otherwise designated as brain meat and milk factors (BMMFs). About 110 number of BMMFs were identified in mammalian tissues (zur Hausen et al., 2017) (Oxley Jimmie, Smith James, Busby Taylor, 2022). The number got enriched in colorectal cancer tissues (König et al., 2021). The inflammatory response induced by BMMFs is predicted to be responsible for cancer induction (Zur Hausen & De Villiers, 2015). A

number of BMMFs show similarity with phage genome, especially in the region coding for *repA* is highly conserved suggesting existence of a common lineage between BMMFs and phage AbDs1 genome. In the background of these results, further studied were designed to ascertain if phage genome is laterally transferred into bovine meat and milk through OMVs.

5.2.10.2 Construction of AbDs1 genome derivative

In a previous study our laboratory has rescue cloned phage genome by tagging a mini transposon (Longkumer et al., 2013). Initially it was assumed as plasmid and later shown to be the genome of phage AbDs1. It is named as pTS4 assuming it is an endogenous plasmid of *A. baumannii* DS002. Using the sequence information of pTS236, a detailed restriction map was generated for pTS236. A single *Mlul* site was found in the non-coding region between *repA* and *orf113*, was exploited to insert R6Ky replication origin containing kanamycin cassette in to the genome of phage pTS236 and the resulting phage DNA is named as pTS236-K1 (Fig 5.23).

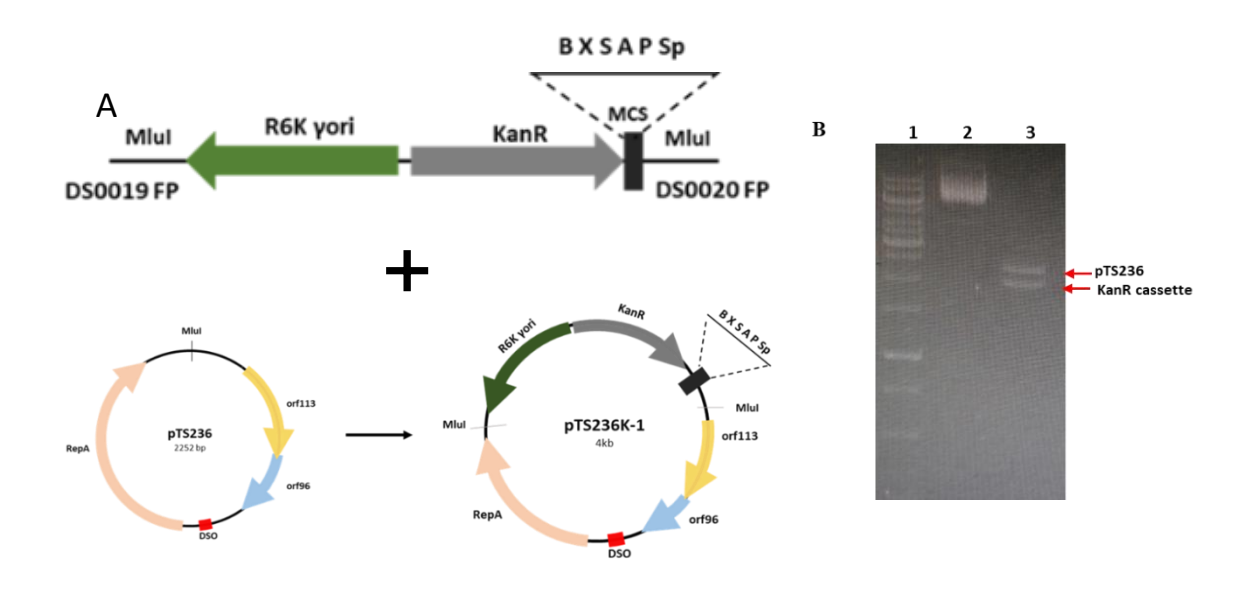


Figure 5. 23 Generation of phage genome derivative pTS236K-1. Physical map of pTS236-K1 is shown in panel A. Panel B shows release of kanamycin cassette (2 kb) after digestion of pTS236-K1 with Mlul enzyme (lane 3). Lane 1 and 2 are 1 kb DNA ladder and undigested pTS236-K1 respectively.

While testing the role of OMVs in lateral mobility of phage genome, the *A. baumannii* DS002 cells (pT236-K1) containing cells were used to isolate OMVs. OMVs were then checked for the presence of phage derivatives pTS236-K1 containing kanamycin resistance cassette and the mini replicative origin R6Kγ. The OMVs containing pTS236-K1 were used to demonstrate lateral mobility of phage genome into gram negative as well as gram positive bacterial cells. The cell pellet prepared from mid-log culture of *E. coli pir*116, *P. stutzeri*, *A. baumannii DS002* and *Bacillus*

subtilis were incubated with OMVs containing phage derivative following the procedure explained in methods section. Cells were plated on LB medium containing kanamycin after being incubated. No colonies appeared when OMVs were incubated with *E. coli pir*116, *P. stutzeri* and *Bacillus subtilis*. However, the OMVs successfully transformed otherwise kanamycin sensitive *A. baumannii* DS002 into a kanamycin resistant strain. A number of colonies were appeared on kanamycin plates when OMVs containing pTS236-K1 were incubated with DS002. The colonies obtained were further confirmed with PCR using primer specific to kanamycin, where kanamycin cassette amplification was observed suggesting that phage AbDs1 associated with OMVs retained infectivity (Fig 5.24 B). The available data do not explain the reason of not obtaining colonies with other bacteria. There may be certain unknown species-specific interaction between OMVs and *A. baumannii* DS002. More research is needed to unravel the species-specific OMV mediated lateral mobility of phage DNA at a molecular level.

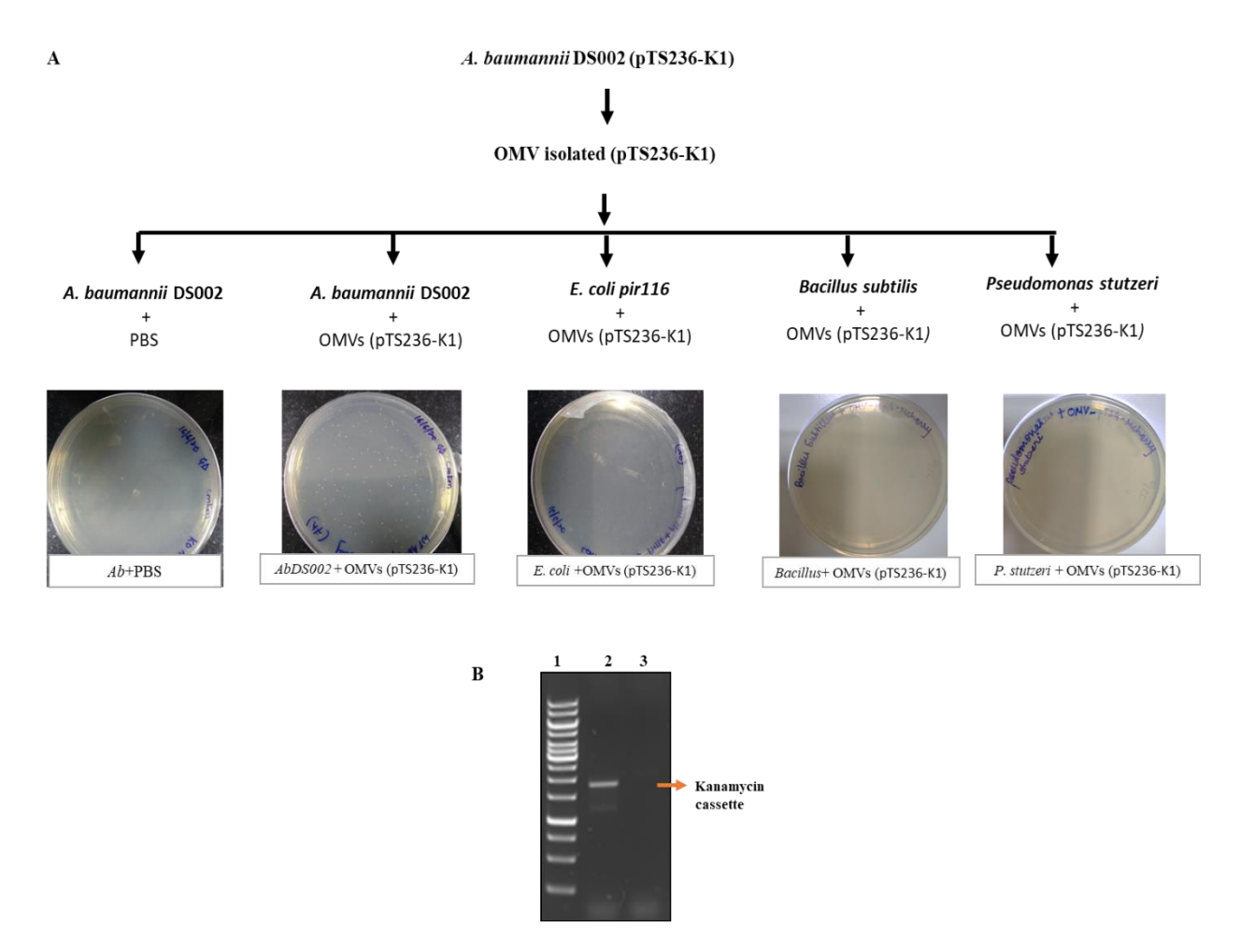


Figure 5. 24 Phage AbDs1 mobility into other bacteria. Panel A represents experimental design followed to test horizontal mobility of phage genome (pTS236-K1) into other bacterial species. The top panel represents the *E. coli* pir116 (iii), *Bacillus subtilis* (iv) and *P. stutzeri* (v) cells incubated with OMVs containing pTS236-K1. Colonies were observed only in *A. baumannii* DS002 cells (ii). *A. baumannii* DS002 incubated with PBS served as control and has shown no colonies (i). Panel B indicate amplification of 2.0 Kb kanamycin cassette from *A. baumannii* DS002 cells incubated with OMVs containing pTS236-K1(lane 2). Lanes 1 and 3 are 1 kb DNA ladder and no template control (NTC) respectively.

5.2.11 Tagging phage AbDs1 genome with GFP

The pTS236 is not suitable to track the lateral mobility of the phage DNA into mammalian cells. Therefore, a DNA sequence codon optimized to express eukaryotic Green Fluorescence Protein (GFP), from a CMV promoter and SV_40_ PA terminator was amplified using pEGFP-C1 plasmid as a template. The primer set used to amplify *GFP* sequence was appended with *BamHI* and *SalI* fragment (Fig 5.25 B lane 2). The amplicon corresponding to the size of 1.5 kb was digested with *BamHI* and *SalI* and cloned into phage genome derivative pTS236-K1 digested with similar enzyme (Fig 5.25 C). Ligation of *GFP* sequence was confirmed by detecting the release of *GFP* at 1. 5 kb after digesting the recombinant plasmid with *BamHI* and *SalI* (Fig 5.25 D lane 3). The construct was designated as pGD5.

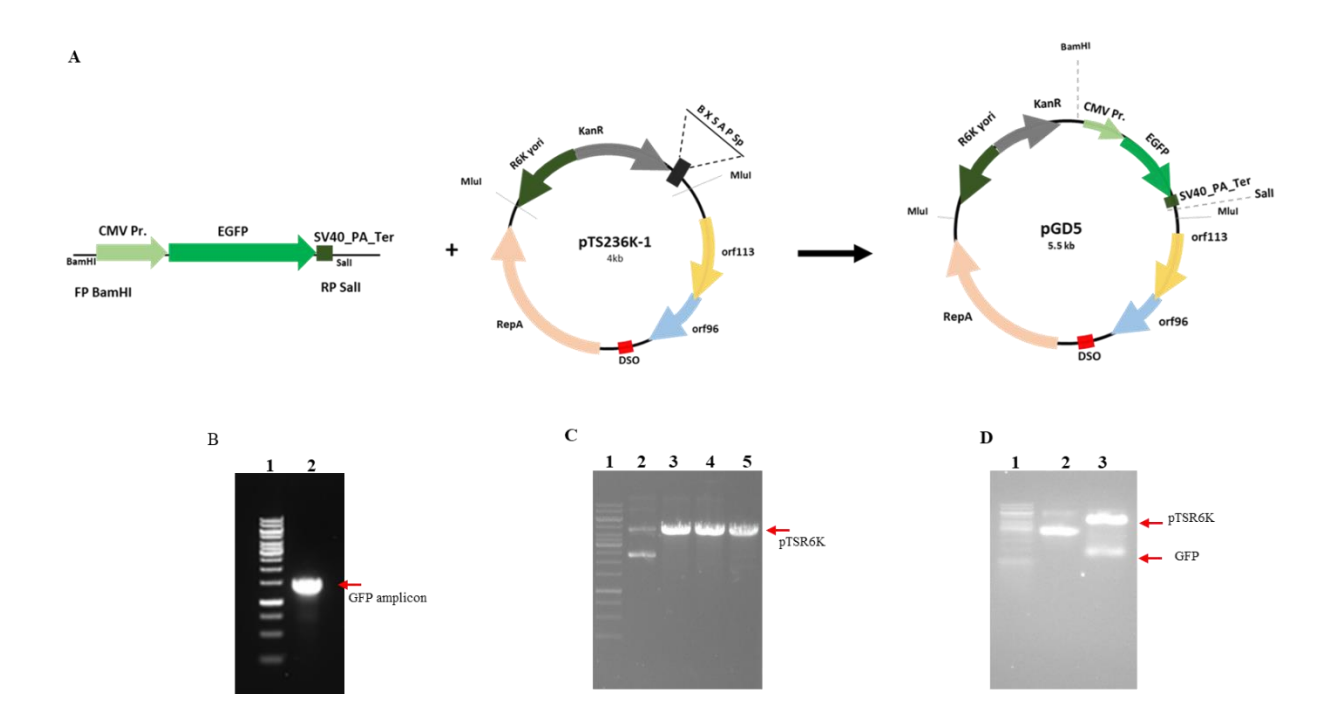


Figure 5. 25 Tagging genome of phage AbDs1 with GFP. Panel A shows the strategy followed for the construction of pGD5. Panel B indicate GFP amplicon at 1.5 kb (lane 2). Panel C shows restriction digestion of pTS236-K1 with *Bam*HI and *Sal*I (lane 5), whereas lane 3 and 4 are loaded with pTS236-K1 independently digested with *Bam*HI and *Sal*I respectively. Undigested pTS236-K1 is shown in lane 2. Panel D shows ligation of GFP fragment to pTS236-K1 (lane 3). Lane 2 is undigested pGD5 plasmid. Lane 1 in all B, C and D panels indicate 1 kb DNA ladder.

5.2.11.1 Lateral transfer of phage genome into Neuronal cell line Neu2A

Plasmid pGD5 (pT236-K1-GFP) was electroporated into *A. baumannii* DS002 strain and the resultant culture, *A. baumannii* DS002 (pT236-K1-GFP) was propagated in a media containing kanamycin. The OMVs isolated from *A. baumannii* DS002 (pGD5) strain was tested for the

presence of pGD5 in their OMVs by performing PCR using primer specific to GFP (Fig 5.26 A). Neuronal cell line Neu2A was seeded at cell density of 5×10⁴ on glass coverslips in DMEM complete media a day before performing the mobilization experiment. Next day, OMVs carrying phage genome derivative pGD5 (20 µg protein concentration) was added to the cells and incubated for different time points (6 h, 12 h and 24 h). After incubation time period, the coverslips were fixed and visualized under fluorescent microscopy. Neu2A cells collected at 24 h post OMV treatment showed fluorescent signal in few cells suggesting mobilization of phage genome AbDs1 into Neuronal cell line (Fig 5.26 B). However, further experiments with various concentration of OMVs along with simultaneous tracking of OMVs in OMV treated cells are required to establish the long-term stability of phage genome AbDs1 in Neu2A neuronal cells

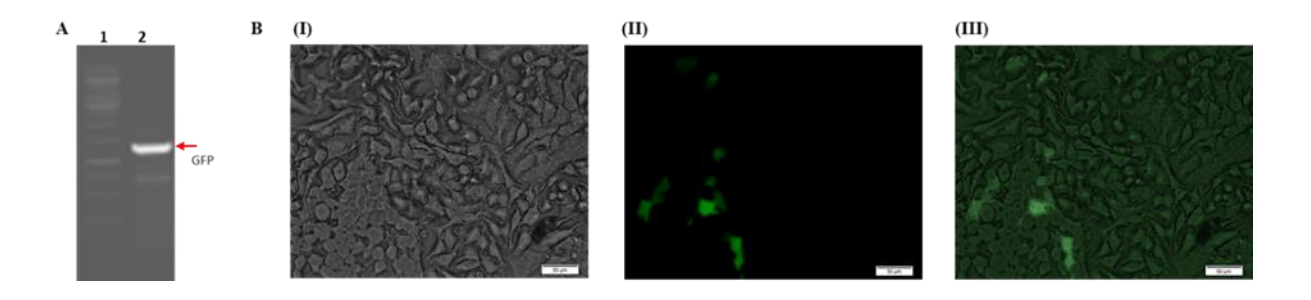


Figure 5. 26 OMV mediated Lateral mobility of phage genome into Neu2A cells: Panel A shows PCR amplification of GFP sequence using OMV isolated from *A. baumannii* (pGD5) as template. Presence of phage derivative pGD5 in OMV is shown in lane 2 of panel A. Panel B shows images of fluorescent microscopy captured after 24 h of post incubation of Neu2A cells with OMVs. (I) is the bright field channel image of Neu2A cells according to their size and morphology. (II) shows fluorescent imaging where green colour represents GFP signal. Merged image is shown in panel (III).

5.3 Discussion

The mobility of genetic information through horizontal gene transfer is dynamic and persistent phenomenon that can have immediate or delayed effects in the recipient hosts (Husnik & McCutcheon, 2017). Recently, several studies have reported the process of HGT being facilitated by OMVs (Dell'annunziata et al., 2020; Domingues & Nielsen, 2017; Tran & Boedicker, 2017).

Present study has interestingly shown the association of four indigenous plasmids out of five, namely pTS4586, pTS9900, pTS11291 and ptTS134338, but not the 37 kb plasmid pTS37365 of *A. baumannii* DS002. Both sequencing results and PCR confirmations using primer specific to plasmids have given same result, suggesting selective sorting of plasmids into the OMVs. These observations are further in line with report from our laboratory, where these plasmid genome sequences were compared with *A. baumannii* plasmid database and a plasmid network was

generated. The network shows extensive similarity among A. baumannii plasmids indicating horizontal mobility and recombination among them. Only pTS37365 was not the part of plasmid network (Samantarrai, Yakkala, et al., 2020). Such selectivity of OMVs pertaining to pTS37365, suggest the packaging of cargo into the OMVs being a regulated process, rather than being a random event during OMV formation. Although it is not yet completely clear, DNA can associate with OMVs in various ways: via cytoplasmic route where DNA could be trapped along with inner membrane, via extracellular route where DNA get incorporated, possibly due to broken OMVs during release from bacteria or due to cell lysis (Gaudin et al., 2014) (Gill et al., 2019). The mechanism(s) for sorting of nucleic acid content in OMVs is not fully understood. The result from our current study where pTS37365 is selectively eliminated from OMVs cargo indicate towards the existence of proper mechanism of cargo selectivity in OMVs. The outer membrane of the OMVs can facilitate fusion of OMVs to compatible Gram-negative bacteria promoting HGT and also act as a barrier to exogenous nucleases. The results from DNase treatment of OMVs has revealed compartmentalization of only two plasmids pTS4586 and pTS9900 inside the lumen of OMVs. Association of four plasmids in OMVs of A. baumannii DS002 suggests its role in HGT. although this system seems logical, but when HGT experiments were performed using pTS4586-K, a kanamycin tagged plasmid it did not demonstrate DNA transformation via OMVs to any bacteria (E. coli pir116, P. stutzeri including A. baumannii DS002) used in the study. It looks pTS4586 vesicle mediated genetic exchange does not occur under the experimental condition followed in this study. The results obtained in this study differ from those of N. gonorrhoeae and E. coli O157: H7, where OMVs successfully transformed WT strains of their own species (David W Dorward et al., 1989; Kolling et al., 1999). It is possible that the A. baumannii DS002 OMVs are inherently different than E. coli and N. gonorrhoeae OMVs.

Current study also demonstrates association of pTS236, a genome of a phage AbDs1 on the surface of OMVs of *A. baumannii* DS002. This conclusion is based on evidences gathered from three independent experiments: PCR amplification using primer specific to pTS236 genome showed clear amplicon of pTS236 (Fig 5.6), western blot using antibody specific to Orf96 protein and mass-spectrometry analysis of proteins associated with OMVs also showed presence of phage protein in OMVs (Fig 5.5 and 5.7). The genome of phage pTS236 gained prominence due to presence of 67% sequence similarity to Sphinx 2.36 sequence co-purified with the Transmissible Spongiform encephalopathy (TSE) particles which were isolated from infected brain samples (Longkumer et al., 2013; Manuelidis, 2011; Yeh et al., 2017). Similar to Sphinx 2.36,

pTS236 also codes for three ORFs, one is *repA* which helps in rolling circle replication of phage genome, other two ORFs *orf96* and *orf113* are believed to be structural proteins of phage.

Further investigation on its association, demonstrate its association with OMVs is via protein-protein interactions. The ligand blot and MALDI TOF/TOF results indicate its association is via one of the porin majorly found in OMVs, outer membrane protein A (OmpA). The pull-down experiments conducted to further validate this interaction has shown interaction of only one of the structural proteins Orf96 but not Orf113 with OmpA. This result suggests Orf96 could be the coat protein of the phage genome. While gaining the genetic evidence the *ompA* gene from *A. baumannii* was successfully replaced with tetracycline cassette and the strain was named as DS003. The OMVs isolated from *A. baumannii* DS002 were checked for the presence of phage genome pTS236 by performing PCR showed absence of phage genome pTS236 specific amplicon. Suggesting, the interaction between OmpA and Orf96 facilitate secretion of phage AbDs1 out of the bacterial cell.

Studies on the horizontal mobility of phage AbDs1genome via OMVs has shown its mobility to only *A. baumannii* DS002 cells. This experiment did not demonstrate phage genome transformation via OMVs to any other bacteria, *E. coli pir* 116, *P. stutzeri* and *Bacillus subtilis*. Indicating that OMV associated phage retains infectivity, but still not mobilizing into other bacteria. This could be due to many unknown factors such as species-specific interactions or replication compatibility in different host conditions. Further studies can be performed taking broad host range in HGT experiments, which might give more conclusive results. Recent studies have shown existence of circular DNA, named as Bovine Meat and Milk Factors (BMMFs), isolated from cattle milk, different serum samples and human brain affected by Multiple sclerosis (MS) (de Villiers et al., 2019). These circular DNAs have been implicated in induction of diseases such as colorectal cancer, MS and BSE (Botsios & Manuelidis, 2016).

Approximately more than hundred BMMFs have been isolated and the characteristic features common among all isolates is the presence of minimum one large open reading frame encoding Rep protein. The phylogenetic tree generated by including complete sequences of approximately hundred BMMF reported till date and genome of phage pTS236, has revealed existence of common lineage between pTS236 and certain BMMFs. The BMMFs, which was categorised as BMMFs group 2 based on its sequence resemblance to sphinx 2.36 has shown highest similarity (Fig from intro chapter). The BLAST Ring Image Generator (BRIG) image generated taking top 18

most significantly similar BMMFs sequences to visualise their similarity to pTS236 sequence indicate highest sequence similarity among the *repA* sequences of all the isolates (Fig 5.27).

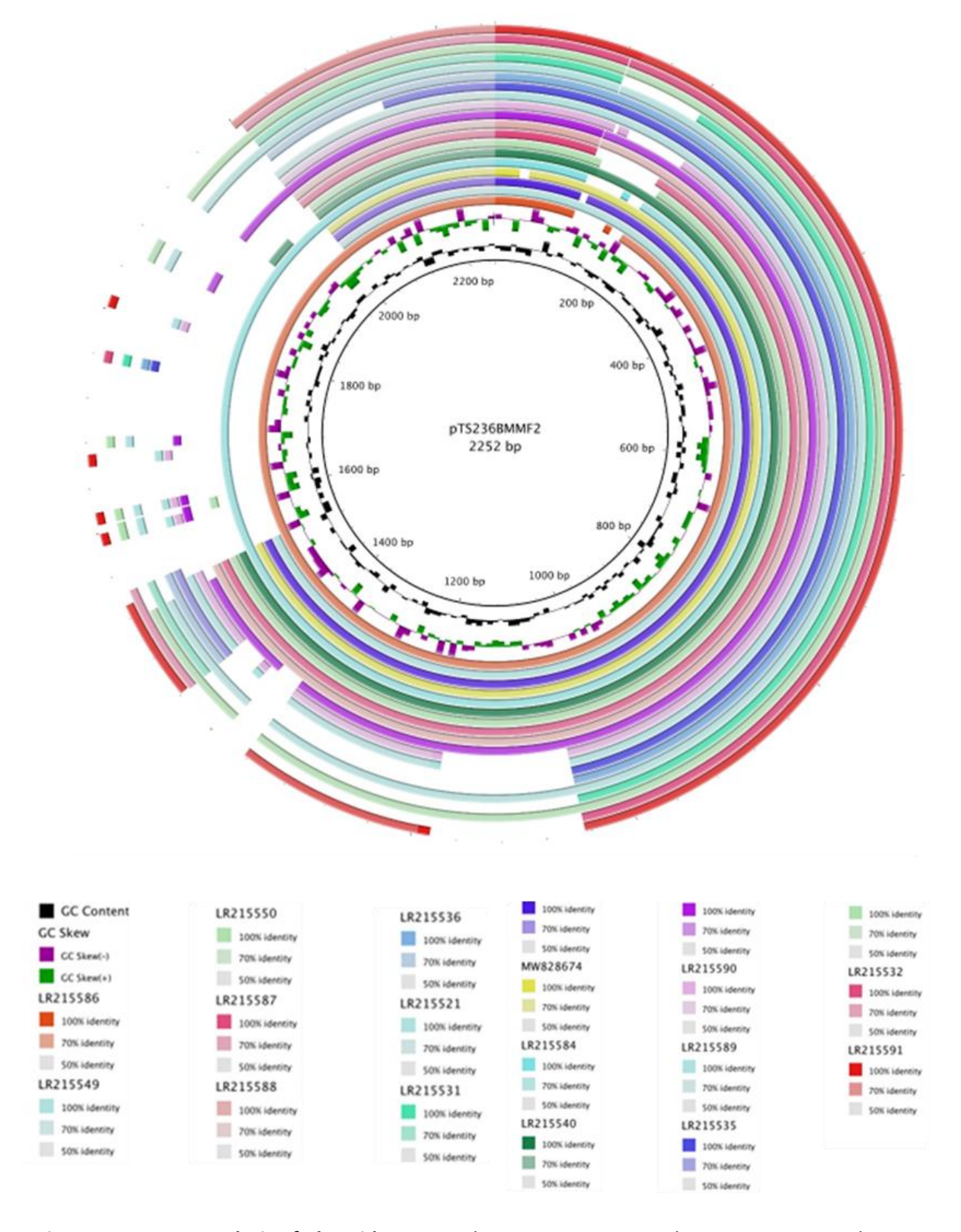


Figure 5. 27 BRIG analysis of plasmid pTS236. The concentric rings indicate sequence similarity among the top 18 BMMF homologues of plasmid pTS236. Lack of colour in a ring indicates the absence of the corresponding region in pTS236 homologues. The region of repA from 48 to 1184 bp shows the highest matched sequence among all homologues. Towards the right size of the ring indicates the BMMFs taken for analysis.

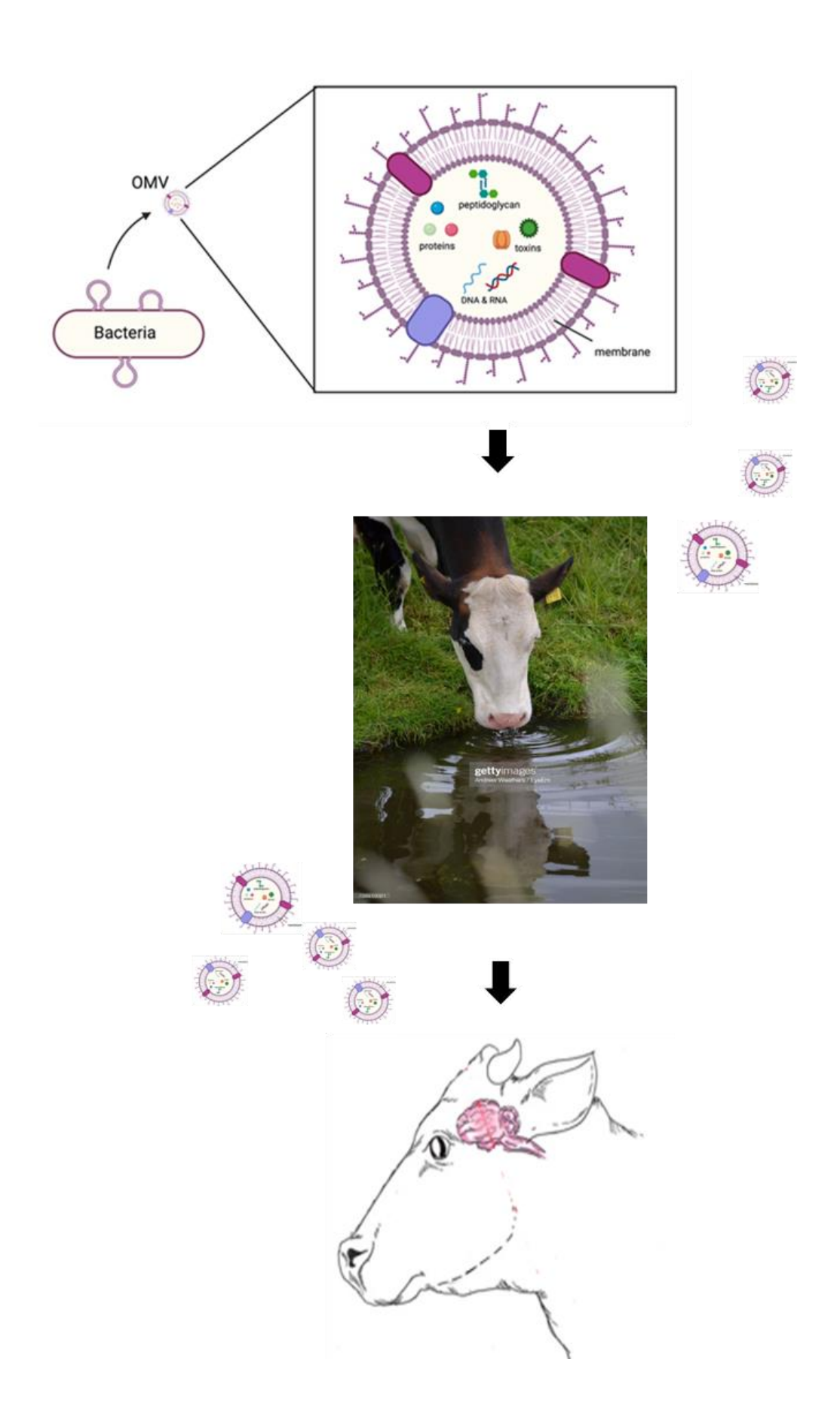


Figure 5. 28 A schematic representation explaining possible route for OMVs to reach brain and mammalian tissue.

Role of OMVs in interkingdom communication is well established. The NGS analysis performed for brain samples of Alzheimer's patient has shown to have more bacterial components than normal brain (Emery et al., 2017). In support of these studies, recently the intracardiac injection of OMVs of *Aggregatibacter actinomycetemcomitans* in mice showed delivery to the brain after crossing blood-brain barrier (BBB) (Han et al., 2019). Considering above findings, first one being similarity of phage AbDs1 genome similarity to Sphinx and BMMF sequences indicating existence of common origin and OMVs and secondly the role of OMVs in crossing blood brain barrier a hypothesis was generated implicating OMVs in delivering these circular DNAs into mammalian cells.

This hypothesis was tested in this study by generating a variant of phage genome tagging with *GFP* coding sequence whose transcription is driven by a CMV promoter. The OMVs were isolated from *A. baumannii* (pTS236-GFP), showed presence of pTS236-GFP phage genome in OMVs. Further, fluorescent microscopy images obtained after HGT studies using Neuronal cell line Neu2A, have shown signal for GFP protein in some of the neuronal cells. These results suggest successful delivery of OMV associated phage DNA, pTS236-GFP inside the Neu2A cells. These preliminary observations acquire significance, if seen together with the published results that suggest crossing of OMVs blood brain barrier (BBB) to reach mammalian brain. *A. baumannii* DS002 was originally, isolated from soil and the OMVs released into soil can reach animals through food chain, especially water. These is an ample scope for these OMVs to gain entry into the brain by crossing blood brain barrier (BBB). A schematic representation given explain possible route for OMVs to reach brain and mammalian tissue (Fig 5.28). Since phage genome showing similarity to the BMMF and Sphinx 2.36 is associating with OMVs it can as well reach this mammalian tissue along with OMVs.

Conclusion

The research work described in the thesis provides a well standardised method for the isolation and purification of OMVs from *Acinetobacter baumannii* DS002. Approximately 600 ug of OMVs were isolated from one litre culture supernatant. The purified OMVs were free from cytoplasmic and inner membrane protein contamination. The OmpA specific signal was seen only in OM and OMVs, not in cytoplasmic fraction. The cytoplasmic marker RepA was exclusively found in cytoplasm fraction not in membrane fraction. As determined by nano tracking analysis, the size of OMVs isolated from *A. baumannii* DS002 are in the range of 74 to 160 nm. The images taken by transmission Electron Microscope (TEM) also confirmed the size distribution of isolated OMVs.

The proteins present in the OMVs are selectively sorted from different subcellular locations, into OMVs. The ESI-MS/MS proteomic analysis revealed association of total 302 proteins with OMVs of *A. baumannii* DS002. The *in-silico* studies showed, 32% of OMV proteins belongs to outer membrane, 22% are periplasmic proteins, 27% are of cytoplasmic origin, 11% of inner membrane origin and 8% belong to extracellular proteins. The OM and periplasmic proteins together represent 54% total OMV proteins.

The COG categorization using EggNOG tool has shown that most of the proteins associated with OMVs are involved in functions such as inorganic ion transport and storage, pathogenesis, cell-wall/membrane biogenesis. Proteins of OMVs are selectively enriched with TonB dependent receptors and in total about 24 TonB dependent transporters (TonRs) were identified.

The TonRs are involved in transporting nutrients, especially iron across energy deprived outer membrane. *A. baumannii* DS002 genome encodes for various TonRs required for transport of three major siderophore types, even in the absence of genetic repertoire needed for synthesis of the corresponding siderophore. The TonRs associated with OMVs appear to facilitate acquisition of iron complexed to the siderophores, which is synthesized and secreted by cohabiting bacteria. The potential of OMVs to transport iron was evaluated using radiolabelled ferric iron (⁵⁵Fe) complexed with enterobactin (Ent). OMVs labelled with ⁵⁵Fe-enterobactin complex positively transported radiolabeled iron into *A. baumannii* DS002 cells grown in iron limiting condition.

The OMVs contained both plasmid and Phage genome sequences. Out of five indigenous plasmids, the OMVs of *A. baumannii* DS002 contained only four of them. The plasmids pTS4586 and pTS9900 are present inside the lumen of OMVs, whereas plasmids, pTS134338 and pTS11232 are associated on the surface of the OMVs. Interestingly, as revealed by sequencing and PCR results, plasmid pTS37365 was not seen OMVs

The genome of bacteriophage, AbDs1 is associated on the surface of OMVs. Association of phage to OMVs is facilitated by interactions between one of the proteins coded by bacteriophage Orf96 and OmpA protein present in outer membrane of the bacteria. The other phage protein Orf113 does not interact with OmpA. The OMVs isolated from *ompA* knockouts strains of *A. baumannii* DS002 were free from phage AbDs1 providing conclusive evidence on association of phage particles with OMVs through establishing interactions with OmpA. The OMV associated page AbDs1 successfully infected *A. baumannii* DS002 but not to any other bacteria.

High sequence similarity was seen between phage AbDs1 genome and closed covalent circular DNAs (BMMFs/ Sphinx) identified in brain tissue of mammals suffering from various neurological disorders. The OMVs when incubated with Neuronal cell lines Neu2A, successfully delivered phage genome pTS236 inside the Neu2A cells. These preliminary observations acquire significance as published results suggest crossing of OMVs blood brain barrier (BBB) and reach mammalian brain. The OMVs of *A. baumannii* DS002 released into soil/water reach food chain, especially via water. These is an ample scope for these OMVs to gain entry into the brain by crossing blood brain barrier (BBB). Since phage genome pTS236 shows similarity to the BMMF and Sphinx2.36 the proposed hypothesis gains significance. However, further research is required to confirm OMVs role in delivering replication competent closed covalent circular DNAs like brain meat and milk factors (BMMFs) and Sphinx sequences into mammalian cells.

References

- Aghajani, Z., Rasooli, I., & Mousavi Gargari, S. L. (2019). Exploitation of two siderophore receptors, BauA and BfnH, for protection against Acinetobacter baumannii infection. *Apmis*, 127(12), 753–763. https://doi.org/10.1111/apm.12992
- Ahmer, B. M. M., Thomas, M. G., Larsen, R. A., & Postle, K. (1995). Characterization of the exbBD operon of Escherichia coli and the role of ExbB and ExbD in TonB function and stability. *Journal of Bacteriology*, *177*(16), 4742–4747. https://doi.org/10.1128/jb.177.16.4742-4747.1995
- Ammari, M. G., Gresham, C. R., McCarthy, F. M., & Nanduri, B. (2016). HPIDB 2.0: a curated database for host-pathogen interactions. *Database: The Journal of Biological Databases and Curation*, 2016, 1–9. https://doi.org/10.1093/database/baw103
- Anand, D., & Chaudhuri, A. (2016). Bacterial outer membrane vesicles: New insights and applications. *Molecular Membrane Biology*, 33(6–8), 125–137. https://doi.org/10.1080/09687688.2017.1400602
- Bai, J., Kim, S. I., Ryu, S., & Yoon, H. (2014). Identification and characterization of outer membrane vesicle-associated proteins in Salmonella enterica serovar Typhimurium. *Infection and Immunity*, 82(10), 4001–4010. https://doi.org/10.1128/IAI.01416-13
- Bailey, T. L., Johnson, J., Grant, C. E., & Noble, W. S. (2015). The MEME Suite. *Nucleic Acids Research*, 43(W1), W39–W49. https://doi.org/10.1093/nar/gkv416
- Bauman, S. J., & Kuehn, M. J. (2006). Purification of outer membrane vesicles from Pseudomonas aeruginosa and their activation of an IL-8 response. *Microbes and Infection / Institut Pasteur, 8*(9–10), 2400. https://doi.org/10.1016/J.MICINF.2006.05.001
- Bedhomme, S., Amorós-Moya, D., Valero, L. M., Bonifaci, N., Pujana, M. À., Bravo, I. G., & Gonzalez, J. (2019). Evolutionary Changes after Translational Challenges Imposed by Horizontal Gene Transfer. *Genome Biology and Evolution*, 11(3), 814–831. https://doi.org/10.1093/gbe/evz031
- Bello-López, J. M., Cabrero-Martínez, O. A., Ibáñez-Cervantes, G., Hernández-Cortez, C., Pelcastre-Rodríguez, L. I., Gonzalez-Avila, L. U., & Castro-Escarpulli, G. (2019). Horizontal Gene Transfer and Its Association with Antibiotic Resistance in the Genus Aeromonas spp. *Microorganisms 2019, Vol. 7, Page 363, 7*(9), 363. https://doi.org/10.3390/MICROORGANISMS7090363
- Berleman, J., & Auer, M. (2013). The role of bacterial outer membrane vesicles for intra- and interspecies delivery. *Environmental Microbiology*, 15(2), 347–354. https://doi.org/10.1111/1462-2920.12048
- Biller, S. J., Mcdaniel, L. D., Breitbart, M., Rogers, E., Paul, J. H., & Chisholm, S. W. (2017). Membrane vesicles in sea water: heterogeneous DNA content and implications for viral abundance estimates. *The ISME Journal*, *11*(2), 394. https://doi.org/10.1038/ISMEJ.2016.134
- Biller, S. J., Schubotz, F., Roggensack, S. E., Thompson, A. W., Summons, R. E., & Chisholm, S. W. (2014). Bacterial vesicles in marine ecosystems. *Science (New York, N.Y.)*, 343(6167), 183–186. https://doi.org/10.1126/SCIENCE.1243457
- Blesa, A., & Berenguer, J. (2015). Contribution of vesicle-protected extracellular DNA to horizontal gene transfer in Thermus spp. International Microbiology, 18(3), 177–187. https://doi.org/10.2436/20.1501.01.248
- Bonnington, K. E., & Kuehn, M. J. (2014). Protein selection and export via outer membrane vesicles. *Biochimica et Biophysica Acta*, 1843(8), 1612–1619. https://doi.org/10.1016/J.BBAMCR.2013.12.011
- Botsios, S., & Manuelidis, L. (2016). CJD and Scrapie Require Agent-Associated Nucleic Acids for Infection. *Journal of Cellular Biochemistry*, 117(8), 1947–1958. https://doi.org/10.1002/jcb.25495
- Bund, T., Nikitina, E., Chakraborty, D., Ernst, C., Gunst, K., Boneva, B., Tessmer, C., Volk, N., Brobeil, A., Weber, A., Heikenwalder, M., Hausen, H. zur, & de Villiers, E. M. (2021). Analysis of chronic inflammatory lesions of the colon for BMMF Rep antigen expression and CD68 macrophage interactions. *Proceedings of the National Academy of Sciences of the United States of America*, 118(12). https://doi.org/10.1073/pnas.2025830118
- Chakraborty, S., & Kenney, L. J. (2018). A new role of OmpR in acid and osmotic stress in salmonella and E. coli. *Frontiers in Microbiology*, *9*(NOV), 1–14. https://doi.org/10.3389/fmicb.2018.02656
- Chatterjee, S., Mondal, A., Mitra, S., & Basu, S. (2017). Acinetobacter baumannii transfers the blaNDM-1 gene via outer membrane vesicles. *Journal of Antimicrobial Chemotherapy*, 72(8). https://doi.org/10.1093/jac/dkx131
- Chatterjee, S. N., & Das, J. (1967). Electron microscopic observations on the excretion of cell-wall material by Vibrio cholerae. Journal of General Microbiology, 49(1), 1–11. https://doi.org/10.1099/00221287-49-1-1
- Choi, K. H., Hwang, S., & Cha, J. (2013). Identification and characterization of malA in the maltose/maltodextrin operon of Sulfolobus acidocaldarius DSM639. *Journal of Bacteriology*, 195(8), 1789–1799. https://doi.org/10.1128/JB.01713-12
- Choi, U., & Lee, C.-R. (2019). Distinct Roles of Outer Membrane Porins in Antibiotic Resistance and Membrane Integrity in Escherichia coli. *Frontiers in Microbiology*, 10(APR), 953. https://doi.org/10.3389/fmicb.2019.00953
- Chowdhury, C., & Jagannadham, M. V. (2013). Virulence factors are released in association with outer membrane vesicles of Pseudomonas syringae pv. tomato T1 during normal growth. *Biochimica et Biophysica Acta Proteins and Proteomics*, 1834(1), 231–239. https://doi.org/10.1016/j.bbapap.2012.09.015
- Davies, J. (1996). Origins and evolution of antibiotic resistance. *Microbiología (Madrid, Spain)*, 12(1), 9–16. https://doi.org/10.1128/MMBR.00016-10/ASSET/BCBFCE98-C6B7-4543-BA59-2D24A5D2B587/ASSETS/GRAPHIC/ZMR9990922530005.JPEG
- Davis, G. S., Flannery, E. L., & Mobley, H. L. T. (2006). Helicobacter pylori HP1512 is a nickel-responsive NikR-regulated outer membrane protein. *Infection and Immunity*, 74(12), 6811–6820. https://doi.org/10.1128/IAI.01188-06
- De Biase, D., Sperandeo, P., Kuehn, M. J., Lynch, J., Contreras-Rodríguez, A., Daniel Avila-Calderón, E., Ed, A.-C., Mds, R.-P., Del, M., Ruiz-Palma, S., Aguilera-Arreola, M. G., Velázquez-Guadarrama, N., Ruiz, E. A., Gomez-Lunar, Z., & Witonsky, S. (2021).

- Outer Membrane Vesicles of Gram-Negative Bacteria: An Outlook on Biogenesis. Frontiers in Microbiology | Www.Frontiersin.Org, 1, 557902. https://doi.org/10.3389/fmicb.2021.557902
- de Villiers, E. M., Gunst, K., Chakraborty, D., Ernst, C., Bund, T., & zur Hausen, H. (2019). A specific class of infectious agents isolated from bovine serum and dairy products and peritumoral colon cancer tissue. *Emerging Microbes and Infections*, 8(1), 1205–1218. https://doi.org/10.1080/22221751.2019.1651620
- Dell'annunziata, F., Ilisso, C. P., Dell'aversana, C., Greco, G., Coppola, A., Martora, F., Piaz, F. D., Donadio, G., Falanga, A., Galdiero, M., Altucci, L., Galdiero, M., Porcelli, M., Folliero, V., & Franci, G. (2020). Outer Membrane Vesicles Derived from Klebsiella pneumoniae Influence the miRNA Expression Profile in Human Bronchial Epithelial BEAS-2B Cells. *Microorganisms 2020, Vol. 8, Page 1985*, 8(12), 1985. https://doi.org/10.3390/MICROORGANISMS8121985
- DeVoe, I. W., & Gilchrist, J. E. (1975). Pili on meningococci from primary cultures of nasopharyngeal carriers and cerebrospinal fluid of patients with acute disease. *Journal of Experimental Medicine*, 141(2), 297–305. https://doi.org/10.1084/jem.141.2.297
- Dhurve, G., Madikonda, A. K., Jagannadham, M. V., & Siddavattam, D. (2022). Outer Membrane Vesicles of Acinetobacter baumannii DS002 Are Selectively Enriched with TonB-Dependent Transporters and Play a Key Role in Iron Acquisition. *Microbiology Spectrum*, e0029322. https://doi.org/10.1128/spectrum.00293-22
- Dineshkumar, K., Aparna, V., Wu, L., Wan, J., Abdelaziz, M. H., Su, Z., Wang, S., & Xu, H. (2020). Bacterial bug-out bags: outer membrane vesicles and their proteins and functions. *Journal of Microbiology*, *58*(7), 531–542. https://doi.org/10.1007/s12275-020-0026-3
- Domingues, S., & Nielsen, K. M. (2017). Membrane vesicles and horizontal gene transfer in prokaryotes. *Current Opinion in Microbiology*, *38*, 16–21. https://doi.org/10.1016/J.MIB.2017.03.012
- Domingues, S., Rosário, N., Cândido, Â., Neto, D., Nielsen, K. M., & Da Silva, G. J. (2019). Competence for Natural Transformation Is Common among Clinical Strains of Resistant Acinetobacter spp. *Microorganisms*, 7(2). https://doi.org/10.3390/MICROORGANISMS7020030
- Dorward, D. W., & Garon, C. F. (1990). DNA is packaged within membrane-derived vesicles of gram-negative but not gram-positive bacteria. *Applied and Environmental Microbiology*, *56*(6), 1960–1962. https://doi.org/10.1128/aem.56.6.1960-1962.1990
- Dorward, David W, Garon, C. F., & Judd1, R. C. (1989). Export and Intercellular Transfer of DNA via Membrane Blebs of Neisseria gonorrhoeae. *JOURNAL OF BACTERIOLOGY*, 171, 2499–2505.
- Eijkelkamp, B. A., Hassan, K. A., Paulsen, I. T., & Brown, M. H. (2011). Investigation of the human pathogen Acinetobacter baumannii under iron limiting conditions. *BMC Genomics*, 12(1), 126. https://doi.org/10.1186/1471-2164-12-126
- Eilebrecht, S., Hotz-Wagenblatt, A., Sarachaga, V., Burk, A., Falida, K., Chakraborty, D., Nikitina, E., Tessmer, C., Whitley, C., Sauerland, C., Gunst, K., Grewe, I., & Bund, T. (2018). Expression and replication of virus-like circular DNA in human cells. Scientific Reports, 8(1), 1–15. https://doi.org/10.1038/s41598-018-21317-w
- Ely, B. (2020). Recombination and gene loss occur simultaneously during bacterial horizontal gene transfer. *PLOS ONE, 15*(1), e0227987. https://doi.org/10.1371/JOURNAL.PONE.0227987
- Emamalipour, M., Seidi, K., Zununi Vahed, S., Jahanban-Esfahlan, A., Jaymand, M., Majdi, H., Amoozgar, Z., Chitkushev, L. T., Javaheri, T., Jahanban-Esfahlan, R., & Zare, P. (2020). Horizontal Gene Transfer: From Evolutionary Flexibility to Disease Progression. Frontiers in Cell and Developmental Biology, 8, 229. https://doi.org/10.3389/FCELL.2020.00229/BIBTEX
- Emery, D. C., Shoemark, D. K., Batstone, T. E., Waterfall, C. M., Coghill, J. A., Cerajewska, T. L., Davies, M., West, N. X., & Allen, S. J. (2017). 16S rRNA next generation sequencing analysis shows bacteria in Alzheimer's Post-Mortem Brain. *Frontiers in Aging Neuroscience*, *9*(JUN), 195. https://doi.org/10.3389/FNAGI.2017.00195/BIBTEX
- Ernst, F. D., Stoof, J., Horrevoets, W. M., Kuipers, E. J., Kusters, J. G., & Van Vliet, A. H. M. (2006). NikR mediates nickel-responsive transcriptional repression of the Helicobacter pylori outer membrane proteins FecA3 (HP1400) and FrpB4 (HP1512). *Infection and Immunity*, 74(12), 6821–6828. https://doi.org/10.1128/IAI.01196-06
- Escolar, L., Pérez-Martín, J., & De Lorenzo, V. (1999). Opening the iron box: Transcriptional metalloregulation by the fur protein. Journal of Bacteriology, 181(20), 6223–6229. https://doi.org/10.1128/jb.181.20.6223-6229.1999
- Ferguson, A. D., & Deisenhofer, J. (2002). TonB-dependent receptors Structural perspectives. *Biochimica et Biophysica Acta Biomembranes*, 1565(2), 318–332. https://doi.org/10.1016/S0005-2736(02)00578-3
- Fernandez-Cassi, X., Timoneda, N., Martínez-Puchol, S., Rusiñol, M., Rodriguez-Manzano, J., Figuerola, N., Bofill-Mas, S., Abril, J. F., & Girones, R. (2018). Metagenomics for the study of viruses in urban sewage as a tool for public health surveillance. Science of The Total Environment, 618, 870–880. https://doi.org/10.1016/J.SCITOTENV.2017.08.249
- Figurski, D. H., & Helinski, D. R. (1979). Replication of an origin-containing derivative of plasmid RK2 dependent on a plasmid function provided in trans (plasmid replication/replication origin/trans-complementation/broad host range/gene cloning). *Proc. Nati. Acad. Sc, 76*(4), 1648–1652.
- Fillol-Salom, A., Alsaadi, A., de Sousa, J. A. M., Zhong, L., Foster, K. R., Rocha, E. P. C., Penadés, J. R., Ingmer, H., & Haaber, J. (2019). Bacteriophages benefit from generalized transduction. *PLOS Pathogens*, *15*(7), e1007888. https://doi.org/10.1371/JOURNAL.PPAT.1007888
- Fournier, P. E., Vallenet, D., Barbe, V., Audic, S., Ogata, H., Poirel, L., Richet, H., Robert, C., Mangenot, S., Abergel, C., Nordmann, P., Weissenbach, J., Raoult, D., & Claverie, J. M. (2006). Comparative Genomics of Multidrug Resistance in Acinetobacter baumannii. *PLOS Genetics*, *2*(1), e7. https://doi.org/10.1371/JOURNAL.PGEN.0020007
- Fulsundar, S., Harms, K., Flaten, G. E., Johnsen, P. J., Chopade, B. A., & Nielsen, K. M. (2014). Gene transfer potential of outer membrane vesicles of Acinetobacter baylyi and effects of stress on vesiculation. *Applied and Environmental Microbiology*, 80(11), 3469–3483. https://doi.org/10.1128/AEM.04248-13/SUPPL_FILE/ZAM999105385SO1.PDF
- Fulsundar, S., Kulkarni, H. M., Jagannadham, M. V., Nair, R., Keerthi, S., Sant, P., Pardesi, K., Bellare, J., & Chopade, B. A. (2015). Molecular characterization of outer membrane vesicles released from Acinetobacter radioresistens and their potential roles in pathogenesis. *Microbial Pathogenesis*, 83–84, 12–22. https://doi.org/10.1016/j.micpath.2015.04.005
- Funk, M., Gunst, K., Lucansky, V., Müller, H., zur Hausen, H., & de Villiers, E. M. (2014). Isolation of protein-associated circular

- DNA from healthy cattle serum. Genome Announcements, 2(4), 2014. https://doi.org/10.1128/genomeA.00846-14
- Gao, L., & van der Veen, S. (2020). Role of Outer Membrane Vesicles in Bacterial Physiology and Host Cell Interactions. *Infectious Microbes and Diseases*, 2(1), 3–9. https://doi.org/10.1097/im9.00000000000017
- Gaudin, M., Krupovic, M., Marguet, E., Gauliard, E., Cvirkaite-Krupovic, V., Le Cam, E., Oberto, J., & Forterre, P. (2014). Extracellular membrane vesicles harbouring viral genomes. *Environmental Microbiology*, 16(4), 1167–1175. https://doi.org/10.1111/1462-2920.12235
- Gill, S., Catchpole, R., & Forterre, P. (2019). Extracellular membrane vesicles in the three domains of life and beyond. *FEMS Microbiology Reviews*, 43(3), 273–303. https://doi.org/10.1093/femsre/fuy042
- Grande, R., Di Marcantonio, M. C., Robuffo, I., Pompilio, A., Celia, C., Marzio, L. Di, Paolino, D., Codagnone, M., Muraro, R., Stoodley, P., Hall-Stoodley, L., & Mincione, G. (2015). Helicobacter pylori ATCC 43629/NCTC 11639 Outer Membrane Vesicles (OMVs) from biofilm and planktonic phase associated with extracellular DNA (eDNA). Frontiers in Microbiology, 6(DEC). https://doi.org/10.3389/fmicb.2015.01369
- Gunst, K., zur Hausen, H., & de Villiers, E. M. (2014). Isolation of bacterial plasmid-related replication-associated circular DNA from a serum sample of a multiple sclerosis patient. *Genome Announcements*, 2(4), 2014. https://doi.org/10.1128/genomeA.00847-14
- Hakami, R. M., Batoni, G., Margolis, L., & Tasleem Jan, A. (2017). Outer Membrane Vesicles (OMVs) of Gram-negative Bacteria: A Perspective Update. *Front. Microbiol*, *8*, 1053. https://doi.org/10.3389/fmicb.2017.01053
- Hall, R. J., Whelan, F. J., McInerney, J. O., Ou, Y., & Domingo-Sananes, M. R. (2020). Horizontal Gene Transfer as a Source of Conflict and Cooperation in Prokaryotes. Frontiers in Microbiology, 11, 1569. https://doi.org/10.3389/FMICB.2020.01569/BIBTEX
- Han, E. C., Choi, S. Y., Lee, Y., Park, J. W., Hong, S. H., & Lee, H. J. (2019). Extracellular RNAs in periodontopathogenic outer membrane vesicles promote TNF-α production in human macrophages and cross the blood-brain barrier in mice. FASEB Journal: Official Publication of the Federation of American Societies for Experimental Biology, 33(12), 13412–13422. https://doi.org/10.1096/fj.201901575R
- Harvey, K. L., Jarocki, V. M., Charles, I. G., & Djordjevic, S. P. (2019). The diverse functional roles of elongation factor tu (Ef-tu) in microbial pathogenesis. *Frontiers in Microbiology*, 10(OCT), 1–19. https://doi.org/10.3389/fmicb.2019.02351
- Haurat, M. F., Aduse-opoku, J., Rangarajan, M., Dorobantu, L., Gray, M. R., Curtis, M. A., & Feldman, M. F. (2011). *Selective Sorting of Cargo Proteins into Bacterial Membrane Vesicles* * □. 286(2), 1269–1276. https://doi.org/10.1074/jbc.M110.185744
- Headd, B., & Bradford, S. A. (2020). The conjugation window in an Escherichia coli K-12 strain with an IncFII plasmid. *Applied and Environmental Microbiology*, 86(17). https://doi.org/10.1128/AEM.00948-20/SUPPL_FILE/AEM.00948-20-SD003.XLSX
- Henderson, B., Nair, S., Pallas, J., & Williams, M. A. (2011). Fibronectin: a multidomain host adhesin targeted by bacterial fibronectin-binding proteins. *FEMS Microbiology Reviews*, *35*(1), 147–200. https://doi.org/10.1111/J.1574-6976.2010.00243.X
- Horspool, A. M., & Schertzer, J. W. (2018). Reciprocal cross-species induction of outer membrane vesicle biogenesis via secreted factors. *Scientific Reports, June*, 1–12. https://doi.org/10.1038/s41598-018-28042-4
- Horstman, A. L., & Kuehn, M. J. (2000). Enterotoxigenic Escherichia coli Secretes Active Heat-labile Enterotoxin via Outer Membrane Vesicles*. *Journal of Biological Chemistry*, 275, 12489–12496. https://doi.org/10.1074/jbc.275.17.12489
- Hu, Y., Zheng, J., & Zhang, J. (2022). Natural Transformation in Acinetobacter baumannii W068: A Genetic Analysis Reveals the Involvements of the CRP, XcpV, XcpW, TsaP, and TonB2. Frontiers in Microbiology, 12, 4187. https://doi.org/10.3389/FMICB.2021.738034/BIBTEX
- Husnik, F., & McCutcheon, J. P. (2017). Functional horizontal gene transfer from bacteria to eukaryotes. https://doi.org/10.1038/nrmicro.2017.137
- Jan, A. T. (2017). Outer Membrane Vesicles (OMVs) of gram-negative bacteria: A perspective update. *Frontiers in Microbiology*, 8(JUN), 1–11. https://doi.org/10.3389/fmicb.2017.01053
- Jarzab, M., Posselt, G., Meisner-Kober, N., & Wessler, S. (2020). Helicobacter pylori-Derived Outer Membrane Vesicles (OMVs):
 Role in Bacterial Pathogenesis? *Microorganisms 2020, Vol. 8, Page 1328, 8*(9), 1328. https://doi.org/10.3390/MICROORGANISMS8091328
- Jawad, A., Seifert, H., Snelling, A. M., Heritage, J., & Hawkey, P. M. (1998). Survival of Acinetobacter baumannii on dry surfaces: comparison of outbreak and sporadic isolates. *Journal of Clinical Microbiology*, *36*(7), 1938–1941. https://doi.org/10.1128/JCM.36.7.1938-1941.1998
- Jiang, Y., Kong, Q., Roland, K. L., & Curtiss, R. (2014). Membrane vesicles of Clostridium perfringens type A strains induce innate and adaptive immunity. *International Journal of Medical Microbiology: IJMM, 304*(3–4), 431–443. https://doi.org/10.1016/J.IJMM.2014.02.006
- Joly-Guillou, M. L. (2005). Clinical impact and pathogenicity of Acinetobacter. Clinical Microbiology and Infection: The Official Publication of the European Society of Clinical Microbiology and Infectious Diseases, 11(11), 868–873. https://doi.org/10.1111/J.1469-0691.2005.01227.X
- Jones, E. J., Booth, C., Fonseca, S., Parker, A., Cross, K., Miquel-Clopés, A., Hautefort, I., Mayer, U., Wileman, T., Stentz, R., & Carding, S. R. (2020). The Uptake, Trafficking, and Biodistribution of Bacteroides thetaiotaomicron Generated Outer Membrane Vesicles. *Frontiers in Microbiology*, *11*(February), 1–14. https://doi.org/10.3389/fmicb.2020.00057
- Jun, S. H., Lee, J. H., Kim, B. R., Kim, S. II, Park, T. I., Lee, J. C., & Lee, Y. C. (2013). Acinetobacter baumannii Outer Membrane Vesicles Elicit a Potent Innate Immune Response via Membrane Proteins. *PLoS ONE*, 8(8), e71751. https://doi.org/10.1371/journal.pone.0071751
- Kadurugamuwa, J. L., & Beveridge, T. J. (1995). Virulence Factors Are Released from. Microbiology, 177(14), 3998-4008.
- Kahn, M. E., Barany, F., & Smith, H. O. (1983). Transformasomes: Specialized membranous structures that protect DNA during Haemophilus transformation. *Proceedings of the National Academy of Sciences of the United States of America*, 80(22 I), 6927–6931. https://doi.org/10.1073/PNAS.80.22.6927

- Kato, S., Kowashi, Y., & Demuth, D. R. (2002). Outer membrane-like vesicles secreted by Actinobacillus actinomycetemcomitans are enriched in leukotoxin. *Microbial Pathogenesis*, 32(1), 1–13. https://doi.org/10.1006/mpat.2001.0474
- Keenan, J., Day, T., Neal, S., Cook, B., Perez-Perez, G., Allardyce, R., & Bagshaw, P. (2000). A role for the bacterial outer membrane in the pathogenesis of Helicobacter pylori infection. *FEMS Microbiology Letters*, *182*(2), 259–264. https://doi.org/10.1111/J.1574-6968.2000.TB08905.X
- Kesty, N. C., & Kuehn, M. J. (2004). Incorporation of Heterologous Outer Membrane and Periplasmic Proteins into Escherichia coli Outer Membrane Vesicles. *Journal of Biological Chemistry*, 279(3), 2069–2076. https://doi.org/10.1074/jbc.M307628200
- Killmann, H., Videnov, G., Jung, G., Schwarz, H., & Braun, V. (1995). Identification of receptor binding sites by competitive peptide mapping: Phages T1, T5, and \$\phi80\$ and colicin M bind to the gating loop of FhuA. *Journal of Bacteriology*, 177(3), 694–698. https://doi.org/10.1128/jb.177.3.694-698.1995
- Kleanthous, C., & Armitage, J. P. (2015). The bacterial cell envelope. *Philosophical Transactions of the Royal Society B: Biological Sciences*, *370*(1679), 1–17. https://doi.org/10.1098/rstb.2015.0019
- Klevens, R. M., Edwards, J. R., Richards, C. L., Horan, T. C., Gaynes, R. P., Pollock, D. A., & Cardo, D. M. (2007). Estimating health care-associated infections and deaths in U.S. Hospitals, 2002. *Public Health Reports*, 122(2), 160–166. https://doi.org/10.1177/003335490712200205
- Klieve, A. V., Yokoyama, M. T., Forster, R. J., Ouwerkerk, D., Bain, P. A., & Mawhinney, E. L. (2005a). Naturally occurring DNA transfer system associated with membrane vesicles in cellulolytic Ruminococcus spp. of ruminal origin. *Applied and Environmental Microbiology*, 71(8), 4248–4253. https://doi.org/10.1128/AEM.71.8.4248-4253.2005
- Klieve, A. V., Yokoyama, M. T., Forster, R. J., Ouwerkerk, D., Bain, P. A., & Mawhinney, E. L. (2005b). Naturally occurring DNA transfer system associated with membrane vesicles in cellulolytic Ruminococcus spp. of ruminal origin. *Applied and Environmental Microbiology*, 71(8), 4248–4253. https://doi.org/10.1128/AEM.71.8.4248-4253.2005
- Klimentová, J., & Stulík, J. (2015). Methods of isolation and purification of outer membrane vesicles from gram-negative bacteria. *Microbiological Research*, *170*, 1–9. https://doi.org/10.1016/J.MICRES.2014.09.006
- Knox, K. W., Vesk, M., & Work, E. (1966). Relation Between Excreted Lipopolysaccharide Complexes and Surface Structures of a Lysine- Limited Culture of Escherichia coli. 92(4).
- Kolling, G. L., Matthews, K. R., & Rd, D. (1999). Export of Virulence Genes and Shiga Toxin by Membrane Vesicles of Escherichia coli O157:H7. APPLIED AND ENVIRONMENTAL MICROBIOLOGY, 65(5), 1843–1848. https://journals.asm.org/journal/aem
- König, M. T., Fux, R., Link, E., Sutter, G., Märtlbauer, E., & Didier, A. (2021). Circular rep-encoding single-stranded dna sequences in milk from water buffaloes (Bubalus arnee f. bubalis). *Viruses*, 13(6), 1–13. https://doi.org/10.3390/v13061088
- Kulkarni, H. M., & Jagannadham, M. V. (2014). Biogenesis and multifaceted roles of outer membrane vesicles from Gram-negative bacteria. *Microbiology (United Kingdom)*, 160, 2109–2121. https://doi.org/10.1099/mic.0.079400-0
- Kulkarni, H. M., Nagaraj, R., & Jagannadham, M. V. (2015). Protective role of E. coli outer membrane vesicles against antibiotics. *Microbiological Research*, 181, 1–7. https://doi.org/10.1016/j.micres.2015.07.008
- Kulkarni, H. M., Swamy, C. V. B., & Jagannadham, M. V. (2014). Molecular characterization and functional analysis of outer membrane vesicles from the Antarctic bacterium Pseudomonas syringae suggest a possible response to environmental conditions. *Journal of Proteome Research*, 13(3), 1345–1358. https://doi.org/10.1021/pr4009223
- Kulp, A., & Kuehn, M. J. (2010a). Biological Functions and biogenesis of secreted bacterial outer membrane vesicles. *Annual Review of Microbiology*, 64(1), 163–184. https://doi.org/10.1146/annurev.micro.091208.073413
- Kulp, A., & Kuehn, M. J. (2010b). Biological Functions and Biogenesis of Secreted Bacterial Outer Membrane Vesicles. *Annual Review of Microbiology*, *64*(1), 163–184. https://doi.org/10.1146/annurev.micro.091208.073413
- Kumawat, M., Karuna, I., Ahlawat, N., & Ahlawat, S. (2020). Identification of Salmonella Typhimurium Peptidyl-prolyl cis-trans Isomerase B (PPlase B) and Assessment of their Role in the Protein Folding. *Protein and Peptide Letters*, 27(8), 744–750. https://doi.org/10.2174/0929866527666200225124104
- Kwon, S. O., Gho, Y. S., Lee, J. C., & Kim, S. II. (2009). Proteome analysis of outer membrane vesicles from a clinical Acinetobacter baumannii isolate. FEMS Microbiology Letters, 297(2), 150–156. https://doi.org/10.1111/j.1574-6968.2009.01669.x
- Laboratories, T., & Road, T. A. (1965). An Extracellular Glycolipid Produced by Escherichia coli Grown under Lysine-Limiting Conditions.
- Lamberto, I., Gunst, K., Müller, H., zur Hausen, H., & de Villiers, E. M. (2014). Mycovirus-like DNA virus sequences from cattle serum and human brain and serum samples from multiple sclerosis patients. *Genome Announcements*, 2(4), 931485. https://doi.org/10.1128/genomeA.00848-14
- Larsen, R. A., Myers, P. S., Skare, J. T., Seachord, C. L., Darveau, R. P., & Postle, K. (1996). Identification of TonB homologs in the family Enterobacteriaceae and evidence for conservation of TonB-dependent energy transduction complexes. *Journal of Bacteriology*, 178(5), 1363–1373. https://doi.org/10.1128/jb.178.5.1363-1373.1996
- Leaden, L., Silva, L. G., Ribeiro, R. A., dos Santos, N. M., Lorenzetti, A. P. R., Alegria, T. G. P., Schulz, M. L., Medeiros, M. H. G., Koide, T., & Marques, M. V. (2018). Iron deficiency generates oxidative stress and activation of the sos response in Caulobacter crescentus. *Frontiers in Microbiology*, *9*(AUG), 1–14. https://doi.org/10.3389/fmicb.2018.02014
- Lee, E. Y., Choi, D. S., Kim, K. P., & Gho, Y. S. (2008). Proteomics in Gram-negative bacterial outer membrane vesicles. *Mass Spectrometry Reviews*, 27(6), 535–555. https://doi.org/10.1002/MAS.20175
- Lee, E. Y., Joo, Y. B., Gun, W. P., Choi, D. S., Ji, S. K., Kim, H. J., Park, K. S., Lee, J. O., Kim, Y. K., Kwon, K. H., Kim, K. P., & Yong, S. G. (2007). Global proteomic profiling of native outer membrane vesicles derived from Escherichia coli. *Proteomics*, 7(17), 3143–3153. https://doi.org/10.1002/PMIC.200700196
- Lee, H. S., Abdelal, A. H. T., Clark, M. A., & Ingraham, J. L. (1991). Molecular characterization of nosA, a Pseudomonas stutzeri gene encoding an outer membrane protein required to make copper-containing N2O reductase. *Journal of Bacteriology*, 173(17), 5406–5413. https://doi.org/10.1128/jb.173.17.5406-5413.1991
- Letunic, I., & Bork, P. (2007). Interactive Tree Of Life (iTOL): An online tool for phylogenetic tree display and annotation. *Bioinformatics*, 23(1), 127–128. https://doi.org/10.1093/bioinformatics/btl529

- Lippmann, E. S., Al-Ahmad, A., Azarin, S. M., Palecek, S. P., & Shusta, E. V. (2014). A retinoic acid-enhanced, multicellular human blood-brain barrier model derived from stem cell sources. *Scientific Reports 2014 4:1*, 4(1), 1–10. https://doi.org/10.1038/srep04160
- Longkumer, T., Kamireddy, S., Muthyala, V. R., Akbarpasha, S., Pitchika, G. K., Kodetham, G., Ayaluru, M., & Siddavattam, D. (2013). Acinetobacter phage genome is similar to Sphinx 2.36, the circular DNA copurified with TSE infected particles. *Scientific Reports*, 3(X), 1–9. https://doi.org/10.1038/srep02240
- MacDonald, I. A., & Kuehn, M. J. (2012). Offense and defense: Microbial membrane vesicles play both ways. *Research in Microbiology*, 163(9–10), 607–618. https://doi.org/10.1016/j.resmic.2012.10.020
- MacDonald, I. A., & Kuehna, M. J. (2013). Stress-induced outer membrane vesicle production by Pseudomonas aeruginosa. Journal of Bacteriology, 195(13), 2971–2981. https://doi.org/10.1128/JB.02267-12
- Magill, S. S., Edwards, J. R., Bamberg, W., Beldavs, Z. G., Dumyati, G., Kainer, M. A., Lynfield, R., Maloney, M., McAllister-Hollod, L., Nadle, J., Ray, S. M., Thompson, D. L., Wilson, L. E., & Fridkin, S. K. (2014). Multistate Point-Prevalence Survey of Health Care—Associated Infections for the Emerging Infections Program Healthcare-Associated Infections and Antimicrobial Use Prevalence Survey Team * Centers for Disease Control and Prevention (. St. Paul (R.L.); Connecticut Department of Public Health Oakland (J.N. Decatur (S.M.R., 370(13), 1198–1208. https://doi.org/10.1056/NEJMoa1306801.Multistate
- Manuelidis, L. (2011). Nuclease resistant circular DNAs copurify with infectivity in scrapie and CJD. *Journal of NeuroVirology*, 17(2), 131–145. https://doi.org/10.1007/s13365-010-0007-0
- Mashburn, L. M., & Whiteley, M. (2005a). *Membrane vesicles traffic signals and facilitate group activities in a prokaryote.* 437(September), 422–425. https://doi.org/10.1038/nature03925
- Mashburn, L. M., & Whiteley, M. (2005b). Membrane vesicles traffic signals and facilitate group activities in a prokaryote. *Nature* 2005 437:7057, 437(7057), 422–425. https://doi.org/10.1038/nature03925
- McBroom, A. J., Johnson, A. P., Vemulapalli, S., & Kuehn, M. J. (2006). Outer Membrane Vesicle Production by Escherichia coli Is Independent of Membrane Instability. *Journal of Bacteriology*, 188(15), 5385. https://doi.org/10.1128/JB.00498-06
- McBroom, A. J., & Kuehn, M. J. (2007). Release of outer membrane vesicles by Gram-negative bacteria is a novel envelope stress response. *Molecular Microbiology*, *63*(2), 545–558. https://doi.org/10.1111/j.1365-2958.2006.05522.x
- McMahon, K. J., Castelli, M. E., Vescovi, E. G., & Feldman, M. F. (2012). Biogenesis of outer membrane vesicles in Serratia marcescens is thermoregulated and can be induced by activation of the Rcs phosphorelay system. *Journal of Bacteriology*, 194(12), 3241–3249. https://doi.org/10.1128/JB.00016-12
- Mergenhagen, S. E., Bladen, H. A., & Hsu, K. C. (1966). Electron Microscopic Localization of Endotoxic Lipopolysaccharide in Gram-Negagive Organisms. *Annals of the New York Academy of Sciences*, 133(2), 279–291. https://doi.org/10.1111/j.1749-6632.1966.tb52371.x
- Mobarak Qamsari, M., Rasooli, I., & Darvish Alipour Astaneh, S. (2020). Identification and immunogenic properties of recombinant ZnuD protein loops of Acinetobacter baumannii: Immunogenicity of ZnuD loops of A. baumannii. *Informatics in Medicine Unlocked*, 19, 100342. https://doi.org/10.1016/j.imu.2020.100342
- Moon, D. C., Choi, C. H., Lee, J. H., Choi, C. W., Kim, H. Y., Park, J. S., Kim, S. II, & Lee, J. C. (2012). Acinetobacter baumannii outer membrane protein a modulates the biogenesis of outer membrane vesicles. *Journal of Microbiology*, 50(1), 155–160. https://doi.org/10.1007/s12275-012-1589-4
- N'Diaye, A. R., Borrel, V., Racine, P. J., Clamens, T., Depayras, S., Maillot, O., Schaack, B., Chevalier, S., Lesouhaitier, O., & Feuilloley, M. G. J. (2019). Mechanism of action of the moonlighting protein EfTu as a Substance P sensor in Bacillus cereus. *Scientific Reports*, *9*(1), 1–14. https://doi.org/10.1038/s41598-018-37506-6
- Nagakubo, T., Nomura, N., & Toyofuku, M. (2020). Cracking Open Bacterial Membrane Vesicles. *Frontiers in Microbiology,* 10(January). https://doi.org/10.3389/fmicb.2019.03026
- Nemec, A., Radolfová-Křížová, L., Maixnerová, M., Nemec, M., Španělová, P., Šafránková, R., Šedo, O., Lopes, B. S., & Higgins, P. G. (2021). Delineation of a novel environmental phylogroup of the genus Acinetobacter encompassing Acinetobacter terrae sp. nov., Acinetobacter terrestris sp. nov. and three other tentative species. *Systematic and Applied Microbiology*, 44(4), 126217. https://doi.org/10.1016/j.syapm.2021.126217
- Noinaj, N., Guillier, M., Barnard, T. J., & Buchanan, S. K. (2010). TonB-dependent transporters: Regulation, structure, and function. *Annual Review of Microbiology*, *64*(75), 43–60. https://doi.org/10.1146/annurev.micro.112408.134247
- Ojima, Y., Sawabe, T., Nakagawa, M., Tahara, Y. O., Miyata, M., & Azuma, M. (2021). Aberrant Membrane Structures in Hypervesiculating Escherichia coli Strain ΔmlaEΔnlpl Visualized by Electron Microscopy. *Frontiers in Microbiology*, *12*, 2291. https://doi.org/10.3389/FMICB.2021.706525/BIBTEX
- Olofsson, A., Vallström, A., Petzold, K., Tegtmeyer, N., Schleucher, J., Carlsson, S., Haas, R., Backert, S., Wai, S. N., Gröbner, G., & Arnqvist, A. (2010). Biochemical and functional characterization of Helicobacter pylori vesicles. *Molecular Microbiology*, 77(6), 1539–1555. https://doi.org/10.1111/j.1365-2958.2010.07307.x
- Orench-Rivera, N., & Kuehn, M. J. (2021). Differential Packaging Into Outer Membrane Vesicles Upon Oxidative Stress Reveals a General Mechanism for Cargo Selectivity. *Frontiers in Microbiology*, 12(July), 1–14. https://doi.org/10.3389/fmicb.2021.561863
- Oxley Jimmie, Smith James, Busby Taylor, K. A. (2022). (12) Patent Application Publication (10) Pub. No.: US 2022/0017431 A1. 2022(19).
- Pantazou, V., Schluep, M., & Du Pasquier, R. (2015). Environmental factors in multiple sclerosis. *Presse Medicale*, 44(4), e113–e120. https://doi.org/10.1016/j.lpm.2015.01.001
- Parapatla, H., Gudla, R., Konduru, G. V., Devadasu, E. R., Nagarajaram, H. A., Sritharan, M., Subramanyam, R., & Siddavattam, D. (2020). Organophosphate hydrolase interacts with ferric-enterobactin and promotes iron uptake in association with TonB-dependent transport system. *Biochemical Journal*, 477(15), 2821–2840. https://doi.org/10.1042/BCJ20200299
- Park, J., Kim, M., Shin, B., Kang, M., Yang, J., Lee, T. K., & Park, W. (2021). A novel decoy strategy for polymyxin resistance in acinetobacter baumannii. *ELife*, 10. https://doi.org/10.7554/ELIFE.66988

- Pérez-Cruz, C., Delgado, L., López-Iglesias, C., & Mercade, E. (2015). Outer-inner membrane vesicles naturally secreted by gramnegative pathogenic bacteria. *PLoS ONE*, *10*(1). https://doi.org/10.1371/journal.pone.0116896
- Pettit, R. K., & Judd, R. C. (1992). The interaction of naturally elaborated blebs from serum-susceptible and serum-resistant strains of Neisseria gonorrhoeae with normal human serum. *Molecular Microbiology*, *6*(6), 729–734. https://doi.org/10.1111/J.1365-2958.1992.TB01522.X
- Prados-Rosales, R., Weinrick, B. C., Piqué, D. G., Jacobs, W. R., Casadevall, A., & Rodriguez, G. M. (2014). Role for mycobacterium tuberculosis membrane vesicles in iron acquisition. *Journal of Bacteriology*, 196(6), 1250–1256. https://doi.org/10.1128/JB.01090-13
- Raetz, C. R. H., & Dowhan, W. (1990). Biosynthesis and function of phospholipids in Escherichia coli. *Journal of Biological Chemistry*, 265(3), 1235–1238. https://doi.org/10.1016/s0021-9258(19)40001-x
- Ramsamy, Y., Essack, S. Y., Sartorius, B., Patel, M., & Mlisana, K. P. (2018). Antibiotic resistance trends of ESKAPE pathogens in Kwazulu-Natal, South Africa: A five-year retrospective analysis. *African Journal of Laboratory Medicine*, 7(2), 1–8. https://doi.org/10.4102/ajlm.v7i2.887
- Redondo-Salvo, S., Fernández-López, R., Ruiz, R., Vielva, L., de Toro, M., Rocha, E. P. C., Garcillán-Barcia, M. P., & de la Cruz, F. (2020). Pathways for horizontal gene transfer in bacteria revealed by a global map of their plasmids. *Nature Communications* 2020 11:1, 11(1), 1–13. https://doi.org/10.1038/s41467-020-17278-2
- Reimer, S. L., Beniac, D. R., Hiebert, S. L., Booth, T. F., Chong, P. M., Westmacott, G. R., Zhanel, G. G., & Bay, D. C. (2021). Comparative Analysis of Outer Membrane Vesicle Isolation Methods With an Escherichia coli tolA Mutant Reveals a Hypervesiculating Phenotype With Outer-Inner Membrane Vesicle Content. *Frontiers in Microbiology*, 12, 383. https://doi.org/10.3389/FMICB.2021.628801/BIBTEX
- Renelli, M., Matias, V., Lo, R. Y., & Beveridge, T. J. (2004). DNA-containing membrane vesicles of Pseudomonas aeruginosa PAO1 and their genetic transformation potential. *Microbiology (Reading, England)*, 150(Pt 7), 2161–2169. https://doi.org/10.1099/MIC.0.26841-0
- Resch, U., Tsatsaronis, J. A., Le Rhun, A., Stübiger, G., Rohde, M., Kasvandik, S., Holzmeister, S., Tinnefeld, P., Nyunt Wai, S., & Charpentier, E. (2016). A two-component regulatory system impacts extracellular membrane-derived vesicle production in group a streptococcus. *MBio*, 7(6), 1–10. https://doi.org/10.1128/mBio.00207-16
- Riva, F., Riva, V., Eckert, E. M., Colinas, N., Di Cesare, A., Borin, S., Mapelli, F., & Crotti, E. (2020). An Environmental Escherichia coli Strain Is Naturally Competent to Acquire Exogenous DNA. *Frontiers in Microbiology*, *11*, 2131. https://doi.org/10.3389/FMICB.2020.574301/BIBTEX
- Rothfield, L., & Pearlman-Kothencz, M. (1969). Synthesis and assembly of bacterial membrane components. *Journal of Molecular Biology*, 44(3), 477–492. https://doi.org/10.1016/0022-2836(69)90374-x
- Rueter, C., & Bielaszewska, M. (2020). Secretion and Delivery of Intestinal Pathogenic Escherichia coli Virulence Factors via Outer Membrane Vesicles. Frontiers in Cellular and Infection Microbiology, 10, 91. https://doi.org/10.3389/FCIMB.2020.00091/BIBTEX
- Rumbo, C., Fernández-Moreira, E., Merino, M., Poza, M., Mendez, J. A., Soares, N. C., Mosquera, A., Chaves, F., & Bou, G. (2011). Horizontal transfer of the OXA-24 carbapenemase gene via outer membrane vesicles: A new mechanism of dissemination of carbapenem resistance genes in Acinetobacter baumannii. *Antimicrobial Agents and Chemotherapy*, 55(7), 3084–3090. https://doi.org/10.1128/AAC.00929-10
- Salvadori, G., Junges, R., Morrison, D. A., & Petersen, F. C. (2019). Competence in streptococcus pneumoniae and close commensal relatives: Mechanisms and implications. *Frontiers in Cellular and Infection Microbiology, 9*(APR), 94. https://doi.org/10.3389/FCIMB.2019.00094/BIBTEX
- Samantarrai, D., Sagar, A. L., Gudla, R., & Siddavattam, D. (2020). Tonb-dependent transporters in sphingomonads: Unraveling their distribution and function in environmental adaptation. *Microorganisms*, 8(3), 359. https://doi.org/10.3390/microorganisms8030359
- Samantarrai, D., Yakkala, H., & Siddavattam, D. (2020). Analysis of indigenous plasmid sequences of A. baumannii DS002 reveals the existence of lateral mobility and extensive genetic recombination among Acinetobacter plasmids. *Journal of Genetics*, 99(1), 71. https://doi.org/10.1007/s12041-020-01232-8
- Schauer, K., Rodionov, D. A., & de Reuse, H. (2008). New substrates for TonB-dependent transport: do we only see the "tip of the iceberg"? *Trends in Biochemical Sciences*, 33(7), 330–338. https://doi.org/10.1016/j.tibs.2008.04.012
- Schertzer, J. W., Whiteley, M., & Kolter, R. (2012). A Bilayer-Couple Model of Bacterial Outer Membrane Vesicle Biogenesis. https://doi.org/10.1128/mBio.00297-11
- Schwechheimer, C., & Kuehn, M. J. (2015). *Outer-membrane vesicles from Gram-negative bacteria: biogenesis and functions*. https://doi.org/10.1038/nrmicro3525
- Schwechheimer, C., Sullivan, C. J., & Kuehn, M. J. (2013). Envelope control of outer membrane vesicle production in Gramnegative bacteria. *Biochemistry*, 52(18), 3031–3040. https://doi.org/10.1021/bi400164t
- Sciences, E., December, R., & February, A. (2010). *Pseudomonas Quinolone Signal Affects Membrane Vesicle Production in not only Gram-Negative but also Gram-Positive Bacteria*. 25(2), 120–125. https://doi.org/10.1264/jsme2.ME09182
- Shrivastava, S. R., Shrivastava, P. S., & Ramasamy, J. (2018). World health organization releases global priority list of antibiotic-resistant bacteria to guide research, discovery, and development of new antibiotics. *JMS Journal of Medical Society*, 32(1), 76–77. https://doi.org/10.4103/jms.jms_25_17
- Shultis, D. D., Purdy, M. D., Banchs, C. N., & Wiener, M. C. (2006). Outer membrane active transport: Structure of the BtuB:TonB complex. *Science*, 312(5778), 1396–1399. https://doi.org/10.1126/science.1127694
- Soler, N., Marguet, E., Verbavatz, J. M., & Forterre, P. (2008). Virus-like vesicles and extracellular DNA produced by hyperthermophilic archaea of the order Thermococcales. *Research in Microbiology*, 159(5), 390–399. https://doi.org/10.1016/J.RESMIC.2008.04.015
- Stentz, R., Carvalho, A. L., Jones, E. J., & Carding, S. R. (2018). Fantastic voyage: The journey of intestinal microbiota-derived

- microvesicles through the body. *Biochemical Society Transactions*, 46(5), 1021–1027. https://doi.org/10.1042/BST20180114
- Tashiro, Y., Inagaki, A., Shimizu, M., Ichikawa, S., Takaya, N., Nakajima-Kambe, T., Uchiyama, H., & Nomura, N. (2011). Characterization of phospholipids in membrane vesicles derived from Pseudomonas aeruginosa. *Bioscience, Biotechnology and Biochemistry*, 75(3), 605–607. https://doi.org/10.1271/bbb.100754
- Tran, F., & Boedicker, J. Q. (2017). Genetic cargo and bacterial species set the rate of vesicle-mediated horizontal gene transfer. Scientific Reports 2017 7:1, 7(1), 1–10. https://doi.org/10.1038/s41598-017-07447-7
- Tucker, A. T., Nowicki, E. M., Boll, J. M., Knauf, G. A., Burdis, N. C. M., Trent, S., & Davies, B. W. (2014). Defining Gene-Phenotype Relationships in Acinetobacter baumannii. *MBio*, 5(4), e01313-14. https://doi.org/10.1128/mBio.01313-14.Editor
- Tuckman, M., & Osburne, M. S. (1992). In vivo inhibition of TonB-dependent processes by a TonB box consensus pentapeptide. *Journal of Bacteriology*, 174(1), 320–323. https://doi.org/10.1128/jb.174.1.320-323.1992
- Turnbull, L., Toyofuku, M., Hynen, A. L., Kurosawa, M., Pessi, G., Petty, N. K., Osvath, S. R., Cárcamo-Oyarce, G., Gloag, E. S., Shimoni, R., Omasits, U., Ito, S., Yap, X., Monahan, L. G., Cavaliere, R., Ahrens, C. H., Charles, I. G., Nomura, N., Eberl, L., & Whitchurch, C. B. (2016). Explosive cell lysis as a mechanism for the biogenesis of bacterial membrane vesicles and biofilms. *Nature Communications 2016 7:1, 7*(1), 1–13. https://doi.org/10.1038/ncomms11220
- Usher, K. C., Özkan, E., Gardner, K. H., & Deisenhofer, J. (2001). The plug domain of FepA, a TonB-dependent transport protein from Escherichia coli, binds its siderophore in the absence of the transmembrane barrel domain. *Proceedings of the National Academy of Sciences of the United States of America*, *98*(19), 10676–10681. https://doi.org/10.1073/pnas.181353398
- von Wintersdorff, C. J. H., Penders, J., van Niekerk, J. M., Mills, N. D., Majumder, S., van Alphen, L. B., Savelkoul, P. H. M., & Wolffs, P. F. G. (2016). Dissemination of Antimicrobial Resistance in Microbial Ecosystems through Horizontal Gene Transfer. Frontiers in Microbiology, 0, 173. https://doi.org/10.3389/FMICB.2016.00173
- Whitley, C., Gunst, K., Müller, H., Funk, M., zur Hausen, H., & de Villiers, E. M. (2014). Novel replication-competent circular DNA molecules from healthy cattle serum and milk and multiple sclerosis-affected human brain tissue. *Genome Announcements*, 2(4), 3–4. https://doi.org/10.1128/genomeA.00849-14
- Wiener, M. C. (2005). TonB-dependent outer membrane transport: Going for Baroque? *Current Opinion in Structural Biology*, 15(4), 394–400. https://doi.org/10.1016/j.sbi.2005.07.001
- Yakkala, H., Samantarrai, D., Gribskov, M., & Siddavattam, D. (2019). Comparative genome analysis reveals nichespecific genome expansion in Acinetobacter baumannii strains. *PLoS ONE*, *14*(6), 1–26. https://doi.org/10.1371/journal.pone.0218204
- Yáñez-Mó, M., Siljander, P. R. M., Andreu, Z., Zavec, A. B., Borràs, F. E., Buzas, E. I., Buzas, K., Casal, E., Cappello, F., Carvalho, J., Colás, E., Cordeiro-Da Silva, A., Fais, S., Falcon-Perez, J. M., Ghobrial, I. M., Giebel, B., Gimona, M., Graner, M., Gursel, I., ... De Wever, O. (2015). Biological properties of extracellular vesicles and their physiological functions. *Journal of Extracellular Vesicles*, 4(2015), 1–60. https://doi.org/10.3402/jev.v4.27066
- Yang, S., Sun, Y., & Zhang, H. (2001). The Multimerization of Human Immunodeficiency Virus Type I Vif Protein: A REQUIREMENT FOR Vif FUNCTION IN THE VIRAL LIFE CYCLE*. *The Journal of Biological Chemistry*, *276*(7), 4889. https://doi.org/10.1074/JBC.M004895200
- Yaron, S., Kolling, G. L., Simon, L., & Matthews, K. R. (2000). Vesicle-mediated transfer of virulence genes from Escherichia coli O157:H7 to other enteric bacteria. *Applied and Environmental Microbiology*, *66*(10), 4414–4420. https://doi.org/10.1128/AEM.66.10.4414-4420.2000/FORMAT/EPUB
- Yeh, Y. H., Gunasekharan, V., & Manuelidis, L. (2017). A prokaryotic viral sequence is expressed and conserved in mammalian brain. *Proceedings of the National Academy of Sciences of the United States of America*, 114(27), 7118–7123. https://doi.org/10.1073/pnas.1706110114
- Yoneyama, H., & Nakae, T. (1996). Protein C (OprC) of the outer membrane of Pseudomonas aeruginosa is a copper-regulated channel protein. *Microbiology*, 142(8), 2137–2144. https://doi.org/10.1099/13500872-142-8-2137
- Zhan, X., Stamova, B., Jin, L. W., Decarli, C., Phinney, B., & Sharp, F. R. (2016). Gram-negative bacterial molecules associate with Alzheimer disease pathology. *Neurology*, *87*(22), 2324–2332. https://doi.org/10.1212/WNL.0000000000003391
- Zhao, Z., Nelson, A. R., Betsholtz, C., & Zlokovic, B. V. (2015). Establishment and Dysfunction of the Blood-Brain Barrier. *Cell*, 163(5), 1064–1078. https://doi.org/10.1016/J.CELL.2015.10.067
- Zur Hausen, H. (2015). Risk factors: What do breast and CRC cancers and MS have in common? *Nature Reviews Clinical Oncology*, 12(10), 569–570. https://doi.org/10.1038/nrclinonc.2015.154
- zur Hausen, H., Bund, T., & de Villiers, E. M. (2017). Infectious Agents in Bovine Red Meat and Milk and Their Potential Role in Cancer and Other Chronic Diseases. *Current Topics in Microbiology and Immunology*, 407, 83–116. https://doi.org/10.1007/82 2017 3
- zur Hausen, H., Bund, T., & de Villiers, E. M. (2019). Specific nutritional infections early in life as risk factors for human colon and breast cancers several decades later. *International Journal of Cancer*, 144(7), 1574–1583. https://doi.org/10.1002/ijc.31882
- Zur Hausen, H., & De Villiers, E. M. (2015). Dairy cattle serum and milk factors contributing to the risk of colon and breast cancers. International Journal of Cancer, 137(4), 959–967. https://doi.org/10.1002/IJC.29466





Outer Membrane Vesicles of *Acinetobacter baumannii* DS002 Are Selectively Enriched with TonB-Dependent Transporters and Play a Key Role in Iron Acquisition

Ganeshwari Dhurve, a Ashok Kumar Madikonda, a Medicharla Venkata Jagannadham, b 🗈 Dayananda Siddavattama

^aDept. of Animal Biology, School of Life Sciences, University of Hyderabad, Hyderabad, India ^bMetabolomics Facility, School of Life Sciences, University of Hyderabad, Hyderabad, India

ABSTRACT Outer membrane vesicles (OMVs) of *Acinetobacter baumannii* DS002 carry proteins which perform selective biological functions. The proteins involved in cell wall/membrane biogenesis and inorganic ion transport and metabolism occupied a significant portion of the 302 proteins associated with OMVs. Interestingly, the TonB-dependent transporters (TonRs), linked to the active transport of nutrients across the energy-deprived outer membrane, are predominant among proteins involved in inorganic ion transport and metabolism. The OMVs of DS002 contain TonRs capable of transporting iron complexed to catecholate, hydroximate, and mixed types of siderophores. Consistent with this observation, the OMVs were firmly bound to ferric-enterobactin (55Fe-Ent) and successfully transported iron into *A. baumannii* DS002 cells grown under iron-limiting conditions. In addition to the TonRs, OMVs also carry proteins known to promote pathogenesis, immune evasion, and biofilm formation. Our findings provide conclusive evidence for the role of OMVs in the transport of nutrients such as iron and show the presence of proteins with proven roles in pathogenicity and immune response.

IMPORTANCE TonB-dependent transporters (TonRs) play a crucial role in transporting nutrients such as iron, nickel, copper, and complex carbohydrates across the energy-deprived outer membrane. Due to their unique structural features, TonRs capture nutrients in an energy-independent manner and transport them across the outer membrane by harvesting energy derived from the inner membrane-localized Ton-complex. In this study, we report the presence of TonRs capable of transporting various nutrients in OMVs and demonstrate their role in capturing and transporting ferric iron complexed with enterobactin into *A. baumannii* DS002 cells. The OMV-associated TonRs appear to play a critical role in the survival of *A. baumannii*, listed as a priority pathogen, under nutrient-deprived conditions.

KEYWORDS proteomics, OMVs, LC-ESI-MS/MS, TonRs, iron uptake, siderophores

uter membrane vesicles (OMVs) of 20 to 300 nm in diameter, released by Gramnegative bacteria, play a crucial role in the survival of bacterial cells under adverse environmental conditions (1). They play critical roles in nutrient acquisition, pathogenesis, quorum-sensing signaling, and horizontal gene transfer (2). Almost all Gram-negative bacteria, including those infecting host tissue and serum, produce OMVs (3). OMVs contribute to the survival of bacterial cells by performing several critical cellular activities. They remove misfolded proteins, perform transport functions, and carry enzymes that generate carbon sources from complex macromolecules (3). The OMVs also contain signaling molecules that influence cellular communication and host immune response (1). Despite significant clues on the physiological relevance of OMVs, no conclusive evidence is available regarding their biogenesis (4). It is widely believed

Editor Ayush Kumar, University of Manitoba
Copyright © 2022 Dhurve et al. This is an
open-access article distributed under the terms
of the Creative Commons Attribution 4.0
International license.

Address correspondence to Dayananda Siddavattam, siddavattam@gmail.com, or Medicharla Venkata Jagannadham, medicharlavj@gmail.com or jagannadhamm_visiting@uohyd.ac.in.

The authors declare no conflict of interest.

Received 2 February 2022 Accepted 17 February 2022 Published 10 March 2022





59th Annual Conference of Association of Microbiologists of India (AMI-2018)



8

International Symposium on Host-Pathogen Interactions

Certificate

This is to certify that

Ganeshwari Dhurve

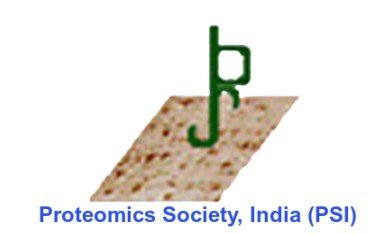
has presented oral/poster/participated in the AMI 2018 conference organized from 9th - 12th December 2018 by School of Life Sciences, University of Hyderabad, Hyderabad, Telangana - 500046, India.

Prof. Appa Rao Podile President

Prof. Pratyoosh Shukla General Secretary

Prof. Ch. Venkata Ramana Organizing Secretary 7/16/2021 1 new message







Virtual Conference on Proteomics in Agriculture and Healthcare

School of Life Sciences, University of Hyderabad

Certificate of Merit

This is to certify that Ms. GANESHWARI DHURVE S/o, D/o Bhagvan Singh Dhurve from University Of Hyderabad, Hyderabad has been awarded the best oral presentation in the conference held during March 13-14, 2021.

Prof. MV Jagannadham

MNJaggz

Convener

Prof. S Rajagopal

Organising Secretary

Prof. S Dayananda

Dean, School of Life Sciences





Functional Characterization of Outer Membrane Vesicles (OMVs) isolated from Acinetobacter baumannii DS002

by Ganeshwari Dhurve

Submission date: 16-Jun-2022 12:22PM (UTC+0530)

Submission ID: 1857788128

File name: i_15LAPH11_for_plagiarism_on_14-6-22_accepted_track_changes.docx (298.41K)

Word count: 26157

Character count: 141900

Functional Characterization of Outer Membrane Vesicles (OMVs) isolated from Acinetobacter baumannii DS002

ORIGINALITY REPORT					
2 SIMIL	6% ARITY INDEX	21% INTERNET SOURCES	23% PUBLICATIONS	6% STUDENT PAPERS	
PRIMAF	RY SOURCES				
1	Madikor Jaganna Outer M Selective Transpo	vari Dhurve, Asl nda, Medicharla dham, Dayanan embrane Vesicl ely Enriched with rters and Play a	Venkata da Siddavatta es of DS002 A n TonB-Deper Key Role in I	ndent ron	6
	Publication	on ", Microbiolo	ogy spectrum,	, 2022	
2	www.nck	oi.nlm.nih.gov		1. 0 mg 7 9,	ó
3	Submitte Hyderab Student Paper		of Hyderaba	d, 4 ₉	ó
4	isolation vesicles	nentová, Jiří Stu and purificatio from gram-nega ological Researc	n of outer me ative bacteria	embrane	ó

repository.ias.ac.in
Internet Source

<1%

	6	Adam Kulp, Meta J. Kuehn. "Biological Functions and Biogenesis of Secreted Bacterial Outer Membrane Vesicles", Annual Review of Microbiology, 2010 Publication	<1%
	7	www.nature.com Internet Source	<1%
	8	Marie-T. König, Robert Fux, Ellen Link, Gerd Sutter, Erwin Märtlbauer, Andrea Didier. "Circular Rep-Encoding Single-Stranded DNA Sequences in Milk from Water Buffaloes (Bubalus arnee f. bubalis)", Viruses, 2021 Publication	<1%
	9	scholarbank.nus.edu.sg Internet Source	<1%
	10	baadalsg.inflibnet.ac.in Internet Source	<1%
	11	academic.oup.com Internet Source	<1%
	12	etheses.whiterose.ac.uk Internet Source	<1%
	13	www.science.gov Internet Source	<1%
	14	Submitted to Mahidol University Student Paper	<1%
4			

15	"Lectin Purification and Analysis", Springer Science and Business Media LLC, 2020 Publication	<1%
16	Monique C. P. Mendonça, Ayse Kont, Maria Rodriguez Aburto, John F. Cryan, Caitriona M. O'Driscoll. "Advances in the Design of (Nano)Formulations for Delivery of Antisense Oligonucleotides and Small Interfering RNA: Focus on the Central Nervous System", Molecular Pharmaceutics, 2021 Publication	<1%
17	Sang-Oh Kwon, Yong Song Gho, Je Chul Lee, Seung Il Kim. "Proteome analysis of outer membrane vesicles from a clinical isolate ", FEMS Microbiology Letters, 2009 Publication	<1%
18	Mariana G. Sartorio, Evan J. Pardue, Mario F. Feldman, M. Florencia Haurat. "Bacterial Outer Membrane Vesicles: From Discovery to Applications", Annual Review of Microbiology, 2021 Publication	<1%
19	krishikosh.egranth.ac.in Internet Source	<1%
20	Régis Stentz, Ana L. Carvalho, Emily J. Jones, Simon R. Carding. "Fantastic voyage: the journey of intestinal microbiota-derived	<1%

microvesicles through the body", Biochemical Society Transactions, 2018

Publication

- Raman Karthikeyan, Pratapa Gayathri,
 Paramasamy Gunasekaran, Medicharla V.
 Jagannadham, Jeyaprakash Rajendhran.
 "Comprehensive proteomic analysis and
 pathogenic role of membrane vesicles of
 Listeria monocytogenes serotype 4b reveals
 proteins associated with virulence and their
 possible interaction with host", International
 Journal of Medical Microbiology, 2019
 Publication
- <1%

Harald zur Hausen, Timo Bund, Ethel-Michele de Villiers. "Chapter 3 Infectious Agents in Bovine Red Meat and Milk and Their Potential Role in Cancer and Other Chronic Diseases", Springer Science and Business Media LLC, 2017

<1%

Publication

Arif Tasleem Jan. "Outer Membrane Vesicles (OMVs) of Gram-negative Bacteria: A Perspective Update", Frontiers in Microbiology, 2017
Publication

<1%

Handoko, Lusy Lusiana. "Functional Characterization of IGHMBP2, the Disease Gene Product of Spinal Muscular Atrophy with

<1%

Respiratory Distress Type 1 (SMARD1)", Universität Würzburg, 2007.

Publication

25	S. Yaron, G. L. Kolling, L. Simon, K. R. Matthews. "Vesicle-Mediated Transfer of Virulence Genes from Escherichia coli O157:H7 to Other Enteric Bacteria", Applied and Environmental Microbiology, 2000 Publication	<1%
26	ebin.pub Internet Source	<1%
27	geb.uni-giessen.de Internet Source	<1%
28	A. T. Tucker, E. M. Nowicki, J. M. Boll, G. A. Knauf, N. C. Burdis, M. S. Trent, B. W. Davies. "Defining Gene-Phenotype Relationships in Acinetobacter baumannii through One-Step Chromosomal Gene Inactivation", mBio, 2014 Publication	<1%
29	C. Whitley, K. Gunst, H. Muller, M. Funk, H. zur Hausen, EM. de Villiers. "Novel Replication- Competent Circular DNA Molecules from Healthy Cattle Serum and Milk and Multiple Sclerosis-Affected Human Brain Tissue",	<1%

Submitted to Oxford Brookes University
Student Paper

'American Society for Microbiology', 2014

Internet Source

Yang, Zhibiao Bian, Yan Li, Hongchao Gou, Zhiyong Jiang, Rujian Cai, Chunling Li.
"Proteome Analysis of Outer Membrane Vesicles From a Highly Virulent Strain of Haemophilus parasuis", Frontiers in Veterinary Science, 2021

<1%

Publication

Submitted to University of Bristol
Student Paper

<1%

Aoife Howard, Michael O'Donoghue, Audrey Feeney, Roy D. Sleator. "Acinetobacter baumannii", Virulence, 2014

Publication

<1%

Steven J Biller, Lauren D McDaniel, Mya Breitbart, Everett Rogers, John H Paul, Sallie W Chisholm. "Membrane vesicles in sea water: heterogeneous DNA content and implications for viral abundance estimates", The ISME Journal, 2016

<1%

Publication

creativecommons.org

<1%

Internet Source

journals.sagepub.com
Internet Source

<1%

37	www.ilovemycarbondioxide.com Internet Source	<1%
38	Submitted to Universiti Sains Malaysia Student Paper	<1%
39	d-nb.info Internet Source	<1%
40	kups.ub.uni-koeln.de Internet Source	<1%
41	bio-protocol.org Internet Source	<1%
42	epdf.pub Internet Source	<1%
43	hdl.handle.net Internet Source	<1%
44	mrc.ac.ir Internet Source	<1%
45	www.freepatentsonline.com Internet Source	<1%
46	eprints.utar.edu.my Internet Source	<1%
47	etd.uwc.ac.za Internet Source	<1%
48	open.bu.edu Internet Source	<1%

Heramb M. Kulkarni, Ch. V. B. Swamy, Medicharla V. Jagannadham. " Molecular Characterization and Functional Analysis of Outer Membrane Vesicles from the Antarctic Bacterium Suggest a Possible Response to Environmental Conditions ", Journal of Proteome Research, 2014 Publication	<1%
Shweta Sharma, Pratibha Chanana, Ravi Bharadwaj, Sudha Bhattacharya, Ranjana Arya. "Functional characterization of GNE mutations prevalent in Asian subjects with GNE myopathy, an ultra-rare neuromuscular disorder", Biochimie, 2022	<1%
Submitted to University of Birmingham Student Paper	<1%
Submitted to University of Essex Student Paper	<1%
docksci.com Internet Source	<1%
Je Chul Lee, Eun Jeoung Lee, Jung Hwa Lee, So Hyun Jun, Chi Won Choi, Seung Il Kim, Sang Sun Kang, Sunghee Hyun. "Klebsiella pneumoniae secretes outer membrane vesicles that induce the innate immune response", FEMS Microbiology Letters, 2012	<1%

55	Submitted to University of Newcastle Student Paper	<1%
56	livrepository.liverpool.ac.uk Internet Source	<1%
57	polen.itu.edu.tr Internet Source	<1%
58	www.patentguru.com Internet Source	<1%

Exclude quotes

Exclude bibliography On

On

Exclude matches

< 14 words